NATIONAL COOPERATIVE HIGHWAY RESEARCH PROGRAM

NCHRP Report 368

Calibration of LRFD Bridge Design Code

Transportation Research Board
National Research Council

NATIONAL COOPERATIVE HIGHWAY RESEARCH PROGRAM

Report 368

Calibration of LRFD Bridge Design Code

ANDRZEJ S. NOWAK
Department of Civil and Environmental Engineering
University of Michigan
Ann Arbor, MI

Subject Areas

Bridges, Other Structures, and Hydraulics and Hydrology

Research Sponsored by the American Association of State Highway and Transportation Officials in Cooperation with the Federal Highway Administration

TRANSPORTATION RESEARCH BOARD
NATIONAL RESEARCH COUNCIL

NATIONAL ACADEMY PRESS
Washington, D.C. 1999

NATIONAL COOPERATIVE HIGHWAY RESEARCH PROGRAM

Systematic, well-designed research provides the most effective approach to the solution of many problems facing highway administrators and engineers. Often, highway problems are of local interest and can best be studied by highway departments individually or in cooperation with their state universities and others. However, the accelerating growth of highway transportation develops increasingly complex problems of wide interest to highway authorities. These problems are best studied through a coordinated program of cooperative research.

In recognition of these needs, the highway administrators of the American Association of State Highway and Transportation Officials initiated in 1962 an objective national highway research program employing modern scientific techniques. This program is supported on a continuing basis by funds from participating member states of the Association and it receives the full cooperation and support of the Federal Highway Administration, United States Department of Transportation.

The Transportation Research Board of the National Research Council was requested by the Association to administer the research program because of the Board's recognized objectivity and understanding of modern research practices. The Board is uniquely suited for this purpose as it maintains an extensive committee structure from which authorities on any highway transportation subject may be drawn; it possesses avenues of communications and cooperation with federal, state and local governmental agencies, universities, and industry; its relationship to the National Research Council is an insurance of objectivity; it maintains a full-time research correlation staff of specialists in highway transportation matters to bring the findings of research directly to those who are in a position to use them.

The program is developed on the basis of research needs identified by chief administrators of the highway and transportation departments and by committees of AASHTO. Each year, specific areas of research needs to be included in the program are proposed to the National Research Council and the Board by the American Association of State Highway and Transportation Officials. Research projects to fulfill these needs are defined by the Board, and qualified research agencies are selected from those that have submitted proposals. Administration and surveillance of research contracts are the responsibilities of the National Research Council and the Transportation Research Board.

The needs for highway research are many, and the National Cooperative Highway Research Program can make significant contributions to the solution of highway transportation problems of mutual concern to many responsible groups. The program, however, is intended to complement rather than to substitute for or duplicate other highway research programs.

Note: The Transportation Research Board, the National Research Council, the Federal Highway Administration, the American Association of State Highway and Transportation Officials, and the individual states participating in the National Cooperative Highway Research Program do not endorse products or manufacturers. Trade or manufacturers' names appear herein solely because they are considered essential to the object of this report.

NCHRP REPORT 368

Project C12-33 FY'88, '89, '90, '91, and '92

ISSN 0077-5614

ISBN 0-309-06613-7

L. C. Catalog Card No. 99-72895

Price $53.00

NOTICE

The project that is the subject of this report was a part of the National Cooperative Highway Research Program conducted by the Transportation Research Board with the approval of the Governing Board of the National Research Council. Such approval reflects the Governing Board's judgment that the program concerned is of national importance and appropriate with respect to both the purposes and resources of the National Research Council.

The members of the technical committee selected to monitor this project and to review this report were chosen for recognized scholarly competence and with due consideration for the balance of disciplines appropriate to the project. The opinions and conclusions expressed or implied are those of the research agency that performed the research, and, while they have been accepted as appropriate by the technical committee, they are not necessarily those of the Transportation Research Board, the National Research Council, the American Association of State Highway and Transportation Officials, or the Federal Highway Administration, U.S. Department of Transportation.

Each report is reviewed and accepted for publication by the technical committee according to procedures established and monitored by the Transportation Research Board Executive Committee and the Governing Board of the National Research Council.

To save time and money in disseminating the research findings, the report is essentially the original text as submitted by the research agency. This report has not been edited by TRB.

Published reports of the

NATIONAL COOPERATIVE HIGHWAY RESEARCH PROGRAM

are available from:

Transportation Research Board
National Research Council
2101 Constitution Avenue, N.W.
Washington, D.C. 20418

and can be ordered through the Internet at:

http://www.nas.edu/trb/index.html

Printed in the United States of America

FOREWORD

By Staff
Transportation Research Board

This report presents the results of a study on the calculation of load and resistance factors for the AASHTO *LRFD Bridge Design Specifications*. Information on various load models, and procedures for determining reliability indices, are included. The contents of this report will be of immediate interest to bridge and structural engineers, bridge researchers, and others interested in the development of the AASHTO LRFD design code and in probabilistic design methods.

The development of a new load and resistance factor design (LRFD) code for the design of bridges in the United States required the calculation of factors that were consistent with both theory and the performance of existing bridges. Load factors account for the variability in live and dead loads that a structure will endure during its design life. Resistance factors account for imperfect knowledge regarding material characteristics (especially strength), structural member geometries, and the static and dynamic behavior of bridges, and the effect this lack of knowledge has on the ability of structures to withstand loads. Because bridge design in the United States through the 1980s was based on the working stress (allowable stress) and load factor methods (neither of which had formal, probabilistically determined factors for both loads and resistances), significant new information was needed to provide the range of factors used in design.

NCHRP Project 12-33, "Development of a Comprehensive Bridge Specification and Commentary," was initiated in 1988 with the objective of developing a comprehensive new design code that could eventually replace the AASHTO *Standard Specifications for Highway Bridges* (which was considered disjointed, fragmented, and not state of the art). The product of Project 12-33 was published by AASHTO in 1994 as the LRFD *Bridge Design Specifications,* and a summary of the project is published in *NCHRP Research Results Digest 198.* A significant part of the project was the development and calibration of the load and resistance factors, and that work is the basis for this report. The research was performed by the University of Michigan, in Ann Arbor, Michigan, under a subcontract to Modjeski and Masters, Inc., of Mechanicsburg, Pennsylvania. The research results are presented in a form that allows researchers and bridge engineers to understand the loads that were considered during the course of the project, the types of structural resistance that were investigated, the concept of reliability and the target reliability indices chosen for the design code, and, finally, the load and resistance factors recommended for inclusion in the design specifications.

The report also describes issues related to the state of the practice—that is, how the factors selected were intended to result in structures that performed as satisfactorily as those designed and built using the "older" methods of working stress or load factors. Detailed information is provided regarding the database of bridges that served to calibrate the new factors; this database represents bridges of many geometries, materials, and span lengths from across the nation.

The report provides the basis for the continuous refinement of the bridge design code as more and better data are generated related to loads, load variability, materials, workmanship, and bridge performance.

CONTENTS

AUTHOR ACKNOWLEDGMENTS

The research reported herein was performed under NCHRP Project 12-33. Dr. John M. Kulicki, Modjeski and Masters, was the principal investigator and Professor Dennis Mertz, University of Delaware, formerly of Modjeski and Masters, was co-principal investigator. Andrzej S. Nowak, Professor of Civil Engineering, University of Michigan, was the Chair of Calibration Task Group. Other members of the Calibration Task Group are Professor C. Allin Cornell, Stanford University, Professor Ted V. Galambos, University of Minnesota, Professor Dan M. Frangopol, University of Colorado, Professor Fred Moses, University of Pittsburgh, Professor Roger Green, University of Waterloo and Professor Kamal Rojiani, Virginia Polytechnic Institute.

Other individuals who contributed by giving their comments and sharing their expertise include Dr. Baidar Bakht, Ontario Ministry of Transportation, Dr. Roy Inbsen, Imbsen and Associates, Hid Grouni, Ontario Ministry of Transportation and Professor Teoman Pekoz, Cornell University.

The work was done under the general supervision of Professor Nowak. A considerable effort was made by former research assistants and doctoral students at the University of Michigan. Dr. Young-Kyun Hong, KOPEC, Korea, and Professor Hani Nassif, Bradley University, assisted in the development of live load model. Dr. Eui-Seung Hwang, Korea Institute of Construction Technology, Korea, developed the simulation procedure for dynamic analysis of girder bridges. The parameters of resistance were calculated using a numerical procedure developed by Dr. Sami W. Tabsh, Gannett and Fleming Inc. (steel girders), Dr. Sheunn-Chern Ting, Williams Brothers Eng., (reinforced concrete and prestressed concrete), Professor Hani Nassif (shear resistance of steel girders) and Professor Ahmed Yamani, King Saud University, (Sheer resistance of reinforced concrete and prestressed concrete). Dr. Nagi Arwashan, Carl Walker Engineers, assisted in calculation of load and resistance parameters for selected bridges provided by the state DOTs. Tadeusz Alberski, New York DOT, and Hassan El-Hor, University of Michigan, helped in the preparation of the final report.

Help was also offered by many state departments of transportation, by providing designs and drawings of selected bridges. The California Department of Transportation also offered assistance in the analysis of prestressed concrete structures. The Federal Highway Administration was helpful in providing the access to the available data on bridge loads and behavior.

SUMMARY OF FINDINGS

The report describes the calculation of load and resistance factors for the LRFD bridge design code, carried out as a part of the NCHRP Project 12-33. The work involved the development of load and resistance models, selection of the reliability analysis method and calculation of the reliability indices.

The statistical data on load and resistance is reviewed. Load models are developed for dead load, live load and dynamic load. Resistance models are developed for girder bridges (steel, reinforced concrete and prestressed concrete). Reliability analysis is performed for selected representative structures.

Three components of dead load are considered; weight of factory-made elements, weight of cast-in-place concrete and bituminous surface (asphalt). The statistical parameters of dead load are based on the available data.

The live load model is based on the available truck survey data. The maximum live load moments and shears are calculated for one lane and two lane girder bridges. Simple spans and continuous spans are considered. For two lanes, the coefficient of correlation between trucks traveling side-by-side is very important. The governing combination is with two fully correlated vehicles, each weighing about 0.85 of the maximum 75 year truck. The resulting mean-to-nominal ratios are not consistent. They vary from about 1.6 to over 2.1. A new design live load has been developed which is a combination of truck load and a uniformly distributed load. The resulting moments and shears provide a consistent mean-to-nominal ratio of about 1.3 to 1.35.

The dynamic load is modeled on the basis of test results and simulations. A special numerical procedure is developed for the analysis of the dynamic behavior of girder bridges. The results of calculations indicate that dynamic load depends not only on the span (natural frequency), but also on road surface roughness and vehicle dynamics (suspension). It is observed that dynamic load, in terms of deflection, is constant. Therefore, the ratio of dynamic-to-static deflection decreases for heavier trucks. Dynamic load, as a fraction of live load, is also lower for two trucks compared to one truck cases. The observed mean dynamic loads (in terms of static live load) are about 0.15 for one truck and less than 0.1 for two trucks. A recommendation is made to use the dynamic load allowance of 0.33 applied to the truck effect only.

The resistance is considered as a product of three factors: material (strength), fabrication (dimensions) and professional (actual-to-theoretical behavior). The statistical parameters are derived using special simulation procedures. Data on material and dimensions is taken from the available literature and special studies. The parameters are calculated for moment carrying capacity and shear carrying capacity.

Reliability indices are calculated using an iterative procedure. The calculations are performed for bridges designed using current AASHTO. The resulting reliability indices vary depending on span length and girder spacing. The calculated reliability indices served as a basis in the selection of the target safety level. The target reliability index for girder bridges is taken as 3.5.

Load and resistance factors are determined so that the reliability index of bridges designed using the new LRFD code will be at the predetermined level. Recommended load factors are γ = 1.25 for dead load, except γ = 1.5 for asphalt overlay, and γ = 1.7 for live load (including impact). Resistance factors depend on statistical parameters (bias factor and coefficient of variation) of material properties and dimensions. It is recommended to use ϕ = 1.00 for moment and shear resistance of steel girders (composite and non-composite), ϕ = 1.00 for moment resistance of prestressed concrete girders, and ϕ = 0.90 for moment resistance of reinforced concrete T-beams and shear resistance of concrete girders (reinforced and/or prestressed).

Reliability indices calculated for bridges designed using the new LRFD code are very close to the target value of 3.5 for all materials and spans. For comparison, the ratio of the required load carrying capacity by the new LRFD code and the current AASHTO is also calculated for the considered bridges. The results are shown in figures and tables.

CHAPTER ONE

INTRODUCTION AND RESEARCH APPROACH

OBJECTIVE AND SCOPE OF THE REPORT

The objective of this report is to provide a background information for load and resistance factors in the LRFD (load and resistance factor design) bridge design code developed as a part of NCHRP Project 12-33.

The report reviews the code development procedures. The current specifications use allowable stresses and/or load factor design. The new code is based on a probability-based approach. Structural performance is measured in terms of the reliability (or probability of failure). Load and resistance factors are derived so that the reliability of bridges designed using the proposed provisions will be at the predefined target level. The report describes the calibration procedure (calculation of load and resistance factors). The major steps include selection of representative structures, calculation of reliability for the selected bridges, selection of the target reliability index and calculation of load factors and resistance factors. The report also reviews some other changes related to loads and resistance models. In particular, a new live load model is proposed which provides a consistent safety margin for a wide spectrum of spans. Dynamic load model takes into account the effect of road roughness, bridge dynamics and vehicle dynamics. Statistical models of resistance (load carrying capacity) are summarized for steel, composite steel, reinforced concrete and prestressed concrete. The reliability indices for bridges designed using the proposed code are compared to the reliability indices corresponding to the current specification.

The allowable stress method and even load factor design, do not provide for a consistent and uniform safety level for various groups of bridges. One of the major goals set for the new code is to provide a uniform safety reserve. The main parts of the current AASHTO (1) specification were written over 40 years ago. There were many changes and adjustments at different times. In the result there are many gaps and inconsistencies. Therefore, the work on the LRFD code also involves the re-writing of the whole document based on the state-of-the-art knowledge in various branches of bridge engineering.

The theory of code writing has been formulated in the last 20 years. Important contributions were made by Lind, Davenport, Cornell, Ferry-Borges, Galambos and MacGregor. The major tool in the development of a new code is the reliability analysis procedure. The reliability theory reached the degree of maturity which simplifies the applications. Structural performance is measured in terms of the reliability, or probability of failure. The code provisions are formulated so that structures designed using the code have a consistent and uniform safety level. Currently, almost all new codes are based on the probabilistic analysis (2).

The available reliability methods are reviewed in several textbooks. The methods vary with regard to accuracy, required input data, computational effort and special features (time-variance). In some cases, a considerable advantage can be gained by use of the system reliability methods. The structure is considered as a system of components. In the traditional reliability analysis, the analysis is performed for individual components. Systems approach allows to quantify the redundancy and complexity of the structure. The proposed LRFD code is based on element reliability. However, system reliability methods are used to verify the selection of redundancy factors.

This report presents the calibration procedure, load models, resistance models, reliability analysis and the development of load and resistance factors. The calibration work is performed to determine the load and resistance factors for non-composite steel girders, composite steel girders, reinforced concrete T-beams and prestressed concrete girders. The major new developments include load and resistance models.

The dead load parameters are summarized. Live load parameters are calculated on the basis of the truck survey data. The analysis is performed for one lane, two and multi-lane bridges. Simple spans and continuous spans are considered. An important part of this study is the dynamic load analysis. Dynamic load is modeled using the specially developed numerical procedure for simulation of bridge behavior. The parameters are also calculated for load combinations.

Resistance models are developed for girder bridges. The structural behavior is simulated using the available statistical data. The resistance models are described for the considered structural types; non-composite steel, composite steel, reinforced concrete T-beams and prestressed concrete girders. The ultimate limit states are considered, flexural capacity and shear. The statistical parameters are derived using specially developed simulation procedures. The results are summarized in a table.

The practical reliability methods used in this study are summarized. Reliability indices are calculated using a numerical procedure based on simulations. The flowchart of the computer program is presented in this report. The calculations are performed for representative bridges designed by the AASHTO (1). The spectrum of these reliability indices, along with the evaluation of performance of existing bridges, serve as a basis for the selection of the target reliability indices.

The procedure for calculation of load and resistance factors for the new code is also described.

CALIBRATION PROCEDURE

The calibration procedure was developed as a part of the project FHWA/RD-87/069 (3). In this project, the work on the new bridge design code was formulated including the following steps:

1. Selection of representative bridges

   About 200 structures are selected from various geographical regions of the United States. These structures cover materials, types and spans which are characteristic for the region. Emphasis is placed on current and future trends, rather than very old bridges. For each selected bridge, load effects (moments, shears, tensions and compressions) are calculated for various components. Load carrying capacities are also evaluated.

2. Establishing the statistical data base for load and resistance parameters.

   The available data on load components, including results of surveys and other measurements, is gathered. Truck survey and weigh-in-motion (WIM) data are used for modeling live load. There is little field data available for dynamic load therefore a numerical procedure is developed for simulation of the dynamic bridge behavior. Statistical data for resistance include material tests, component tests and field measurements. Numerical procedures are developed for simulation of behavior of large structural components and systems.

3. Development of load and resistance models.

   Loads and resistance are treated as random variables. Their variation is described by cumulative distribution functions (CDF) and correlations. For loads, the CDF's are derived using the available statistical data base (Step 2). Live load model includes multiple presence of trucks in one lane and in adjacent lanes. Multilane reduction factors are calculated for wider bridges. Dynamic load is modeled for single trucks and two trucks side-by-side. Resistance models are developed for girder bridges. The variation of the ultimate strength is determined by simulations. System reliability methods are used to quantify the degree of redundancy.

4. Development of the reliability analysis procedure.

   Structural performance is measured in terms of the reliability, or probability of failure. Limit states are defined as mathematical formulas describing the state (safe or failure). Reliability is measured in terms of the reliability index, β. Reliability index is calculated using an iterative procedure described by Rackwitz and Fiessler (4). The developed load and resistance models (Step 3) are part of the reliability analysis procedure.

5. Selection of the target reliability index.

   Reliability indices are calculated for a wide spectrum of bridges designed according to the current AASHTO (1). The performance of existing bridges is evaluated to determine whether their reliability level is adequate. The target reliability index, β_T, is selected to provide a consistent and uniform safety margin for all structures.

6. Calculation of load and resistance factors.

   Load factors, γ, are calculated so that the factored load has a predetermined probability of being exceeded. Resistance factors, ϕ, are calculated so that the structural reliability is close to the target value, β_T.

RESEARCH APPROACH

The work on the project followed the calibration procedure. Load and resistance models were developed on the basis of the available data and simulations. Reliability analysis procedure was developed to calculate the reliability of bridge girders. Structural performance was measured in terms of the reliability index.

The load and resistance factors were derived for girder bridges including non-composite steel, composite steel, reinforced concrete and prestressed concrete.

A very important part of the project was the selection of the target reliability index. The selection was based on the reliability indices of bridges design according to the current AASHTO (1) and evaluation of the structural performance by AASHTO engineers.

Load factors were calculated on the basis of statistical model. The major parameters considered were bias factor (ratio of mean to nominal) and coefficient of variation.

Resistance factors were determined for the considered bridge types and limit states. The selection criterion was closeness to the target reliability index.

CHAPTER TWO

FINDINGS

The major findings of this study is a procedure for calculation of load and resistance factors for the new LRFD bridge code. The work involved the development of load models, resistance models, reliability analysis procedure, selection of the target reliability index and calculation of the load and resistance factors for the new code.

BRIDGE LOADS

The major load components of highway bridges are dead load, live load (static and dynamic), environmental loads (temperature, wind, earthquake) and other loads (collision, emergency braking). Each load group includes several subcomponents. The load models are developed using the available statistical data, surveys and other observations. Load components are treated as random variables. Their variation is described by the cumulative distribution function (CDF), mean value or bias factor (ratio of mean to nominal) and coefficient of variation. The relationship among various load parameters is described in terms of the coefficients of correlation. The derivation of the statistical parameters for bridge load components is summarized in Appendix B.

Dead Load

Dead load, D, is the gravity load due to the self weight of the structural and non structural elements permanently connected to the bridge. Because of different degrees of variation, it is convenient to consider the following components of D:

D_1 = weight of factory made elements (steel, precast concrete),
D_2 = weight of cast-in-place concrete,
D_3 = weight of the wearing surface (asphalt),
D_4 = miscellaneous weight (e.g. railing, luminaries).

All components of D are treated as normal random variables. The statistical parameters (bias factors and coefficients of variation) used in the calibration are listed in Table 1.

Live Load

Live load, L, covers a range of forces produced by vehicles moving on the bridge. Traditionally, the static and dynamic effects are

Table 1. Statistical Parameters of Dead Load

Component	Bias Factor	Coefficient of Variation
Factory-made members	1.03	0.08
Cast-in-place members	1.05	0.10
Asphalt	3.5 inch*	0.25
Miscellaneous	1.03-1.05	0.08-0.10

*mean thickness

Table 2. Multilane Live Load Factors

ADTT	Number of lanes			
(in one direction)	1	2	3	4 or more
100	1.15	0.95	0.65	0.55
1,000	1.20	1.00	0.85	0.60
5,000	1.25	1.05	0.90	0.65

considered separately. Therefore, in this study, L covers only the static component. The dynamic component is denoted by I.

The effect of live load depends on many parameters including the span length, truck weight, axle loads, axle configuration, position of the vehicle on the bridge (transverse and longitudinal), traffic volume (ADTT), number of vehicles on the bridge (multiple presence), girder spacing, and stiffness of structural members (slab and girders) (5).

The design live load specified by AASHTO (1989) is shown in Fig. 1. The live load model is based on the available truck survey data. Multiple presence is considered by simulations. Girder distribution factors were taken from (6).

Live load effect is considered in terms of a positive moment, negative moment (continuous spans) and shear force. The available data is extrapolated to determine the maximum expected load effects for various periods of time, up to 75 years. For longer spans, two vehicles per lane govern. For a single lane and 75 years, the bias factors as a function of span, are shown in Fig. 2 for a positive moment, negative moment and shear. The corresponding coefficient of variation is 0.11 for spans larger than 30 ft and 0.14 for 10 ft span.

The bias factors presented in Fig. 2 correspond to ADTT (average daily truck traffic) equal to 1,000 (in one direction). For ADTT = 5,000, the bias factors are increased by 5%. For ADTT = 100, the bias factors are decreased by 5%.

For multilane bridges, the maximum load effect is determined by simulations. The parameters considered include the number of trucks, their weights and correlation between weights. For a two lane bridge, the maximum 75 year live load effect is caused by two side-by-side trucks, each representing the maximum two month vehicle. The ratio of the mean maximum two month truck and 75 year truck is about 0.85 for all the spans. Multilane live load factors are listed in Table 2 for ADTT = 100, 1,000 and 5,000. It is assumed, that the multilane factor is 1.00 for two lanes and ADTT = 1,000. Therefore, for one lane bridge it is 1.20 (inverse of 0.85).

The analysis of two lane (or multilane) loading involves multiple presence (side-by-side) and distribution of truck load to girders. The actual girder distribution factors (GDF) were calculated using finite element method. For comparison, the actual GDF's and GDF's specified in the current AASHTO (1) are shown in Fig. 3. GDF's in AASHTO are considerably more conservative for larger girder spacings and longer spans.

The bias factor for live load moment per girder, λ_g, is

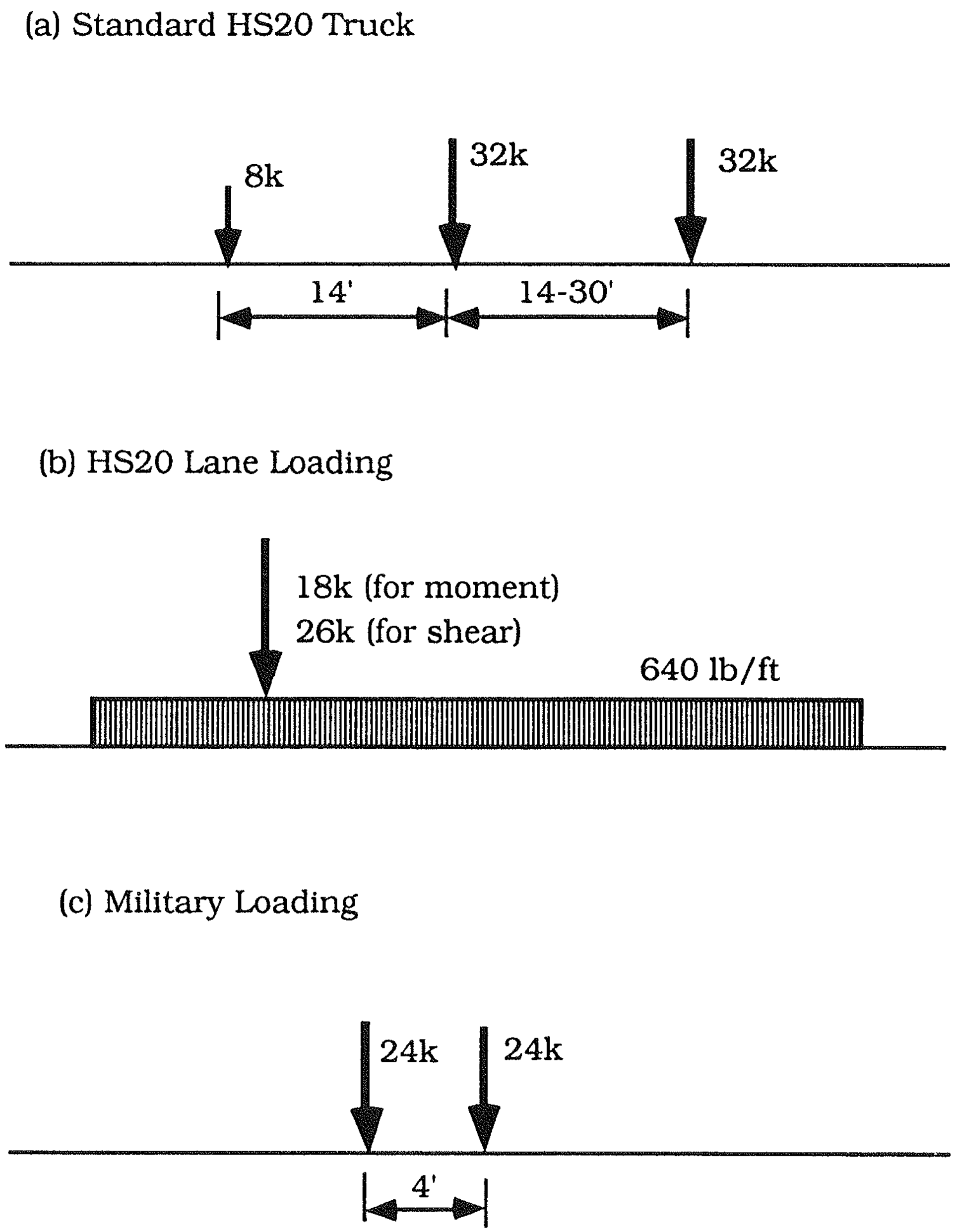

Fig. 1. Design Live Load in Current AASHTO.

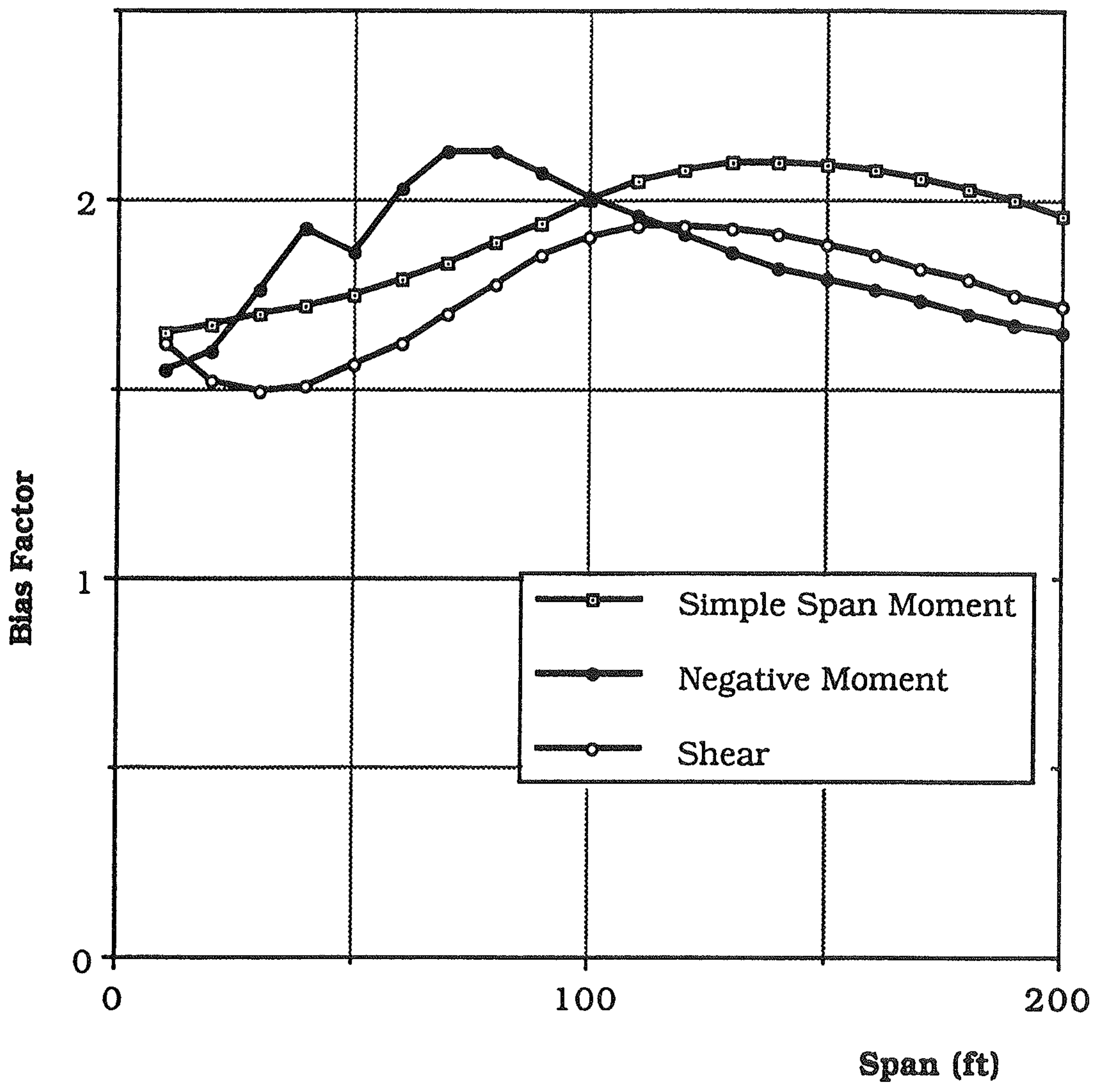

Fig. 2. Bias Factor for the Maximum 75 Year Live Load per Lane, Current AASHTO.

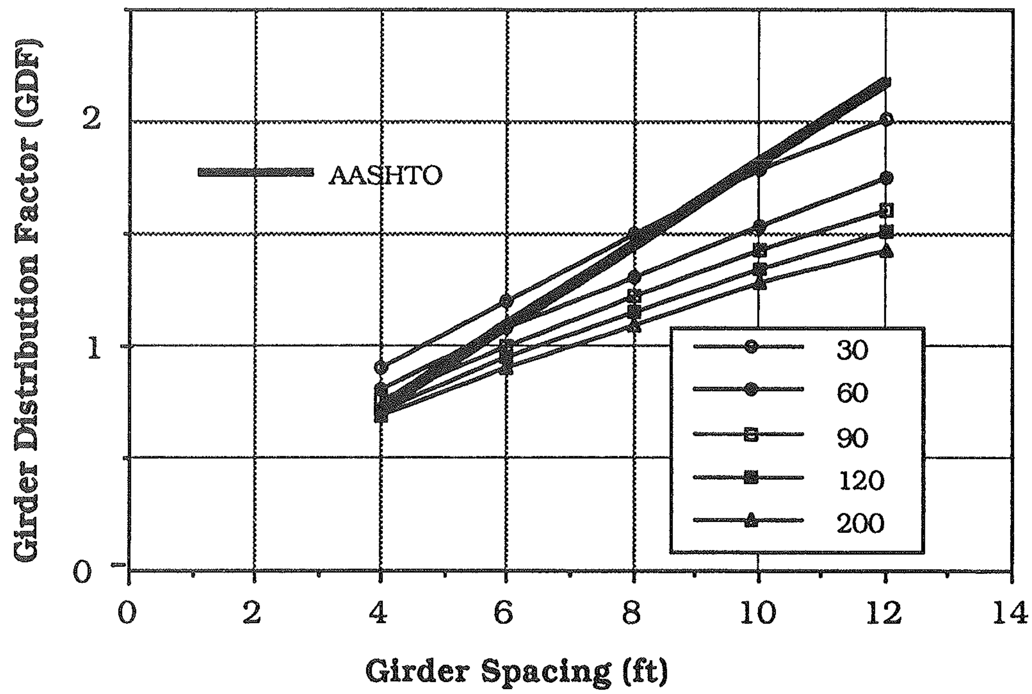

Fig. 3. Actual GDF's and AASHTO Specified GDF's.

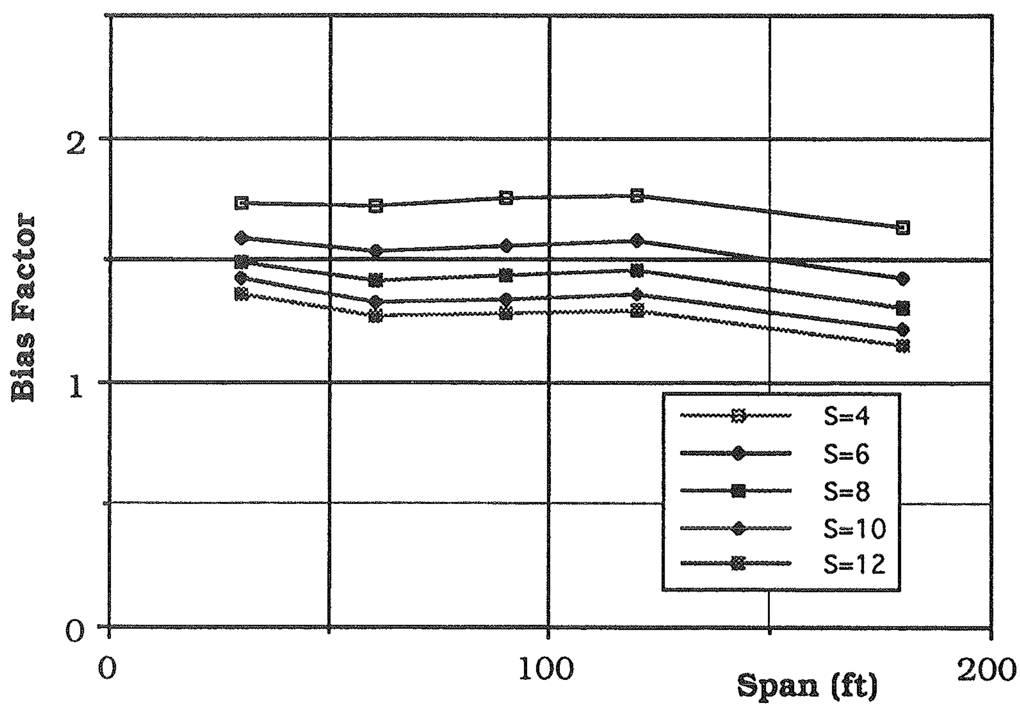

Fig. 4. Bias Factor for the Maximum 75 Year Moment per Girder, Current AASHTO.

$$\lambda_g = (0.85)(\lambda_1)(\lambda_D) \quad (1)$$

where λ_1 = bias factor for the maximum 75 year moment for a single lane (shown in Fig. 2); λ_D = ratio of the actual GDF and GDF specified by AASHTO.

In Fig. 4, λ_g is plotted as a function of span length and girder spacing. The resulting values indicate a considerable degree of variation.

One of the major objectives of the LRFD code is to provide a uniform bias factor for load effects. Therefore, a new live load model is specified, as shown in Fig. 5. For a single lane, the bias factors for the maximum 75 year live load effects are shown in Fig. 6 for a simple span moment, negative moment and shear, respectively. For two lane bridges, the bias factor for LRFD live load per girder, λ_g, is presented in Fig. 7.

Dynamic Load

The dynamic load is a function of three major parameters: road surface roughness, bridge dynamics (frequency of vibration) and vehicle dynamics (suspension system). The developed model includes the effect of these three parameters. The derivations are based on the numerical simulations (7, 8). Dynamic load effect, I, is considered as an equivalent static load effect added to the live load, L.

Static and dynamic load effects are measured in terms of deflection. The results of simulations indicate that dynamic deflections are almost constant while static deflection increase for heavier trucks. Therefore the dynamic load factors (DLF), defined as I/L, are lower for two trucks than for one truck. In general, DLF is reduced for a larger number of axles. To determine the maximum 75 load effect, DLF is applied to the maximum 75 year live load. The dynamic load corresponding to an extremely heavy truck is close to the mean of DLF. For longer spans, the maximum live load is a resultant of two or more trucks in lane. This corresponds to a reduced DLF. The mean DLF for a single truck is about 0.15 and for two trucks side-by-side, DLF is about 0.10. The coefficient of variation is 0.8.

The proposed nominal (design) DLF = 0.33, applied to the truck effect only, with no DLF applied to the uniformly distributed portion of live load (Fig. 5). For wood bridges, the DLF is reduced by 50%.

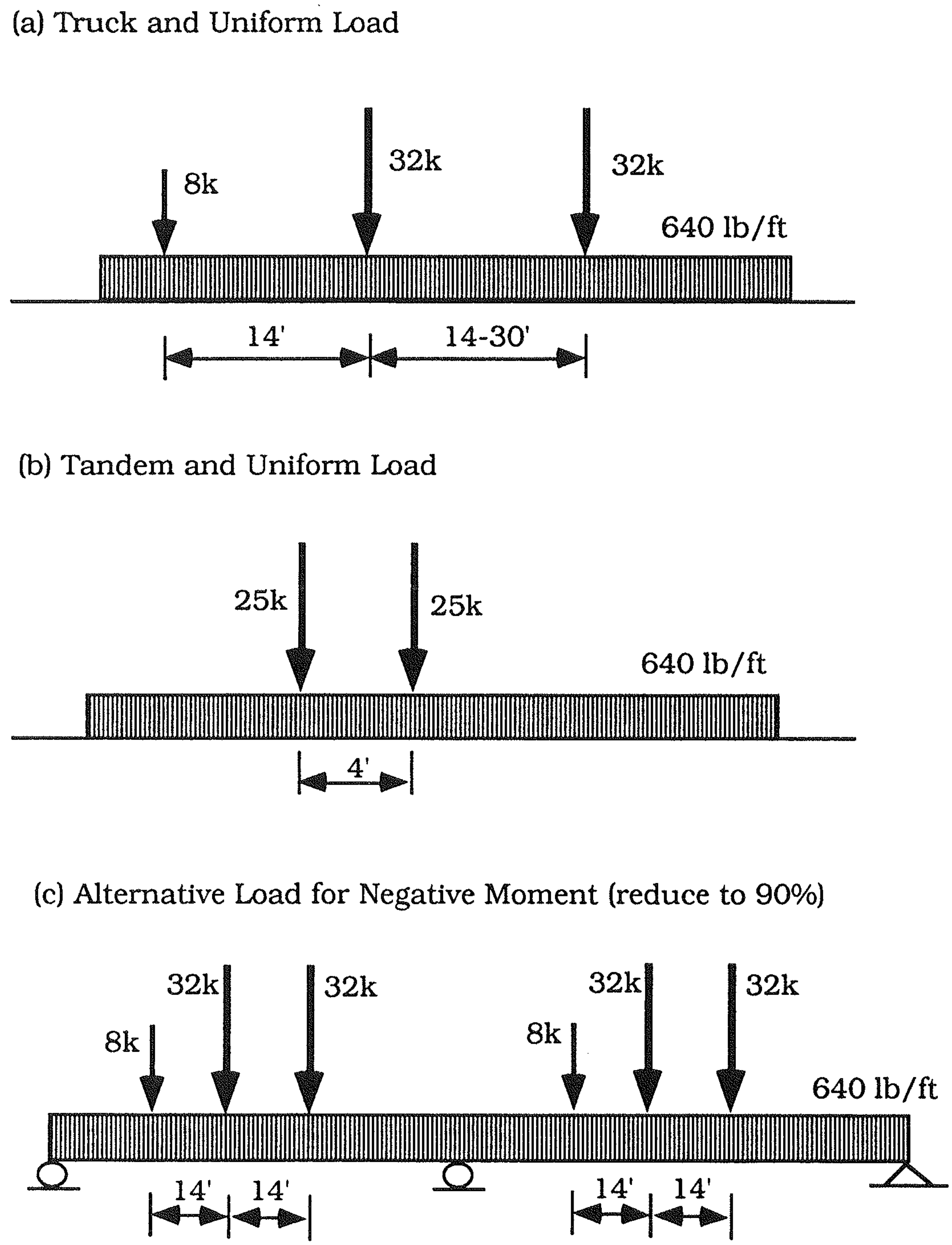

Fig. 5. Design Live Load in LRFD Code.

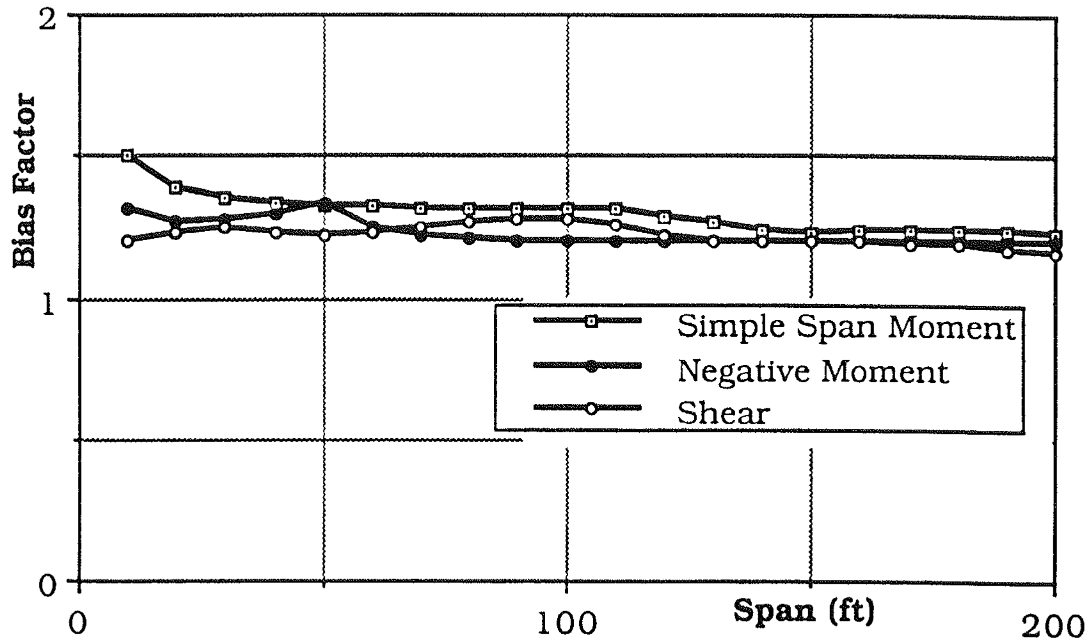

Fig. 6. Bias Factor for the Maximum 75 Year Live Load Effects per Lane, LRFD Code.

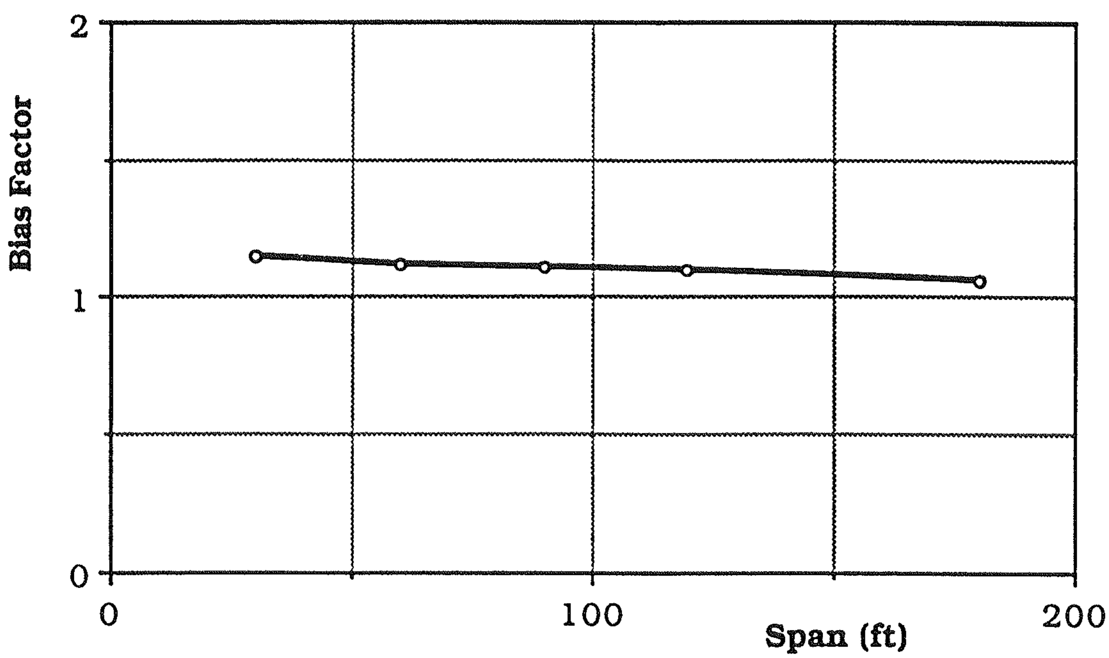

Fig. 7. Bias Factor for the Maximum 75 Year Moment per Girder, LRFD Code.

Environmental Loads

Environmental loads include wind, earthquake, temperature, water pressure, ice pressure. The statistical models for wind load and earthquake are based on the available information, in particular (9). For the maximum 75 year wind, the bias factor, λ =0.64, and coefficient of variation, V = 0.37. For the maximum 75 year earthquake, λ = 0.30 and V = 0.70.

Load Combinations

Load components occur simultaneously. However, there is a reduced probability of a simultaneous occurrence of extreme values. Therefore, the following load combinations are considered:

(1) $D + L + I$ (2)

This is the basic combination with D and L taking the maximum values simultaneously.

(2) $D + W$ (3)

Wind and dead load take the maximum 75 year values simultaneously. Live load is not considered as it is assumed that the bridge is closed for traffic during an extreme wind.

(3) $D + L + I + W$ (4)

This combination includes the maximum daily live load simultaneous with an average daily wind.

(4) $D + L + I + E$ (5)

The maximum earthquake occurs simultaneously with an average (arbitrary-point-in-time) live load. Arbitrary-point-in-time live load depends on ADTT.

BRIDGE RESISTANCE

The capacity of a bridge depends on the resistance of its components and connections. The component resistance, R, is determined mostly by material strength and dimensions. R is a random variable and it can be considered as a product of the following parameters (9):

$$R = M\ F\ P\ R_n \tag{6}$$

where M = material factor representing properties such as strength, modulus of elasticity, cracking stress, and chemical composition; F = fabrication factor including geometry, dimensions, and section modulus; P = analysis factor such as approximate method of analysis, idealized stress and strain distribution model.

The variation of resistance has been modeled by tests, simulations, observations of existing structures and by engineering judgment. The statistical parameters are developed for non-composite and composite steel girders, reinforced concrete T-beams, and prestressed concrete AASHTO-type girders. The derivations are described in Appendix C.

Bias factors and coefficients of variation are determined for material factor, M, fabrication factor, F, and analysis factor, P. Factors M and F are combined. The parameters of R are calculated as follows:

$$\lambda_R = (\lambda_{FM})(\lambda_P) \tag{7}$$

where λ_R = bias factor of R; λ_{FM} = bias factor of FM; and λ_P = bias factor of P, and

$$V_R = (V_{FM}^2 + V_P^2)^{1/2} \tag{8}$$

where V_R = coefficient of variation of R; V_{FM} = coefficient of variation of FM; and V_P = coefficient of variation of P.

The statistical parameters of resistance for steel girders, reinforced concrete T-beams and prestressed concrete girders are shown in Table 3.

RELIABILITY ANALYSIS

Structural performance is measured in terms of the reliability index, β (10). Reliability index is defined as a function of the probability of failure, P_F,

$$\beta = -\Phi^{-1}(P_F) \tag{9}$$

where Φ^{-1} = inverse standard normal distribution function.

In this study, the reliability index is calculated using an iterative procedure described in Appendix D. It is assumed that the total load, Q, is a normal random variable. The resistance, R, is considered as a lognormal random variable.

Table 3. Statistical Parameters of Resistance

Type of Structure	F M		P		R	
	λ	V	λ	V	λ	V
Non-composite steel girders						
Moment (compact)	1.095	0.075	1.02	0.06	1.12	0.10
Moment (non-com.)	1.085	0.075	1.03	0.06	1.12	0.10
Shear	1.12	0.08	1.02	0.07	1.14	0.105
Composite steel girders						
Moment	1.07	0.08	1.05	0.06	1.12	0.10
Shear	1.12	0.08	1.02	0.07	1.14	0.105
Reinforced concrete						
Moment	1.12	0.12	1.02	0.06	1.14	0.13
Shear w/steel	1.13	0.12	1.075	0.10	1.20	0.155
Shear no steel	1.165	0.135	1.20	0.10	1.40	0.17
Prestressed concrete						
Moment	1.04	0.045	1.01	0.06	1.05	0.075
Shear w/steel	1.07	0.10	1.075	0.10	1.15	0.14

The formula for reliability index can be expressed in terms of the given data (R_n, λ_R, V_R, m_Q, σ_Q) and parameter k as follows,

$$\beta = \frac{R_n \lambda_R (1 - kV_R)[1 - \ln(1 - kV_R)] - m_Q}{\sqrt{[R_n V_R \lambda_R (1 - kV_R)]^2 + \sigma_Q^2}} \tag{10}$$

where R_n = nominal (design) value of resistance; λ_R = bias factor of R; V_R = coefficient of variation of R; m_Q = mean load; σ_Q = standard deviation of load. Value of parameter k depends on location of the design point. In practice, k is about 2.

RELIABILITY INDICES FOR CURRENT AASHTO

The code calibration is based on calculations performed for a selected set of structures. The selection was based on structural type, material, and geographical location. Current and future trends were considered. The selected set also includes representative existing bridges. The list of structures and calculated reliability indices are provided in Appendix E.

The basic design requirement according to AASHTO (1) is expressed in terms of moments or shears (Load Factor Design),

$$1.3\ D + 2.17\ (L + I) < \phi R \tag{11}$$

where D, L and I are moments (or shears) due to dead load, live load and impact, R is the moment (or shear) carrying capacity, and ϕ is the resistance factor. Values of the resistance factor are given in Table 4.

For given loads, D, L and I, the required resistance, R, according to the current AASHTO (1), is calculated as,

$$R = [1.3\ D + 2.17\ (L + I)]/\phi \tag{12}$$

The reliability indices are calculated for girder bridges and the limit states (moment and shear) described by the representative load components and resistance (11). The results are presented in Fig. 8 to 11, for simple span moments in non-composite steel, composite steel, reinforced concrete and prestressed concrete girders, respectively. For shears the results are given in Fig. 12 to 15.

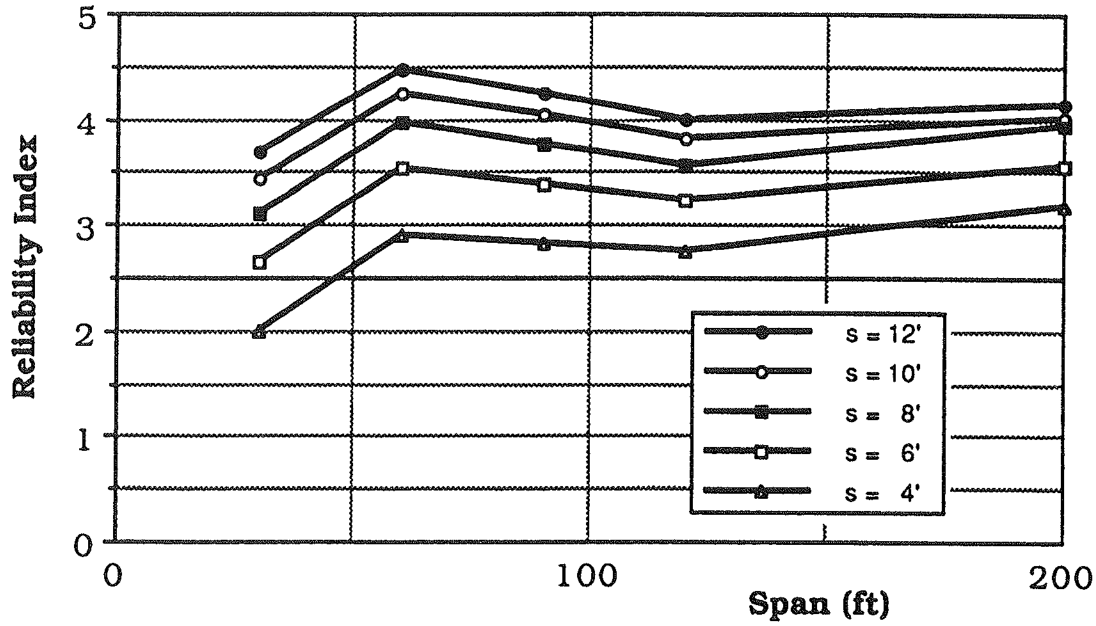

Fig. 8. Reliability Indices for Current AASHTO; Simple Span Moment in Non-Composite Steel Girders.

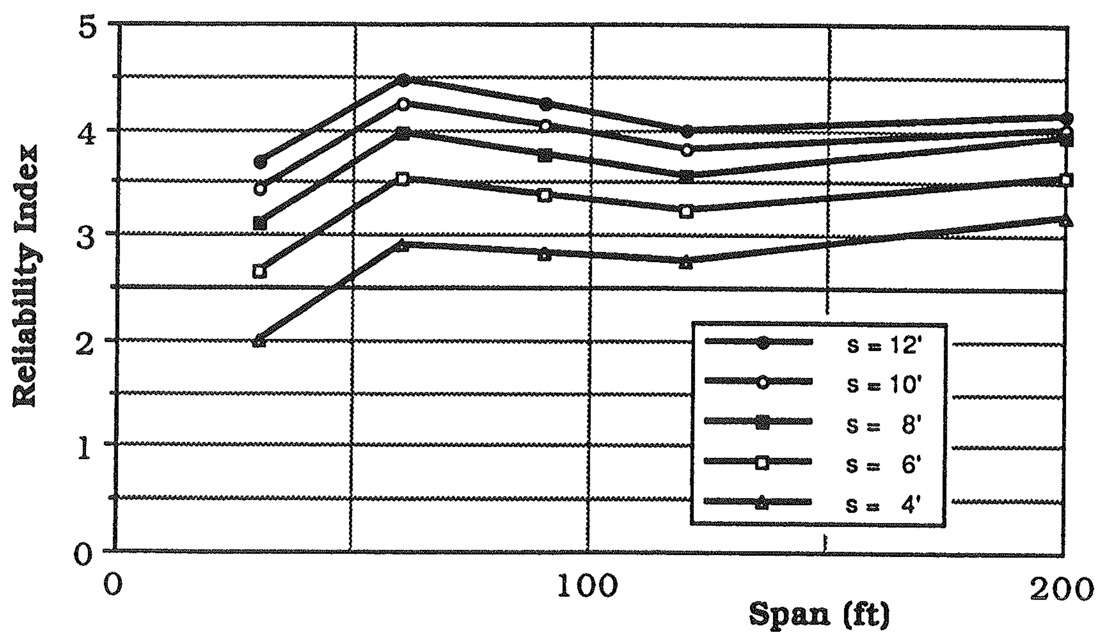

Fig. 9. Reliability Indices for Current AASHTO; Simple Span Moment in Composite Steel Girders.

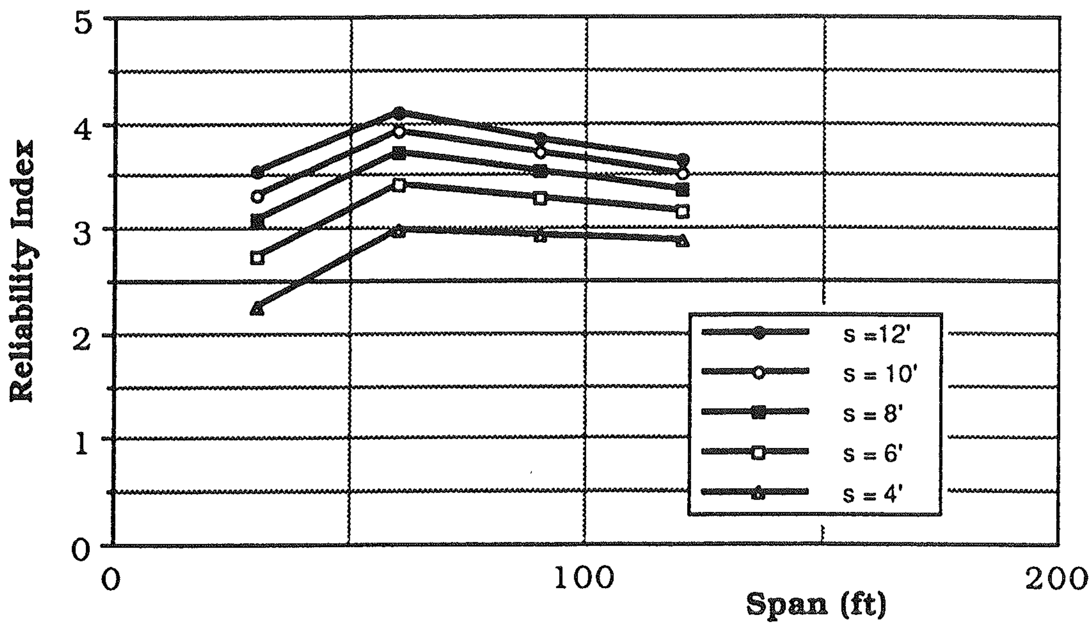

Fig. 10. Reliability Indices for Current AASHTO;
Simple Span Moment in Reinforced Concrete T-Beams.

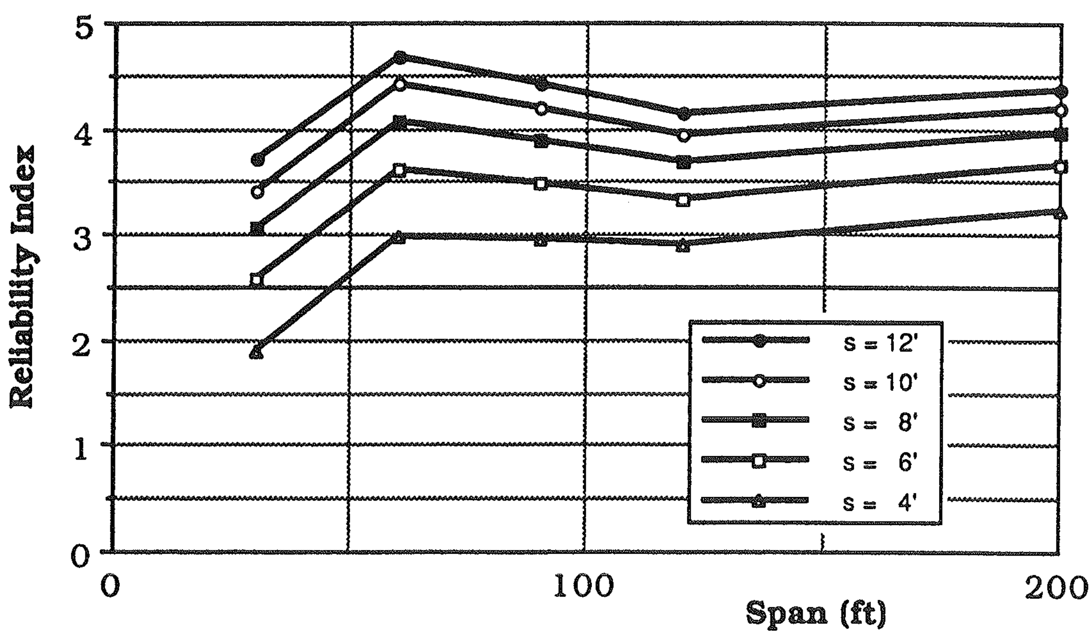

Fig. 11. Reliability Indices for Current AASHTO;
Simple Span Moment in Prestressed Concrete Girders.

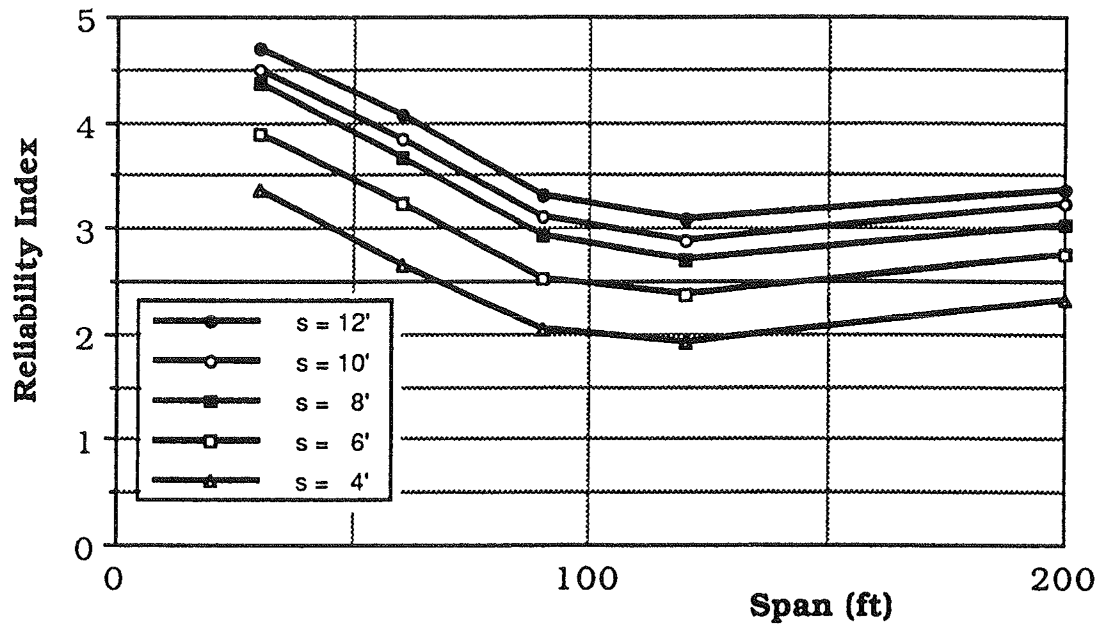

Fig. 12. Reliability Indices for Current AASHTO;
Shear in Steel Girders.

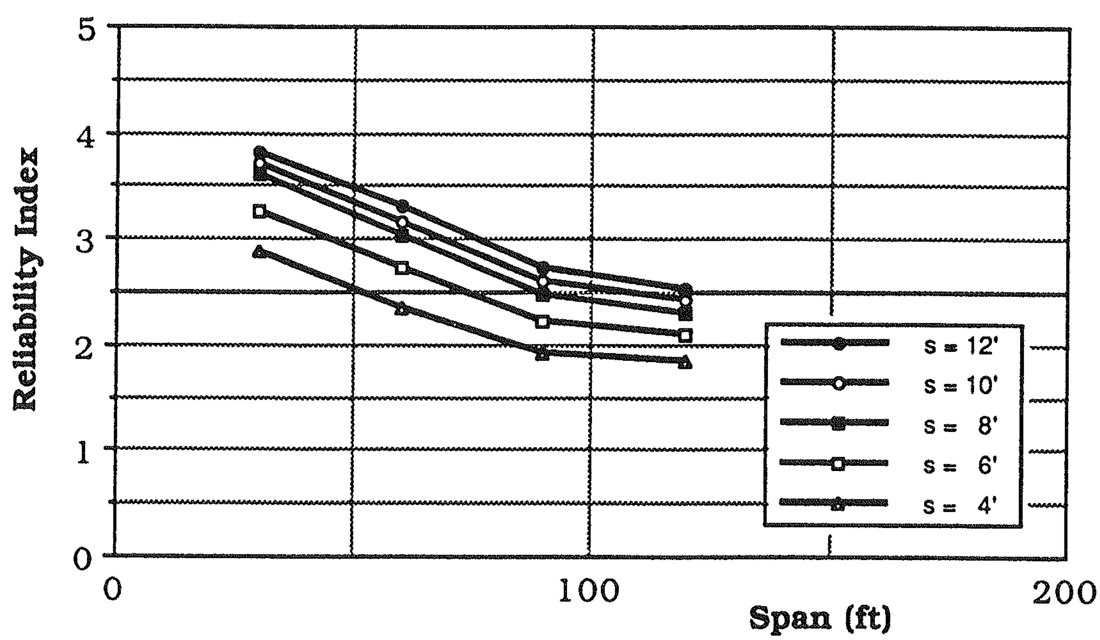

Fig. 13. Reliability Indices for Current AASHTO;
Shear in Reinforced Concrete T-Beams.

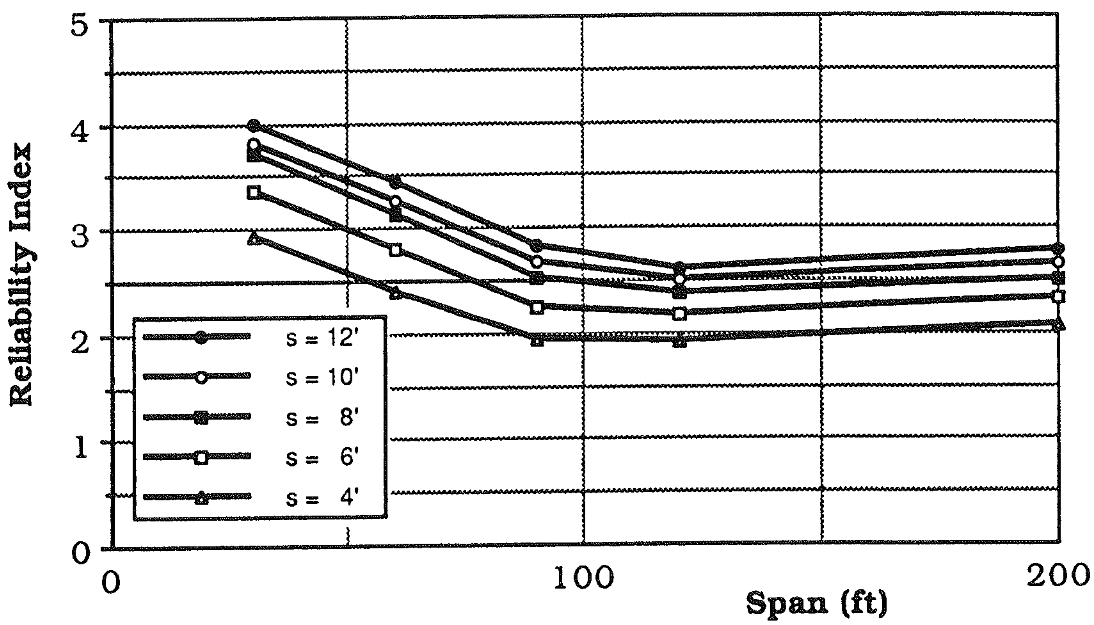

Fig. 14. Reliability Indices for Current AASHTO;
Shear in Prestressed Concrete Girders.

Table 4. Resistance Factors in Current AASHTO (1).

Material	Limit State	Resistance Factor, ϕ
Non-composite steel	Moment	1.00
	Shear	1.00
Composite steel	Moment	1.00
	Shear	1.00
Reinforced concrete	Moment	0.90
	Shear	0.85
Prestressed concrete	Moment	1.00
	Shear	0.90

Table 5. Recommended Resistance Factors.

Material	Limit State	Resistance Factor, ϕ
Non-Composite Steel	Moment	1.00
	Shear	1.00
Composite Steel	Moment	1.00
	Shear	1.00
Reinforced Concrete	Moment	0.90
	Shear	0.90
Prestressed Concrete	Moment	1.00
	Shear	0.90

TARGET RELIABILITY INDEX

The calculated reliability indices served as a basis for the selection of the target reliability index, β_T. The most important parameters which determine the reliability index are girder spacing and span length. In general, β's are higher for larger girder spacing. This is due to more conservative values of GDF (girder distribution factor) compared to shorter spacings. It is assumed that the safety level determined for simple span moment and corresponding to girder spacing of 6 ft and span of 60 ft is acceptable. Therefore, for girder bridges, the target reliability index is taken as $\beta_T = 3.5$.

LOAD AND RESISTANCE FACTORS

Load Factors

The objective in the selection of load and resistance factors is closeness to the target reliability index, β_T. The procedure is described in Appendix F. For each load component, X_i, load factor, γ_i, is calculated as the following function of the bias factor (mean to nominal ratio), λ_i, and the coefficient of variation, V_i,

$$\gamma_i = \lambda_i (1 + kV_i) \qquad (13)$$

where $k = 2$.

Therefore, the resulting load factors are: 1.20 for D_1; 1.25 for D_2; 1.50 for D_3; and 1.60 for live load (see Fig. F-2). For simplicity of the designer, one factor is recommended for D_1 and D_2, $\gamma = 1.25$. For D_3, weight of asphalt, $\gamma = 1.50$. For negative dead load, $\gamma = 0.85$-0.90. The calculated live load factor corresponds to ADTT = 1,000 trucks (in one direction). For ADTT = 5,000, the recommended live load factor is 1.70.

For the considered load combinations, the following factors are recommended:

(1) $$1.25\ D + 1.50\ D_A + 1.70\ (L + I) \qquad (14)$$

(2a) $$1.25\ D + 1.50\ D_A + 1.40\ W \qquad (15)$$

(2b) $$-\ 0.85\ D - 0.50\ D_A + 1.40\ W \qquad (16)$$

(3) $$1.25\ D + 1.50\ D_A + 1.35\ (L + I) + 0.45\ W \qquad (17)$$

(4) $$1.25\ D + 1.50\ D_A + \gamma_L\ (L + I) + 1.00\ E \qquad (18)$$

(4) $$1.25\ D + 1.50\ D_A + \gamma_L\ (L + I) + 1.00\ E \qquad (18)$$

where γ_L = 0.25-0.50 for ADTT = 5,000 (smaller load factor for longer spans); γ_L = 0.10-0.20 for ADTT = 1,000; and γ_L = 0 for ADTT = 100.

Resistance Factors

In the selection of resistance factors, the acceptance criterion is closeness to the target value of the reliability index, β_T. Various sets of resistance factors, ϕ, are considered as described in Appendix F. Resistance factors are rounded off to the nearest 0.05.

The recommended resistance factors are given in Table 5.

CHAPTER THREE

INTERPRETATION, APPRAISAL, APPLICATION

The study has several important implications. The calculated load and resistance factors for the new LRFD code provide a uniform safety level for various bridges. The statistical analysis of load and resistance models served as a basis for the development of more rational design criteria.

BRIDGE LOADS

The major new development resulting from the project, is the new design live load and dynamic load. The statistical parameters (bias factors and coefficients of variation) are calculated for various time periods and ADTT's.

The live load parameters are derived with the assumption of no future growth of truck weights. If there is an increase in legal loads then the design criteria may have to be revised. The data and procedures presented in this report, can serve as a basis for recalculation of load factors.

BRIDGE RESISTANCE

The developed statistical parameters for girder bridges can be used in the reliability analysis of a wide range of structural types. The developed procedures are also applicable to new materials.

RELIABILITY INDICES

Reliability index is an efficient measure of structural performance. The developed procedures can be used for an objective comparison of different variants of design alternatives, acceptance of new materials and types of structures.

Optimum safety level can be expressed in terms of the target reliability index, β_T. In this research, the same $\beta_T = 3.5$ is selected for various materials and spans. However, the optimum value of β_T, can be determined by considering consequences of potential failure and the cost of increasing safety to a higher level. Therefore, for other materials and structural types, β_T can be different than 3.5.

LOAD AND RESISTANCE FACTORS

The calculated load and resistance factors provide a consistently uniform reliability of design. However, bridges designed using the new LRFD Code are different than those designed by the current AASHTO (1). For comparison, the minimum required resistance is calculated for LRFD Code, R(LRFD), and current AASHTO, R(HS20). The calculations are performed for non-composite and composite steel girders, reinforced concrete T-beams and prestressed concrete AASHTO-type girders. The ratios of R(LRFD) and R(HS20) are plotted for various girder spacings in Fig. 15-18 for moments and Fig. 19-21 for shears.

For comparison, the calculations are also carried out for other values of live load factor and resistance factors. The results are presented in Appendix F.

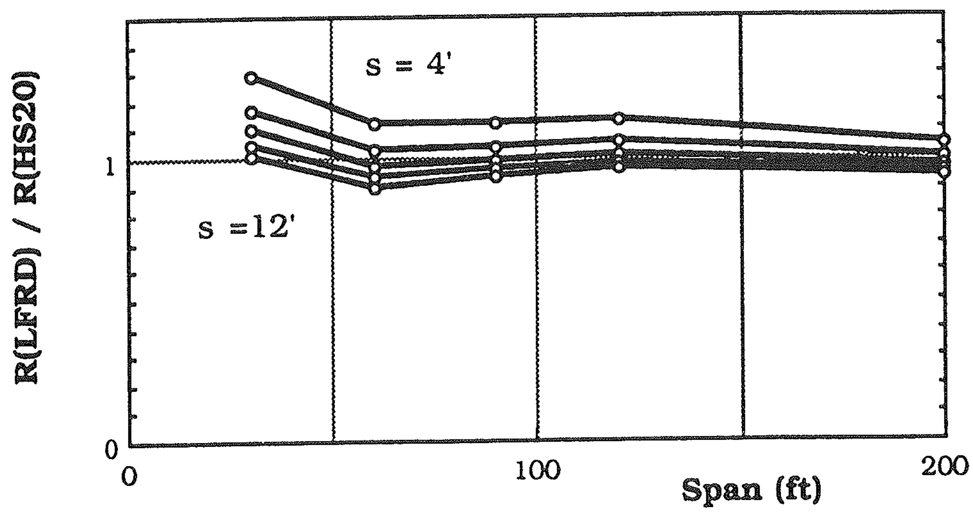

Fig. 15. Resistance Ratios; Simple Span Moment in Non-Composite Steel Girders.

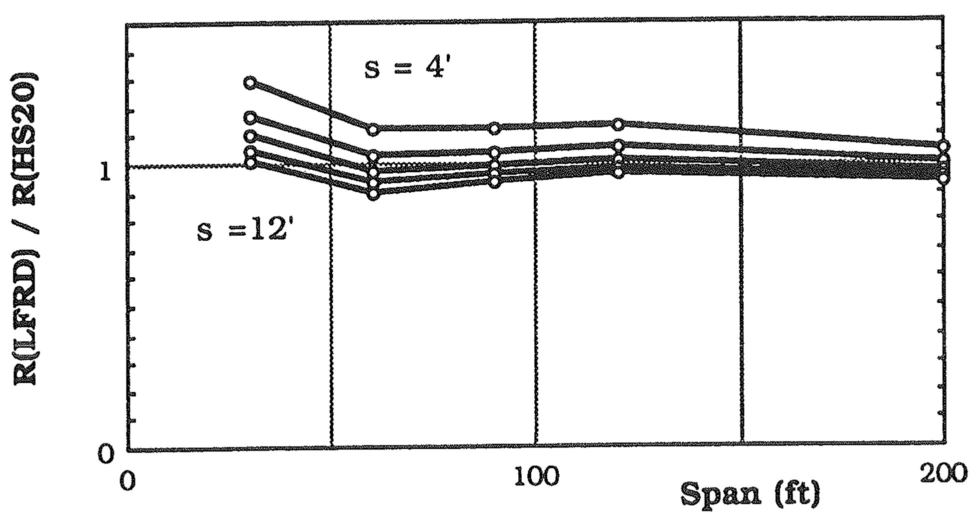

Fig. 16. Resistance Ratios; Simple Span Moment in Composite Steel Girders.

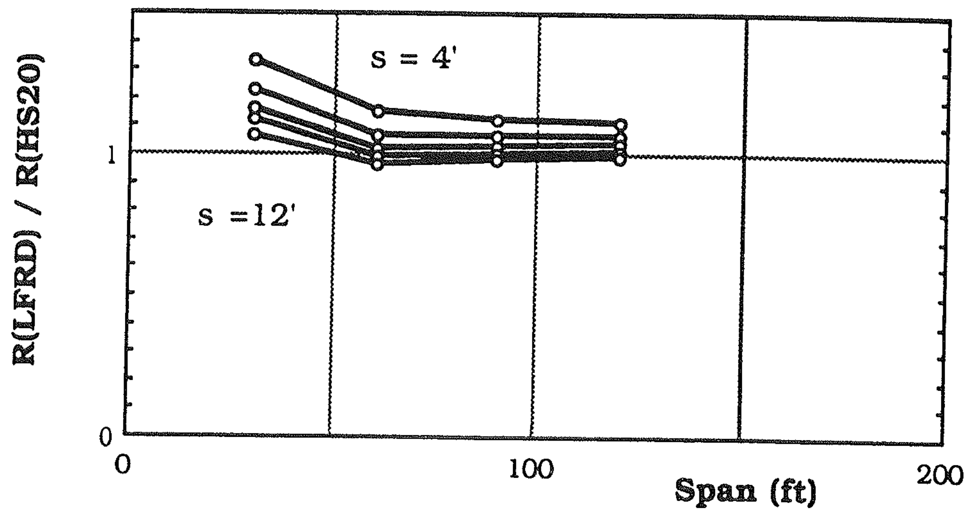

Fig. 17. Resistance Ratios; Simple Span Moment in Reinforced Concrete T-Beams.

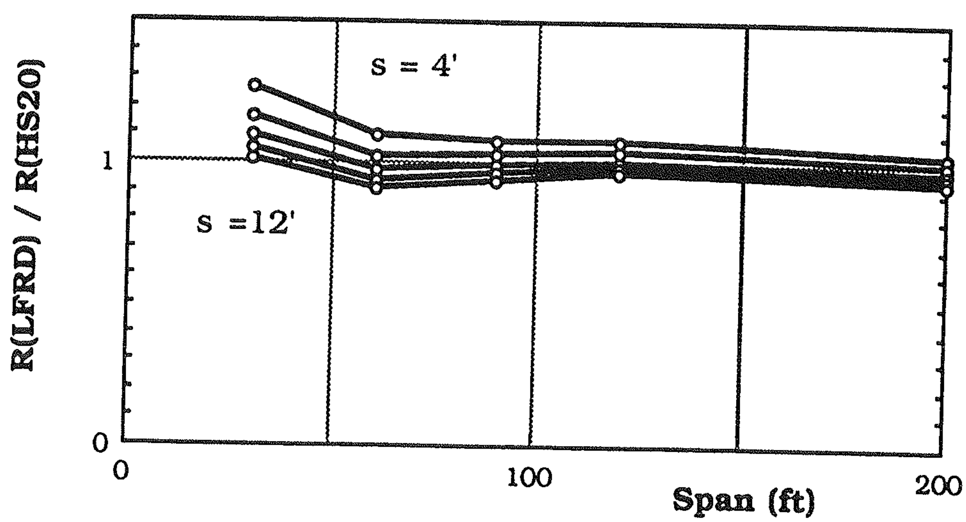

Fig. 18. Resistance Ratios; Simple Span Moment in Prestressed Concrete Girders.

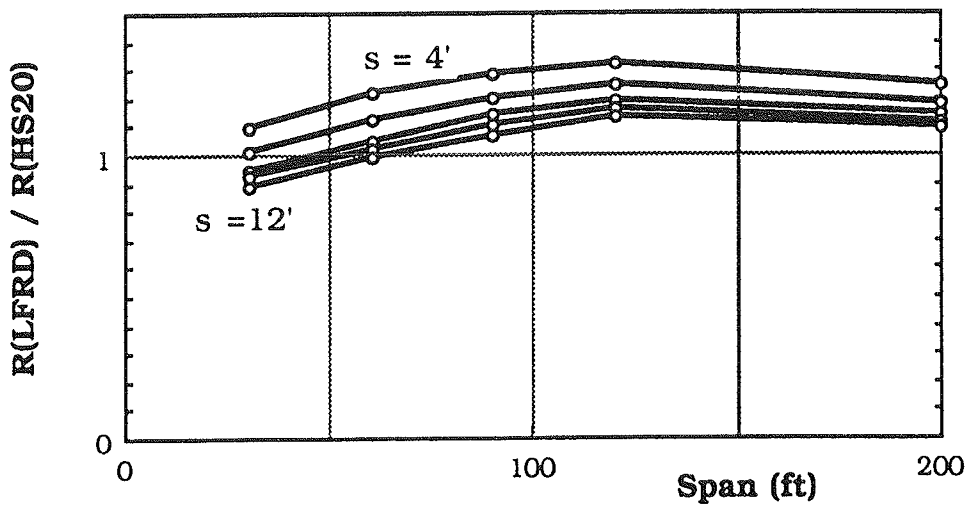

Fig. 19. Resistance Ratios; Shear in Steel Girders.

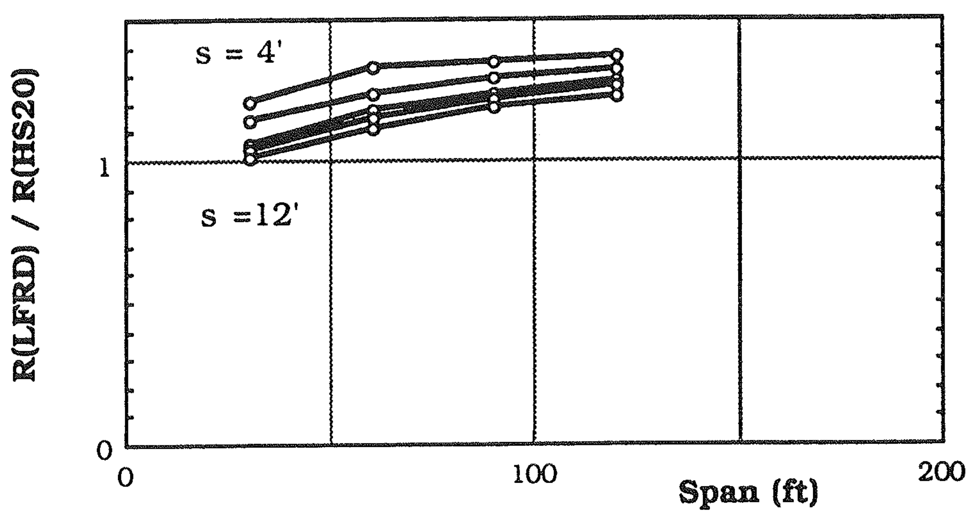

Fig. 20. Resistance Ratios; Shear in Reinforced Concrete T-Beams.

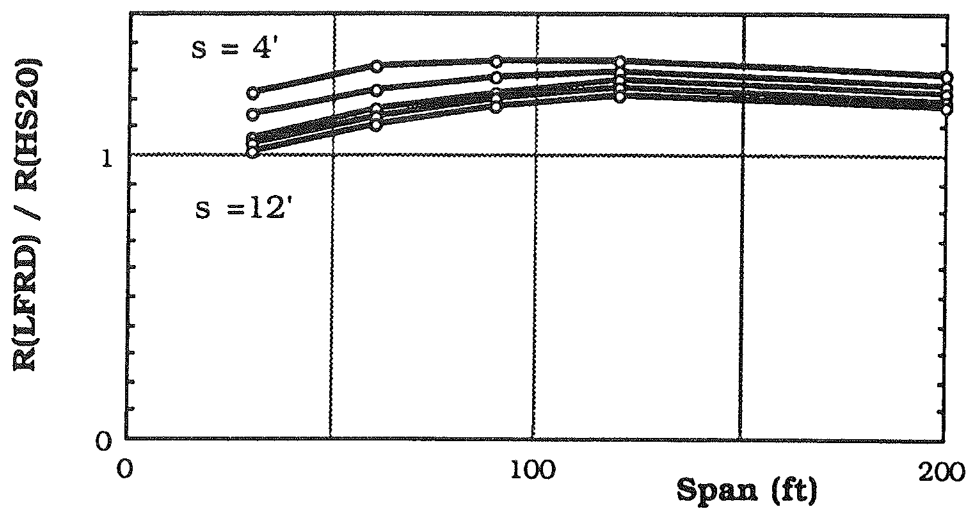

Fig. 21. Resistance Ratios; Shear in Prestressed Concrete Girders.

CHAPTER FOUR

CONCLUSIONS AND SUGGESTED RESEARCH

CONCLUSIONS

The calculated load and resistance factors provide a rational basis for the design of bridges. They also provide a basis for comparison of different materials and structural types.

Bridge components designed using the proposed LRFD Code have reliability index larger than 3.5.

SUGGESTED RESEARCH

The study revealed a need for further research in various related areas as follows.

1. Bridge live load; there is a need for a large and reliable data base, more weigh-in-motion (WIM) measurements; site-specific live load models; component-specific live load models; verification of the multiple presence model.

2. Bridge dynamic load; a data base is needed for verification of the analytical model; dynamic load for multiple presence; dynamic load at the ultimate limit state (should dynamic load be included in the design?); what is the effect of a load of a very-short duration on the ultimate capacity?

3. Serviceability limit states (cracking, vibration, deflection); what are acceptability criteria?; what is the optimum reliability level(s).

4. Wood structures; perform calibration for wood bridges.

5. Resistance models; there is a need for more test data for components; shear in concrete; steel connections.

6. Other load models; verify the statistical data for wind, earthquake, temperature, other loads; load combinations.

7. Deterioration; how to handle deterioration of bridge components in the code.

8. Substructure; verify the statistical data; perform calibration.

REFERENCES

1. AASHTO, Standard Specifications for Highway Bridges, American Association of State Highway and Transportation Officials, Washington, D.C. (1989).

2. Nowak, A. S. and Lind, N. C., "Practical Bridge Code Calibration," ASCE Journal of the Structural Division, Vol. 105, No. 12, (1979) pp. 2497-2510.

3. Nowak, A. S., Czernecki, J., Zhou, J. and Kayser, R., "Design Loads for Future Bridges," Report UMCE 87-1, University of Michigan, Ann Arbor, MI (1987).

4. Rackwitz, R. and Fiessler, B., 1978, "Structural Reliability under Combined Random Load Sequences", Computer and Structures, 9, (1978) pp. 489-494.

5. Nowak, A.S. and Hong, Y-K., "Bridge Live Load Models", ASCE Journal of Structural Engineering, Vol. 117, No. 9, (1991) pp. 2757-2767.

6. Zokaie, T., Osterkamp, T.A. and Imbsen, R.A., "Distribution of Wheel Loads on Highway Bridges", NCHRP 12-26/1, (1992).

7. Hwang, E.S., "Dynamic Loads for Girder Bridges", PhD Thesis, Department of Civil Engineering, University of Michigan, Ann Arbor, MI (1990).

8. Hwang, E-S. and Nowak, A.S., "Simulation of Dynamic Load for Bridges", ASCE Journal of Structural Engineering, Vol. 117, No. 5, (1991) pp. 1413-1434.

9. Ellingwood, B. Galambos, T.V., MacGregor, J.G. and Cornell C.A., "Development of a Probability Based Load Criterion for American National Standard A58", National Bureau of Standards, NBS Special Publication 577, Washington, D.C. (1980).

10. Thoft-Christensen, P. and Baker, M.J., Structural Reliability Theory and Its Applications, Springer-Verlag, (1982) p. 267.

11. Tabsh, S.W. and Nowak, A.S., "Reliability of Highway Girder Bridges," ASCE Journal of Structural Engineering, Vol. 117, No. 8, (1991), pp. 2373-2388.

APPENDIX A Presentation of Statistical Parameters

In the code calibration, load and resistance are treated as random variables. The statistical models are derived using the available data base on load components, materials, dimensions and other parameters. The basic formulas and definitions are presented in numerous textbooks on the theory of probability and statistics (for example A-1). The most important ones used in this report are summarized below.

A random variable, X, is described by the cumulative distribution function (CDF), denoted by $F_X(x)$. The first derivative of $F_X(x)$ is called the probability density function, PDF, and it is denoted by $f_X(x)$. The most important parameters which describe a random variable are the mean, m_X, and standard deviation, σ_X. The coefficient of variation of a random variable X, V_X, is defined as,

$$V_X = \frac{\sigma_X}{m_X} \tag{A-1}$$

The most important random variables used in this report are normal and lognormal. PDF of a normal random variable is given as follows,

$$f_X(x) = \frac{1}{\sigma_X \sqrt{2\pi}} e^{-\frac{(x - m_X)^2}{2\sigma_X^2}} \tag{A-2}$$

PDF of a normal random variable is symmetrical about the mean. Random variable, Y, is lognormal, if lnY is normal. Therefore, a lognormal variable is defined for positive values only.

Standard normal random variable, Z, is a normal random variable with the mean, $m_Z = 0$, and standard deviation, $\sigma_Z = 1$. The CDF of a standard normal random variable is denoted by $\Phi(z)$ and PDF is denoted by $\phi(z)$, and they are widely available in tables and computers (PC's and mainframe systems).

For any normal random variable, X, CDF can be calculated using Φ as follows,

$$F_X(x) = \Phi\left(\frac{x - m_X}{\sigma_X}\right) \tag{A-3}$$

Similarly, for any lognormal random variable, X, CDF can be calculated using Φ as follows,

$$F_X(x) = \Phi\left(\frac{\ln x - m_{\ln X}}{\sigma_{\ln X}}\right) \tag{A-4}$$

where

$$\sigma^2_{\ln X} = \ln(V_X^2 + 1) \tag{A-5}$$

$$m_{\ln X} = \ln m_X - \frac{1}{2}\sigma^2_{\ln X} \tag{A-6}$$

If V_X is not very large (< 0.20), then Eq. 1-5 and 1-6 can be simplified as follows,

$$\sigma^2_{\ln X} = V^2_X \tag{A-7}$$

$$m_{\ln X} = \ln(m_X) \tag{A-8}$$

Consider a simple example with a random variable, X, representing test results. Let the test data (readings) consist of nine readings: 4.6, 4.9, 5.0, 5.1, 5.1, 5.2, 5.2, 5.3, 5.5, arranged in an increasing order. This data can be used to plot a PDF and CDF for X, as shown in Fig. A-1 and A-2, respectively. However, the most important parts of the curves are either lower or upper tails of the distribution. Yet, they are difficult to see on a regular scale. Therefore, in this report a normal probability paper is used. Normal probability paper is a special scale which replaces the vertical scale in Fig. A-2. The basic property of the normal probability paper is that any normal CDF is represented by a straight line, and any straight line represents a normal random variable. The construction of the normal probability paper is described by Benjamin and Cornell (A-1).

Normal probability paper is commercially available. Let the data base to be plotted include n test results (readings): $x_1, \ldots, x_n$. It is assumed that the readings (values of $x_1, \ldots, x_n$) are arranged in an increasing order (x_1 is the smallest and x_n is the largest value). Then, the first test result is plotted at the intersection of x_1 on the horizontal scale and the probability $p_1 = 1/(n+1)$ on the vertical scale. The i-th test result is plotted at the intersection of x_i and the probability $p_i = i/(n+1)$.

It is convenient to replace the irregular vertical scale (probability, p) with the inverse standard normal distribution scale, z, using the following transformation,

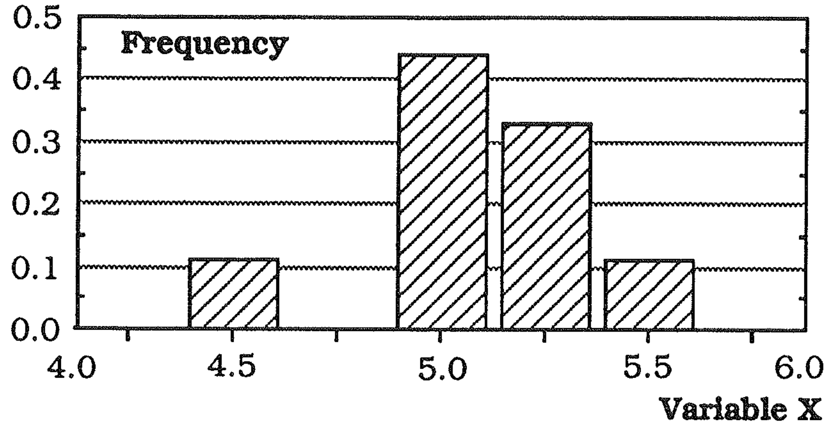

Fig. A-1. Frequency Histogram for Test Data (PDF)

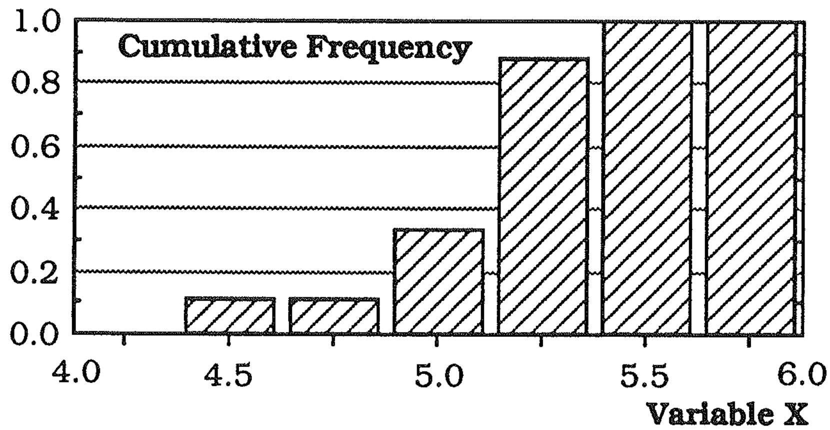

Fig. A-2. Cumulative Frequency Histogram for Test Data (CDF).

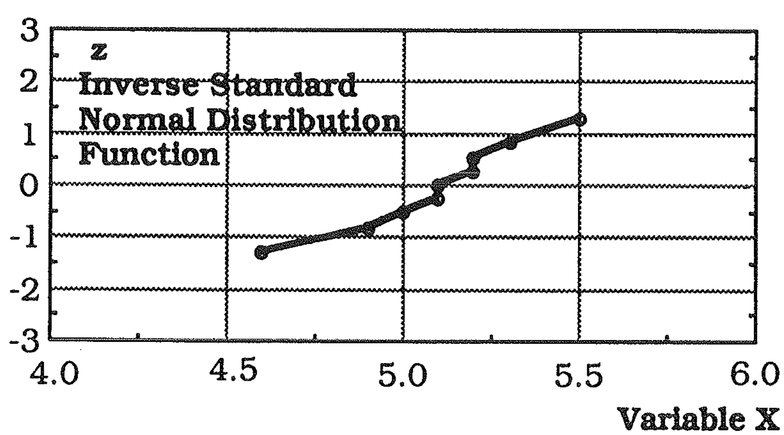

Fig. A-3. Test Data on Normal Probability Paper.

$$z = \Phi^{-1}(p) \tag{A-9}$$

where Φ^{-1} is the inverse standard normal distribution function. In this report, the CDF's of load and resistance parameters are plotted on the normal probability paper using z, as defined by Eq. A-9, on the vertical scale. An example is shown in Fig. A-3. The data includes the same readings as plotted in Fig. A-2. The lowest reading, 4.6, corresponds to the probability, $p_1 = 1/(9+1) = 0.1$. Value of the inverse standard normal distribution corresponding to $p_1 = 0.1$ is $z_1 = \Phi^{-1}(0.1) = -1.28$. The second lowest reading, 4.9, corresponds to $p_2 = 2/(9+1) = 0.2$, and $z_2 = \Phi^{-1}(0.2) = -0.84$.

The degree of correlation between random variables X and Y is expressed in terms of the coefficient of correlation, ρ_{XY}. Values of ρ_{XY} are between -1 and 1. Perfect correlation between X and Y means that Y is a linear function of X, and this corresponds to $\rho_{XY} = 1$ (positive correlation) or $\rho_{XY} = -1$ (negative correlation). Random variables X and Y are linearly uncorrelated if $\rho_{XY} = 0$. Uncorrelated random variables are not necessarily independent.

References to Appendix A

A-1. Benjamin, J.R. and Cornell, C.A., Probability, Statistics and Decision for Civil Engineers. McGraw-Hill, New York (1970).

APPENDIX B Load Models

The major load components of highway bridges are dead load, live load (static and dynamic), environmental loads (temperature, wind, earthquake) and other loads (collision, emergency braking). Each load group includes several subcomponents. The load models are developed using the available statistical data, surveys and other observations. Load components are treated as random variables. Their variation id described by the cumulative distribution function (CDF), mean value and coefficient of variation. The relationship among various load parameters is described in terms of the coefficients of correlation.

The basic load combination for highway bridges is a simultaneous occurrence of dead load, live load and dynamic load. The combinations involving other load components (wind, earthquake, collision forces) require a special approach.

It is assumed that the economic life time for newly designed bridges is 75 years. Therefore, the extreme values of live load and environmental loads are extrapolated accordingly from the available data base.

Nominal values of load components are calculated according to AASHTO (B-1).

DEAD LOAD

Dead load, D, is the gravity load due to the self weight of the structural and non structural elements permanently connected to the bridge. Because of different degrees of variation, it is convenient to consider the following components of D:

D_1 = weight of factory made elements (steel, precast concrete members),
D_2 = weight of cast-in-place concrete members,
D_3 = weight of the wearing surface (asphalt),
D_4 = miscellaneous weight (e.g. railing, luminaries).

All components of D are treated as normal random variables. The statistical parameters used in the calibration are listed in Table 1. The bias factors (mean-to-nominal ratio), λ, are taken as used in the previous bridge code calibration work (B-2). However, the coefficients of variation are increased to include human error as recommended in (B-3).

The thickness of asphalt was modeled on the basis of the statistical data available from the Ontario Ministry of Transportation (MTO) and reported by Nowak and Zhou (B-4). The distributions of D_3 (thickness of asphalt), for various regions of Ontario, are plotted on the normal probability paper in Fig. B-1. The average thickness of asphalt is 3.5 inch. There is a need to verify this value for the United States. The coefficient of variation, calculated from the slope of the distributions in Fig. B-1, is 0.25.

For miscellaneous items (weight or railings, curbs, luminaries, signs, conduits, pipes, cables, etc.), the statistical parameters (means and coefficients of variation) are similar to those of D_1, if the considered item is factory-made with the high quality control measures, and D_2, if the item is cast-in-place, with less strict quality control.

LIVE LOAD

Live load, L, covers a range of forces produced by vehicles moving on the bridge. Traditionally, the static and dynamic effects are considered separately. Therefore, in this study, L covers only the static component. The dynamic component is denoted by I.

The effect of live load depends on many parameters including the span length, truck weight, axle loads, axle configuration, position of the vehicle on the bridge (transverse and longitudinal), number of vehicles on the bridge (multiple presence), girder spacing, and stiffness of structural members (slab and girders). Because of the complexity of the model, the variation in load and load distribution properties are considered separately.

The live load model is based on the available truck survey data. The considered data include weigh-in-motion (WIM) measurements performed as part of the FHWA project (B-5), weigh-in-motion measurements carried out as a part of Michigan DOT project (B-6) and truck measurements performed by the Ontario Ministry of Transportation (B-7). Other available WIM data was analyzed as part of NCHRP Project 12- 28(11) Development of Site-Specific Load Models for Bridge Rating. However, it was found that the data collected in mid 1980's by various states (including Wisconsin and Florida) was not reliable, with errors estimated at 30-40%. Therefore, in this calibration, the data base consists of the results of truck survey performed in 1975 by the Ontario Ministry of Transportation. The study covered about 10,000 selected trucks (only trucks which appeared to be heavily loaded were measured and included in the data base). At the time of the survey, in 1975, the truck population in Ontario was representative of the U.S. trucks.

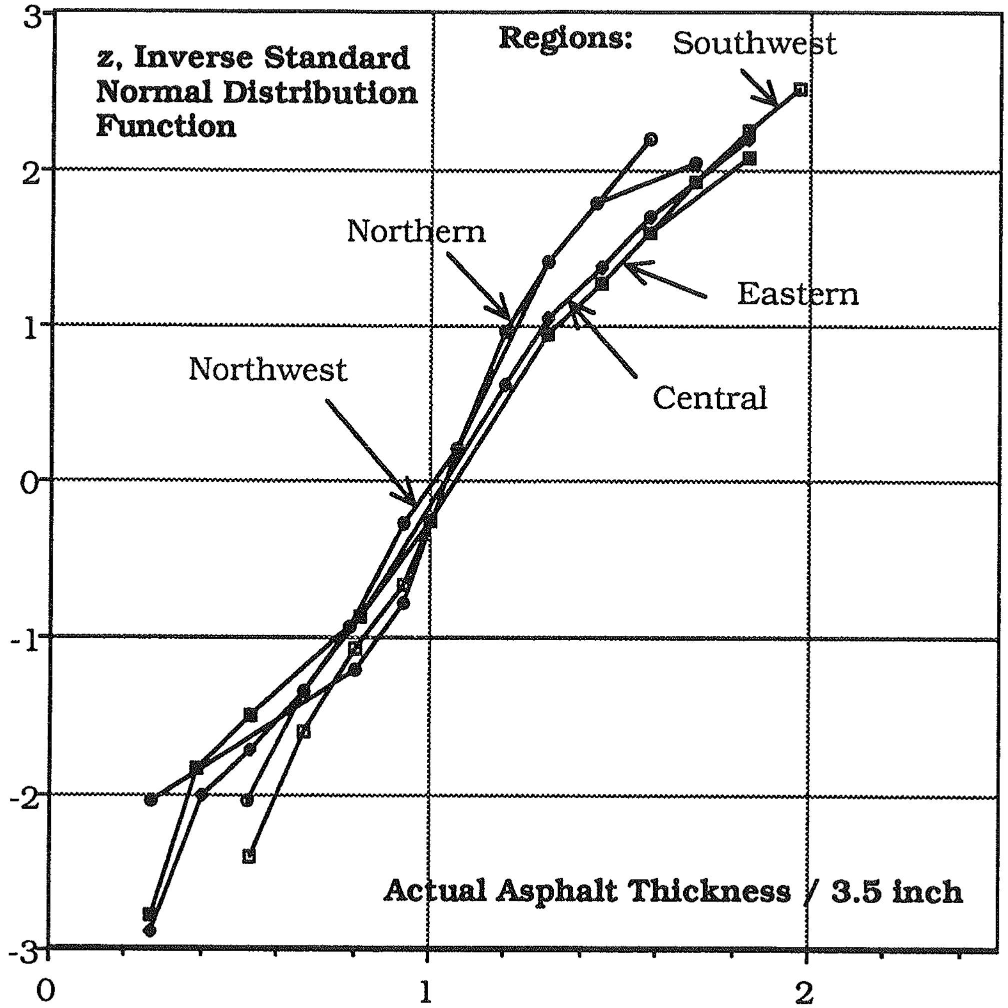

Fig. B-1 Cumulative Distribution Functions of Asphalt Thickness.

The uncertainties involved in the analysis are due to limitations and biases in the survey data. Even though 10,000 trucks is a large number, it is very small compared to the actual number of heavy vehicles in a 75 year life time. It is also reasonable to expect that some extremely heavy trucks purposefully avoided the weighing stations. A considerable degree of uncertainty is caused by unpredictability of the future trends with regard to configuration of axles and weights.

The maximum load effects corresponding to longer periods of time are calculated by extrapolation of the available truck survey data. Furthermore, it is assumed that the legal load limits will not be changed in the future and the truck population will remain as it is now. A similar assumption was made in the development of the Ontario Highway Bridge Design Code (B-8).

Truck Survey Data

The study is based on the truck survey including 9,250 heavy vehicles (B-7). The data includes truck configuration (number of axles and axle spacing) and weights (axle loads and gross vehicle weight). For each truck in the survey, bending moments, M, and shear forces, V, are calculated for a wide range of spans. Simple spans and continuous two equal spans are considered. The moments and shears are calculated in terms of the standard HS20 truck or lane loading, whichever governs (B-1), as shown in Fig. 1. The cumulative distribution functions (CDF) are plotted on normal probability paper in Fig. B-2 for simple span moments, Fig. B-3 for shears, and Fig. B-4 for negative moments (continuous spans), for spans from 30 to 200 ft. The vertical scale, z, is,

$$z = \Phi^{-1} [F(x)] \qquad \text{(B-1)}$$

where F(x) = cumulative distribution function of X, where X is the moment M or shear V; Φ^{-1} = inverse of the standard normal distribution function, as defined in Appendix A of this report.

Maximum Truck Moments and Shears

The maximum moments and shears for various time periods are determined by extrapolation of the distributions shown in Fig. B-2, B-3 and Fig. B-4. The extrapolated distributions are shown in Fig. B-5, B-6 and B-7. Let N be the total number of trucks in time period of T. It is assumed that the surveyed trucks represent about two week traffic. Therefore, in T = 75 years, the number of trucks, N, will be about 2,000 times larger than in the survey. This will result in N = 20

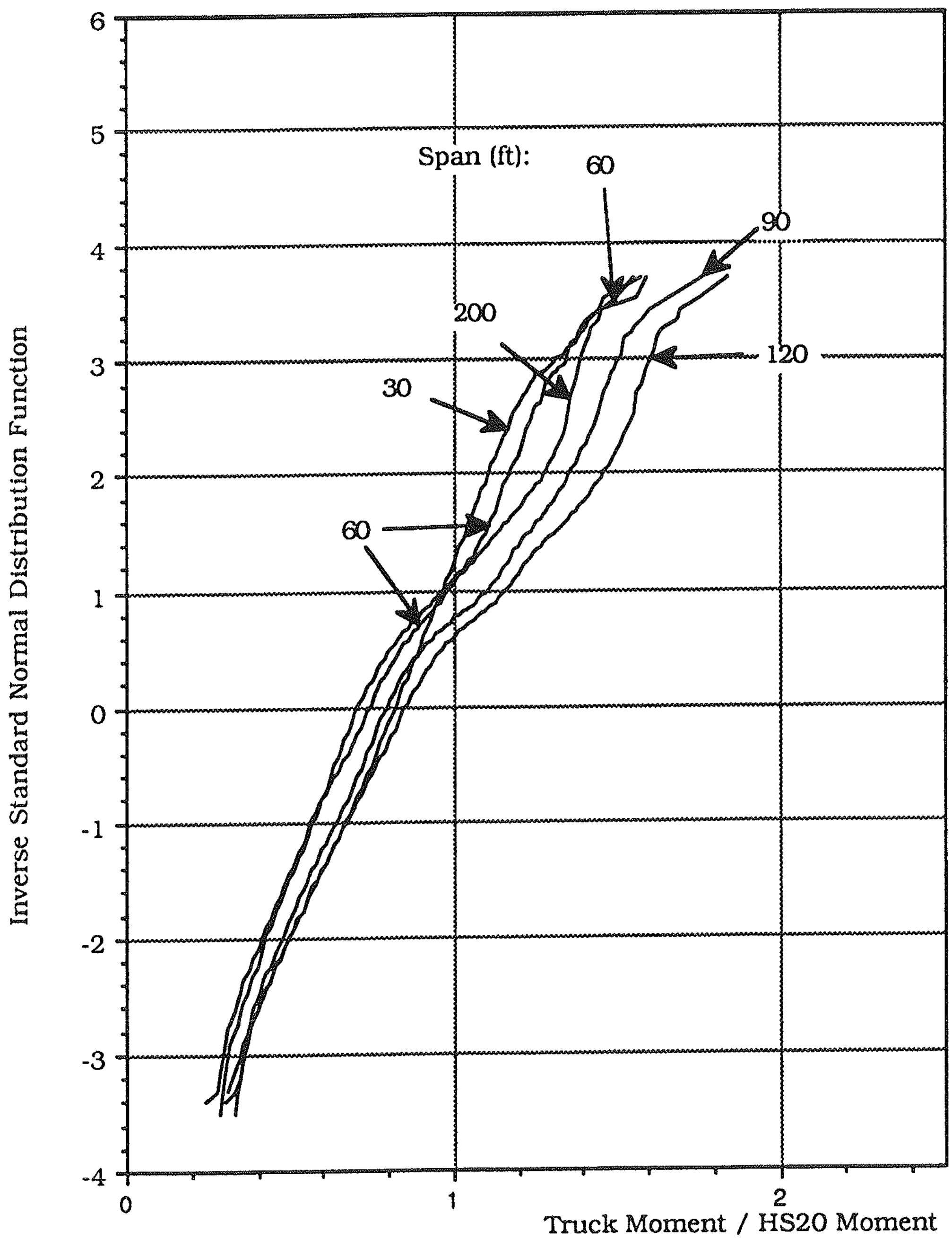

Fig. B-2. Moments from Truck Survey for Simple Spans.

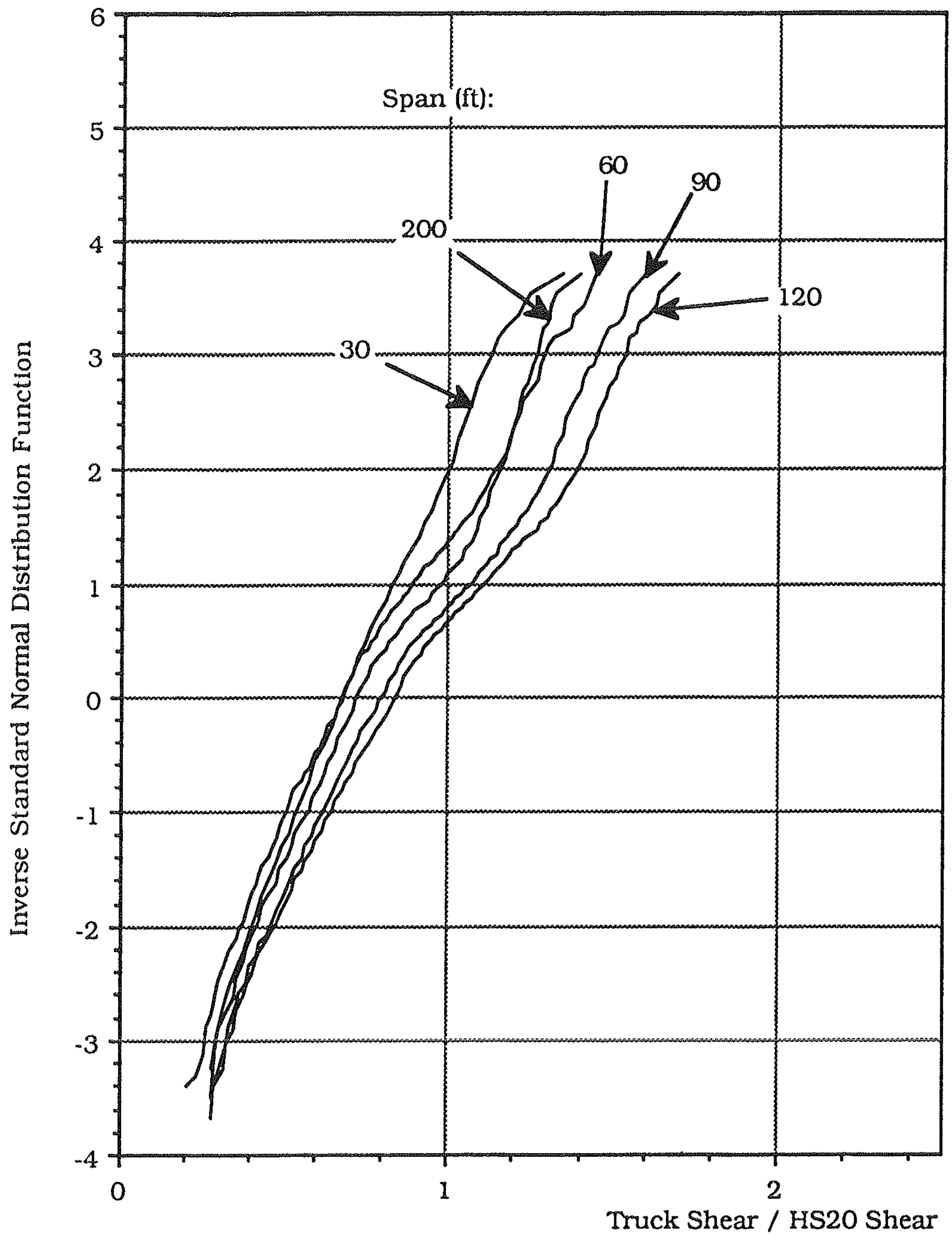

Fig. B-3. Shears from Truck Survey for Simple Spans.

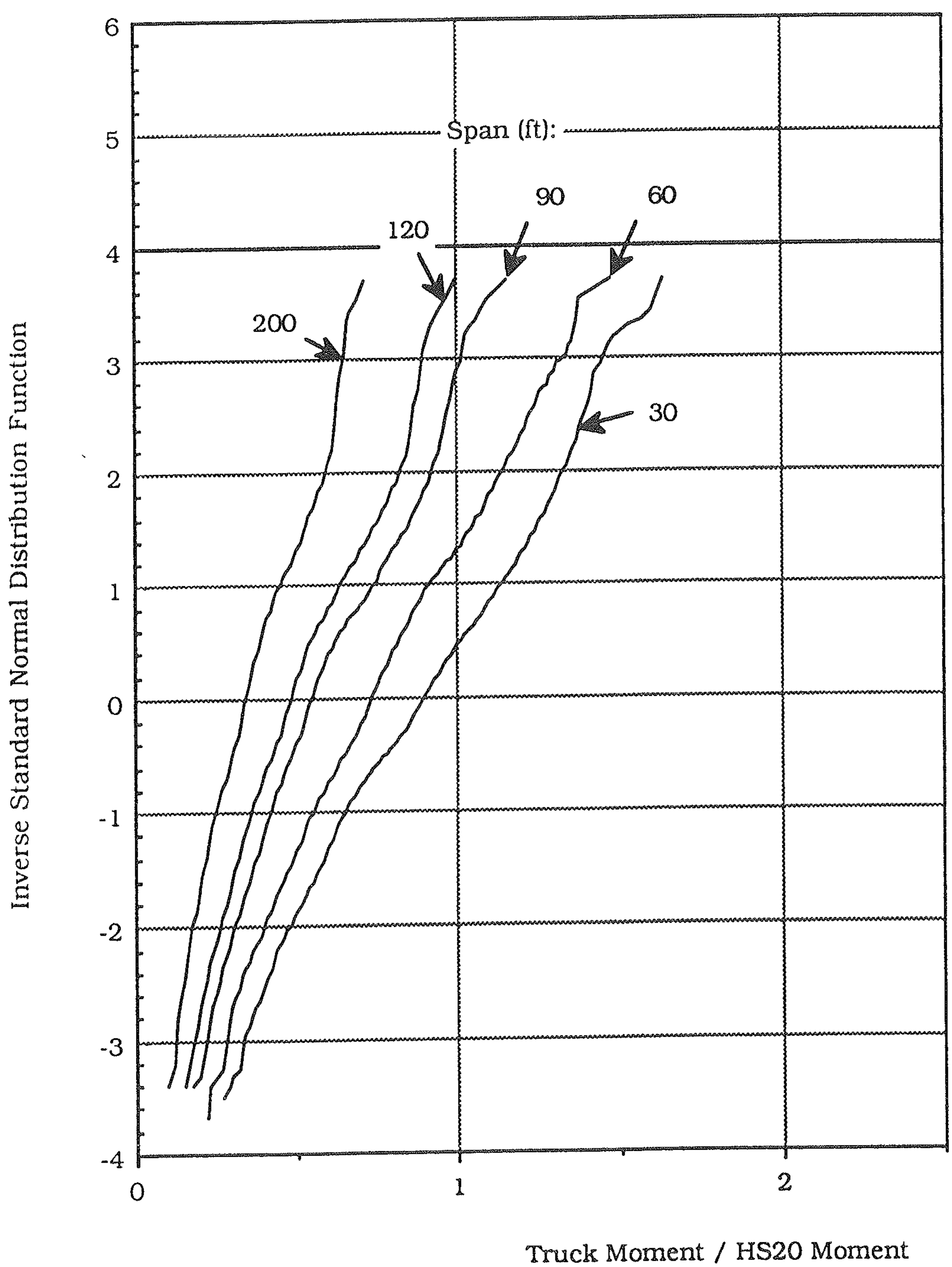

Fig. B-4. Negative Moments from Truck Survey for Two Equal Continuous Spans.

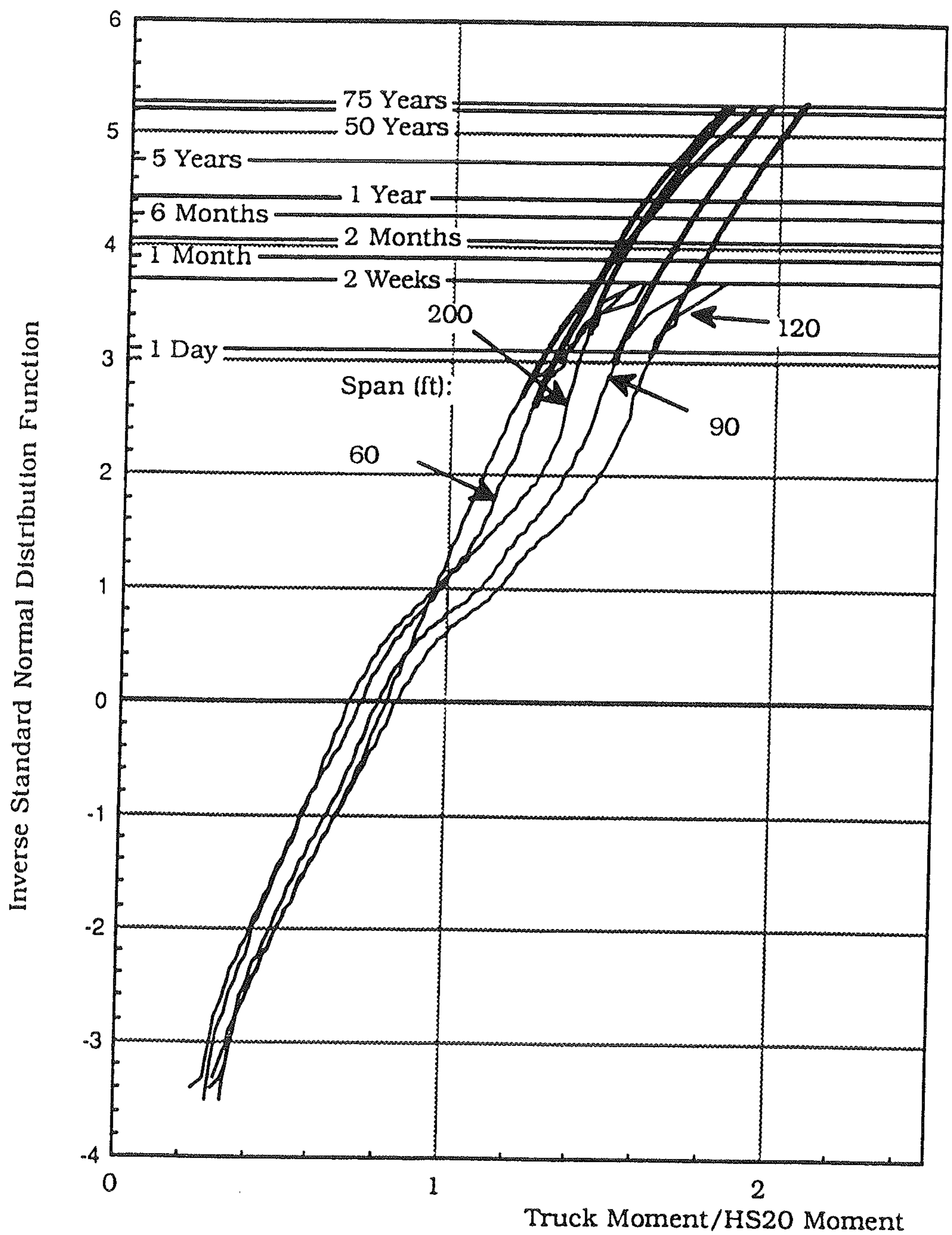

Fig. B-5. Extrapolated Moments for Simple Spans.

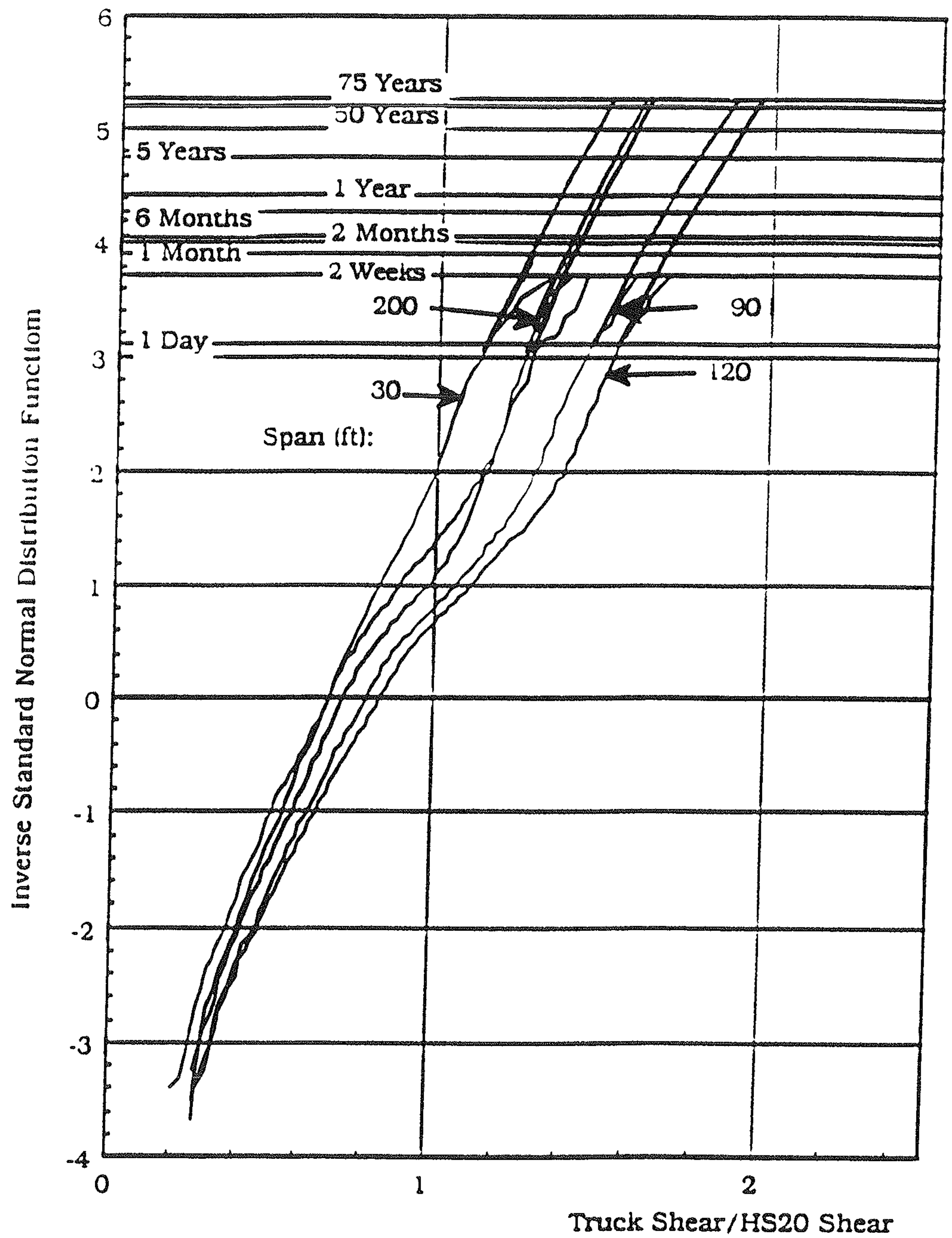

Fig. B-6. Extrapolated Shears for Simple Spans.

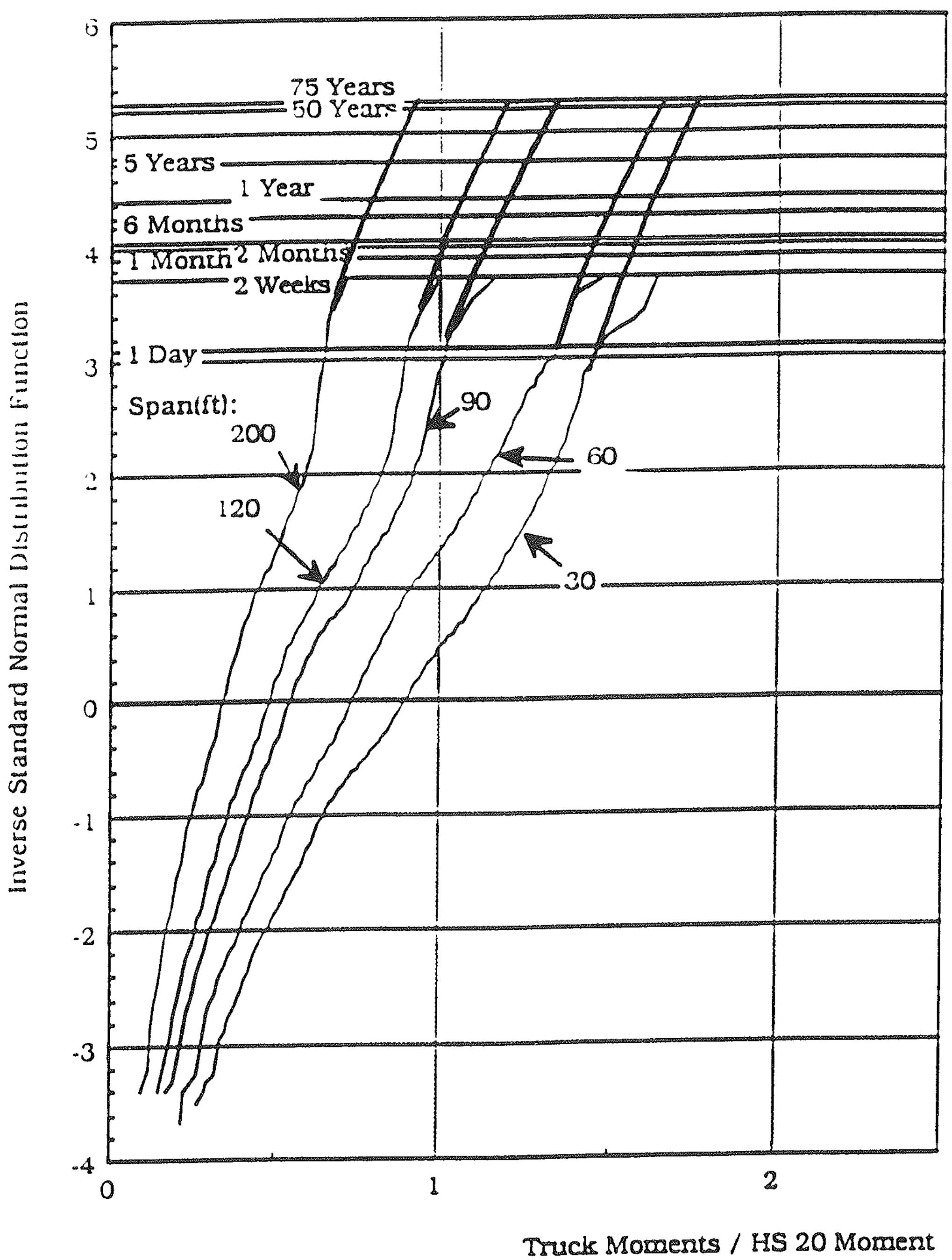

Fig. B-7. Extrapolated Negative Moments for Two Equal Continuous Spans.

million trucks. The probability level corresponding to N is 1/N, and for N = 20 million, it is 1/20,000,000 = 5_{10}-8, which corresponds to z = 5.33 on the vertical scale, as shown in Fig. B-5, B-6 and B-7.

The number of trucks, N, probabilities, 1/N, and inverse normal distribution values, z, corresponding to various time periods T from 1 day to 75 years, are shown in Table B-1. The lines corresponding to some of these probability levels are also shown in Fig. B-5, B-6 and B-7.

The mean maximum moments and shears corresponding to various periods of time can be read from the graph. For example, for 120 span and T = 75 years, the mean maximum moment = 2.08 (HS20 moment) (horizontal coordinate of intersection of the extrapolated distribution and z = 5.33 on the vertical scale). For comparison, the number of heavy trucks passing through the bridge in 5 years is about 1,500,000. This corresponds to z = 4.83 on the vertical scale (Fig. B-5, B-6 and B-7), and the resulting moment is 1.94 (HS20 moment). Similar calculations can be performed for other periods of time. The difference between the mean maximum 50 year moment and the mean maximum 75 year moment is about 1%.

The mean moments and shears calculated for various time periods from 1 day to 75 years are presented in Tables B-2, B-3 and B-4, for simple span moments, shears and negative moments, respectively. For comparison, the means are also given for an average truck. All the moments and shears are divided by the corresponding HS20 moments and shears. The results are also plotted in Fig. B-8, B-9 and B-10.

The coefficients of variation for the maximum truck moments and shears can be calculated by transformation of the cumulative distribution functions (CDF) in Fig. B-5, B-6 and B-7. Each function can be raised to a certain power, so that the calculated earlier mean maximum moment (or shear) becomes the mean value after the transformation. The slope of the transformed CDF determines the coefficient of variation. The results are plotted in Fig. B-11 and Fig. B-12 for moments and shears, respectively.

One Lane Moments and Shears

The maximum one lane moment or shear is caused either by a single truck or two (or more) trucks following behind each other, as shown in Fig. B-13. For a multiple truck occurrence, the important parameters are the headway distance and degree of correlation between truck weights. The maximum one lane effect (moment or shear) is derived as the largest of the following two cases:

Table B-1. Number of Trucks vs. Time Period and Probability

Time period T	Number of Trucks N	Probability 1/N	Inverse Normal z
75 years	20,000,000	$5\,10^{-8}$	5.33
50 years	15,000,000	$7\,10^{-8}$	5.27
5 years	1,500,000	$7\,10^{-7}$	4.83
1 year	300,000	$3\,10^{-6}$	4.50
6 months	150,000	$7\,10^{-6}$	4.36
2 months	50,000	$2\,10^{-5}$	4.11
1 month	30,000	$3\,10^{-5}$	3.99
2 weeks	10,000	$1\,10^{-4}$	3.71
1 day	1,000	$1\,10^{-3}$	3.09

Table B-2. Mean Maximum Moments for Simple Spans Due to a Single Truck (Divided by Corresponding HS20 Moment).

Span (ft)	average	1 day	2 weeks	1 month	2 months	6 months	1 year	5 years	50 years	75 years
10	0.62	0.97	1.12	1.18	1.23	1.30	1.37	1.46	1.63	1.65
20	0.71	1.15	1.25	1.31	1.36	1.41	1.47	1.56	1.66	1.68
30	0.74	1.20	1.32	1.37	1.42	1.47	1.52	1.61	1.70	1.72
40	0.75	1.31	1.42	1.46	1.50	1.55	1.58	1.64	1.72	1.74
50	0.72	1.32	1.43	1.47	1.52	1.56	1.60	1.65	1.73	1.75
60	0.72	1.37	1.47	1.52	1.56	1.60	1.64	1.69	1.77	1.79
70	0.74	1.42	1.51	1.56	1.60	1.64	1.68	1.74	1.81	1.83
80	0.77	1.47	1.55	1.60	1.64	1.68	1.73	1.79	1.86	1.89
90	0.79	1.51	1.60	1.64	1.68	1.72	1.78	1.84	1.92	1.94
100	0.82	1.55	1.64	1.68	1.72	1.76	1.82	1.89	1.98	2.00
110	0.84	1.60	1.68	1.72	1.76	1.81	1.86	1.94	2.03	2.05
120	0.85	1.63	1.72	1.76	1.80	1.85	1.90	1.97	2.06	2.08
130	0.86	1.66	1.75	1.80	1.83	1.87	1.92	1.99	2.08	2.10
140	0.86	1.67	1.76	1.80	1.83	1.87	1.92	1.99	2.08	2.10
150	0.85	1.64	1.73	1.78	1.81	1.84	1.88	1.96	2.05	2.07
160	0.84	1.60	1.68	1.73	1.76	1.80	1.84	1.91	2.01	2.03
170	0.81	1.56	1.63	1.69	1.72	1.76	1.80	1.87	1.96	1.98
180	0.78	1.50	1.58	1.64	1.67	1.71	1.75	1.82	1.91	1.94
190	0.75	1.45	1.53	1.58	1.62	1.66	1.70	1.77	1.86	1.88
200	0.70	1.38	1.48	1.54	1.57	1.60	1.64	1.71	1.80	1.82

Table B-3. Mean Maximum Shears for Simple Spans Due to a Single Truck (Divided by Corresponding HS20 Shear).

Span (ft)	average	1 day	2 weeks	1 month	2 months	6 months	1 year	5 years	50 years	75 years
10	0.78	1.20	1.31	1.38	1.40	1.44	1.48	1.52	1.61	1.62
20	0.72	1.14	1.25	1.30	1.31	1.36	1.38	1.43	1.51	1.52
30	0.68	1.14	1.24	1.29	1.31	1.35	1.38	1.42	1.48	1.49
40	0.66	1.18	1.28	1.32	1.34	1.37	1.40	1.43	1.50	1.51
50	0.69	1.24	1.33	1.37	1.39	1.43	1.45	1.48	1.55	1.56
60	0.73	1.30	1.40	1.44	1.46	1.49	1.52	1.56	1.61	1.62
70	0.74	1.37	1.47	1.50	1.52	1.55	1.58	1.62	1.69	1.70
80	0.77	1.43	1.53	1.57	1.59	1.63	1.66	1.70	1.77	1.78
90	0.80	1.48	1.58	1.62	1.64	1.69	1.72	1.76	1.84	1.85
100	0.81	1.53	1.63	1.67	1.70	1.73	1.77	1.82	1.89	1.90
110	0.82	1.58	1.67	1.70	1.72	1.76	1.80	1.85	1.92	1.93
120	0.83	1.58	1.67	1.71	1.73	1.77	1.80	1.86	1.92	1.93
130	0.83	1.57	1.66	1.70	1.72	1.75	1.78	1.83	1.90	1.91
140	0.82	1.53	1.63	1.66	1.68	1.72	1.74	1.79	1.86	1.87
150	0.79	1.48	1.58	1.62	1.64	1.67	1.70	1.74	1.82	1.83
160	0.76	1.44	1.53	1.57	1.59	1.62	1.65	1.70	1.79	1.80
170	0.74	1.40	1.48	1.52	1.54	1.57	1.60	1.66	1.74	1.75
180	0.72	1.35	1.44	1.47	1.49	1.52	1.56	1.62	1.69	1.70
190	0.70	1.31	1.40	1.43	1.45	1.48	1.51	1.57	1.64	1.65
200	0.68	1.27	1.36	1.39	1.41	1.43	1.47	1.52	1.59	1.60

Table B-4. Mean Max. Negative Moments for Continuous Spans Due to a Single Truck (Divided by Corresponding HS20 Negative Moment).

Span (ft)	average	1 day	2 weeks	1 month	2 months	6 months	1 year	5 years	50 years	75 years
10	0.63	1.12	1.25	1.30	1.33	1.37	1.40	1.46	1.54	1.55
20	0.67	1.30	1.40	1.43	1.44	1.47	1.50	1.54	1.59	1.60
30	0.89	1.50	1.59	1.62	1.64	1.66	1.68	1.72	1.76	1.77
40	0.93	1.63	1.73	1.75	1.77	1.81	1.83	1.86	1.92	1.93
50	0.83	1.51	1.63	1.67	1.68	1.72	1.74	1.78	1.84	1.85
60	0.73	1.34	1.44	1.49	1.51	1.54	1.56	1.61	1.66	1.67
70	0.63	1.24	1.33	1.37	1.39	1.42	1.43	1.47	1.51	1.53
80	0.59	1.16	1.24	1.27	1.29	1.31	1.33	1.35	1.39	1.40
90	0.55	1.11	1.18	1.21	1.22	1.25	1.26	1.29	1.32	1.33
100	0.53	1.07	1.13	1.16	1.17	1.19	1.20	1.22	1.26	1.27
110	0.50	1.03	1.09	1.11	1.12	1.15	1.16	1.18	1.22	1.22
120	0.48	1.00	1.06	1.08	1.09	1.11	1.12	1.15	1.17	1.18
130	0.46	0.97	1.02	1.04	1.05	1.07	1.09	1.10	1.14	1.14
140	0.44	0.94	1.00	1.01	1.02	1.03	1.05	1.07	1.09	1.10
150	0.42	0.90	0.96	0.97	0.99	1.00	1.01	1.03	1.06	1.07
160	0.40	0.86	0.92	0.94	0.95	0.96	0.97	1.00	1.02	1.03
170	0.38	0.84	0.90	0.92	0.93	0.94	0.95	0.97	0.99	1.00
180	0.37	0.82	0.87	0.89	0.90	0.92	0.92	0.94	0.96	0.97
190	0.35	0.80	0.84	0.86	0.87	0.88	0.89	0.91	0.93	0.94
200	0.33	0.78	0.83	0.84	0.85	0.87	0.88	0.89	0.91	0.92

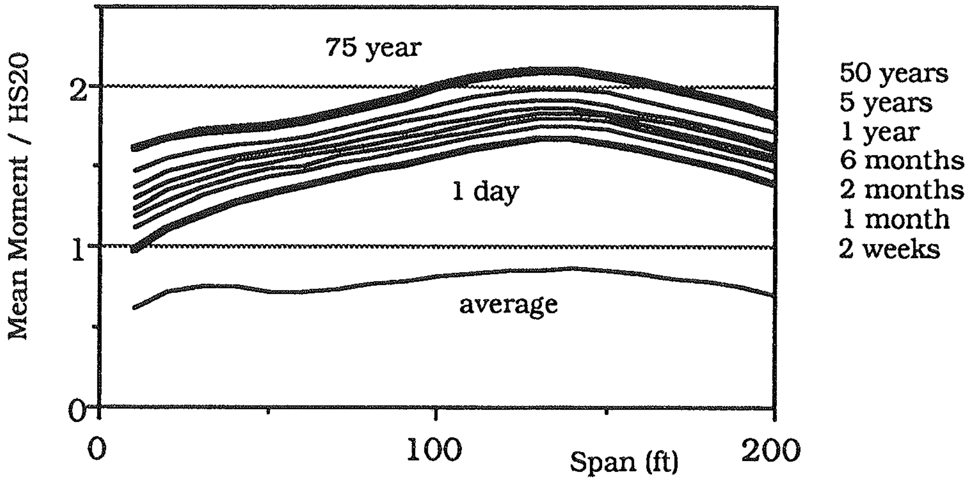

Fig. B-8. Mean Maximum Moments for Simple Spans Due to a Single Truck.

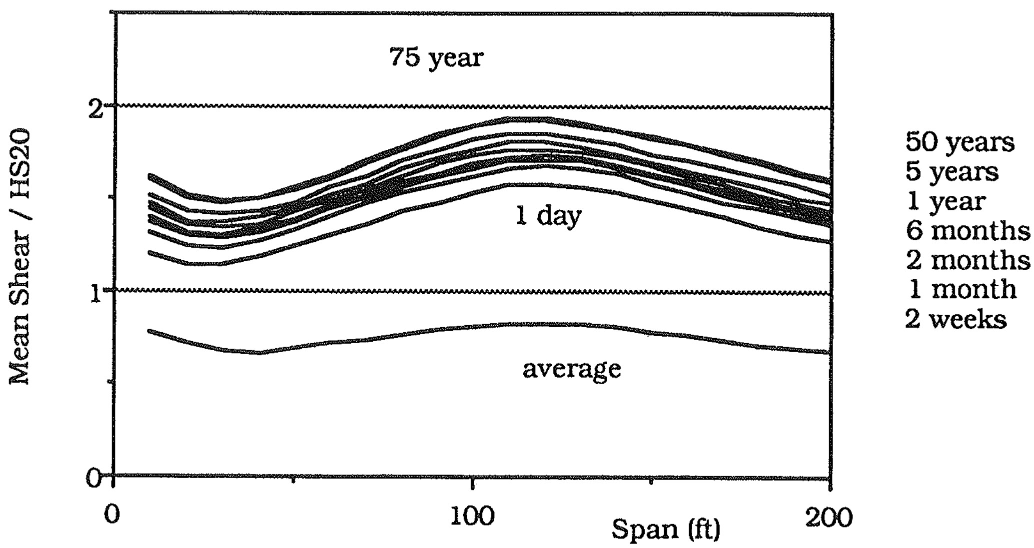

Fig. B-9. Mean Maximum Shears for Simple Spans Due to a Single Truck.

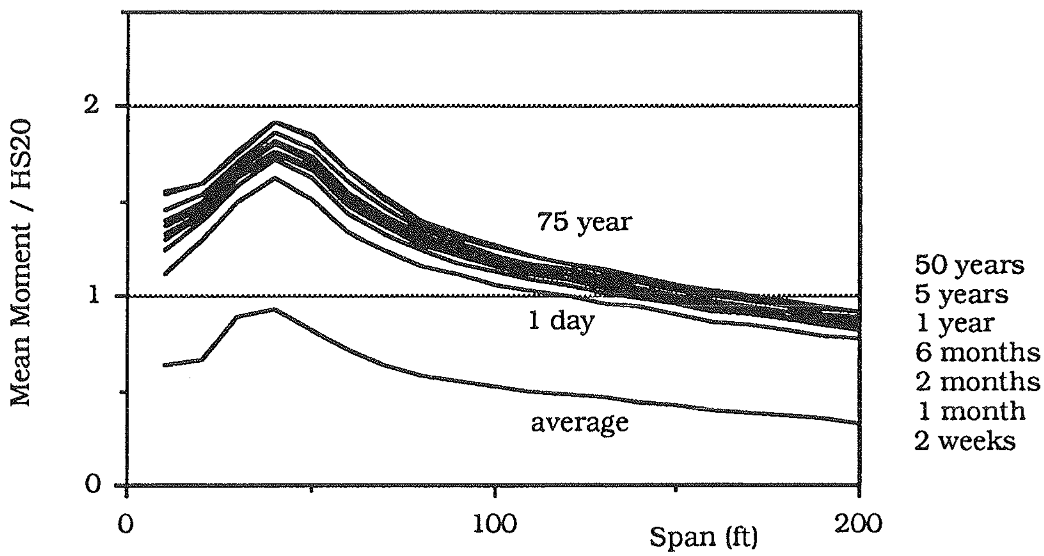

Fig. B-10. Mean Maximum Negative Moments for Two Equal Continuous Spans Due to a Single Truck.

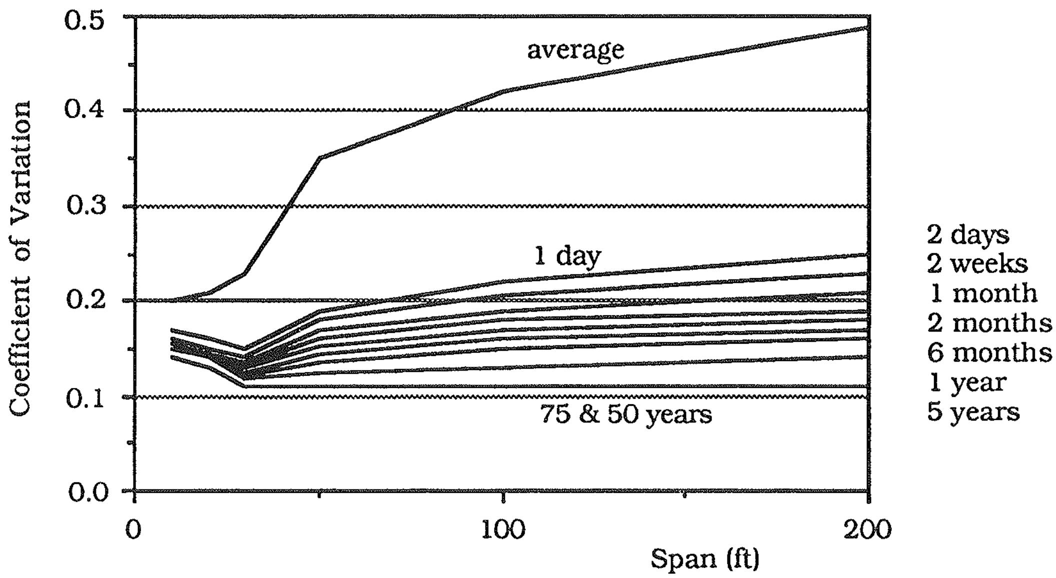

Fig. B-11. Coefficient of Variation of the Maximum Moment Due to a Single Truck.

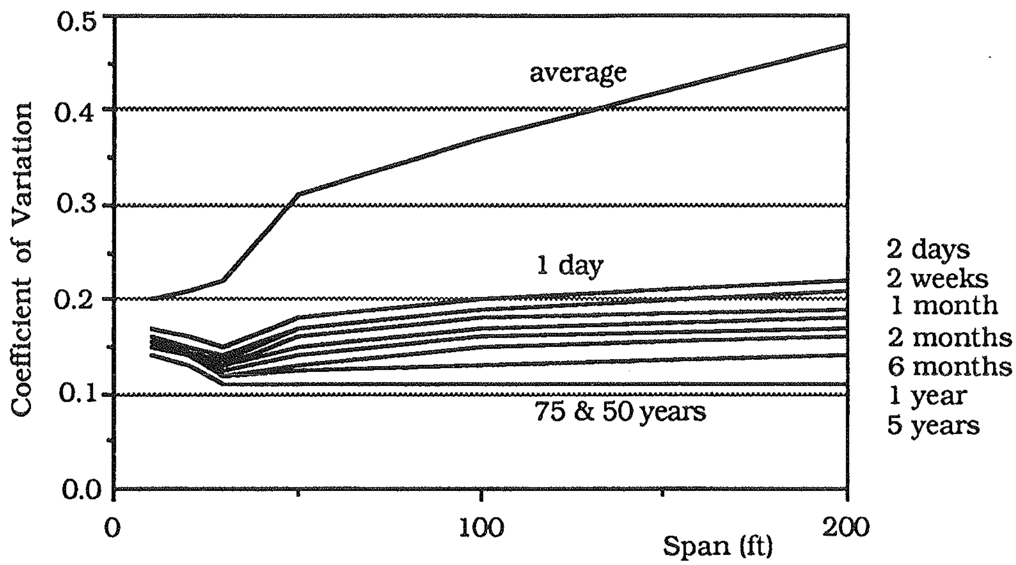

Fig. B-12. Coefficient of Variation of the Maximum Shear Due to a Single Truck.

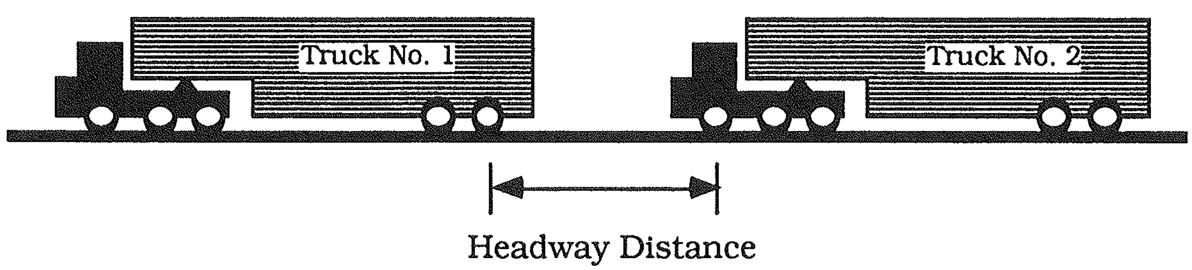

Fig. B-13. Two Truck in One Lane.

a) One truck effect, equal to the maximum 75 year moment (or shear) with the parameters (mean and coefficient of variation) given in Fig. B-7, B-8 and B-10 for the mean and in Fig. B-11 and B-12 for the coefficient of variation;

b) Two trucks, each with the weight smaller than that of a single truck in (a). Various headway distances are considered, from 15 to 100 ft. Headway distance is measured from the rear axle of one vehicle to the front axle of the following vehicle, therefore 15 ft means bumper to bumper traffic. Three degrees of correlation between truck weights are considered: $\rho = 0$ (no correlation), $\rho = 0.5$ (partial) and $\rho = 1$ (full correlation), where ρ is the coefficient of correlation.

There is little data available to verify the statistical parameters for multiple presence. Some measurement results are reported by Nowak, Nassif and DeFrain (B-9). On the basis of this limited data it is assumed that, on average, about every 50th truck is followed by another truck with the headway distance less than 100 ft, about every 150th truck is followed by a partially correlated truck, and about every 500th truck is followed by a fully correlated truck. The two trucks are denoted by T_1 and T_2. The parameters of these two trucks, including N (the considered truck is a maximum of N trucks), corresponding $z = -\Phi^{-1}(1/N)$, and T (the considered truck is the maximum for time period T) are given in Table B-5.

The maximum values of moments and shears are calculated by simulations. The parameters considered include truck configuration, weight, headway distance and frequency of occurrence. For simple spans, the results of calculations are presented in Fig. B-14 for mean maximum 75 year moments and Fig. B-15 for corresponding shears. For the mean maximum 75 year negative moments, the results are shown in Fig. B-16. For simple span moments, one truck governs for spans up to about 140 ft, for shears up to about 120 ft, and for negative moments in continuous bridges (two equal spans) up to about 50 ft (one span length). The minimum headway distance is associated with non-moving vehicles or trucks moving at reduced speeds. This is important in consideration of dynamic loads. Therefore, it is assumed that either headway distance is minimum 50 ft for live load plus dynamic load, or it is 15 ft (bumper-to-bumper traffic) for just live load (no dynamic load).

For simple spans, the calculated mean maximum one lane moments are presented in Table B-6, for time periods from 1 day to 75 years. The mean maximum one lane shears are presented in Table B-7. For continuous spans, the mean maximum negative moments are presented in Table B-8. The results are also plotted in Fig. B-17, B-18 and B-19.

Table B-5. Truck Parameters for Two Trucks in One Lane

One/Two Trucks		N	z	T
One		20,000,000	5.33	75 years
Two: $\rho = 0$	T_1	300,000	4.50	1 year
	T_2	1	0.00	average
$\rho = 0.5$	T_1	150,000	4.36	6 months
	T_2	1,000	3.09	1 day
$\rho = 1$	T_1	30,000	3.99	1 month
	T_2	30,000	3.99	1 month

Table B-6. Mean Maximum Moments for Simple Spans Due to Multiple Trucks in One Lane (Divided by Corresponding HS20 Moment).

Span (ft)	1 day	2 weeks	1 month	2 months	6 months	1 year	5 years	50 years	75 years
10	0.97	1.12	1.18	1.23	1.30	1.37	1.46	1.65	1.65
20	1.08	1.18	1.23	1.28	1.33	1.38	1.47	1.58	1.58
30	1.20	1.32	1.37	1.42	1.46	1.52	1.78	1.72	1.72
40	1.31	1.42	1.46	1.50	1.55	1.58	1.64	1.74	1.74
50	1.32	1.43	1.47	1.52	1.56	1.60	1.65	1.75	1.75
60	1.37	1.47	1.52	1.56	1.60	1.64	1.69	1.79	1.79
70	1.42	1.51	1.56	1.60	1.64	1.68	1.74	1.83	1.83
80	1.47	1.55	1.60	1.64	1.68	1.73	1.79	1.89	1.89
90	1.51	1.60	1.64	1.68	1.72	1.78	1.84	1.94	1.94
100	1.55	1.64	1.68	1.72	1.76	1.82	1.89	2.00	2.00
110	1.60	1.68	1.72	1.76	1.81	1.86	1.94	2.05	2.05
120	1.63	1.72	1.76	1.80	1.85	1.90	1.97	2.08	2.08
130	1.66	1.75	1.80	1.83	1.87	1.92	1.99	2.10	2.10
140	1.67	1.76	1.81	1.84	1.87	1.92	1.99	2.10	2.10
150	1.67	1.76	1.80	1.83	1.87	1.92	1.99	2.10	2.10
160	1.65	1.74	1.79	1.82	1.85	1.90	1.97	2.08	2.08
170	1.63	1.71	1.77	1.80	1.84	1.88	1.95	2.06	2.06
180	1.60	1.68	1.73	1.77	1.81	1.85	1.92	2.03	2.03
190	1.56	1.65	1.70	1.74	1.78	1.82	1.89	2.00	2.00
200	1.52	1.62	1.67	1.71	1.74	1.79	1.85	1.96	1.96

Table B-7. Mean Maximum Shears for Simple Spans Due to Multiple Trucks in One Lane (Divided by Corresponding HS20 Shear).

Span (ft)	1 day	2 weeks	1 month	2 months	6 months	1 year	5 years	50 years	75 years
10	1.20	1.31	1.38	1.40	1.44	1.48	1.52	1.61	1.62
20	1.14	1.25	1.30	1.31	1.36	1.38	1.43	1.51	1.52
30	1.14	1.24	1.29	1.31	1.35	1.38	1.42	1.48	1.49
40	1.18	1.28	1.32	1.34	1.37	1.40	1.43	1.50	1.51
50	1.24	1.33	1.37	1.39	1.43	1.45	1.48	1.55	1.56
60	1.30	1.40	1.44	1.46	1.49	1.52	1.56	1.61	1.62
70	1.37	1.47	1.50	1.52	1.55	1.58	1.62	1.69	1.70
80	1.43	1.53	1.57	1.59	1.63	1.66	1.70	1.77	1.78
90	1.48	1.58	1.62	1.64	1.69	1.72	1.76	1.84	1.85
100	1.53	1.63	1.67	1.70	1.73	1.77	1.82	1.89	1.90
110	1.57	1.66	1.70	1.72	1.76	1.80	1.85	1.92	1.93
120	1.59	1.67	1.71	1.73	1.77	1.80	1.86	1.92	1.93
130	1.59	1.68	1.71	1.73	1.77	1.79	1.85	1.91	1.92
140	1.57	1.67	1.70	1.72	1.75	1.77	1.82	1.90	1.91
150	1.53	1.63	1.67	1.69	1.72	1.75	1.79	1.87	1.88
160	1.50	1.59	1.63	1.65	1.68	1.71	1.76	1.84	1.85
170	1.47	1.56	1.60	1.62	1.65	1.68	1.74	1.81	1.82
180	1.44	1.53	1.56	1.58	1.61	1.65	1.71	1.78	1.79
190	1.41	1.50	1.53	1.55	1.58	1.61	1.67	1.74	1.75
200	1.39	1.48	1.51	1.53	1.55	1.59	1.64	1.71	1.72

Table B-8. Mean Max. Negative Moments for Continuous Spans Due to Multiple Trucks in One Lane (Divided by HS20 Neg. Moment).

Span (ft)	1 day	2 weeks	1 month	2 months	6 months	1 year	5 years	50 years	75 years
10	1.12	1.25	1.30	1.33	1.37	1.40	1.46	1.54	1.55
20	1.30	1.40	1.43	1.44	1.47	1.50	1.54	1.59	1.60
30	1.50	1.59	1.62	1.64	1.66	1.68	1.72	1.75	1.76
40	1.63	1.73	1.75	1.77	1.81	1.83	1.86	1.91	1.92
50	1.58	1.67	1.69	1.71	1.75	1.77	1.80	1.85	1.86
60	1.72	1.83	1.85	1.87	1.92	1.94	1.97	2.02	2.03
70	1.80	1.92	1.94	1.96	2.01	2.03	2.06	2.12	2.13
80	1.80	1.91	1.94	1.96	2.00	2.03	2.06	2.12	2.13
90	1.75	1.86	1.88	1.90	1.95	1.97	2.00	2.06	2.07
100	1.70	1.81	1.83	1.85	1.89	1.91	1.94	2.00	2.01
110	1.66	1.76	1.78	1.80	1.84	1.86	1.89	1.95	1.96
120	1.62	1.72	1.74	1.76	1.80	1.82	1.85	1.90	1.91
130	1.58	1.68	1.70	1.72	1.76	1.78	1.81	1.85	1.86
140	1.55	1.64	1.66	1.68	1.72	1.74	1.77	1.81	1.82
150	1.52	1.61	1.63	1.65	1.69	1.70	1.73	1.78	1.79
160	1.49	1.58	1.60	1.62	1.66	1.67	1.70	1.75	1.76
170	1.46	1.55	1.57	1.59	1.63	1.64	1.67	1.72	1.73
180	1.44	1.53	1.55	1.57	1.60	1.62	1.64	1.69	1.70
190	1.42	1.51	1.52	1.54	1.58	1.59	1.62	1.66	1.67
200	1.42	1.48	1.50	1.52	1.55	1.57	1.60	1.64	1.65

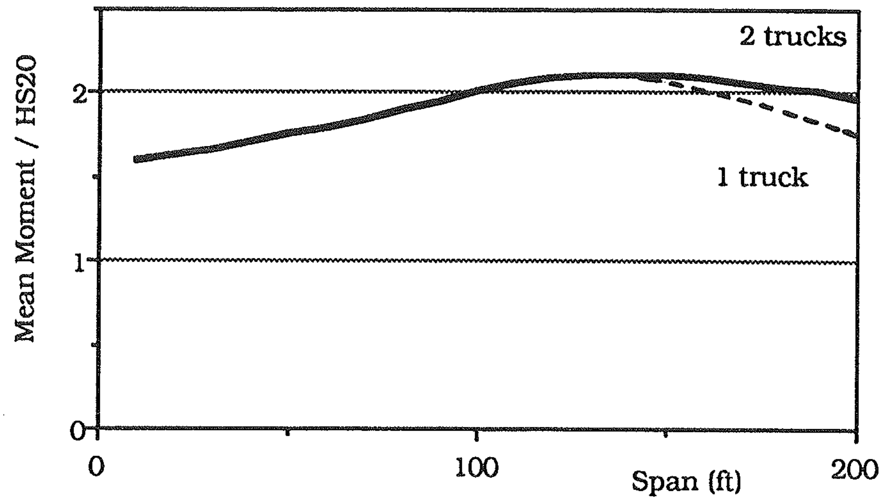

Fig. B-14. Mean Maximum 75 Year Moments Due to One Truck and Two Trucks in One Lane.

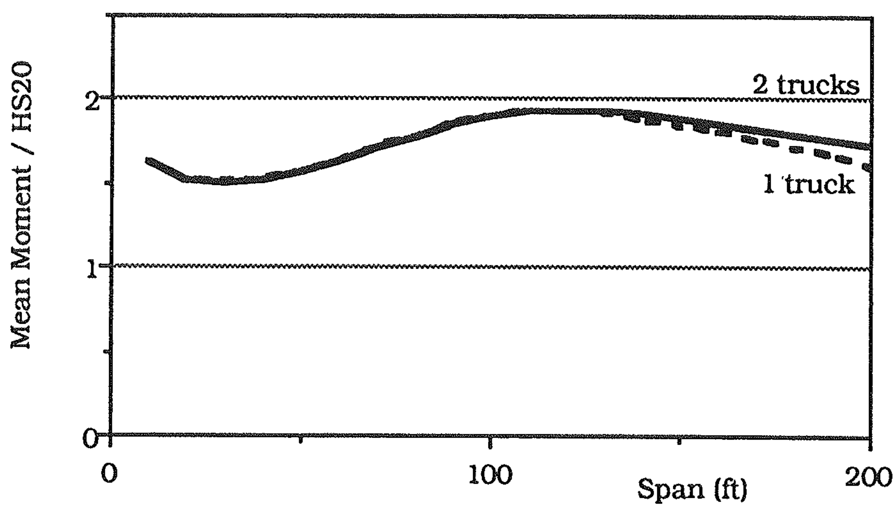

Fig. B-15. Mean Maximum 75 Year Shears Due to One Truck and Two Trucks in One Lane.

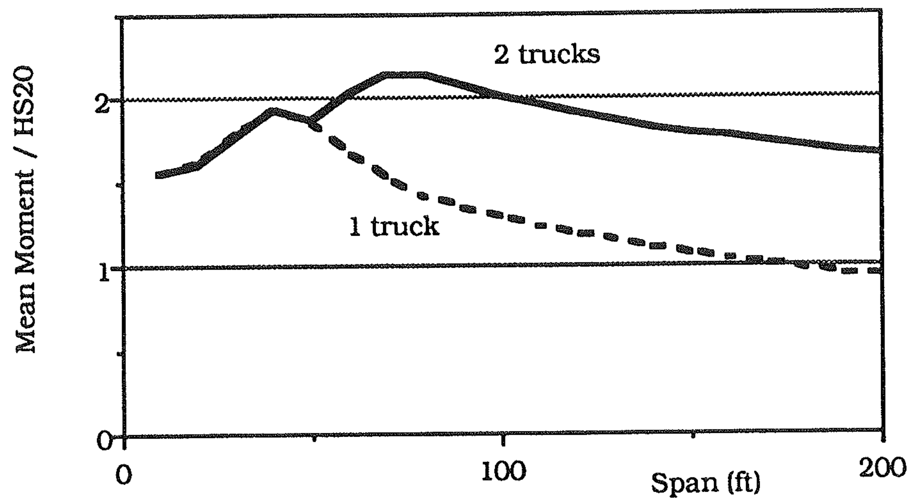

Fig. B-16. Mean Maximum 75 Year Negative Moments Due to One Truck and Two Trucks in One Lane.

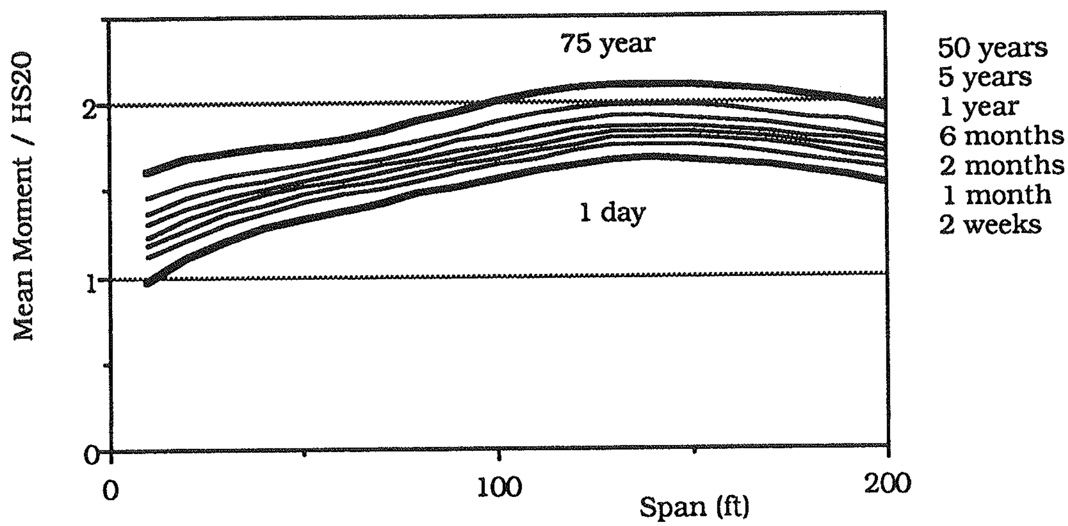

Fig. B-17. Mean Maximum Moments for Simple Spans Due to Multiple Trucks in One Lane.

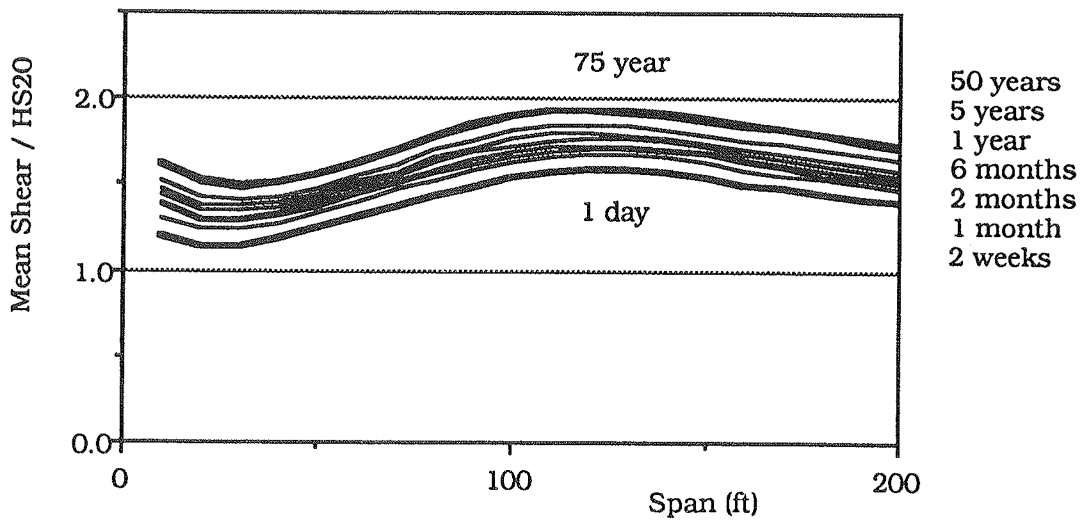

Fig. B-18. Mean Maximum Shears for Simple Spans Due to Multiple Trucks in One Lane.

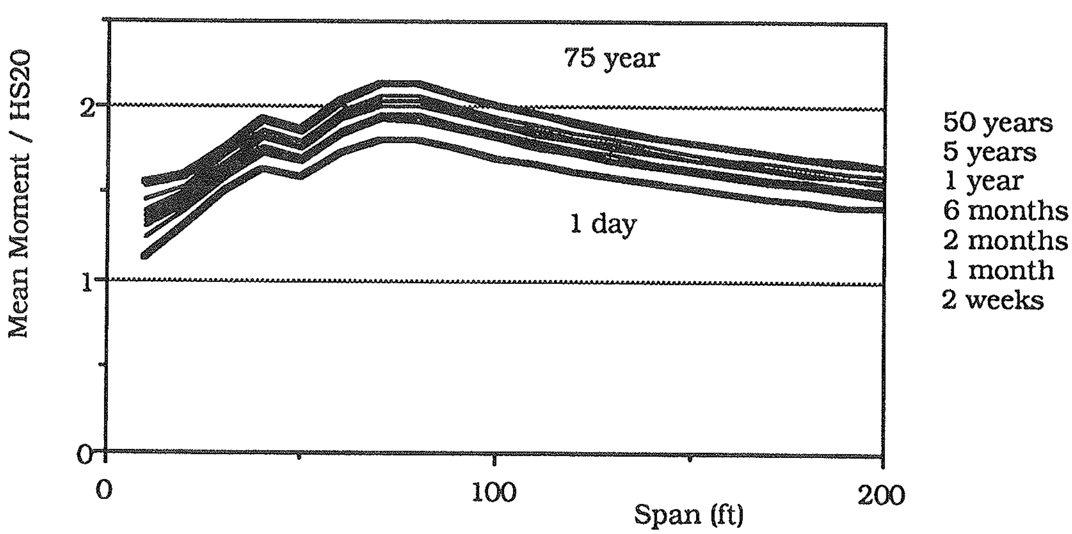

Fig. B-19. Mean Maximum Negative Moments for Two Equal Continuous Spans Due to Multiple Trucks in One Lane.

Girder Distribution Factors

The analysis of two lane loading involves the distribution of truck load to girders. The structural analysis was performed using the finite element method. The model is based on a linear behavior of girders and slab. The calculations were performed for spans ranging from 30 to 200 ft. Five cases of girder spacing were considered: 4, 6, 8, 10 and 12 ft. For each case of span and girder spacing, girder distribution factors were calculated for various truck positions, by moving the truck transversely by 1 ft at a time. The resulting truck "influence lines" are used for calculation of the joint effect of two trucks in adjacent lanes, by superposition.

The resulting girder distribution factors (GDF) are compared with the AASHTO (B-1) values and those recommended by Zokaie, Osterkamp and Imbsen (B-10).

For moment in an interior girder, AASHTO (B-1) specifies a GDF as follows,

$$GDF = s/D, \qquad (B-2)$$

where s is the girder spacing and D is a constant, equal to 5.5 for steel girders and prestressed concrete girders, and D = 6.0 for reinforced concrete T-beams. The design moment in a girder is equal to the product of s/D and 0.5 of the HS20 moment.

Zokaie, Osterkamp and Imbsen (B-10) proposed GDF as a function of girder spacing, s (ft), and span length, L (ft). For interior girders (steel, prestressed concrete and reinforced concrete T-beams) the formula is

$$GDF = 0.15 + (s/3)^{0.6} (s/L)^{0.2} \qquad (B-3)$$

For shear, AASHTO (B-1) specifies GDF's given by Eq. B-2, except of the axle directly over the support. It is assumed that over support the slab is simply supported by the girders.

Zokaie, Osterkamp and Imbsen (B-10) developed the following formula for GDF for shear,

$$GDF = 0.4 + (s/6) - (s/25)^2 \qquad (B-4)$$

The results of calculations performed as a part of this study, along with the GDF's obtained using Eq. B-2, B-3 and B-4, are listed in Table B-9. AASHTO (B-1) values are calculated for steel and prestressed concrete girders using D = 5.5 (denoted by S & P/C in Table B-9), and for reinforced concrete T-beams using D = 6 (denoted by R/C in Table B-9). In Table B-9, the GDF's calculated in

Table B-9. Girder Distribution Factors for Interior Girders.

Span	Girder	Moments				Shears		
	Spacing	AASHTO (1989)		Nowak	Zokaie	AASHTO (1989)		Zokaie
(ft)	(ft)	S & P/C	R/C		et al	S & P/C	R/C	et al
30	4	0.73	0.67	0.88	0.94	0.90	0.88	1.04
30	6	1.09	1.00	1.20	1.25	1.25	1.21	1.34
30	8	1.45	1.33	1.50	1.53	1.65	1.60	1.63
30	10	1.82	1.67	1.79	1.80	1.94	1.88	1.91
30	12	2.18	2.00	2.06	2.06	2.28	2.21	2.17
60	4	0.73	0.67	0.83	0.84	0.87	0.84	1.04
60	6	1.09	1.00	1.10	1.11	1.22	1.17	1.34
60	8	1.45	1.33	1.35	1.35	1.61	1.55	1.63
60	10	1.82	1.67	1.59	1.59	1.91	1.84	1.91
60	12	2.18	2.00	1.82	1.82	2.26	2.18	2.17
90	4	0.73	0.67	0.78	0.79	0.86	0.83	1.04
90	6	1.09	1.00	1.03	1.03	1.21	1.16	1.34
90	8	1.45	1.33	1.26	1.26	1.60	1.54	1.63
90	10	1.82	1.67	1.48	1.48	1.91	1.83	1.91
90	12	2.18	2.00	1.69	1.69	2.26	2.17	2.17
120	4	0.73	0.67	0.73	0.75	0.86	0.83	1.04
120	6	1.09	1.00	0.98	0.98	1.21	1.16	1.34
120	8	1.45	1.33	1.20	1.20	1.60	1.53	1.63
120	10	1.82	1.67	1.40	1.40	1.91	1.83	1.91
120	12	2.18	2.00	1.60	1.60	2.25	2.16	2.17
200	4	0.73	0.67	0.69	0.69	0.75	0.71	1.04
200	6	1.09	1.00	0.90	0.90	1.12	1.06	1.34
200	8	1.45	1.33	1.10	1.10	1.50	1.41	1.63
200	10	1.82	1.67	1.28	1.28	1.87	1.76	1.91
200	12	2.18	2.00	1.46	1.46	2.23	2.10	2.17

this study are denoted by Nowak, and those obtained using Eq. B-3 and B-4 are denoted by Zokaie et al.

The GDF's calculated for moments as a part of this study are also plotted as a function of girder spacing for spans 30, 60, 90, 120 and 200 ft in Fig. 3. For comparison, AASHTO (B-1) GDF's are also shown. The ratios of calculated GDF and AASHTO specified GDF are plotted in Fig. B-20. Girder distribution factors specified by AASHTO are conservative for larger girder spacing. For shorter spans and girder spacings, AASHTO produces smaller GDF than calculated values.

For the proposed LRFD bridge design code, it is assumed that the GDF's are calculated using Eq. B-3 and B-4.

Two Lane Moments and Shears

The analysis involves the determination of the load in each lane and load distribution to girders. The effect of multiple trucks is calculated by superposition. The maximum moments are calculated as the largest of the following cases:

(1) One lane fully loaded and the other lane unloaded.

(2) Both lanes loaded; three degrees of correlation between the lane loads are considered: no correlation ($\rho = 0$), partial correlation ($\rho = 0.5$) and full correlation ($\rho = 1$).

It has been observed that, on average, about every 15th truck is on the bridge simultaneously with another truck (side-by-side). For each such a simultaneous occurrence, it is assumed that every 10th time the trucks are partially correlated and every 30th time they are fully correlated (with regard to weight). It is also assumed that the transverse distance between two side-by-side trucks is 4 ft (wheel center-to-center), as shown in Fig. B-21.

The parameters of lane load, including N (the considered lane load is the maximum of N occurrences), $z = -\Phi^{-1}(1/N)$, and T (the considered lane load is the maximum in time period T) are given in Table B-10.

The results of simulations indicate that for interior girders, the case with two fully correlated side-by-side trucks governs, with each truck equal to the maximum 2 month truck. The ratio of a mean maximum 75 year moment (or shear) and a mean 2 month moment (or shear) is about 0.85 for all the spans. The mean maximum 75 year girder moments depend on the span and girder spacing.

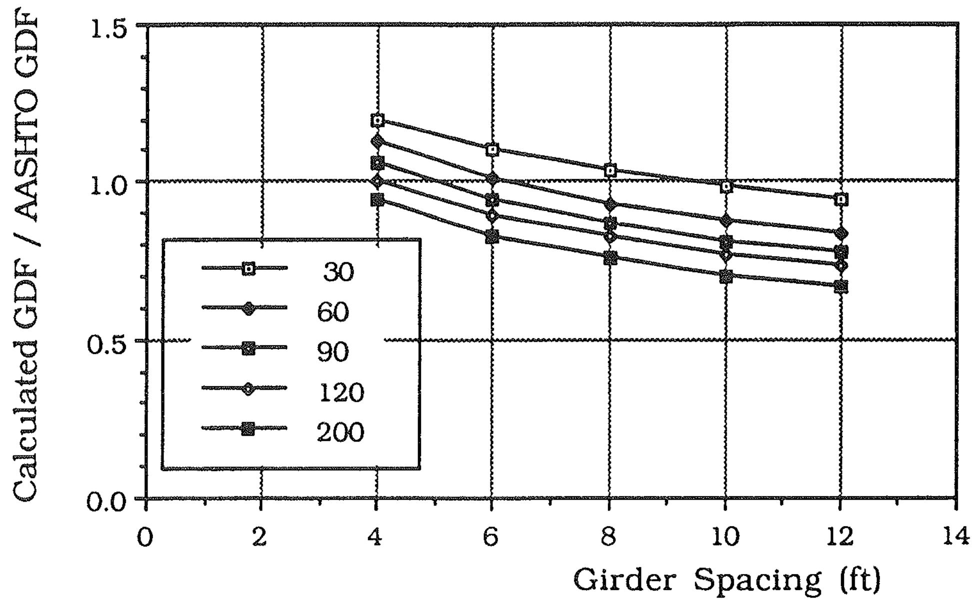

Fig. B-20. Ratios of Calculated GDF and AASHTO Specified GDF.

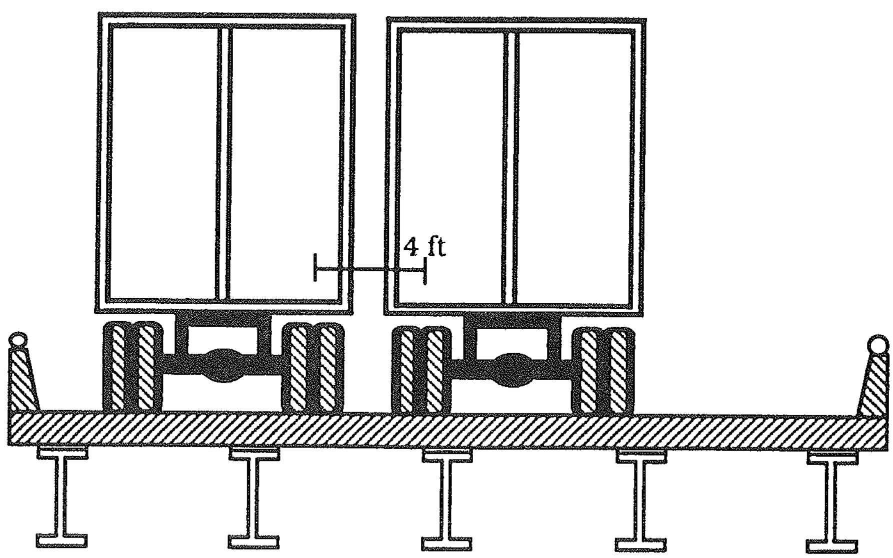

Fig. B-21. Two Trucks Side-by-Side in Adjacent Lanes.

Table B-10. Lane Load Parameters for Two Lane Traffic

One/Two Lanes Loaded		N	z	T
One		20,000,000	5.33	75 years
Two: $\rho = 0$	L_1	1,500,000	4.83	5 years
	L_2	1	0.00	average
$\rho = 0.5$	L_1	150,000	4.36	6 months
	L_2	1,000	3.09	1 day
$\rho = 1$	L_1	50,000	4.11	2 month
	L_2	50,000	4.11	2 month

Proposed Design Live Load

The objective in the selection of the live load model for the LRFD bridge design code is a uniform ratio of the nominal (design) moments (or shears) and the mean maximum 75 year moments (or shears). Various live load models were considered. For the considered models, the ratios of moments and shears were calculated for a wide range of spans. Good results are obtained for a model which combines the HS20 truck with a uniformly distributed load of 640 lb/ft (B-1). For shorter spans, a tandem of two equal axles, each 25 kips, spaced at 4 ft, also combined with a uniform load of 640 lb/ft, is specified. For negative moment in continuous spans, the design live load (per lane) is the larger of:

(a) One HS20 truck plus a uniformly distributed loading of 640 lb/ft,

(b) 90% of the effect of two HS20 trucks, placed in two different spans, with headway distance at least 50 ft, plus 90% of the uniformly distributed loading of 640 lb/ft. The headway distance, 50 ft, corresponds to the minimum value for moving vehicles.

The proposed new live load is shown in Fig. 5.

Values of moments and shears caused by the proposed LRFD live load are calculated for various spans. The results are presented in Table B-11 for simple span moments, M(LRFD), Table B-12 for shears, S(LRFD), and Table B-13 for negative moments in continuous spans, Mn(LRFD). Also included are moments and shears corresponding to HS20 (B-1), denoted by M(HS20), S(HS20) and Mn(HS20), and the mean maximum 75 year values, denoted by M(75), S(75) and Mn(75). For comparison, the ratio of new live load moment for simple spans, and HS20 moment, is plotted in Fig. B-23. For shear and negative moment, the ratios are presented in Fig. B-24 and B-25, respectively.

The mean-to-nominal ratio (bias factor) of live load is equal to the ratio of the mean maximum 75 year load effect and the design value. The calculated bias factors for HS20 loading (B-1) and the new live load (Fig. 5) are shown in Fig. B-26 for simple span moment, Fig. B-27 for shear, and Fig. B-28 for negative moment in continuous spans. The bias factor varies as a function of span, however, the variation is reduced for the proposed LRFD live load.

For various time periods, the mean maximum live load effects are listed in Table B-14, B-15 and B-16, for the simple span moment, shear and negative moment in continuous spans, respectively. The load effects are expressed in terms of the new LRFD live load (Fig. 5). Values of the new LRFD moments and shears are also given in Tables B-14 to B-16.

Table B-11. Simple Span Moment Specified by Current AASHTO, M(HS20), Proposed Live Load, M(LRFD), and Mean Maximum 75 Year Moment, M(75).

Span	M(HS20)	M(LRFD)	M(75)
(ft)	(k-ft)	(k-ft)	(k-ft)
10	80	88	132
20	181	217	302
30	315	399	537
40	450	588	783
50	628	832	1099
60	807	1093	1444
70	986	1376	1804
80	1165	1675	2202
90	1344	1989	2608
100	1524	2323	3048
110	1704	2669	3492
120	1883	3034	3917
130	2063	3414	4333
140	2243	3808	4710
150	2475	4220	5185
160	2768	4648	5757
170	3077	5092	6323
180	3402	5552	6906
190	3743	6028	7486
200	4100	6520	8036

Table B-12. Shear Specified by Current AASHTO, S(HS20), Proposed Live Load, S(LRFD), and Mean Maximum 75 Year Shear, S(75).

Span (ft)	S(HS20) (kips)	S(LRFD) (kips)	S(75) (kips)
10	32.0	43.2	51.8
20	41.6	51.4	63.2
30	49.6	59.2	73.9
40	55.2	68.0	83.4
50	58.5	74.6	91.3
60	60.8	80.0	98.5
70	62.4	84.8	106.1
80	63.6	89.2	112.9
90	64.5	93.3	119.3
100	65.3	97.3	124.1
110	65.9	101.1	127.2
120	66.4	104.8	128.2
130	67.6	108.4	130.0
140	70.8	112.0	134.9
150	74.0	115.5	139.1
160	77.2	119.0	142.8
170	80.4	122.5	146.3
180	83.6	125.9	149.6
190	86.8	129.3	151.9
200	90.0	132.6	154.8

Table B-13. Negative Moment for Continuous Spans Specified by Current AASHTO, Mn(HS20), Proposed Live Load, Mn(LRFD), and Mean Maximum 75 Year Negative Moment, Mn(75).

Span (ft)	Mn(HS20) (k-ft)	Mn(LRFD) (k-ft)	Mn(75) (k-ft)
10	44	52	68
20	123	155	197
30	192	264	338
40	267	393	512
50	373	521	694
60	496	806	1008
70	634	1107	1351
80	789	1386	1677
90	960	1652	1982
100	1146	1918	2302
110	1349	2199	2639
120	1568	2493	2992
130	1802	2800	3360
140	2053	3122	3746
150	2320	3458	4150
160	2602	3808	4570
170	2901	4172	5006
180	3216	4550	5460
190	3546	4943	5932
200	3893	5350	6420

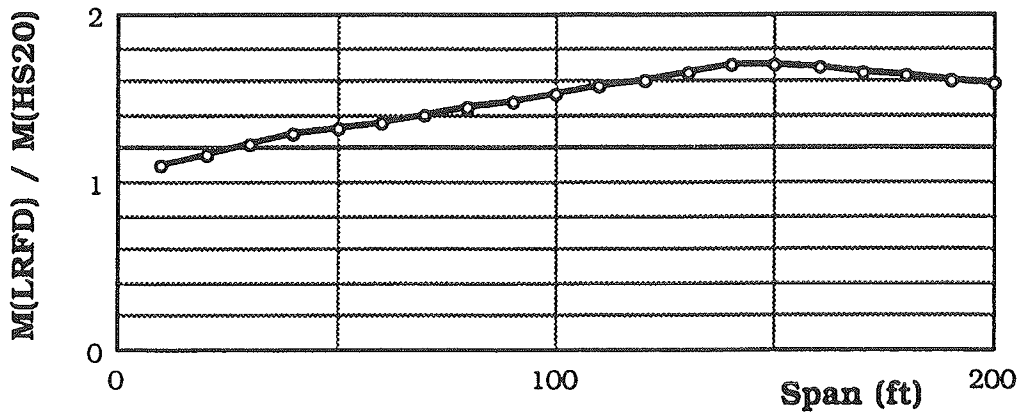

Fig. B-23. Ratio of the New Live Load Simple Span Moment, M(LRFD), and HS20 Moment, M(HS20).

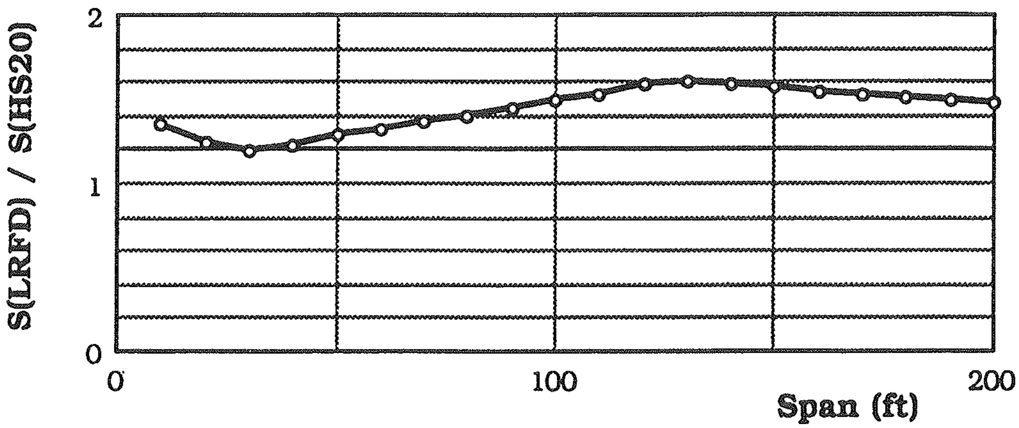

Fig. B-24. Ratio of the New Live Load Shear, S(LRFD), and HS20 Shear, S(HS20).

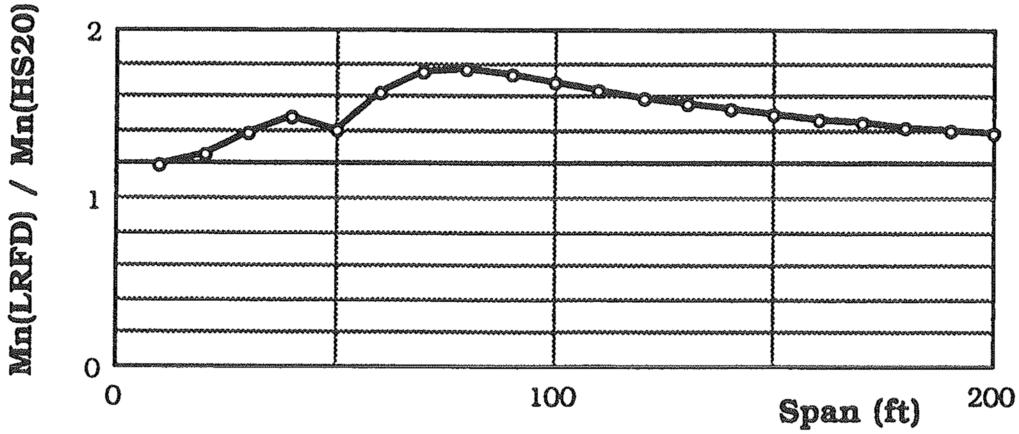

Fig. B-25. Ratio of the New Live Load Negative Moment, Mn(LRFD), and HS20 Negative Moment, Mn(HS20).

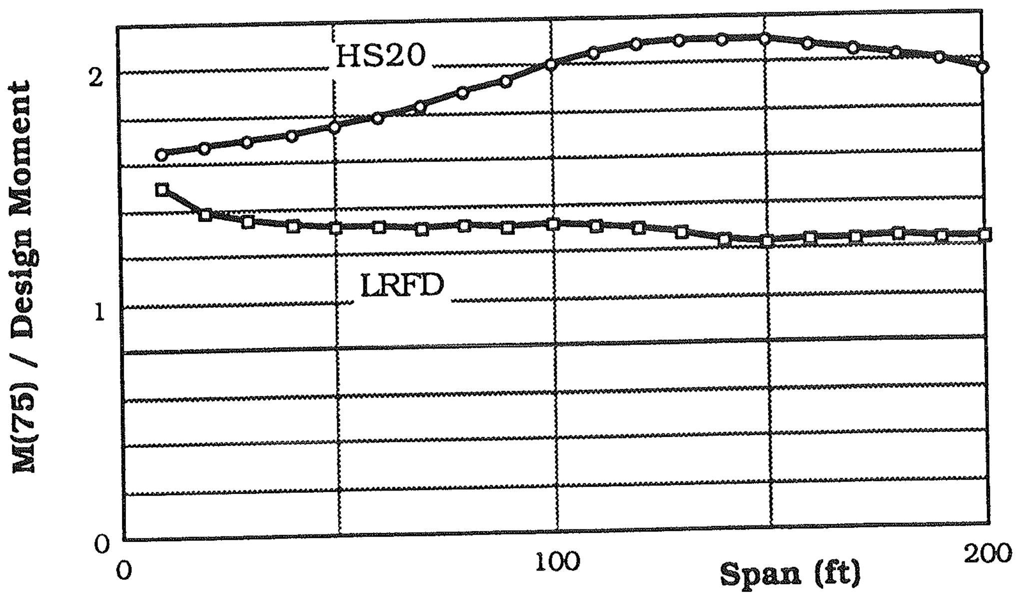

Fig. B-26. Bias Factors for Simple Span Moment; Ratio of M(75)/ M(LRFD) and M(75)/M(HS20).

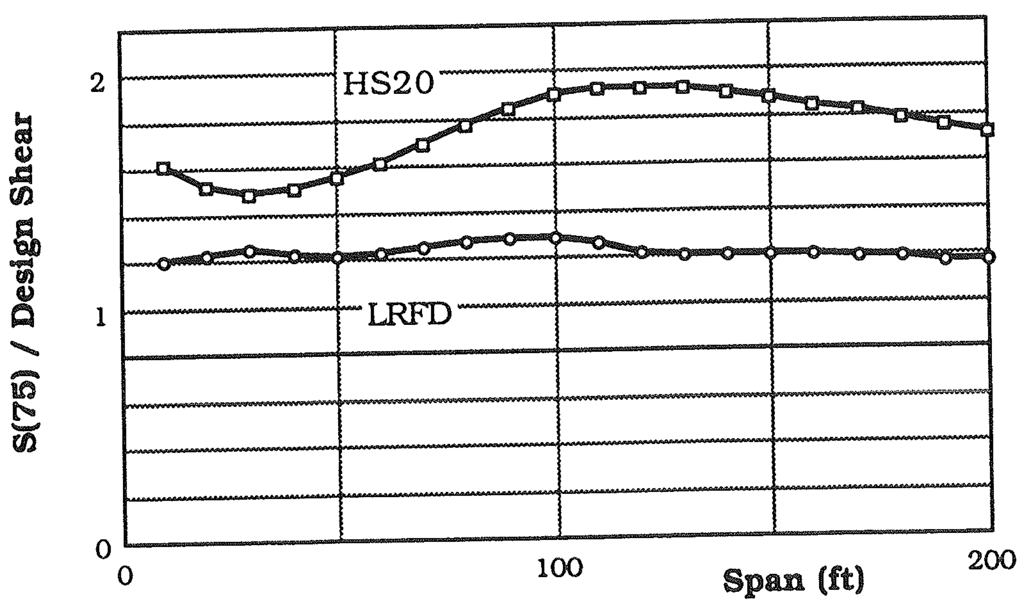

Fig. B-27. Bias Factors for Shear; Ratio of S(75)/S(LRFD) and S(75)/ S(HS20).

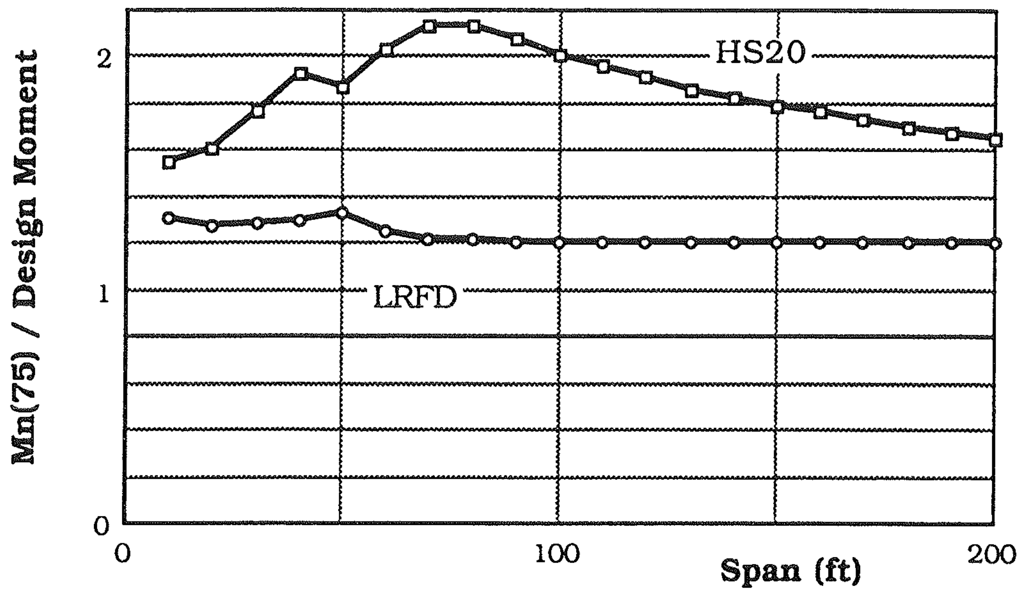

Fig. B-28. Bias Factors for Negative Moment; Ratio of Mn(75)/Mn(LRFD) and Mn(75)/Mn(HS20).

Table B-14. Mean Maximum Moments for Simple Spans Divided by Corresponding New LRFD Moments, M(LRFD).

Span (ft)	M(LRFD) (k-ft)	1 day	2 weeks	1 month	2 months	6 months	1 year	5 years	50 years	75 years
10	88	0.88	1.02	1.07	1.12	1.18	1.25	1.33	1.50	1.50
20	232	0.90	0.98	1.02	1.06	1.10	1.14	1.21	1.30	1.30
30	397	0.95	1.04	1.08	1.12	1.15	1.19	1.26	1.35	1.35
40	578	1.02	1.11	1.14	1.17	1.21	1.23	1.28	1.35	1.35
50	826	1.00	1.08	1.12	1.15	1.18	1.22	1.25	1.33	1.33
60	1093	1.02	1.09	1.12	1.15	1.18	1.21	1.24	1.32	1.32
70	1376	1.02	1.08	1.12	1.15	1.18	1.21	1.25	1.31	1.31
80	1675	1.02	1.08	1.11	1.14	1.17	1.21	1.25	1.32	1.32
90	1990	1.02	1.08	1.11	1.14	1.16	1.20	1.24	1.31	1.31
100	2322	1.02	1.08	1.10	1.13	1.16	1.20	1.24	1.31	1.31
110	2670	1.02	1.07	1.10	1.12	1.15	1.19	1.24	1.31	1.31
120	3033	1.01	1.07	1.09	1.12	1.15	1.18	1.22	1.29	1.29
130	3413	1.00	1.06	1.09	1.11	1.13	1.16	1.20	1.27	1.27
140	3809	0.98	1.03	1.06	1.08	1.10	1.13	1.17	1.24	1.24
150	4220	0.98	1.03	1.06	1.07	1.09	1.12	1.16	1.23	1.23
160	4648	0.98	1.03	1.07	1.09	1.10	1.13	1.17	1.24	1.24
170	5092	0.99	1.03	1.07	1.09	1.11	1.13	1.18	1.24	1.24
180	5552	0.98	1.03	1.06	1.08	1.11	1.13	1.17	1.24	1.24
190	6028	0.97	1.02	1.06	1.08	1.10	1.13	1.17	1.24	1.24
200	6520	0.96	1.02	1.05	1.08	1.09	1.12	1.16	1.23	1.23

Table B-15. Mean Maximum Shears for Simple Spans Divided by Corresponding New LRFD Shears, S(LRFD).

Span (ft)	S(LRFD) (k)	1 day	2 weeks	1 month	2 months	6 months	1 year	5 years	50 years	75 years
10	43.2	0.89	0.97	1.02	1.04	1.07	1.09	1.13	1.19	1.20
20	51.4	0.92	1.01	1.05	1.06	1.10	1.12	1.16	1.22	1.23
30	59.2	0.95	1.03	1.08	1.09	1.13	1.15	1.19	1.24	1.25
40	68.0	0.96	1.04	1.07	1.09	1.11	1.14	1.16	1.22	1.23
50	74.6	0.97	1.04	1.07	1.09	1.12	1.14	1.16	1.22	1.22
60	80.0	0.99	1.06	1.09	1.11	1.13	1.15	1.19	1.22	1.23
70	84.8	1.00	1.08	1.10	1.12	1.14	1.16	1.19	1.24	1.25
80	89.2	1.02	1.09	1.12	1.13	1.16	1.18	1.21	1.26	1.27
90	93.3	1.02	1.09	1.12	1.13	1.17	1.19	1.22	1.27	1.28
100	97.3	1.03	1.09	1.12	1.14	1.16	1.18	1.22	1.27	1.28
110	101.1	1.02	1.08	1.11	1.12	1.15	1.17	1.21	1.25	1.26
120	104.8	1.00	1.06	1.08	1.10	1.12	1.14	1.18	1.22	1.22
130	108.4	0.99	1.04	1.07	1.08	1.10	1.12	1.15	1.19	1.20
140	112.0	0.99	1.05	1.07	1.08	1.11	1.12	1.15	1.20	1.20
150	115.5	0.98	1.04	1.07	1.08	1.10	1.12	1.15	1.20	1.20
160	119.0	0.97	1.03	1.05	1.07	1.09	1.11	1.14	1.19	1.20
170	122.5	0.96	1.02	1.05	1.06	1.08	1.10	1.14	1.19	1.19
180	125.9	0.96	1.02	1.04	1.05	1.07	1.10	1.13	1.18	1.19
190	129.3	0.95	1.01	1.03	1.04	1.06	1.08	1.12	1.17	1.17
200	132.6	0.94	1.00	1.02	1.04	1.05	1.08	1.11	1.16	1.17

Table B-16. Mean Maximum Negative Moments for Two Equal Continuous Spans (Divided by Corresponding New LRFD Negative Moments, Mn(LRFD).

Span (ft)	Mn(LRFD) (k-ft)	1 day	2 weeks	1 month	2 months	6 months	1 year	5 years	50 years	75 years
10	52	0.94	1.06	1.10	1.12	1.15	1.18	1.23	1.30	1.31
20	155	1.03	1.11	1.14	1.14	1.17	1.19	1.22	1.26	1.27
30	264	1.09	1.15	1.18	1.19	1.21	1.22	1.25	1.27	1.28
40	393	1.11	1.17	1.19	1.20	1.22	1.24	1.26	1.30	1.30
50	521	1.13	1.20	1.21	1.23	1.26	1.27	1.29	1.33	1.33
60	806	1.06	1.13	1.14	1.15	1.18	1.19	1.21	1.24	1.25
70	1107	1.03	1.10	1.11	1.12	1.15	1.16	1.18	1.22	1.22
80	1386	1.03	1.09	1.10	1.12	1.14	1.15	1.17	1.21	1.21
90	1652	1.02	1.08	1.09	1.11	1.13	1.14	1.16	1.20	1.20
100	1918	1.02	1.08	1.09	1.11	1.13	1.14	1.16	1.20	1.20
110	2199	1.02	1.08	1.09	1.11	1.13	1.14	1.16	1.20	1.20
120	2493	1.02	1.08	1.09	1.11	1.13	1.14	1.16	1.19	1.20
130	2800	1.02	1.08	1.09	1.11	1.13	1.14	1.16	1.19	1.20
140	3122	1.02	1.08	1.09	1.11	1.13	1.14	1.16	1.19	1.20
150	3458	1.02	1.08	1.09	1.11	1.13	1.14	1.16	1.19	1.20
160	3808	1.02	1.08	1.09	1.11	1.13	1.14	1.16	1.20	1.20
170	4172	1.02	1.08	1.09	1.11	1.13	1.14	1.16	1.20	1.20
180	4550	1.02	1.08	1.09	1.11	1.13	1.14	1.16	1.19	1.20
190	4943	1.02	1.08	1.09	1.11	1.13	1.14	1.16	1.19	1.20
200	5350	1.03	1.08	1.09	1.11	1.13	1.14	1.16	1.19	1.20

DYNAMIC LOAD

The derivation of the dynamic load model is based on the numerical simulations (B-11, B-12). The available test results are also presented. Dynamic load effect, I, is considered as an equivalent static load effect added to the live load, L. The objective of this analysis is to determine the parameters (mean and coefficient of variation) of the dynamic load to be added to the maximum 75 year live load.

Test Results

The dynamic bridge tests were carried out by Billing (B-13). The results are available for 22 bridges and 30 spans, including prestressed concrete girders and slabs, steel girders (hot-rolled sections, plate girders, box girders), steel trusses and rigid frames. The measurements were taken for four test vehicles (weights from 54 to 130 kips), and a normal traffic. The distribution functions of DLF (dynamic load factor) are plotted on normal probability paper in Fig. B-29, B-30 and B-31 for steel girders, prestressed concrete girders and other types, respectively. The means and standard deviations, as a fraction of the static live load, are given in Table B-17.

Considerable differences between the distribution functions for very similar structures indicate the importance of other factors mentioned above (e.g. surface condition). Results collected from the weigh-in-motion studies (B-14) indicate an average DLF of 0.11. This value falls in the middle range of the data plotted from the tests.

Interpretation of these results is difficult because the observed loads are separated from the static live loads. It has been observed that the dynamic load, as a fraction of live load, decreases for heavier trucks. It is expected, that the largest dynamic load fractions recorded in the tests correspond to light-weight trucks.

Simulations Procedure

To verify these observations, a computer procedure was developed for simulation of the dynamic bridge behavior (B-11, B-12). The flowchart is shown in Fig. B-32. The dynamic load is a function of three major parameters: road surface roughness, bridge dynamics (frequency of vibration) and vehicle dynamics (suspension system). The developed model includes the effect of these three parameters.

Road surface roughness is one of the major parameters. The quantification of the degree of roughness is very difficult. Present Serviceability Index (PSI) was used in the past. However, the ratings depend very much on the subjective judgment of individuals. Since

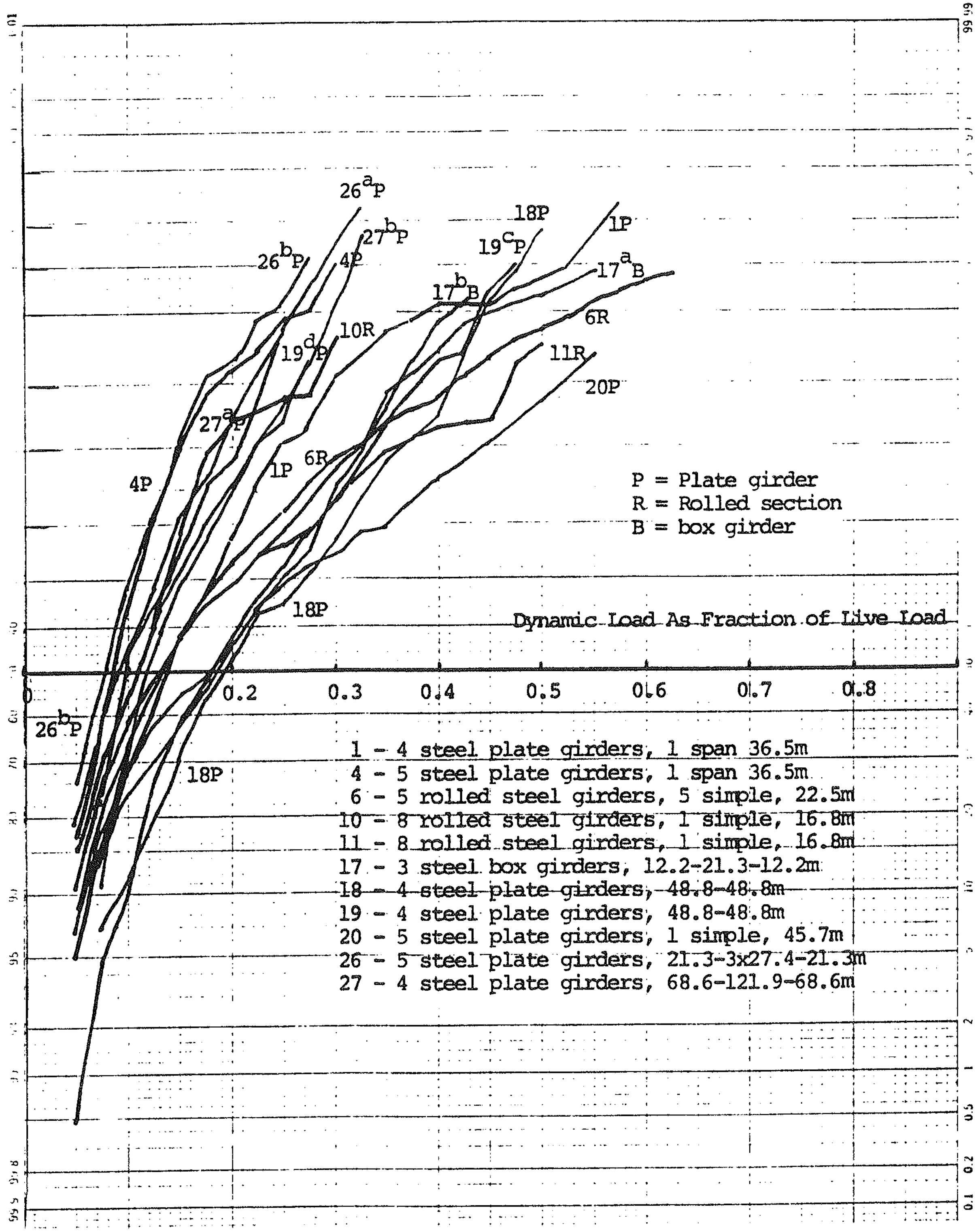

Fig. B-29. Cumulative Distribution Function of the DLF for Steel Bridges.

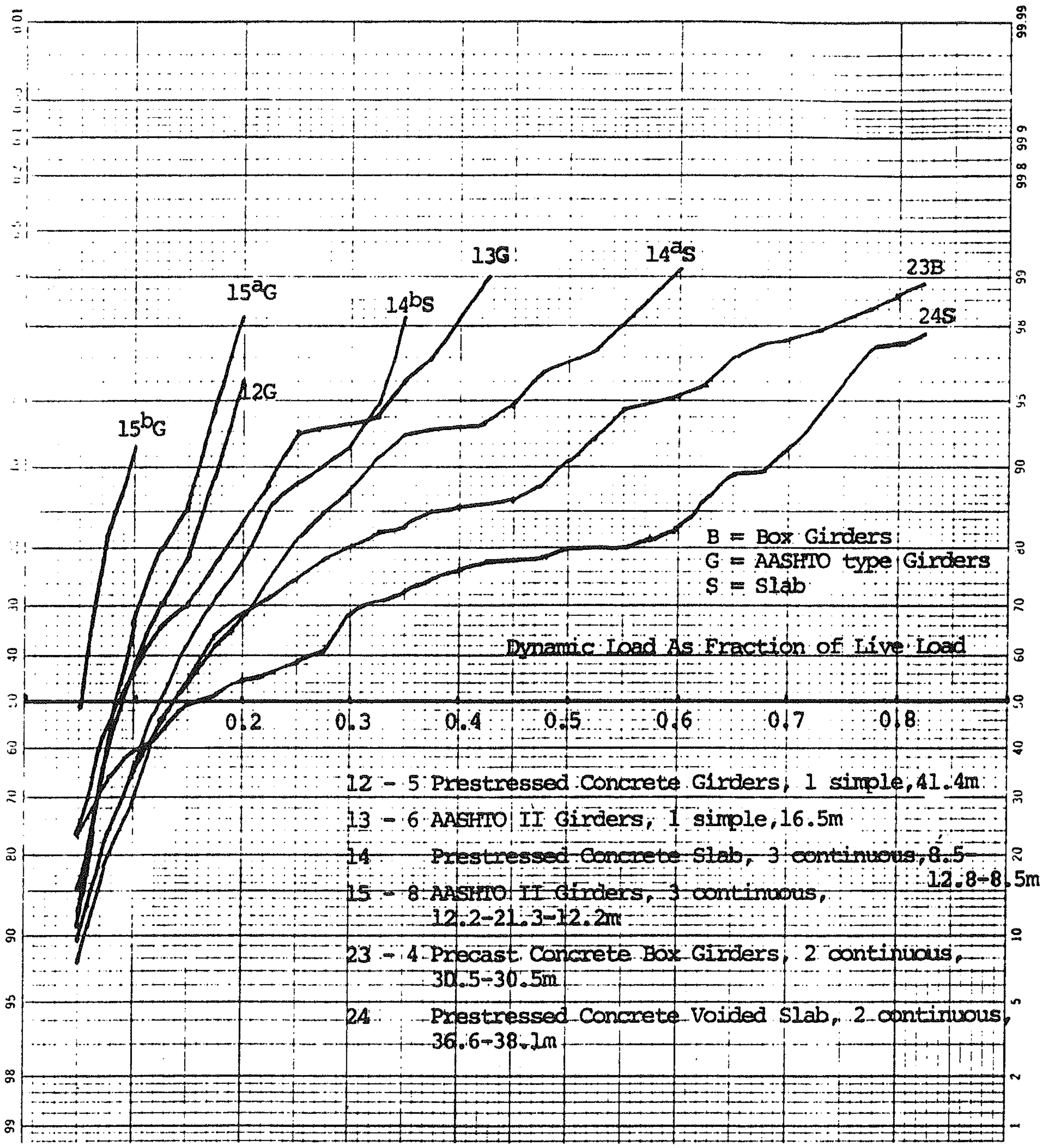

Fig. B-30. Cumulative Distribution Function of the DLF for Prestressed Concrete Bridges.

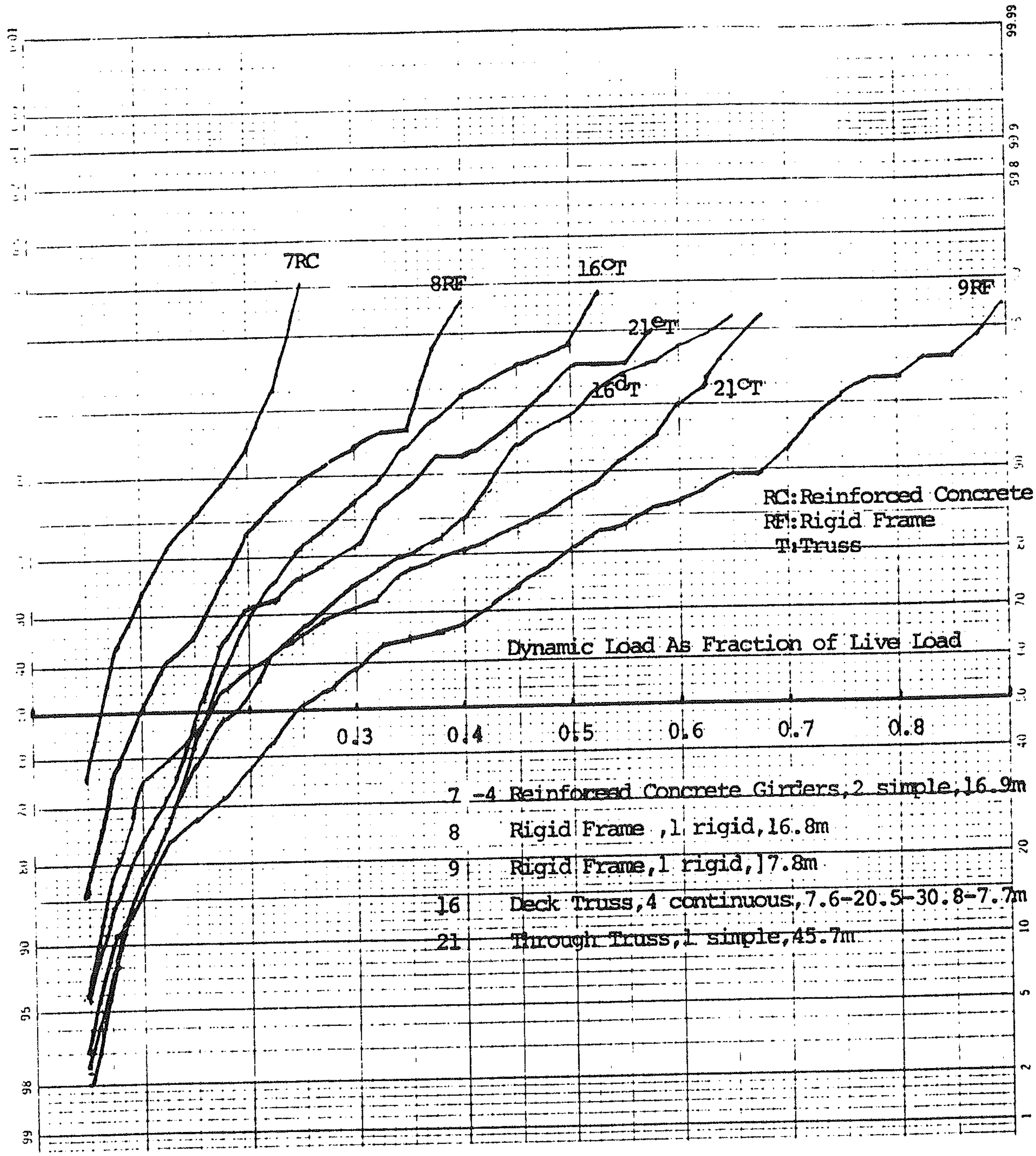

Fig. B-31. Cumulative Distribution Function of the DLF for Other Types of Bridges.

Table B-17 Dynamic Load Factors from Test Results

Type of Structure	Mean		Standard deviation	
	Range	Average	Range	Average
P/C AASHTO girders	0.05-0.10	0.09	0.03-0.07	0.05
P/C box & slabs	0.10-0.15	0.14	0.08-0.40	0.30
Steel girders	0.08-0.20	0.14	0.05-0.20	0.10
Rigid frame, truss	0.10-0.25	0.17	0.12-0.30	0.26

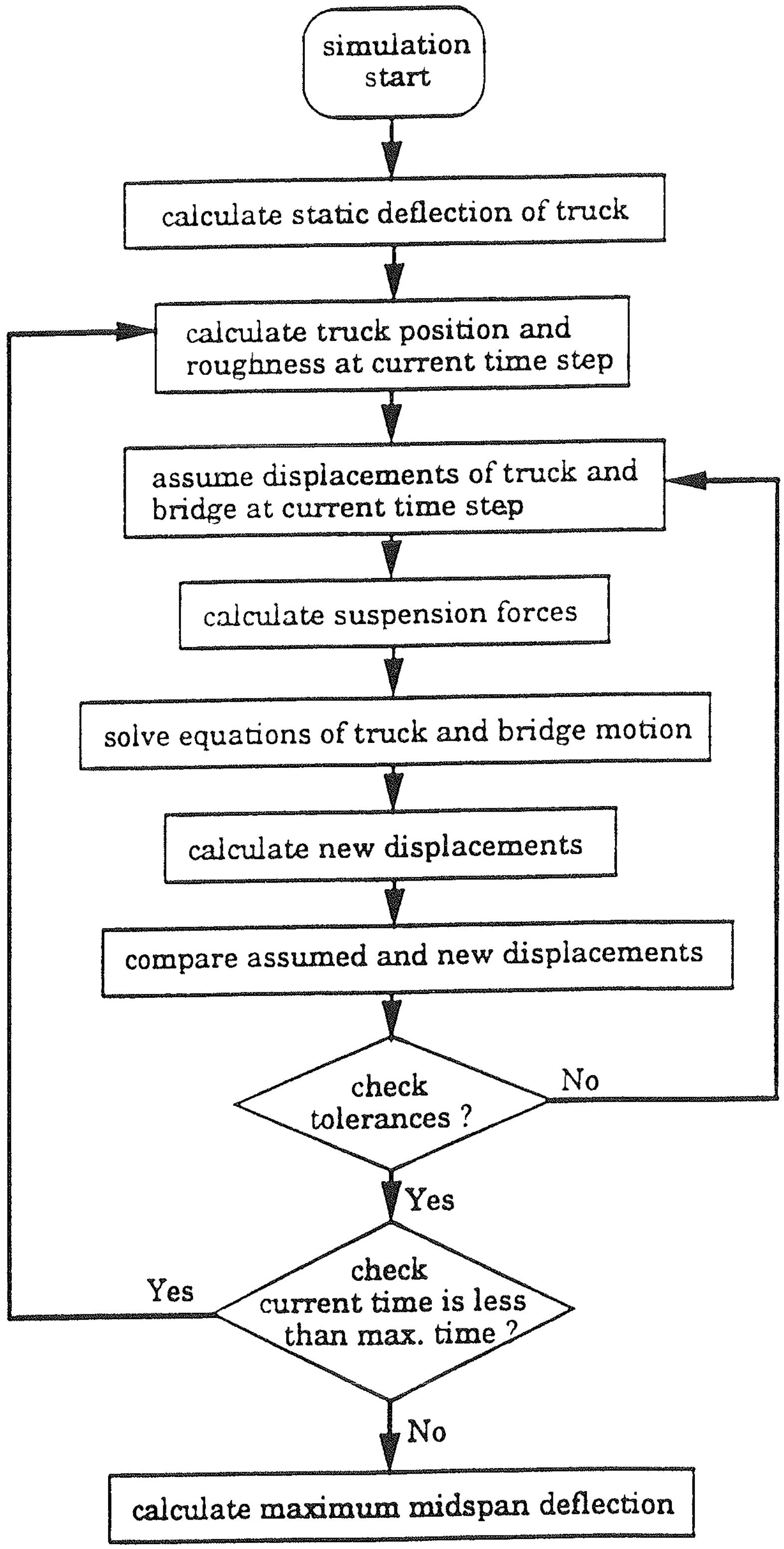

Fig. B-32. Flowchart of Computer Program (B-12).

1982, the International Roughness Index (IRI) is gaining ground as the roughness measure in many parts of the world. The approximate relationship between IRI and type of the pavement is shown in Fig. B-33. Also shown are some corresponding values of PSI.

Simulation of the dynamic load requires the generation of a road profile, which is done by using a Fourier transform of the power spectral density (PSD) function. The PSD function of the road profile has, in general, an exponential form. The relationship between the roughness coefficient a and IRI is shown in Fig. B-34. For the worst condition of older pavements, IRI = 6. This number corresponds to roughness coefficient a = 0.64_{10}^{-6}. It is also close to the mean value of the survey data collected on highway M-14 and I-94 in Southeastern Michigan. Therefore, IRI = 6 is used in this code calibration. Examples of simulated load profiles are shown in Fig. B-35.

The bridge is modeled as a prismatic beam. Modal equations of motion are formulated. Three fundamental modes of vibration are considered. It is assumed that the load is a mixture of 3 axle single trucks and 5 axle tractor-trailers. Dynamic models are shown in Fig. B-36 and B-37. The axle configurations and weight distributions are shown in Fig. B-38 and B-39. Each truck is composed of a body, suspension system and tires. The body is subjected to a rigid body motion including the vertical displacement and pitching rotation. Suspensions are assumed to be of multi-leaf type springs. Their characteristics were measured by Fancher (B-15). In the simulations a nonlinear force-deflection equation was used (B-15). Tires are assumed as linear elastic springs. A typical force deflection diagram for a tractor multi-leaf rear spring is shown in Fig. B-40. Examples of time history of trailer bouncing are shown in Fig. B-41.

Results of Simulations

The dynamic load factor (DLF) is defined as the maximum dynamic deflection, D_{dyn}, divided by the maximum static deflection, D_{sta}, as shown in Fig. B-42.

Static and dynamic deflections are calculated for typical girder bridges with the cross sections shown in Fig. B-43. A three axle truck and a five axle tractor trailer are considered. The obtained static and dynamic deflections vs. gross vehicle weight are presented in Fig. B-44, B-45 and B-46 for a five axle truck on steel bridge, three axle truck on steel bridge and a five axle truck on prestressed concrete bridge, respectively. The dynamic load factor (ratio of dynamic to static deflection) is shown in Fig. B-47, B-48, and B-49 for the three cases considered. As the gross vehicle weight is increased, the dynamic load factor is decreased. Decrease of DLF is mainly due to the

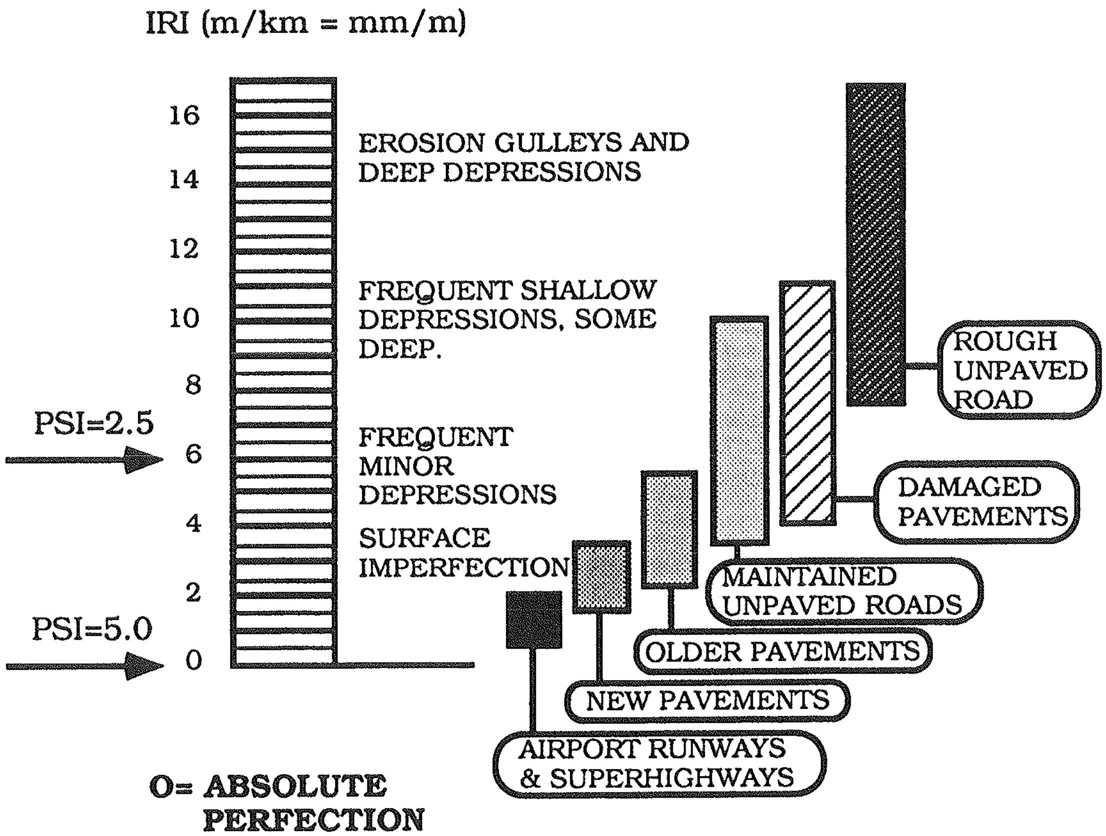

Fig. B-33. IRI, Type of Pavement and Subjective Ratings.

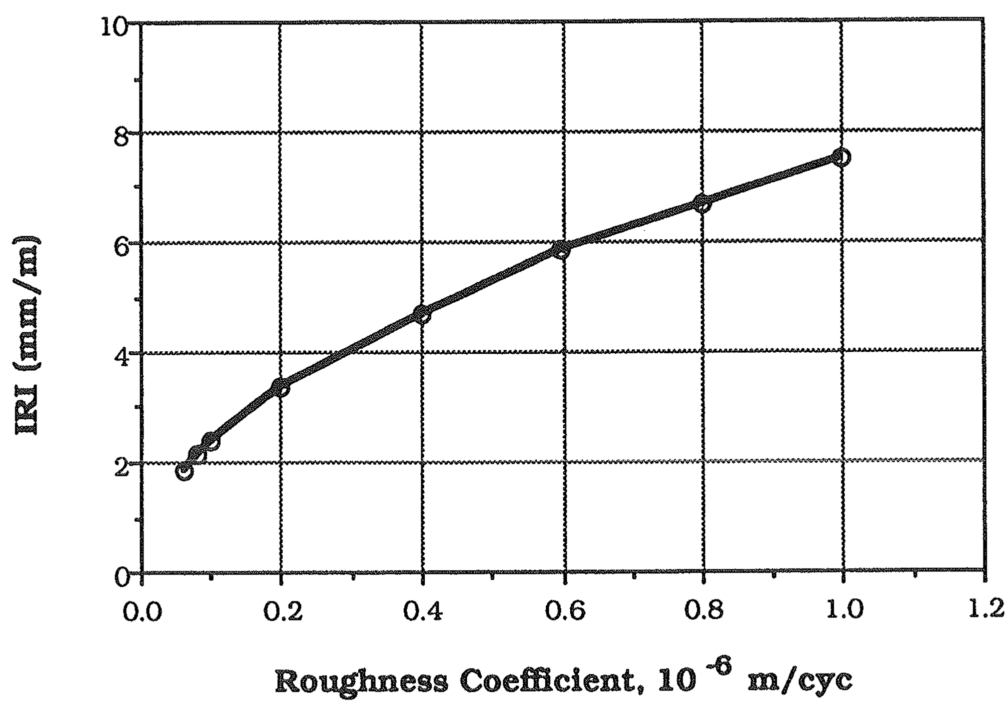

Fig. B-34. Roughness Coefficient of PSD vs. IRI.

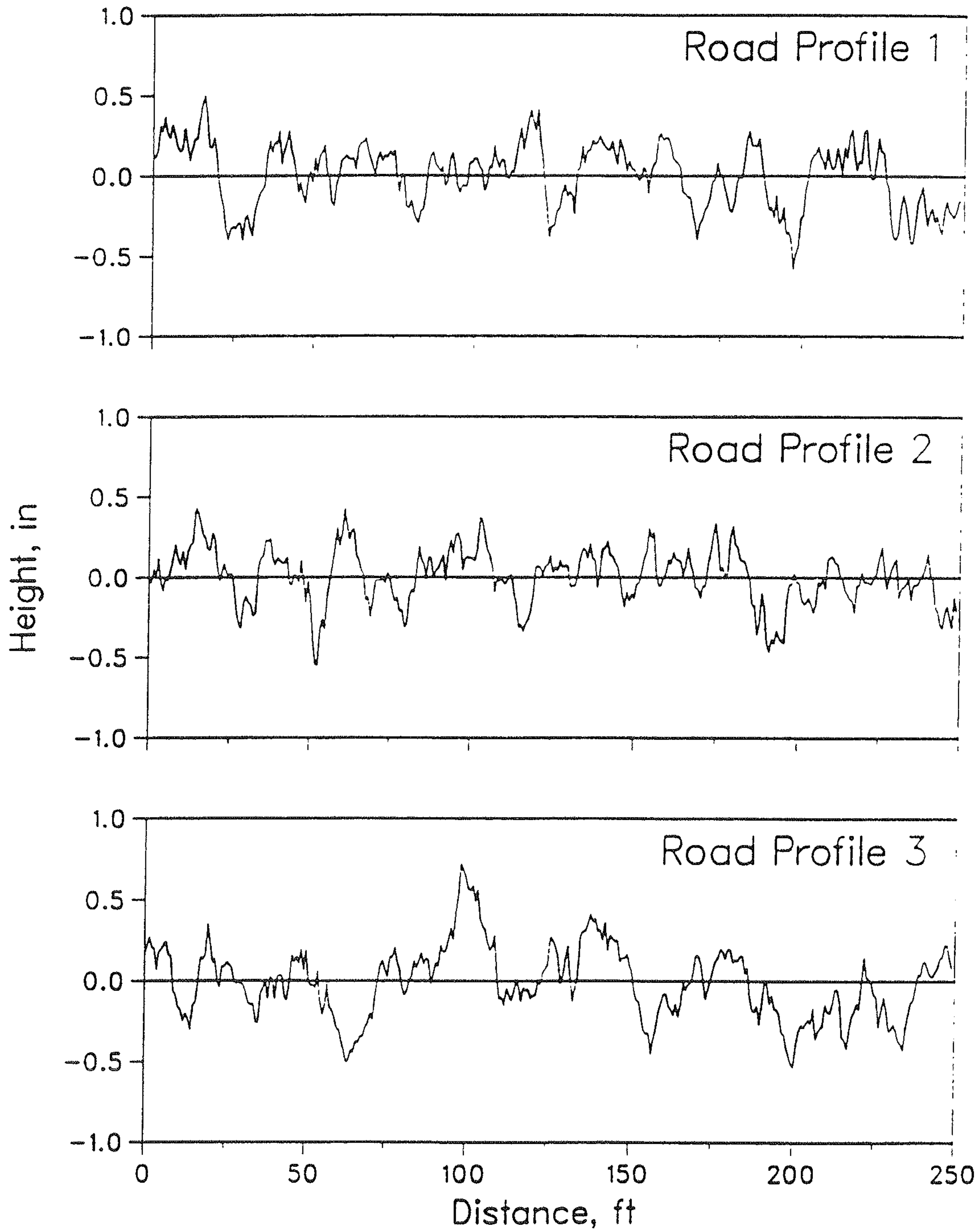

Fig. B-35. Three Independent Random Road Profiles.

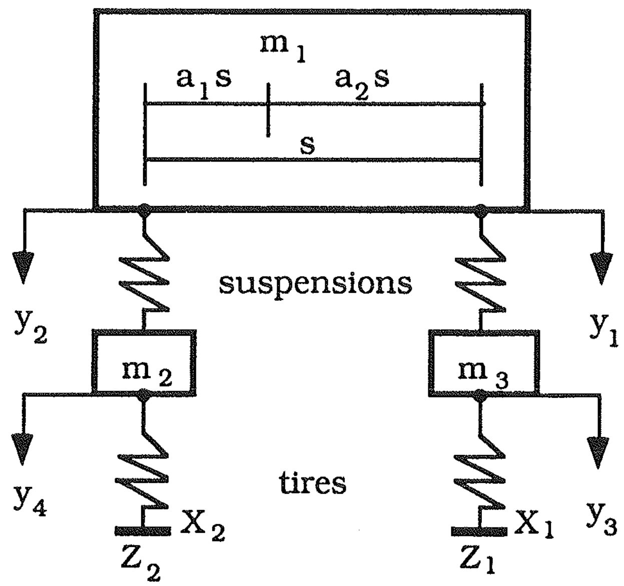

X_1, X_2: front and rear roughness (elevation)
Z_1, Z_2: front and rear bridge deflection

SF_1, SF_2: forces generated from suspension
TF_1, TF_2 : forces generated from tires

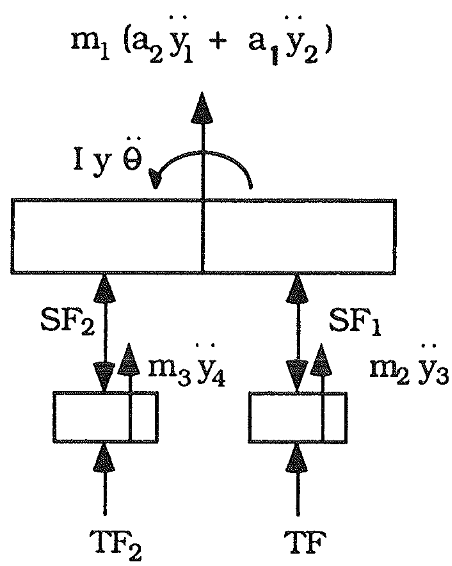

Fig. B-36. Model of a Three Axle Truck.

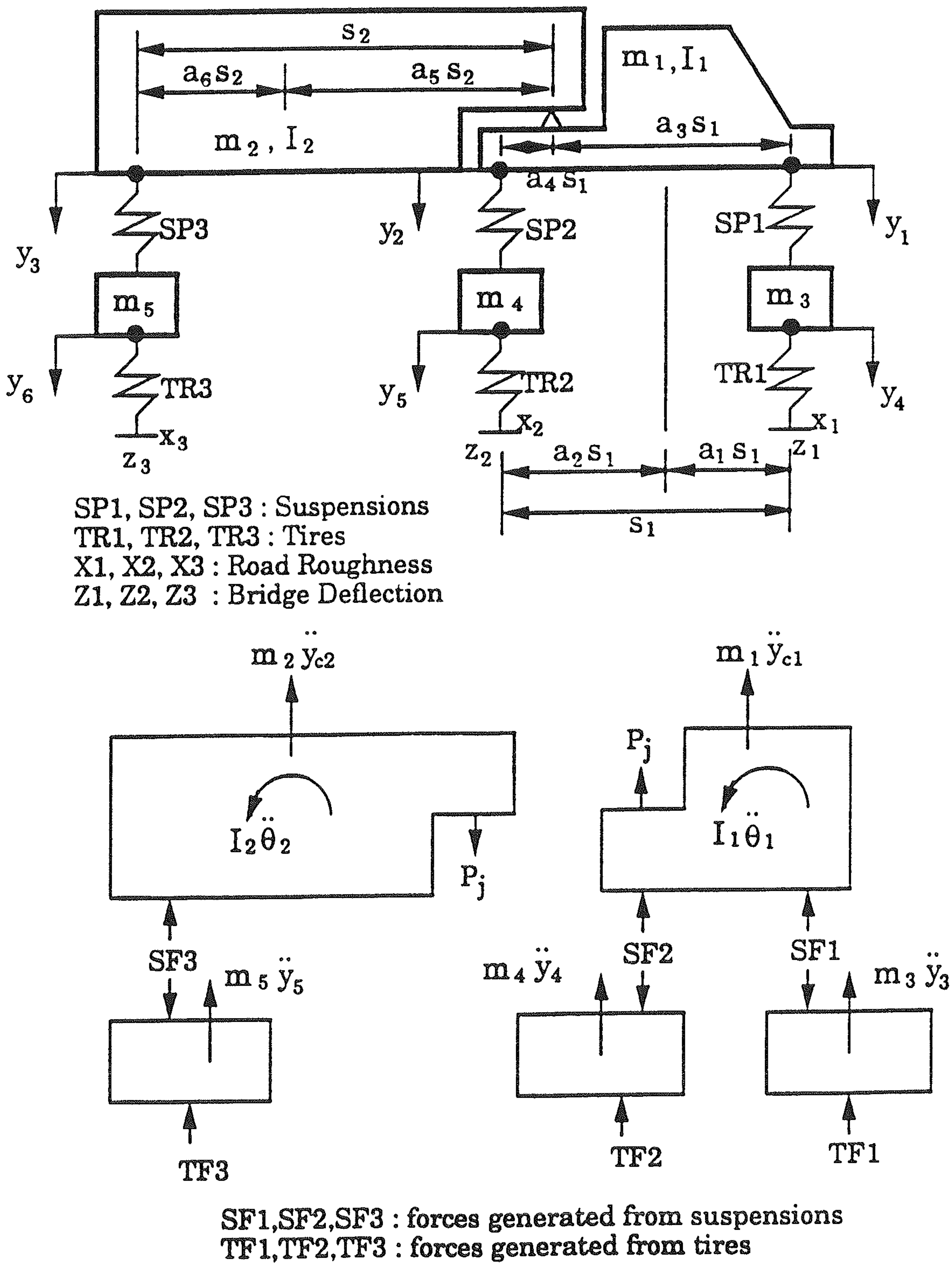

Fig. B-37. Model of a Five Axle Truck.

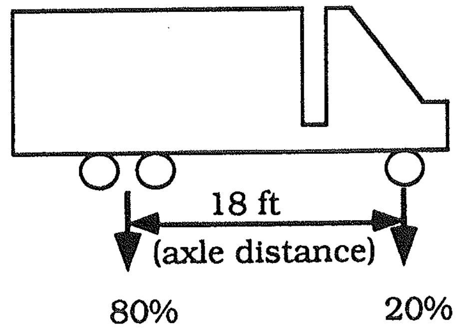

Fig. B-38. Load Distribution for the Three Axle Truck.

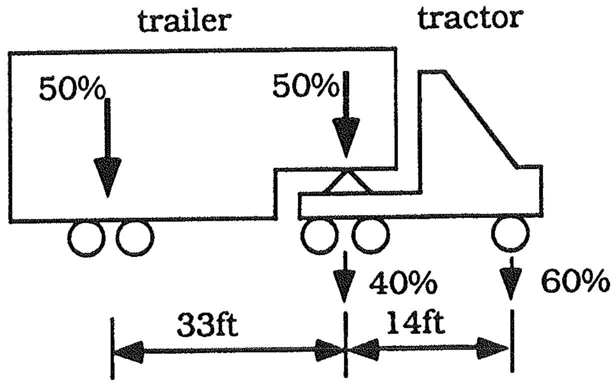

Fig. B-39. Load Distribution for the Tractor Trailer.

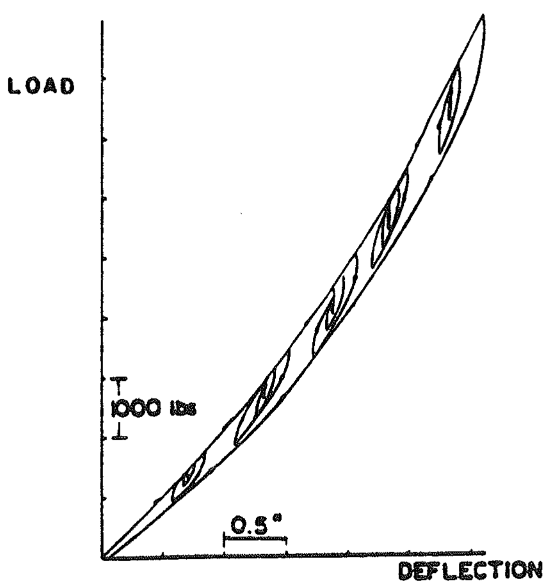

Fig. B-40. Force Deflection Diagram of Multi-Leaf Rear Spring for Tractors (B-15).

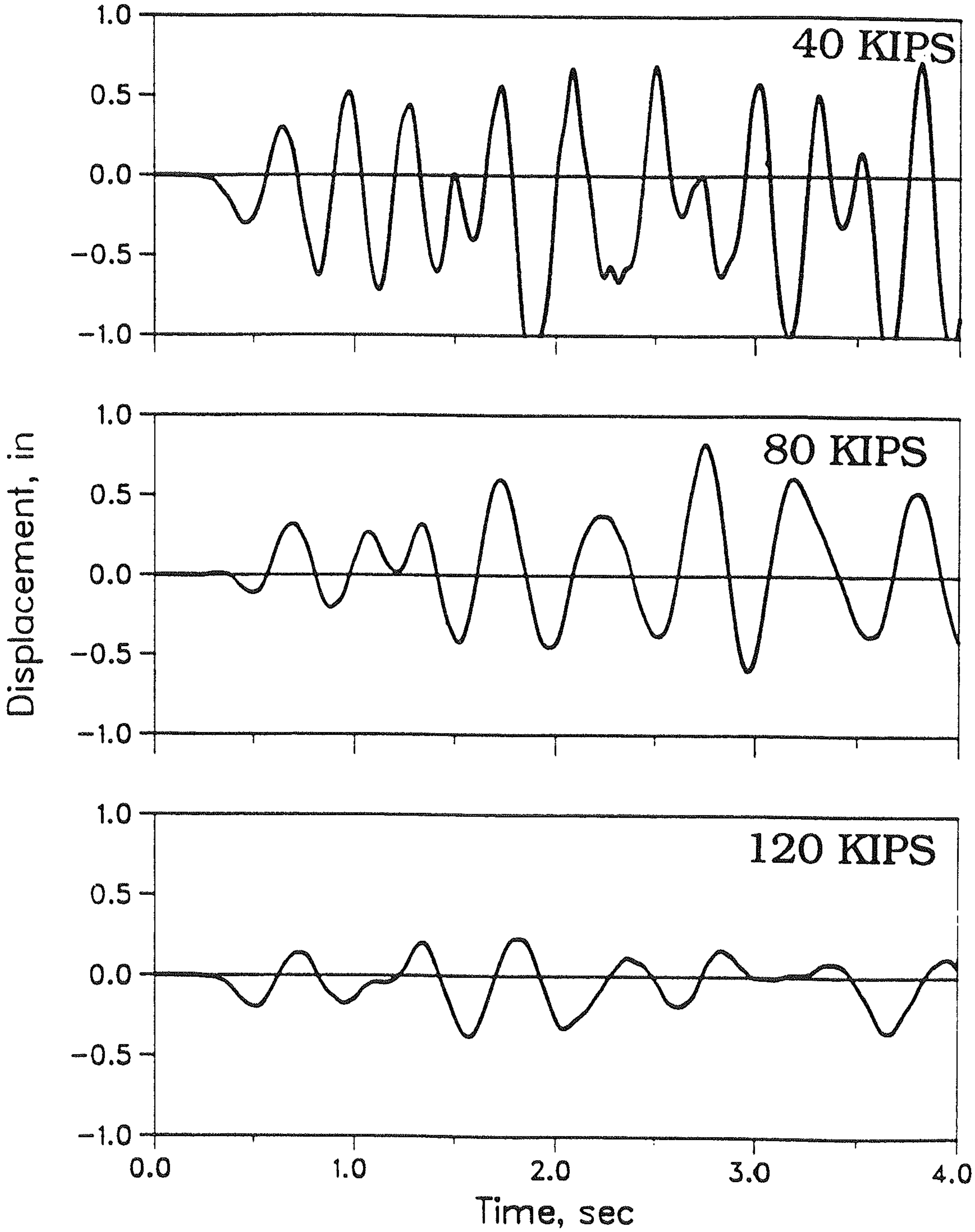

Fig. B-41. Time History of Trailer Bouncing for 40, 80 and 120 kip Tractor-Trailer.

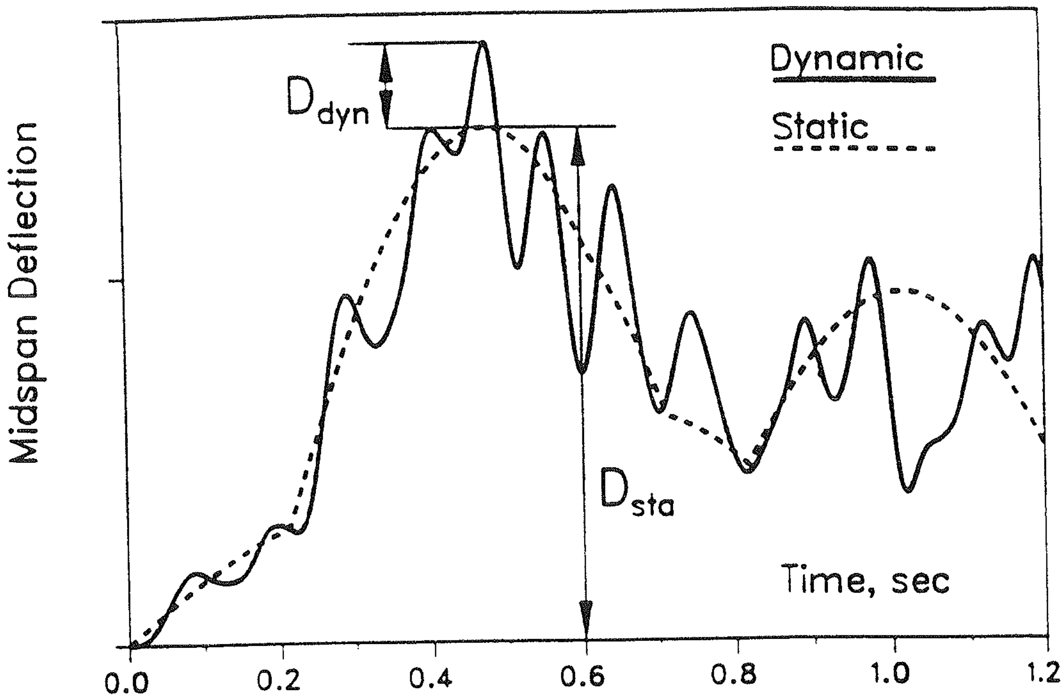

Fig. B-42. Time History for a Typical Bridge Midspan Deflection.

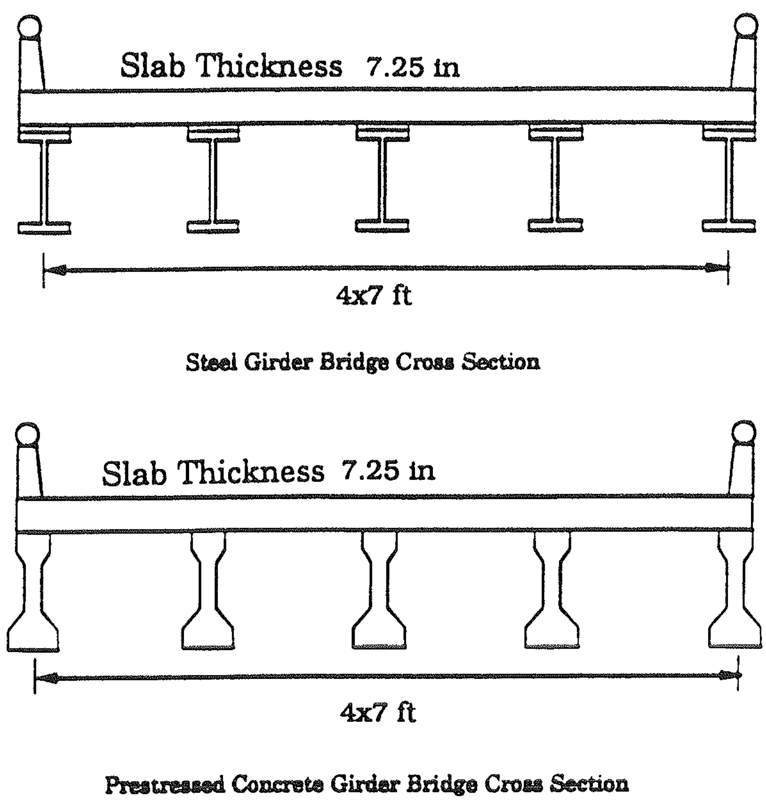

Fig. B-43. Cross Sections of Bridges Considered in Simulations.

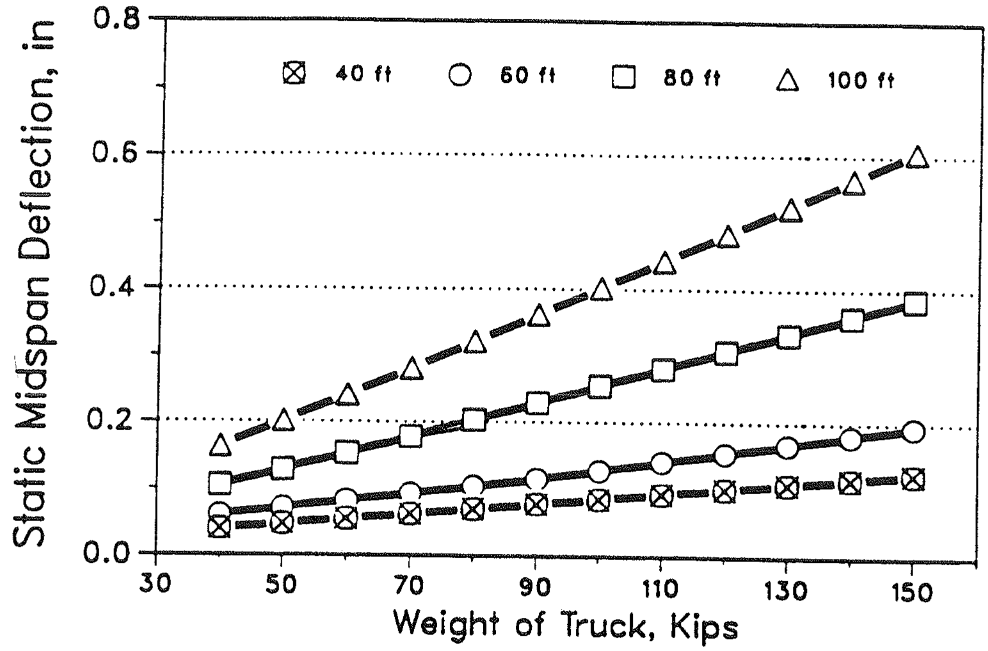

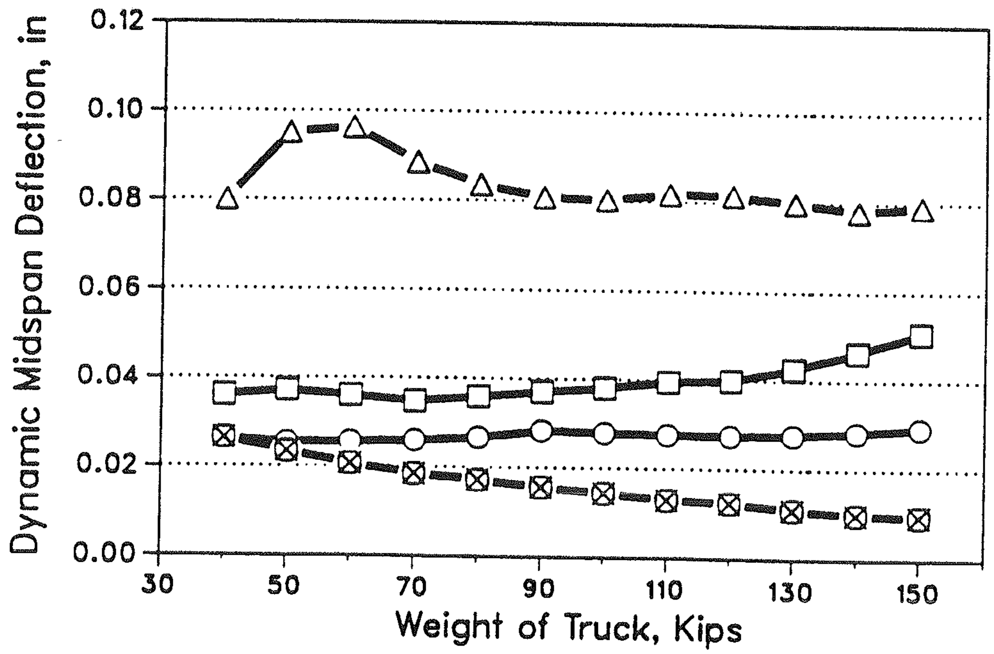

Fig. B-44. Static and Dynamic Deflections vs. Gross Vehicle Weight for a Five Axle Truck on Steel Girder Bridge.

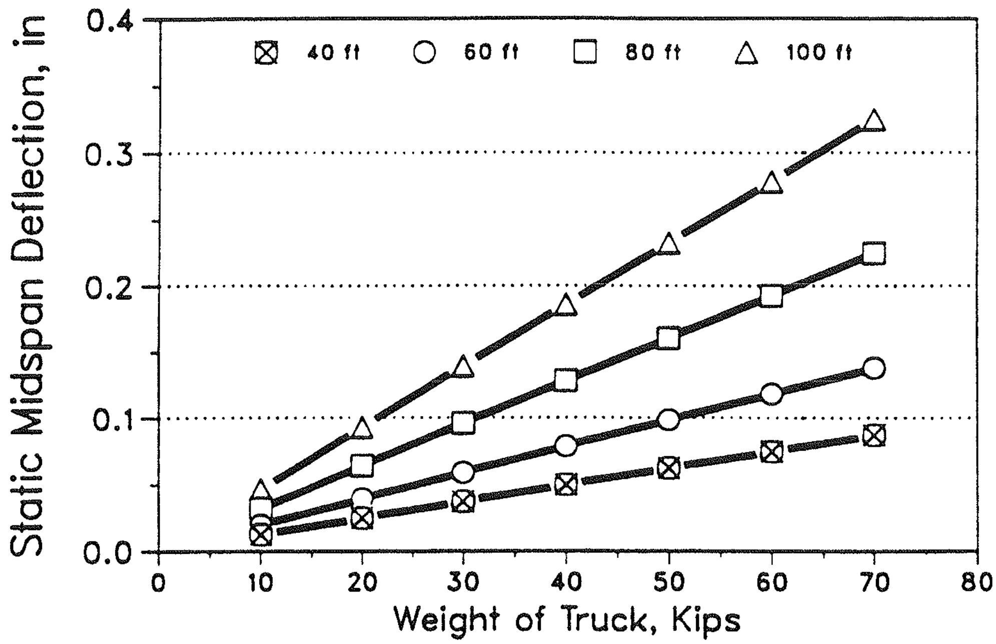

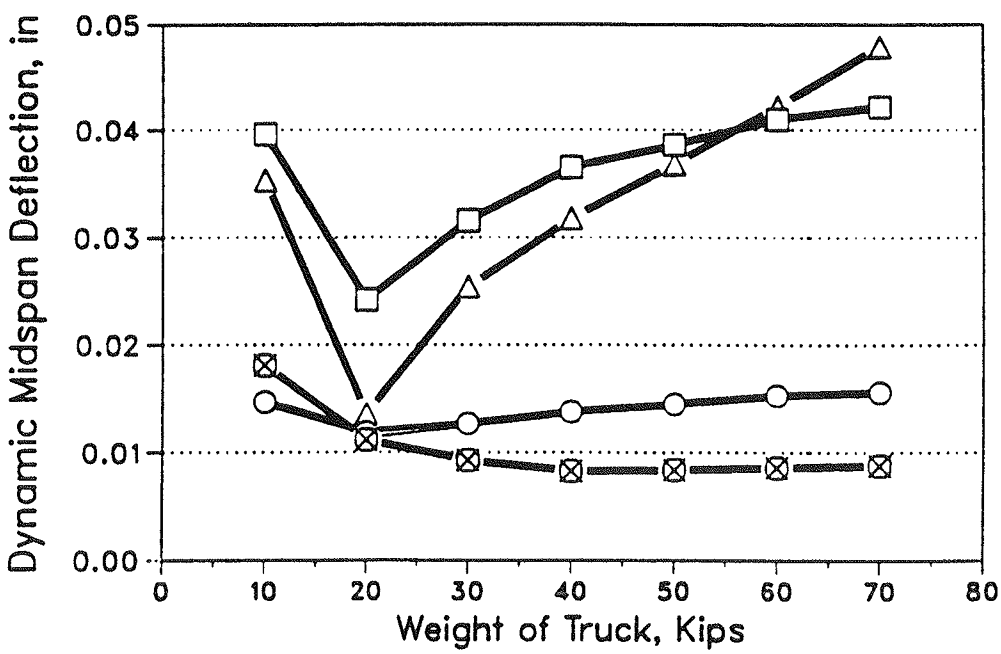

Fig. B-45. Static and Dynamic Deflections vs. Gross Vehicle Weight for a Three Axle Truck on Steel Girder Bridge.

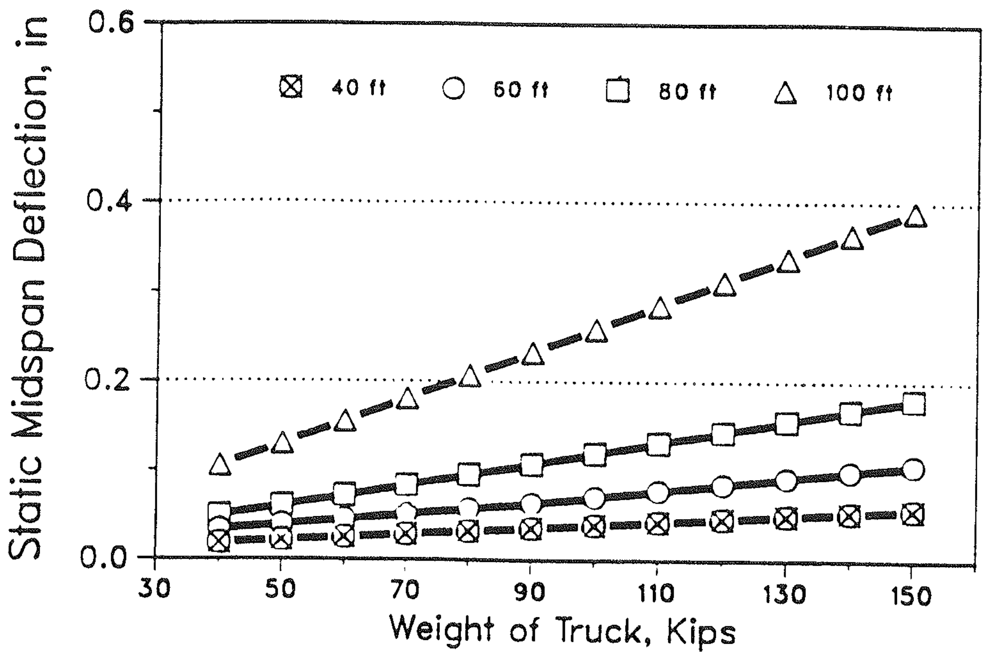

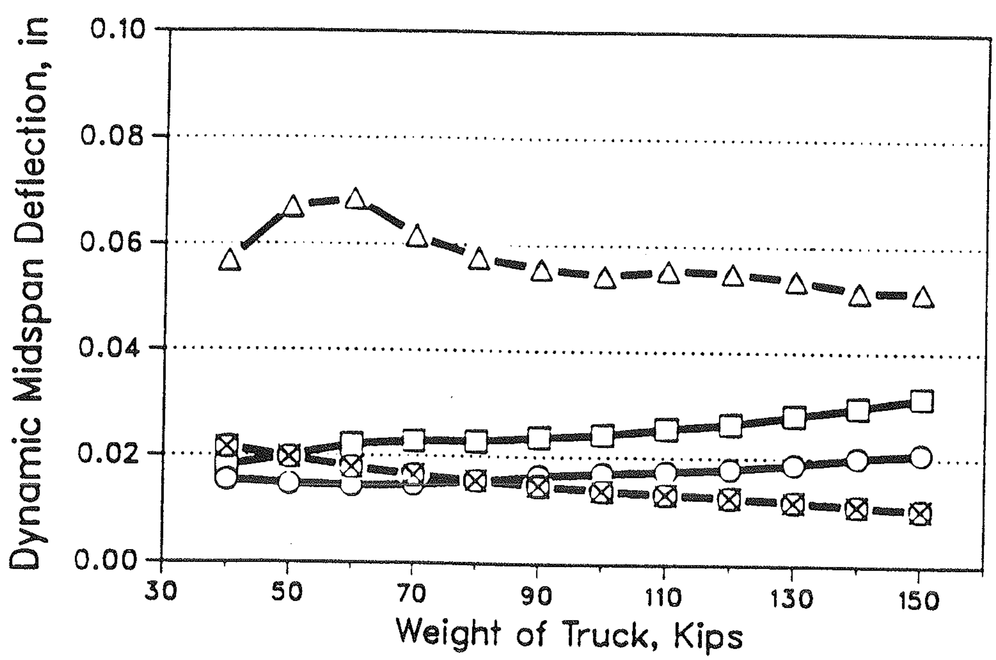

Fig. B-46. Static and Dynamic Deflections vs. Gross Vehicle Weight for a Five Axle Truck on Prestressed Concrete Girder Bridge.

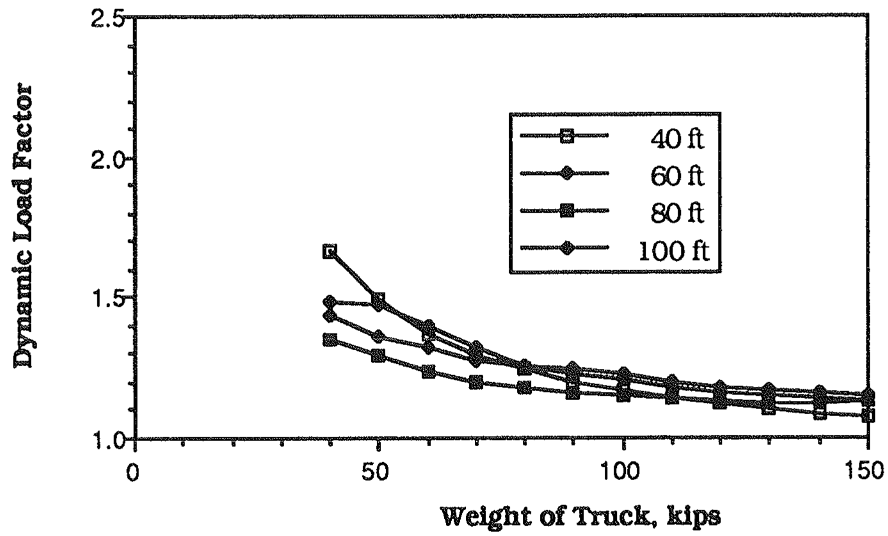

Fig. B-47. Dynamic Load vs. Gross Vehicle Weight for a Five Axle Truck on Steel Girder Bridge.

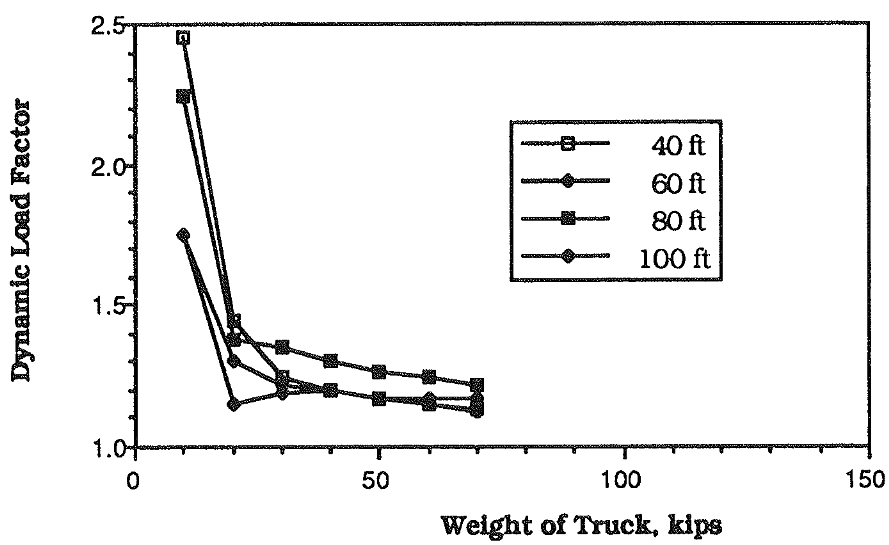

Fig. B-48. Dynamic Load vs. Gross Vehicle Weight for a Three Axle Truck on Steel Girder Bridge.

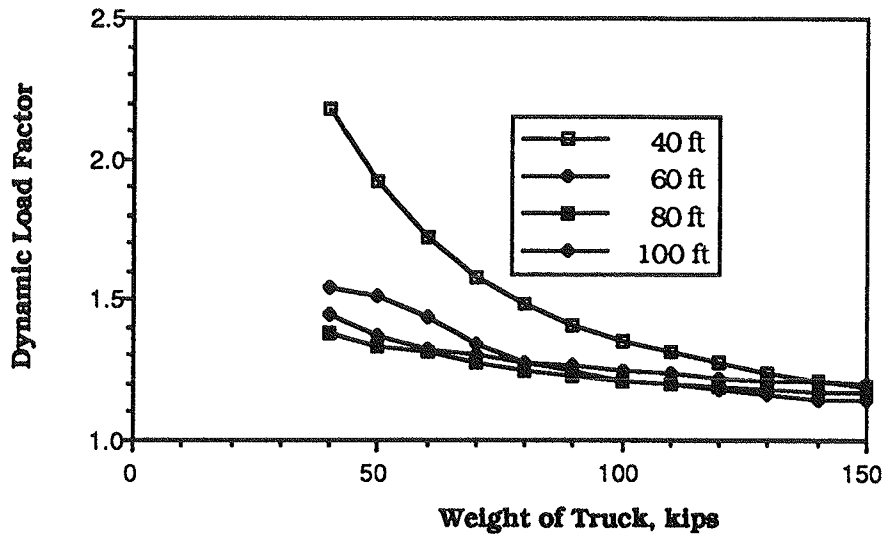

Fig. B-49. Dynamic Load vs. Gross Vehicle Weight for a Five Axle Truck on Prestressed Concrete Girder Bridge.

increase of static deflection. It was observed that the dynamic deflection is almost constant.

Effect of truck speed varies for different gross vehicle weights, as shown in Fig. B-50. It is also observed that the truck suspension characteristics depend on the vehicle speed and weight.

Effect of road roughness is shown in Fig. B-51. Road roughness is measured in terms of roughness coefficient of the power spectral density function of the road profile. As the coefficient is increased, DLF is increased for any gross vehicle weight.

The maximum 75 year value of DLF is calculated using Monte Carlo simulations. It is assumed that 20% of total truck traffic on highways are three axle single trucks and 80% are five axle tractor-trailers. Each truck is described by three random variables: weight, speed, and axle distance (for five axle tractor-trailer, axle distance is the distance between tractor rear axle and trailer axle). Statistical parameters of the random variables are shown in Tables B-18 and B-19. A hundred simulations were performed for each road profile, and 20 road profiles are considered for each case (2,000 computer runs).

The maximum static vs. dynamic deflections from simulations are shown in Fig. B-52 to B-55. To estimate the maximum 75 year value ($z = 5.32$), the simulated static deflections are plotted on the normal probability paper in Fig. B-56 to B-59. For each static deflection, the corresponding dynamic deflection is also plotted so that their vertical coordinates are the same. The DLF's associated with the mean maximum 75 year live loads are calculated using extrapolations.

In most cases, the maximum live load is governed by two trucks side-by-side. Therefore, the corresponding DLF's are calculated for two trucks by superposition of one truck effects as shown in Fig. B-60. Two identical five axle tractor-trailers are used, each weighing 120 kips. The obtained average DLF's for two trucks are presented in Fig. B-61. For comparison, DLF's are also plotted for one truck cases. The results are summarized in Table B-20.

In further calculations, the mean dynamic load is taken as 0.10 of the mean live load, m_L, for two trucks and 0.15 m_L for one truck. The coefficient of variation is taken as 0.80.

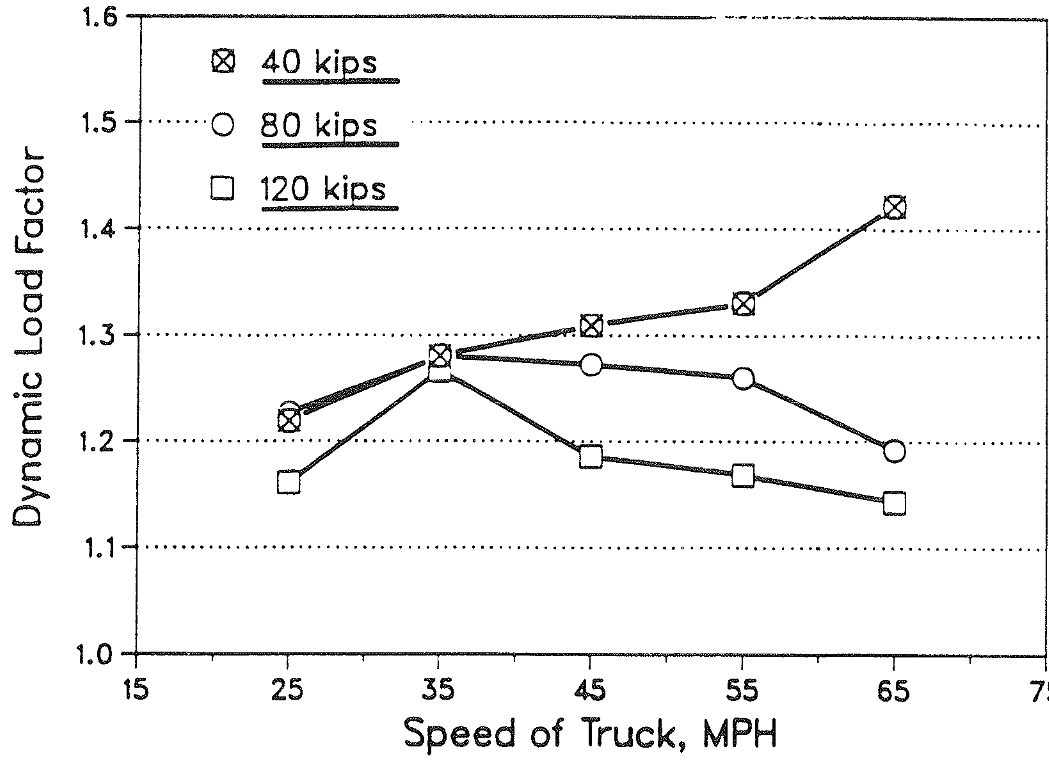

Fig. B-50. Dynamic Load vs. Truck Speed for a Five Axle Truck on Steel Girder Bridge.

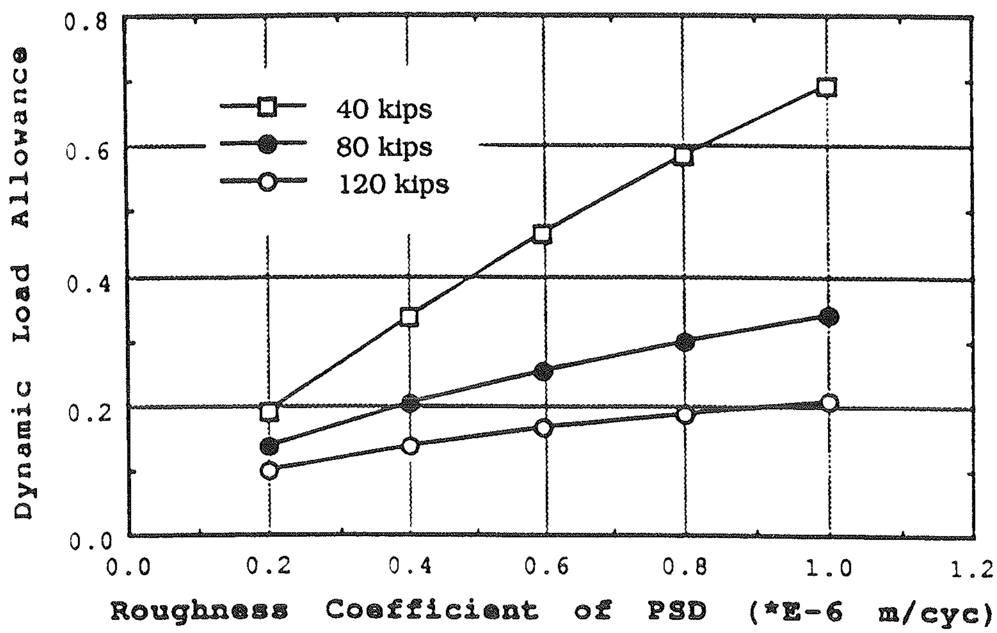

Fig. B-51. Dynamic Load vs. Roughness Coefficient of PSD.

Table B-18. Statistical Parameters For Three Axle Single Trucks.

Random Variable	Distribution Type	Mean	Coefficient of Variation	Min.	Max.
Gross Vehicle Weight	Normal	40 kips	0.21		
Axle distance	Uniform			10ft	25ft
Speed	Normal	55 mph	0.165		

Table B-19. Statistical Parameters For Five Axle Tractor Trailers.

Random Variable	Distribution Type	Mean	Coefficient of Variation	Min.	Max.
Gross Vehicle Weight	Normal	65 kips	0.26		
Axle distance	Uniform			27ft	42ft
Speed	Normal	55 mph	0.165		

Table B-20. Dynamic Load Factors from Simulations.

	Mean	Standard Deviation
One Truck	0.13 m_L	0.10 m_L
Two Trucks	0.09 m_L	0.06 m_L

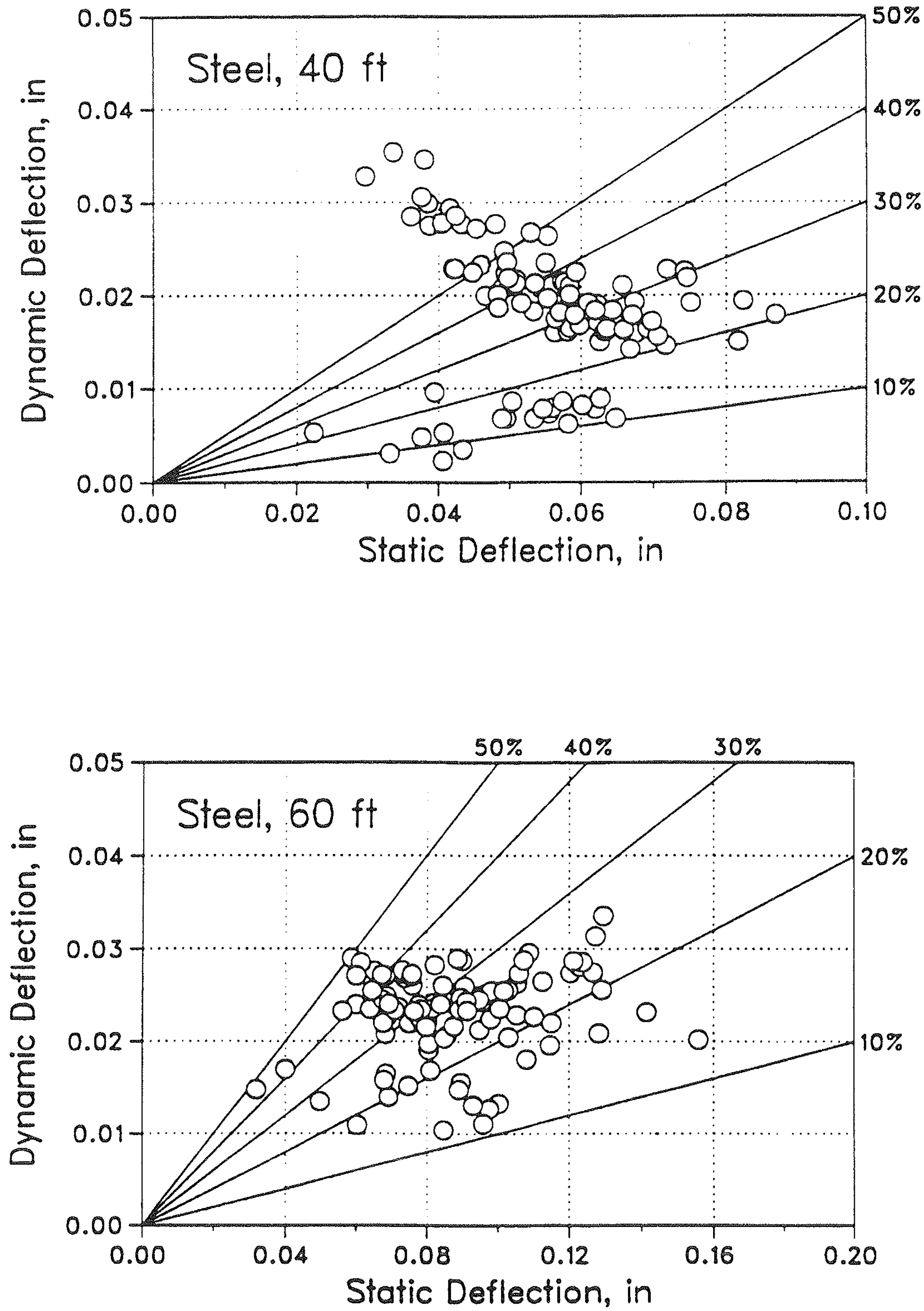

Fig. B-52. Static vs. Dynamic Deflections for 40 and 60 ft Steel Girder Bridges.

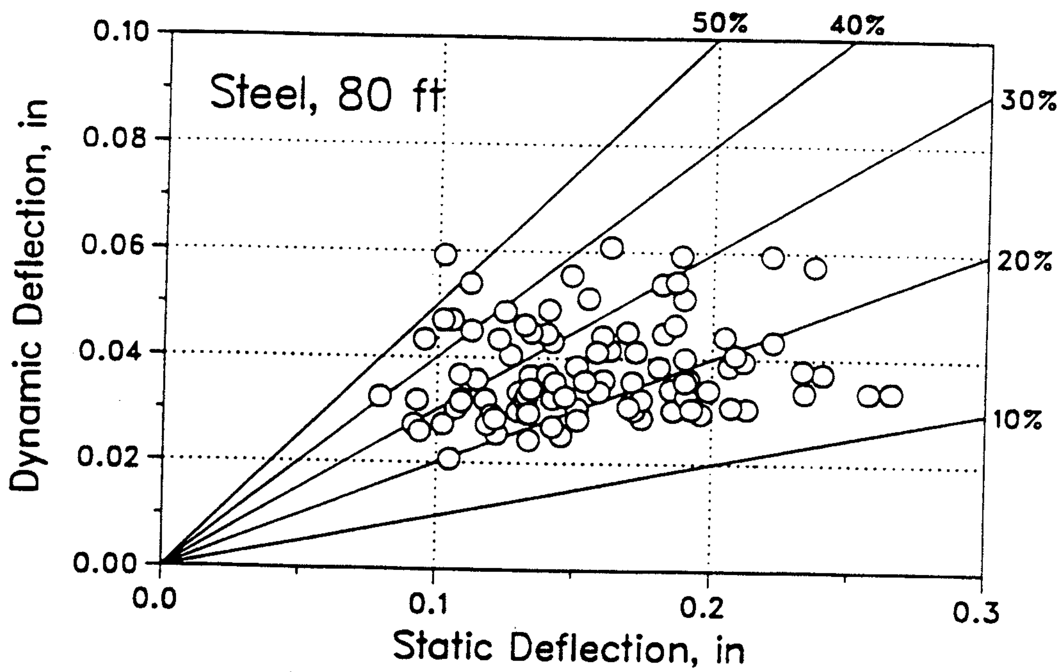

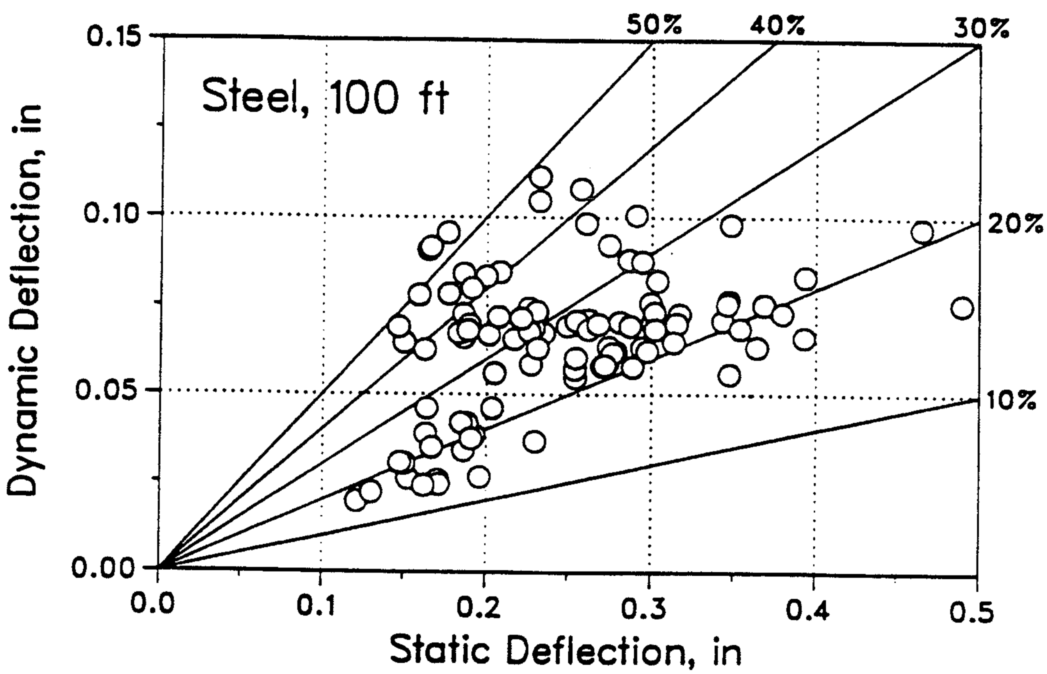

Fig. B-53. Static vs. Dynamic Deflections for 80 and 100 ft Steel Girder Bridges.

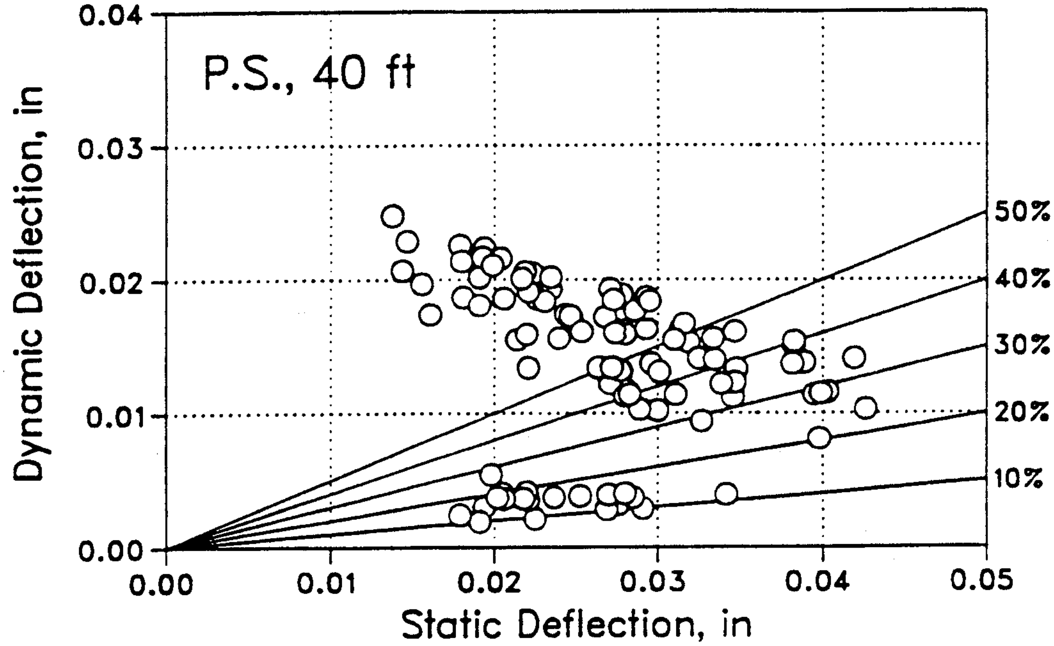

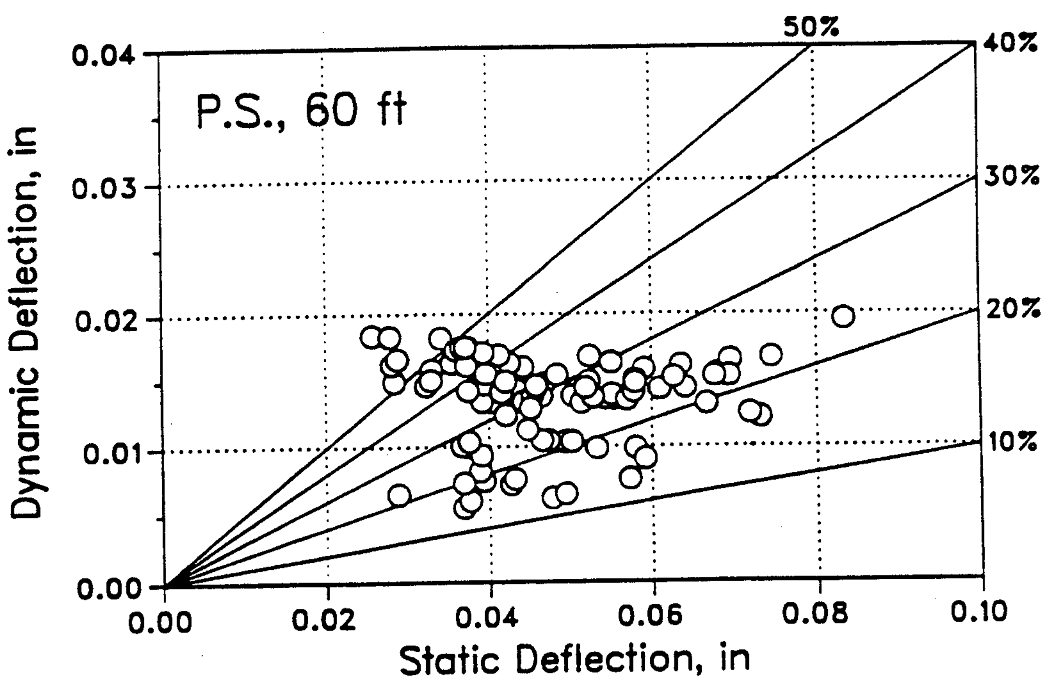

Fig. B-54. Static vs. Dynamic Deflections for 40 and 60 ft Prestressed Concrete Girder Bridges.

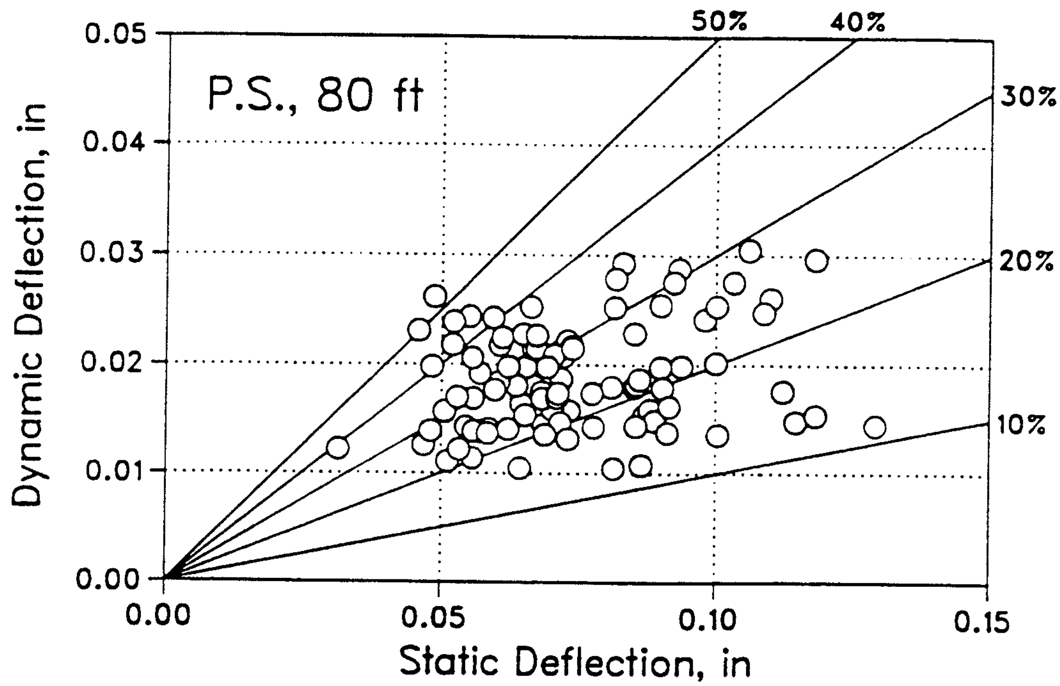

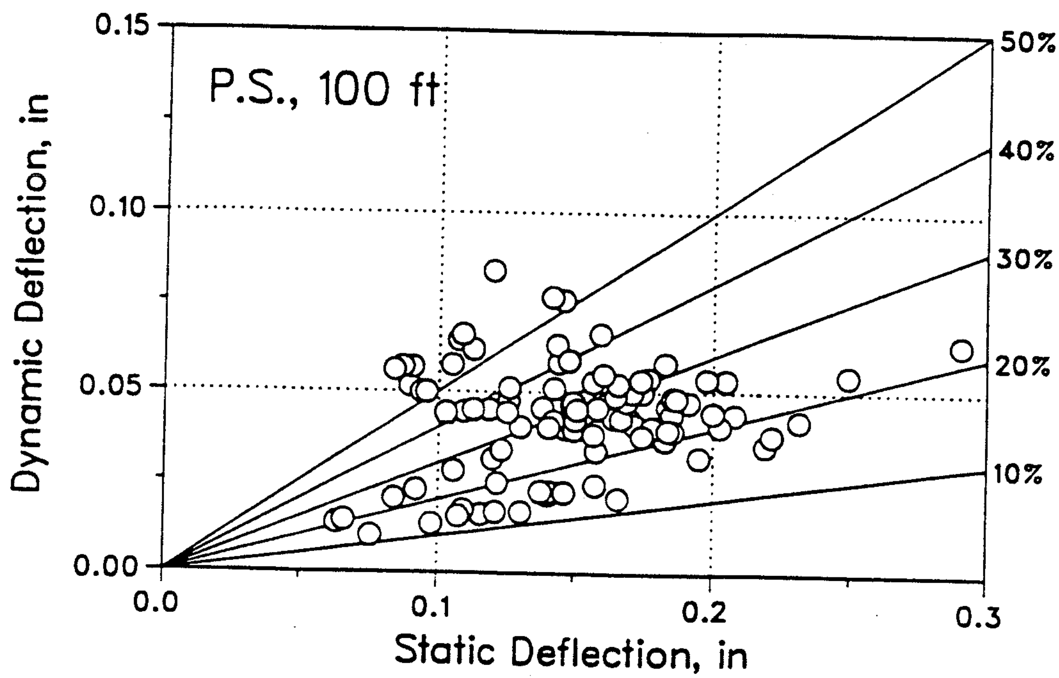

Fig. B-55. Static vs. Dynamic Deflections for 80 and 100 ft Prestressed Concrete Girder Bridges.

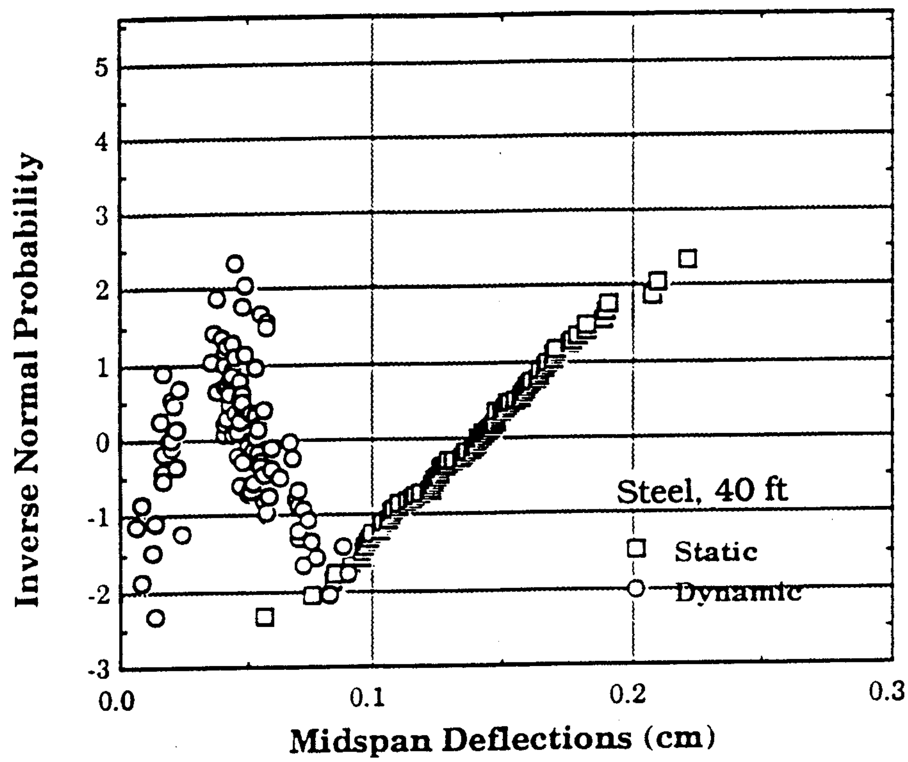

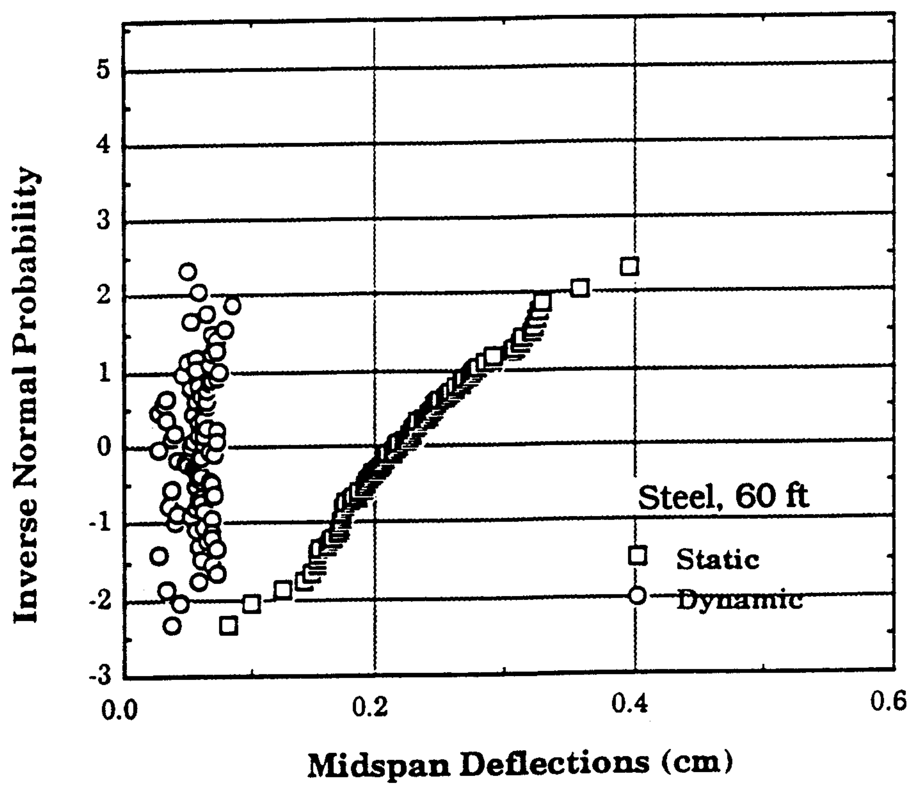

Fig. B-56. Simulation Results for 40 and 60 ft Steel Girder Bridges.

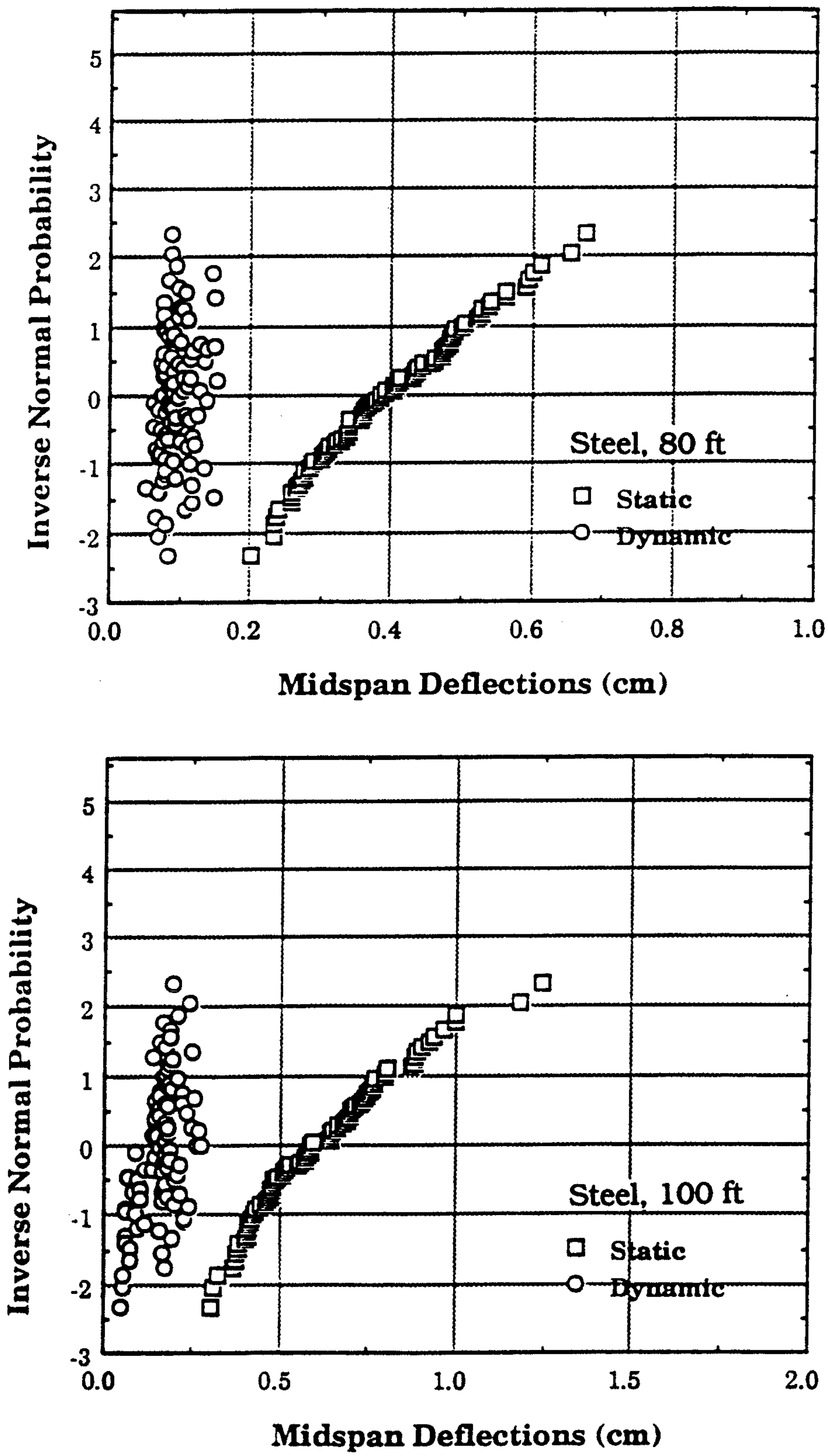

Fig. B-57. Simulation Results for 80 and 100 ft Steel Girder Bridges.

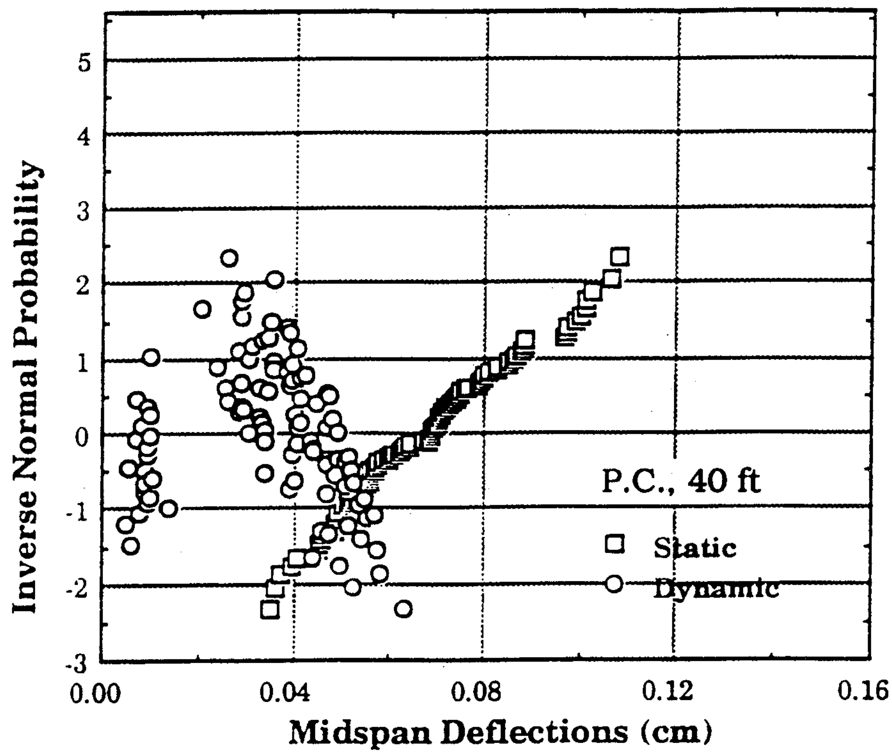

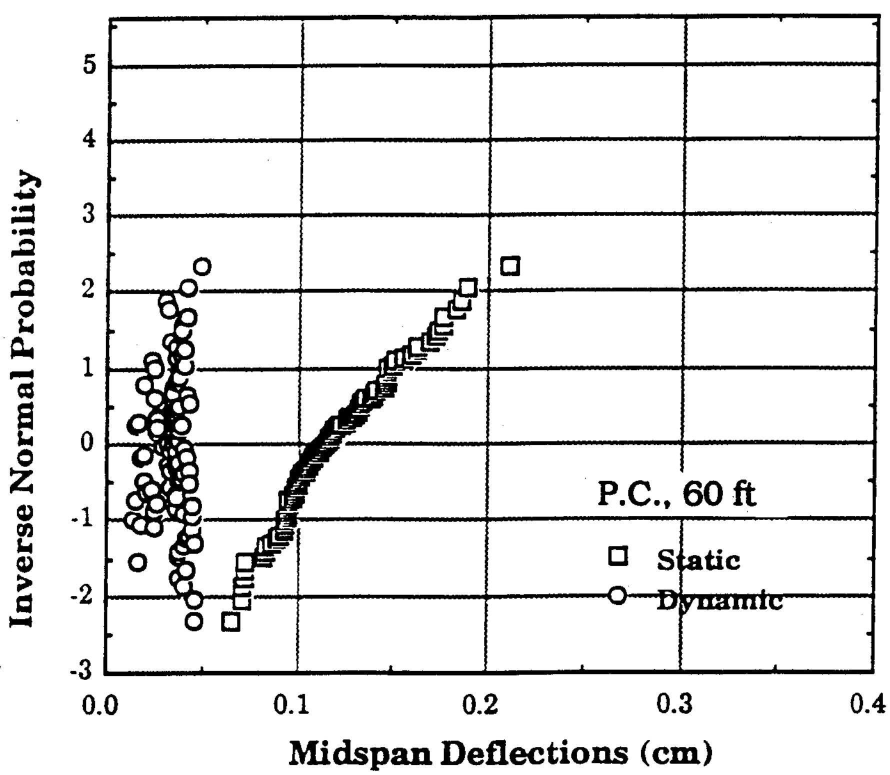

Fig. B-58. Simulation Results for 40 and 60 ft Prestressed Concrete Girder Bridges.

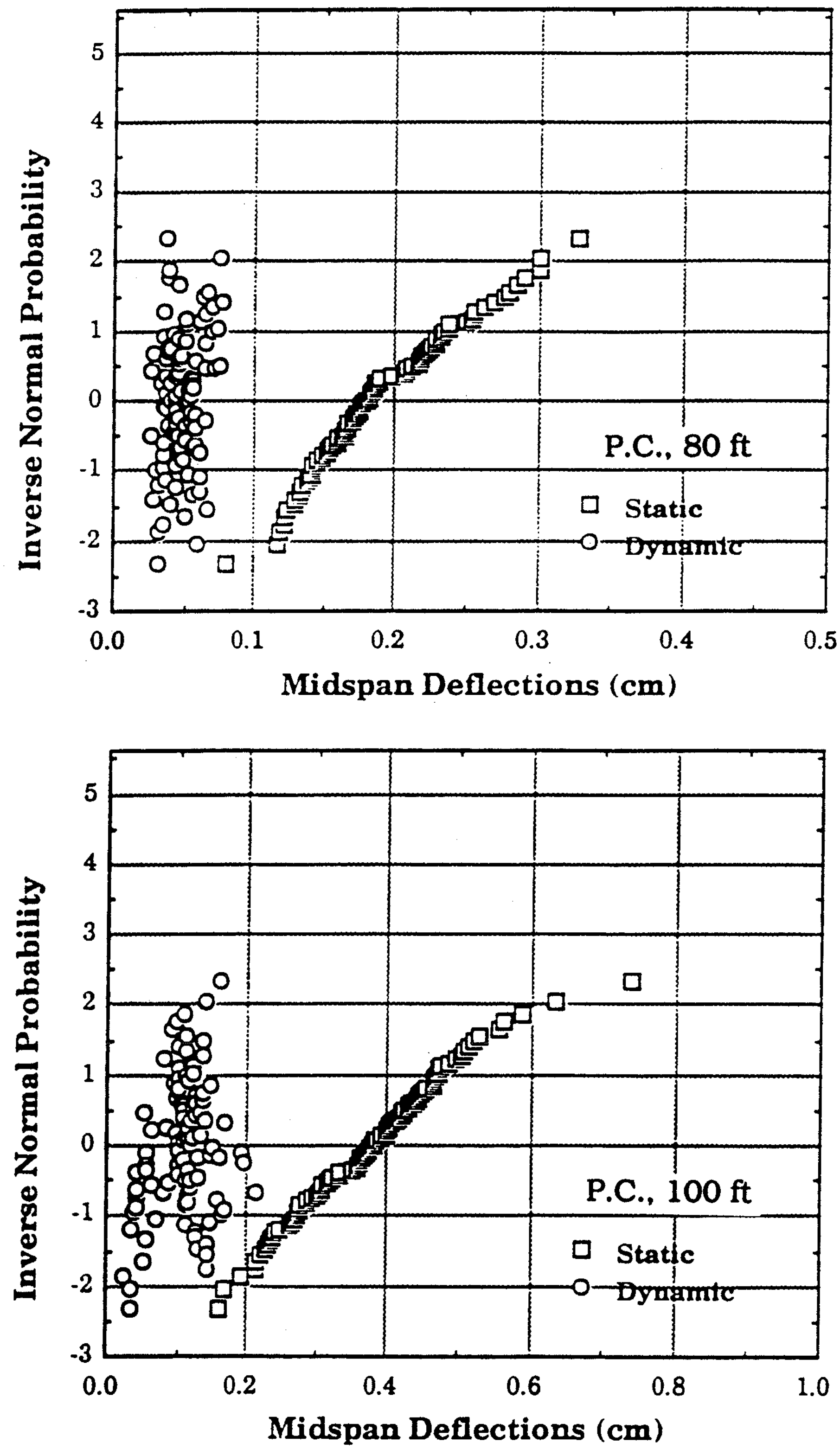

Fig. B-59. Simulation Results for 80 and 100 ft Prestressed Concrete Girder Bridges.

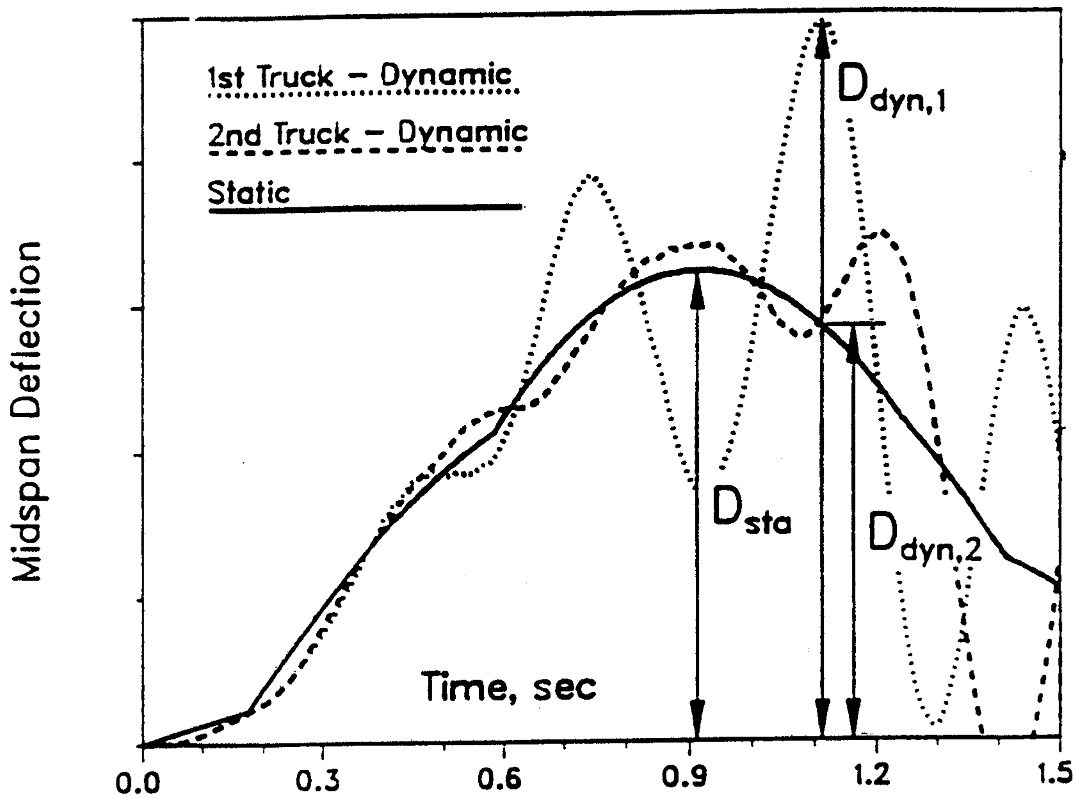

Fig. B-60. Time History for Two Trucks on the Bridge.

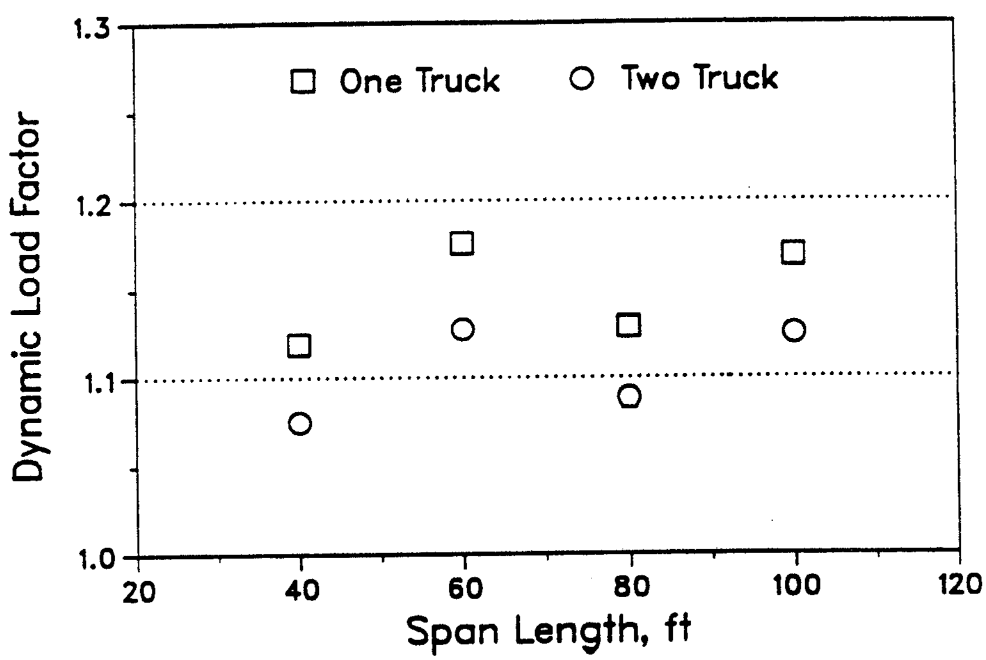

Fig. B-61. Average Dynamic Load vs. Span for One Truck and Two Trucks.

Recommended DLF Values

The results of simulations indicate that the DLF values are lower for two trucks than for one truck. In general, DLF is reduced for a larger number of axles. To determine the maximum 75 load effect, DLF is applied to the maximum 75 year live load. The dynamic load corresponding to an extremely heavy truck is close to the mean of DLF. For longer spans, the maximum live load is a resultant of two or more truck in lane. This corresponds to a reduced DLF. Therefore, the proposed nominal (design) DLF = 0.33, applied to the truck effect only, with no DLF applied to the uniformly distributed portion of live load. For wood bridges, the DLF is reduced by 50%.

LOAD COMBINATIONS

The total load, Q, is a combination of several components. However, the probability of a simultaneous occurrence of the extreme values is very low. The following combinations are considered in this report:

(1) D + L + I
(2) D + L + I + W
(3) D + L + I + EQ (B-5)

where W = wind and EQ = earthquake.

Live Load and Dynamic Load

The maximum 75 year combination of live load, L, and dynamic load, I, is modeled using the statistical parameters derived for L and I in this report.

It is assumed that the live load is a product of two parameters, LP, where L is the static live load and P is the live load analysis factor (influence factor). The mean value of P is 1.0 and the coefficient of variation is 0.12. The coefficient of variation of LP can be calculated using the following formula,

$$V_{LP} = (V_L^2 + V_P^2)^{1/2} \qquad \text{(B-6)}$$

where V_L = coefficient of variation of L and V_P = coefficient of variation of P.

The mean maximum 75 year LP+I, m_{LP+I}, can be calculated by multiplying the mean L by the mean value of P (equal to 1.0) and by (1+I), where I is the mean dynamic load.

The standard deviation of the maximum 75 year LP+I, σ_{LP+I}, is

$$\sigma_{LP+I} = (\sigma_{LP}^2 + \sigma_I^2)^{1/2} \tag{B-7}$$

where $\sigma_{LP} = V_{LP}\ m_{LP}$; m_{LP} = mean LP, equal to mean L, because mean P = 1; $\sigma_I = V_I\ m_I$, standard deviation of the dynamic load.

The coefficient of variation of LP+I, V_{LP+I}, is

$$V_{LP+I} = \sigma_{LP+I}/m_{LP+I} \tag{B-8}$$

The statistical parameters of L and I depend on span length and they are different for a single lane and two lanes. For a single lane V_{LP+I} = 0.19 for most spans, and 0.205 for very short spans. For two lane bridges, V_{LP+I} = 0.18 for most spans, and 0.19 for very short spans.

Dead Load, Live Load and Dynamic Load

The basic load combination for highway bridges is a simultaneous occurrence of dead load, live load and dynamic load. The uncertainty involved in the load analysis is expressed by load analysis factor E. The mean E is 1.0 and the coefficient of variation is 0.04 for simple spans and 0.06 for continuous spans.

The load, Q is given in the following form,

$$Q = E\ (D_1 + D_2 + D_3 + L + I) \tag{B-9}$$

The mean Q, m_Q, is equal to the sum of the means of components (D_1, D_2, D_3, L and I). Coefficient of variation of Q, V_Q, is

$$V_Q = (V_E^2 + V_{D1+D2+D3+L+I}^2)^{1/2} \tag{B-10}$$

where

$$V_{D1+D2+D3+L+I} = \sigma_{D1+D2+D3+L+I}/m_Q; \tag{B-11}$$

and

$$\sigma_{D1+D2+D3+L+I} = (\sigma_{D1}^2 + \sigma_{D2}^2 + \sigma_{D3}^2 + \sigma_{LP+I}^2)^{1/2} \tag{B-12}$$

Other Load Combinations

The total load effect, Q, is the result of dead load, live load, dynamic load and other effects (environmental, other). There are several load combinations for consideration in the reliability analysis of bridges.

For time varying loads, the model depends on the considered time interval. This particularly applies to environmental loads including wind, earthquake, snow, ice, temperature, water pressure, etc. The load models can be based on the report by Ellingwood, Galambos, MacGregor and Cornell (B-3) or Nowak and Curtis (B-16). The basic data has been gathered for building structures, rather than bridges. However, in most cases the same model can be used. Some special bridge related problems can occur because of the unique design conditions, such as foundation conditions, extremely long spans, or wind exposure.

Load effect is a resultant of several components. It is unlikely, that all components take their maximum values simultaneously. There is a need for a formula to calculate the parameters of Q (mean and coefficient of variation). In general all load components are time-variant, except for dead load. There are sophisticated load combination techniques available to calculate the distribution of the total load, Q. However, they involve a considerable numerical effort. Some of these methods are summarized by Thoft-Christensen and Baker (B-17) and Melchers (B-18).

The total load effect in highway bridge members is a joint effect of dead load D, live load L+I (static and dynamic), environmental loads E (wind, snow, ice, earthquake, earth pressure and water pressure), and other loads A (emergency braking, collision forces),

$$Q = D + L + I + E + A \tag{B-13}$$

The effect of a sum of loads is not always equal to the sum of effects of single loads. In particular this may apply to the nonlinear behavior of the structure. Nevertheless, it is further assumed that Eq. B-12 represents the joint effect. The distribution of the joint effect is based on the so called Turkstra's rule. Turkstra (B-19) observed that a combination of several load components reaches its extreme when one of the components takes an extreme value and all other components are at their average (arbitrary-point-in-time) level. For example, the combination of live load with earthquake produces a maximum effect for the lifetime T, when either,

1. Earthquake takes its maximum expected value for T and live load takes its maximum expected value corresponding to the duration of earthquake (about 30 seconds), or

2. Live load takes its maximum expected value for T and earthquake takes its maximum expected value corresponding to duration of this maximum live load (time of truck passage on the bridge).

In practice, the expected value of an earthquake in any short time interval is almost zero. The expected value of truck load for a short time interval depends on the class of the road. For a very busy highway it is likely that there is some traffic at any point in time. Therefore, the maximum earthquake may occur simultaneously with an average truck passing through the bridge.

In the general case, Turkstra's rule can be expressed as follows,

$$Q(\max) = \max Q_i \quad \text{for } i = 1, 2, 3 \text{ and } 4 \tag{B-14}$$

where,

$$Q_1 = D(\max) + (L + I)(ave) + E(ave) + A(ave)$$
$$Q_2 = D(ave) + (L + I)(\max) + E(ave) + A(ave)$$
$$Q_3 = D(ave) + (L + I)(ave) + E(\max) + A(ave)$$
$$Q_4 = D(ave) + (L + I)(ave) + E(ave) + A(\max)$$

In all cases, the average load value is calculated for the period of time corresponding to the duration of the maximum load. The formula can be extended to include various components of D, E, and A.

The joint distribution can be modeled using the central limit theorem of the theory of probability (B-20). A sum of several random variables is a normal random variable if the number of components is large, and if the average values of the components are of the same order. If one variable dominates (its mean value is much larger than any other), then the joint distribution is close to that of the dominating variable.

For each sum Q_i in Eq. B-14, the mean and variance of the sum are equal to the sum of means and the sum of variances of components, respectively.

The distribution of Q is that which minimizes the overall structural reliability. Usually, it is Q_i with the largest mean value. If the means are similar, then the largest standard deviation may point to the governing combination. In some cases, the analysis has to be performed for several Q_i's to determine the one which governs. The identification of the governing load combination is important in the selection of the optimum load factors (including load combination factors).

Therefore, for each load component, the maximum and average values are estimated. Dead load does not vary with time. Therefore, the maximum and average values are the same. The maximum 75 year live load (including dynamic load) is described in this report. For shorter duration the values are also available.

The statistical parameters of wind and earthquake are given in Table B-21.

The probability of an earthquake EQ or heavy wind W, occurring in a short period of time is very small. Therefore, simultaneous occurrence of EQ and W is not considered. In the result, the number of load combinations considered in the code can be reduced as follows,

$$Q_{max} = D + \max \begin{cases} (L+I)_{max} \\ W_{max}; \\ (L+I)_{4\ hour} + W_{daily} \\ EQ_{max} \end{cases} \tag{B-15}$$

where $(L+I)_{max}$ = maximum 75 year L+I; $(L+I)_{4\ hour}$ = maximum 4 hour L+I; W_{max} = maximum 75 year wind; W_{daily} = maximum daily wind; EQ_{max} = maximum 75 year earthquake.

The mean maximum 4 hour live load moment, $(L+I)_{4\ hour}$, can be read directly from Fig. B-2, B-3 and B-4, for z = 2.5 (maximum of 200 trucks). The parameters of $(L+I)_{4\ hour}$ are also shown in Table B-21.

Therefore, if the load factors for the first load combination are:

$$1.25\ D + 1.70\ (L + I) \tag{B-16}$$

and for the second one they are,

$$1.25\ D + 1.40\ W \tag{B-17}$$

then for the third combination, the load factors are,

$$1.25\ D + 1.35\ (L + I) + 0.45\ W \tag{B-18}$$

where live load factor = (0.80)(1.70) = 1.36 (mean maximum daily truck is 0.8-0.9 of the mean maximum 75 year truck); wind load factor = (0.33)(1.40) = 0.46 (mean maximum daily wind is 0.33 of the mean maximum 75 year wind).

Environmental loads include a wide range of components. Some of these components, e.g. water pressure, have a longer duration period (weeks or even months rather than minutes or hours). Therefore, a simultaneous occurrence with a maximum monthly or annual live load may govern.

Table B-21 Statistical Parameters of Wind and Earthquake

Load Component	Maximum 75 Year Load Bias	Maximum 75 Year Load COV	Basic Time Period	Live Load Corresponding to Basic Time Period Bias	Live Load Corresponding to Basic Time Period COV
Wind	0.875	0.20	4 hours	0.80-0.90	0.25
Earthquake	0.30	0.70	30 sec.	0-0.50	0.50

References for Appendix B

B-1. AASHTO, Standard Specifications for Highway Bridges, American Association of State Highway and Transportation Officials, Washington, D.C., (1989).

B-2. Nowak, A. S. and Lind, N. C., "Practical Bridge Code Calibration," ASCE Journal of the Structural Division, Vol. 105, No. 12, (1979), pp. 2497-2510.

B-3. Ellingwood, B. Galambos, T.V., MacGregor, J.G. and Cornell C.A., "Development of a Probability Based Load Criterion for American National Standard A58", National Bureau of Standards, NBS Special Publication 577, Washington, D.C. (1980).

B-4. Nowak, A.S. and Zhou, J.H., "Reliability Models for Bridge Analysis", Report UMCE 85R3, University of Michigan, Ann Arbor, MI, (1985).

B-5. Goble, G. et al., "Load Prediction and Structural Response", Draft of the Report prepared for FHWA, University of Colorado, Boulder, CO. (1991).

B-6. Nowak, A.S. and Nassif, H., "Effect of Truck Loading on Bridges", Report UMCE 91-11, Department of Civil Engineering, University of Michigan, Ann Arbor, MI, (1991).

B-7. Agarwal, A.C. and Wolkowicz, M., "Interim Report on 1975 Commercial Vehicle Survey", Research and Development Division, Ministry of Transportation, Downsview, Ontario, Canada, (1976).

B-8. OHBDC, Ontario Highway Bridge Design Code, Ministry of Transportation, Downsview, Ontario, Canada, (1979; 1983; 1993).

B-9. Nowak, A.S., Nassif, H. and DeFrain, L., "Effect of Truck Loads on Bridges", ASCE Journal of Transportation Engineering, Vol. 119, No. 6, (1993), pp. 853-867.

B-10. Zokaie, T., Osterkamp, T.A. and Imbsen, R.A., "Distribution of Wheel Loads on Highway Bridges", NCHRP 12-26/1, Proposed changes in AASHTO, Imbsen and Associates, Sacramento, CA, (1992).

B-11. Hwang, E-S. and Nowak, A.S., "Simulation of Dynamic Load for Bridges", ASCE Journal of Structural Engineering, Vol. 117, No. 5, (1991), pp. 1413-1434.

B-12. Hwang, E.S., "Dynamic Loads for Girder Bridges", PhD Thesis, Department of Civil Engineering, University of Michigan, Ann Arbor, MI, (1990).

B-13. Billing, J.R., "Dynamic Loading and Testing of Bridges in Ontario', Canadian Journal of Civil Engineering, Vol. 11, No. 4, December, (1984), pp. 833-843.

B-14. Moses, F. et al., "Loading Spectrum Experienced by Bridge Structures in the United States", Report No. FHWA/RD-85/012, Case Western Reserve University, Cleveland, OH, (1985).

B-15. Fancher, P.S., Ervin, R.D., MacAdam, C.C. and Winkler, C.B., "Measurement and Representation of the Mechanical Properties of Truck Leaf Springs", Society of Automotive Engineers, Technical Paper Series 800905, Warrendale, PA. (1980).

B-16. Nowak, A.S. and Curtis, J.D., "Risk Analysis Computer Program", Report UMCE 80R2, University of Michigan, Ann Arbor, MI. (1980).

B-17. Thoft-Christensen, P. and Baker, M.J., Structural Reliability Theory and Its Applications, Springer-Verlag, (1982), p. 267.

B-18. Melchers, R.E., "Structural Reliability Analysis and Prediction," Ellis Horwood Limited, Chichester, England, (1987).

B-19. Turkstra, C.J., "Theory of Structural Design Decisions", Study No. 2, Solid Mechanics Division, University of Waterloo, Waterloo, Ontario, Canada, (1970).

B-20. Benjamin, J.R. and Cornell, C.A., "Probability, Statistics and Decision for Civil Engineers, McGraw-Hill, New York, (1970).

APPENDIX C Resistance Models

GENERAL

The capacity of a bridge depends on the resistance of its components and connections. The component resistance, R, is determined mostly by material strength and dimensions. R is a random variable. The causes of uncertainty can be put into three categories:

- material; strength of material, modulus of elasticity, cracking stress, and chemical composition.
- fabrication; geometry, dimensions, and section modulus.
- analysis; approximate method of analysis, idealized stress and strain distribution model.

The resulting variation of resistance has been modeled by tests, observations of existing structures and by engineering judgment. The information is available for the basic structural materials and components. However, bridge members are often made of several materials (composite members) which require special methods of analysis. Verification of the analytical model may be very expensive because of the large size of bridge members. Therefore, the resistance models are developed using the available material test data and by numerical simulations.

In this study, R is considered as a product of the nominal resistance, R_n and three parameters: strength of material, M, fabrication (dimensions) factor, F, and analysis (professional) factor, P,

$$R = R_n\, M\, F\, P \qquad \text{(C-1)}$$

The mean value of R, m_R, is

$$m_R = R_n\, m_M\, m_F\, m_P \qquad \text{(C-2)}$$

and the coefficient of variation, V_R, is,

$$V_R = (V_M^2 + V_F^2 + V_P^2)^{1/2} \qquad \text{(C-3)}$$

where, m_M, m_F, and m_P are the means of M, F, and P, and V_M, V_F, and V_P are the coefficients of variation of M, F, and P, respectively.

The statistical parameters are developed for steel girders, composite and non-composite, reinforced concrete T-beams, and prestressed concrete AASHTO-type girders.

STEEL GIRDERS

Moment Capacity of Non-composite Steel Girders

The behavior of non-composite steel girders depends on the strength of steel (F_y), and on compactness of the section. The dimensions of hot rolled steel beams can be treated as deterministic values, the corresponding coefficients of variation are less than 0.03. The linear and nonlinear flexural behavior of a cross section is described by the moment-curvature relationship. From such a diagram, the elastic and plastic flexural rigidities and level of ductility can be determined. The shape of the moment-curvature relationship depends on the shape factor of the steel section. The shape factor is defined as the ratio of the plastic section modulus to the elastic section modulus.

In a simple bending test on a section, yielding will not initiate until the bending moment reaches a value of $M_p Z_x$, where M_p is moment causing yielding of the whole section and Z_x is plastic section modulus. The benefit in strength derived from exploiting the plastic range is small for I-sections, since the shape is already efficient under elastic conditions, in the sense that most of the material in the section is positioned furthest away from the neutral axis and is therefore fully stressed.

The response to bending moment has been evaluated for representative sizes using a computer procedure developed by Tabsh (C-1). The resulting moment-curvature relationships are shown in Figs. C-1 to C-4. The middle lines correspond to the average. Also shown are curves corresponding to one standard deviation above and one standard deviation below the average.

From simulations, the mean-to-nominal ratio (bias factor) and coefficient of variation of non-compact sections are $\lambda = 1.075$ and $V = 0.10$. For compact sections they are 1.085 and 0.10, respectively. However, the steel industry (American Iron and Steel Institute) provided recent test data which is used to revise the statistical parameters. On the basis of this data, the observed bias factor is assumed $\lambda = 1.095$ and the coefficient of variation is $V = 0.075$. The parameters of the professional factor, P, are: $\lambda = 1.02$ and $V = 0.06$ (C-2). Therefore, for the resistance, R, the parameters are $\lambda_R = 1.12$ and $V_R = 0.10$.

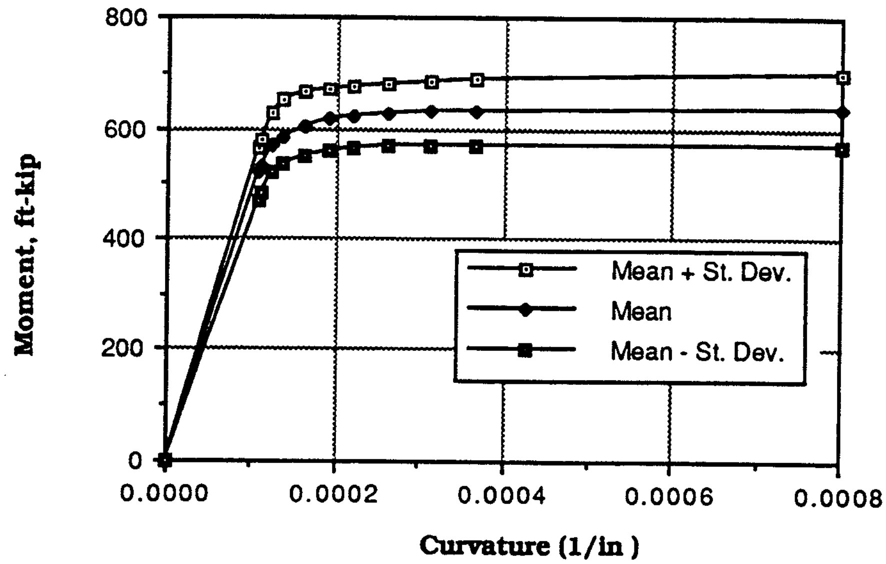

Fig. C-1 Moment-Curvature Curves for a Non-Composite W24x76 Steel Section.

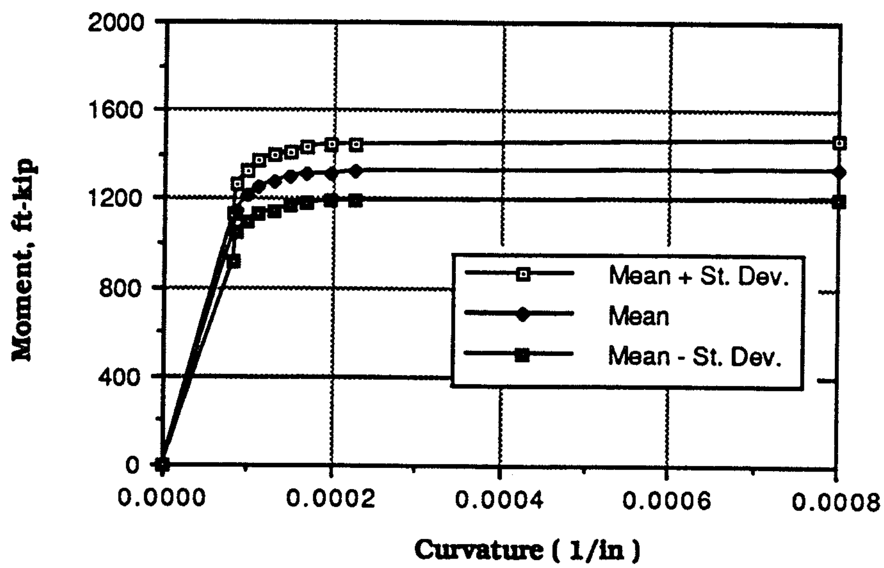

Fig. C-2 Moment-Curvature Curves for a Non-Composite W33x118 Steel Section.

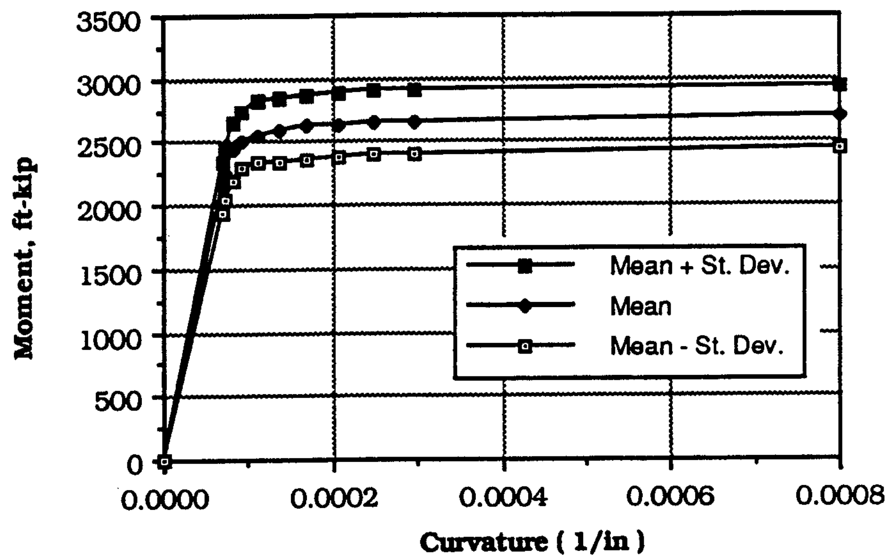

Fig. C-3 Moment-Curvature Curves for a Non-Composite W36x210 Steel Section.

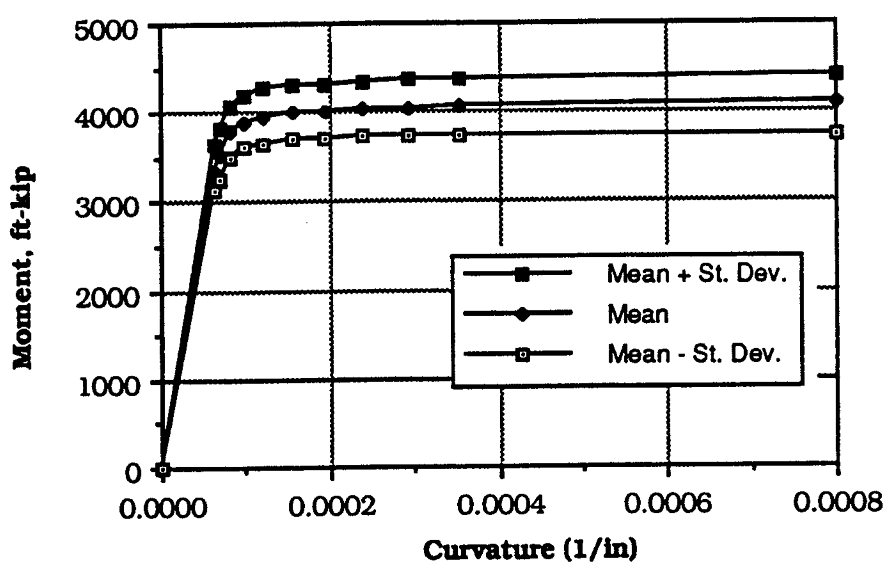

Fig. C-4 Moment-Curvature Curves for a Non-Composite W36x300 Steel Section.

Moment Capacity of Composite Steel Girders

The behavior of composite steel concrete cross sections has been summarized by Tantawi (C-3). The major stresses considered are flexural, torsional and shear. The ultimate torsional capacity of the cross section is also considered. Material properties (strength and dimensions) are modeled using the data provided by Kennedy (C-4) and Ellingwood, Galambos, MacGregor and Cornell (C-2). Crushing of concrete in the positive moment region is the dominant failure mode, provided the longitudinal reinforcement in the cross section is at the minimum level.

Moment-curvature relationship in a composite beam depends on the stress-strain relationship for the structural steel, concrete and reinforcing steel, and the effective flange width of the cross section.

A computer procedure developed by Tabsh (C-1) was used to calculate the moment-curvature relationship under monotonically increasing loading. Several different cross sections were considered. The following assumptions were made:

- A complete composite action between concrete and steel section. The effect of slip was neglected based on experimental and theoretical work done by Kurata and Shodo (C-5).
- The typical stress-strain curves for concrete, reinforcing steel and structural steel are used. In the analysis, the curves were generated by Monte Carlo simulations.
- The tensile strength of concrete is neglected.
- Effect of existing stress and strain in the cross section before composite action takes place in case of unshored construction is not considered.

An iterative method is used for the development of the nonlinear moment-curvature relationship (C-3). The section is idealized as a set of uniform rectangular layers. Strain is increased gradually by increments. At each strain level the corresponding moment is calculated using the nonlinear stress-strain relationships for the materials. The strain throughout the section is assumed constant during the analysis.

A closed form expression for moment-curvature relationship was developed by Zhou (C-6) and Zhou and Nowak (C-7). The formula is fairly flexible and accurate for most engineering purposes. Moreover, it can be used for a wide variety of cross sections. The basic equation is:

$$\phi = M/EI_e + C_1(M/M_y)^{C2} \qquad \text{(C-4)}$$

where: ϕ = curvature; EI_e = elastic bending rigidity; M_y = yield moment; and M = internal moment due to applied load; C_1 and C_2 are constants controlling the shape of the curve. These constants can be determined from the conditions at yield and at ultimate stress or strain. For composite girders C_2 ranges between 16 and 24 whereas C_1 ranges between 0.00015/ft and 0.0003/ft.

Moment-curvature relationship at the mean, mean plus one standard deviation and mean minus one standard deviation for typical sections are shown in Figs. C-5 to C-8. The concrete slab width considered is 6 ft, whereas the thickness is 7 in. The analysis showed that for MF, the bias factor, λ = 1.06 and V = 0.105. Based on the data from the American Iron and Steel Institute, the statistical parameters are λ = 1.07, and V = 0.08. For the analysis factor, P, λ = 1.05 and V = 0.06. Hence for the ultimate moment, λ = 1.12 and V = 0.10.

Shear Capacity of Steel Girders

The ultimate shear capacity of steel sections, V_u, is computed using the following formula,

$$V_u = \sqrt{1/3}\, A_w F_y \tag{C-5}$$

where A_w = area of the web.

The statistical parameters of MF were obtained by simulations; mean-to-nominal, λ = 1.11, and V = 0.10. However, using the recent test data provided by the American Iron and Steel Institute, the statistical parameters are λ = 1.12, and V = 0.08. The parameters for the analysis factor are taken as λ = 1.02 and V = 0.07. Therefore the resulting parameters of R are λ_R = 1.14 and V_R = 0.105.

REINFORCED CONCRETE GIRDERS

Moment Capacity of Reinforced Concrete Girders

The statistical data on material and dimensions is based on the available literature, in particular as summarized in the report by Ellingwood, Galambos, MacGregor and Cornell (C-2). The calculations were performed using the numerical procedures developed by Ting (C-8).

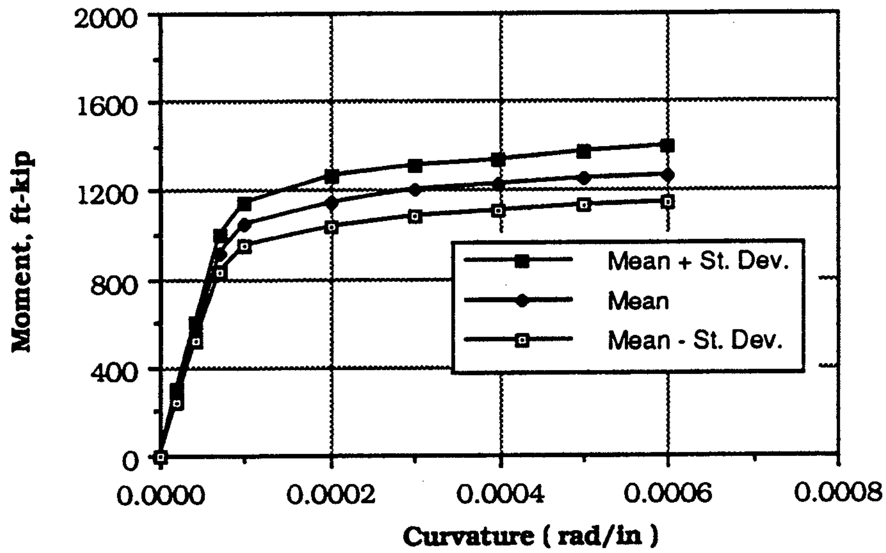

Fig. C-5 Moment-Curvature Curves for a Composite W24x76 Steel Section.

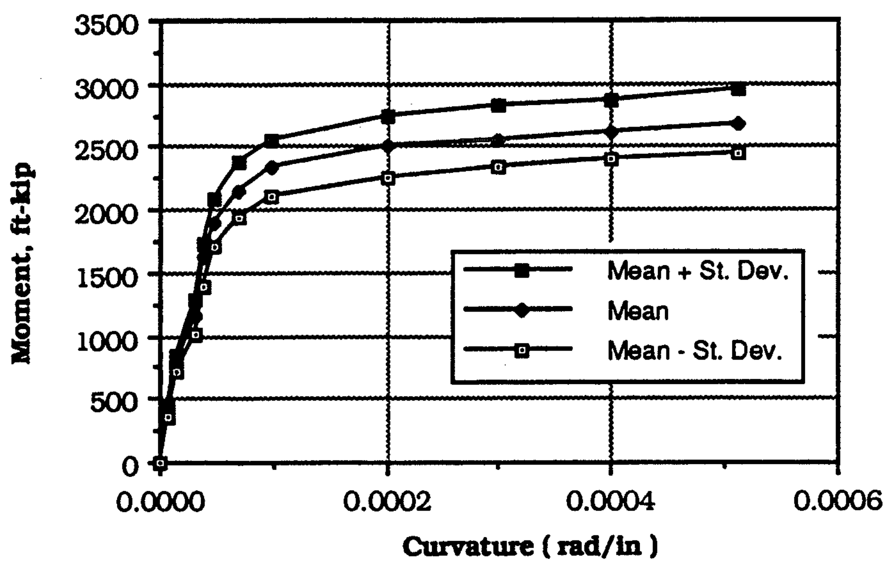

Fig. C-6 Moment-Curvature Curves for a Composite W33x130 Steel Section.

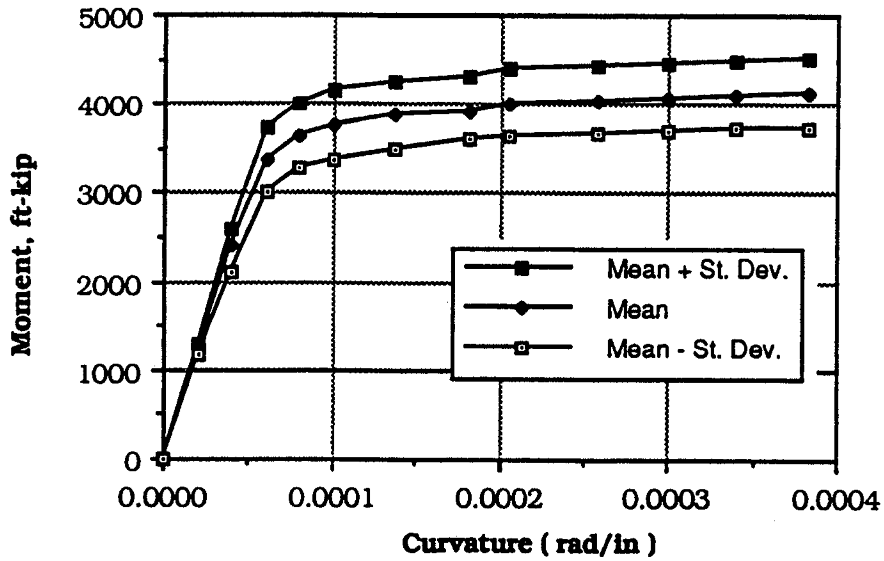

Fig. C-7 Moment-Curvature Curves for a Composite W36x210 Steel Section.

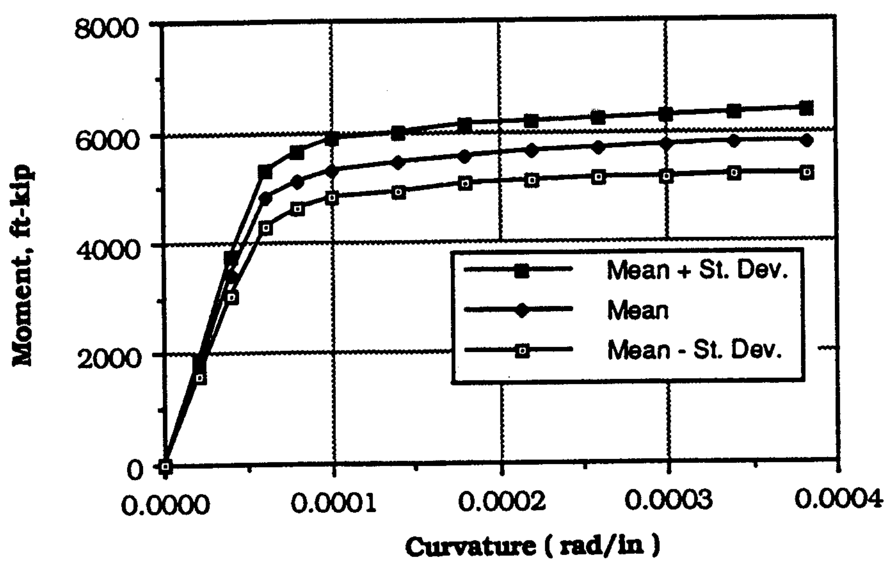

Fig. C-8 Moment-Curvature Curves for a Composite W36x300 Steel Section.

The moment-curvature relationships are developed for typical bridge T-beams. Three sections are considered, with the flange width 7 ft and the slab thickness 7.25 in. These beams are used for spans 40 to 80 ft. The major parameters which determine the structural performance include the amount of reinforcement, steel yield stress and concrete strength.

The sections and the results of simulations are shown in Fig. C-9 to C-11. As in the case of steel girders, the middle curve represents the mean, and the other two correspond to one standard deviation above and below the mean.

The parameters of MF for lightly reinforced concrete T-beams are $\lambda = 1.12$ and $V = 0.12$ (the mean-to-nominal and coefficient of variation). The parameters for analysis factors are $\lambda = 1.00$ and $V = 0.06$. Therefore, for R the parameters are $\lambda_R = 1.12$ and $V_R = 0.135$.

Shear Capacity of Reinforced Concrete Girders

The shear capacity is calculated using the Modified Compression Field Theory (C-9; C-10). The statistical parameters are determined on the basis of simulations performed by Yamani (C-11). The relationship between shear force and shear strain is established for representative T-beams. The results are shown in Fig. C-12 to C-14. The nominal (design) value of shear capacity is calculated according to current AASHTO.

The parameters of the shear capacity, V_n, depend on the amount of shear reinforcement. If shear reinforcement is used, $\lambda = 1.13$ and $V = 0.12$. For the analysis factor, P, $\lambda = 1.075$ and the coefficient of variation is $V = 0.10$. Therefore, for the shear resistance, $\lambda_R = 1.20$ and $V_R = 0.155$. If no shear reinforcement is used, then $\lambda_R = 1.40$ and $V_R = 0.17$.

Collins (yet unpublished) observed that, in most cases, failure in flexure occurs before failure in shear. Flexural capacity, M_n, and shear capacity, V_n, are correlated in the statistical sense. An increase of M_n causes an increase of V_n. In practice, shear governs only in cross sections with zero bending moment and large shear (e.g. some sections in box culverts).

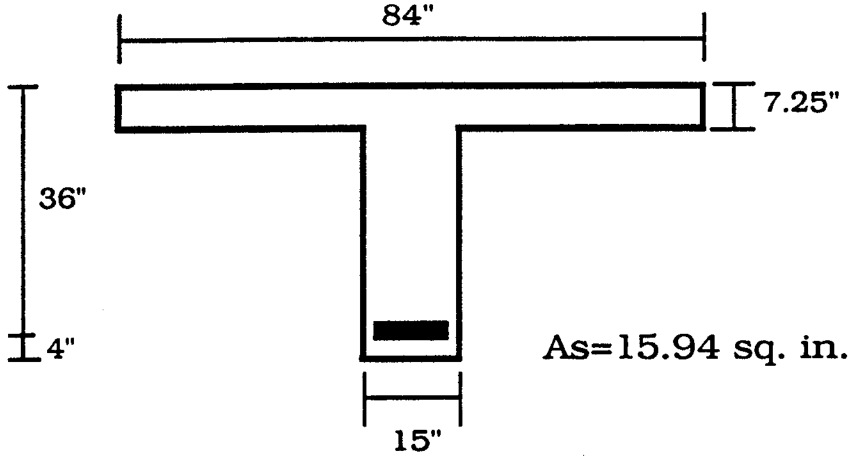

Layout of Section A

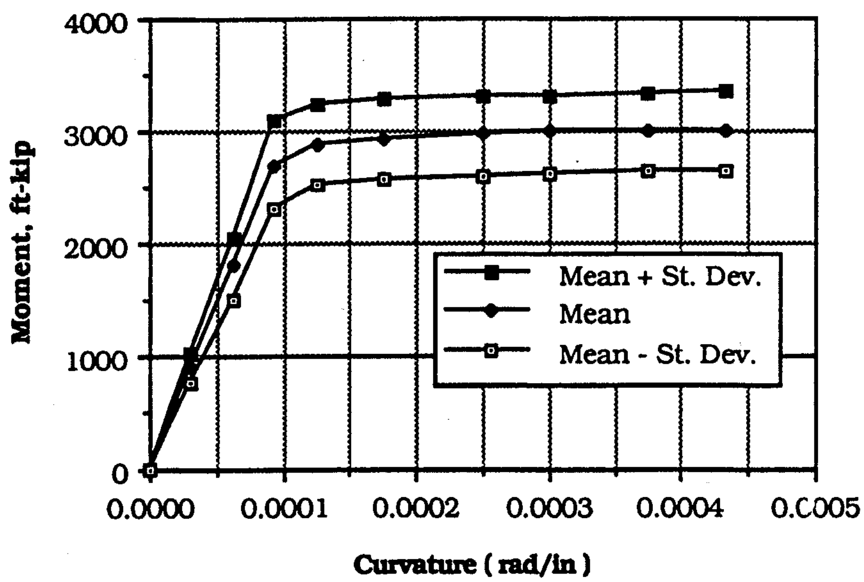

Fig. C-9 Moment-Curvature Curves for R/C Section A.

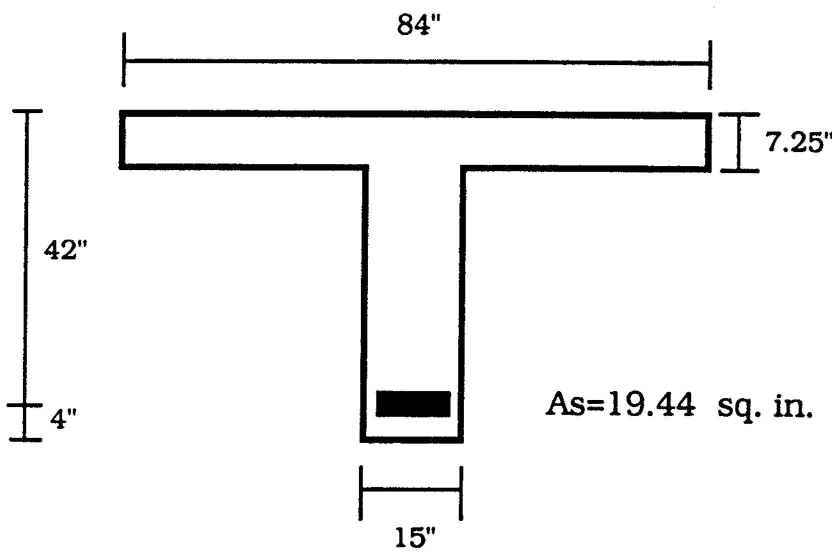

Layout of Section B

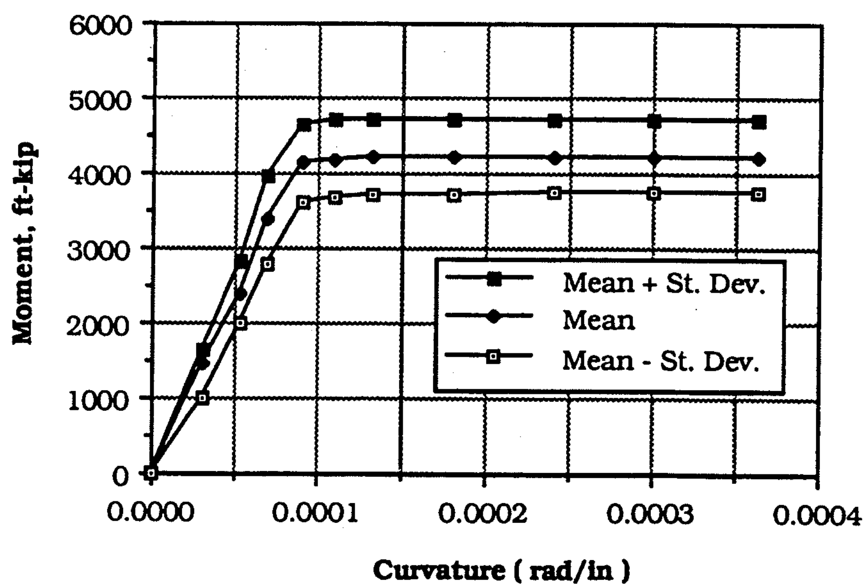

Fig. C-10 Moment-Curvature Curves for R/C Section B.

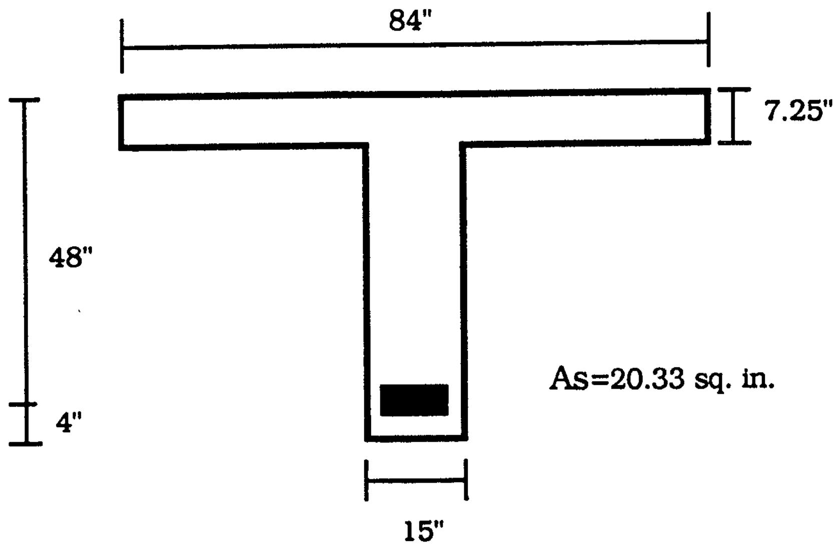

Layout of Section C

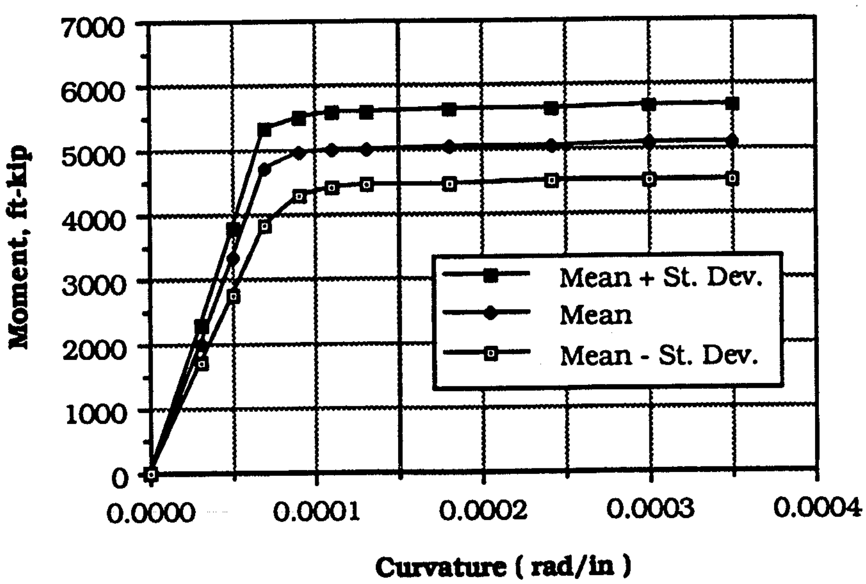

Fig. C-11 Moment-Curvature Curves for R/C Section C.

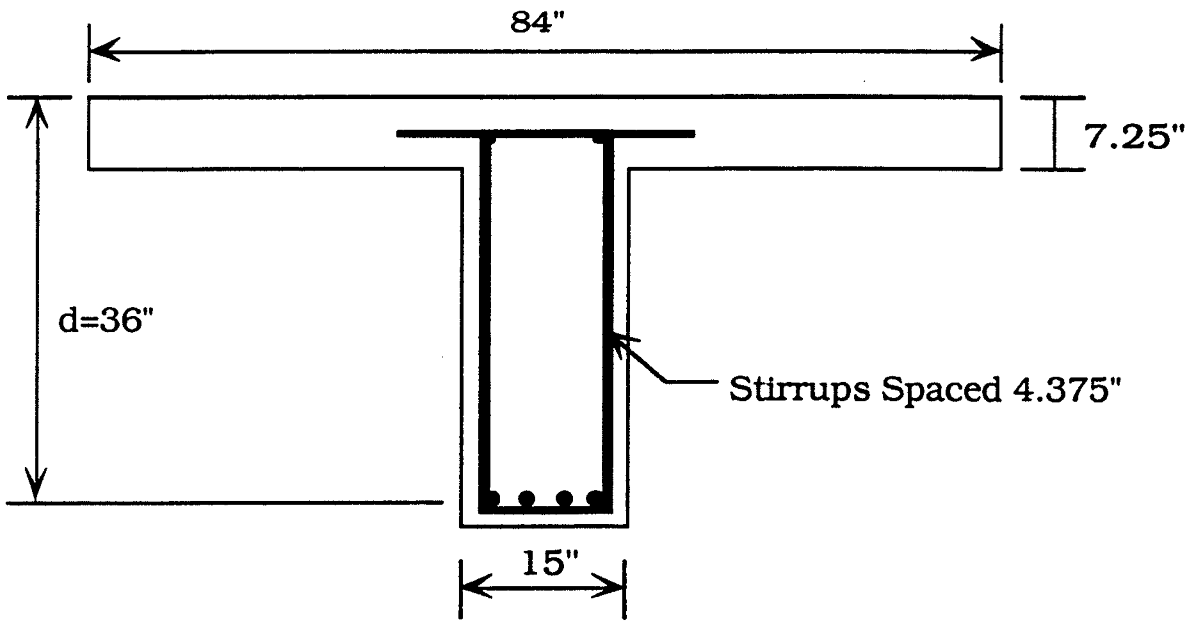

Layout of R/C Section A.

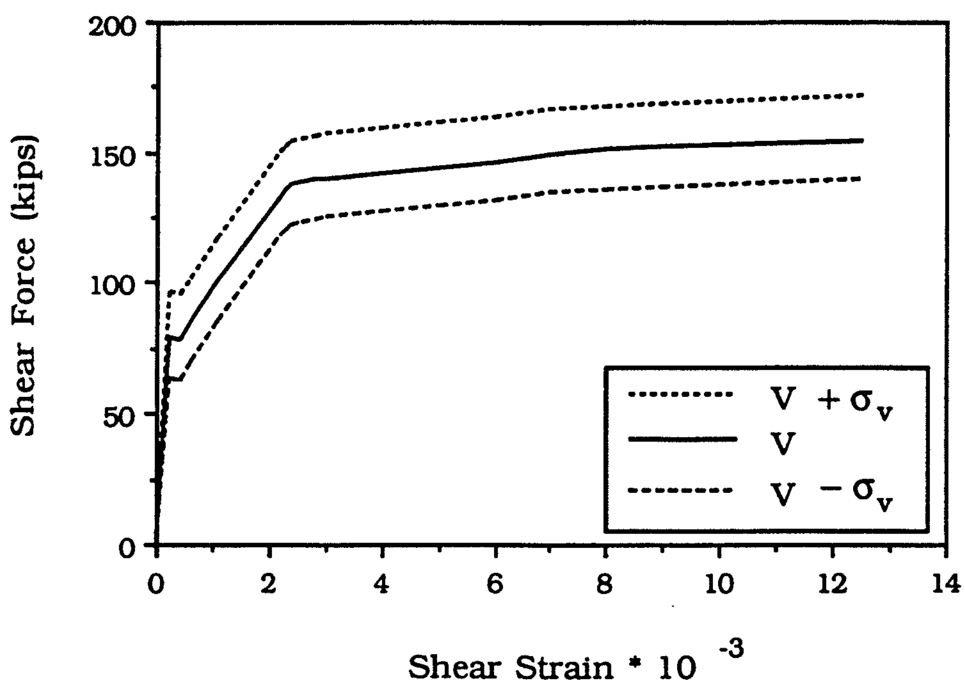

Fig. C-12 Shear Force - Shear Strain Curves for R/C Section A.

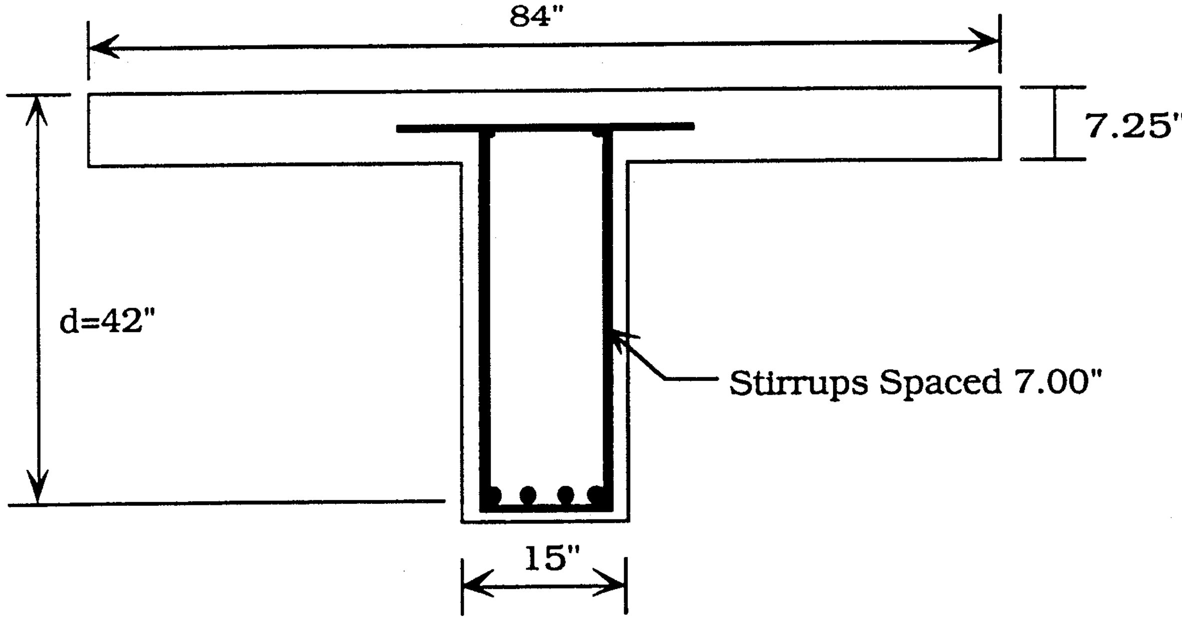

Layout of R/C Section B.

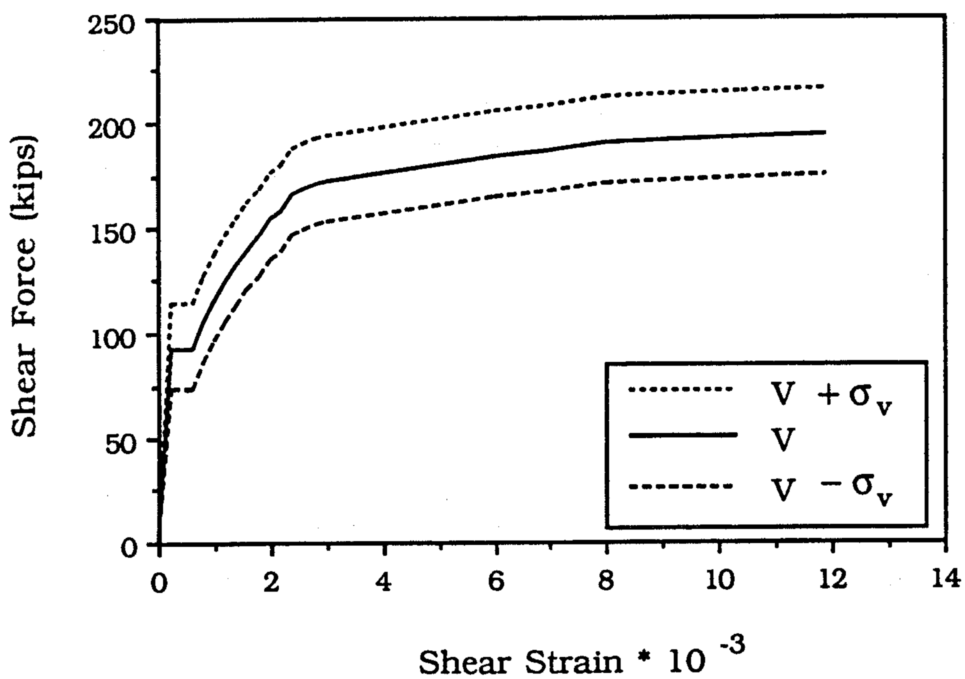

Fig. C-13 Shear Force - Shear Strain Curves for R/C Section B.

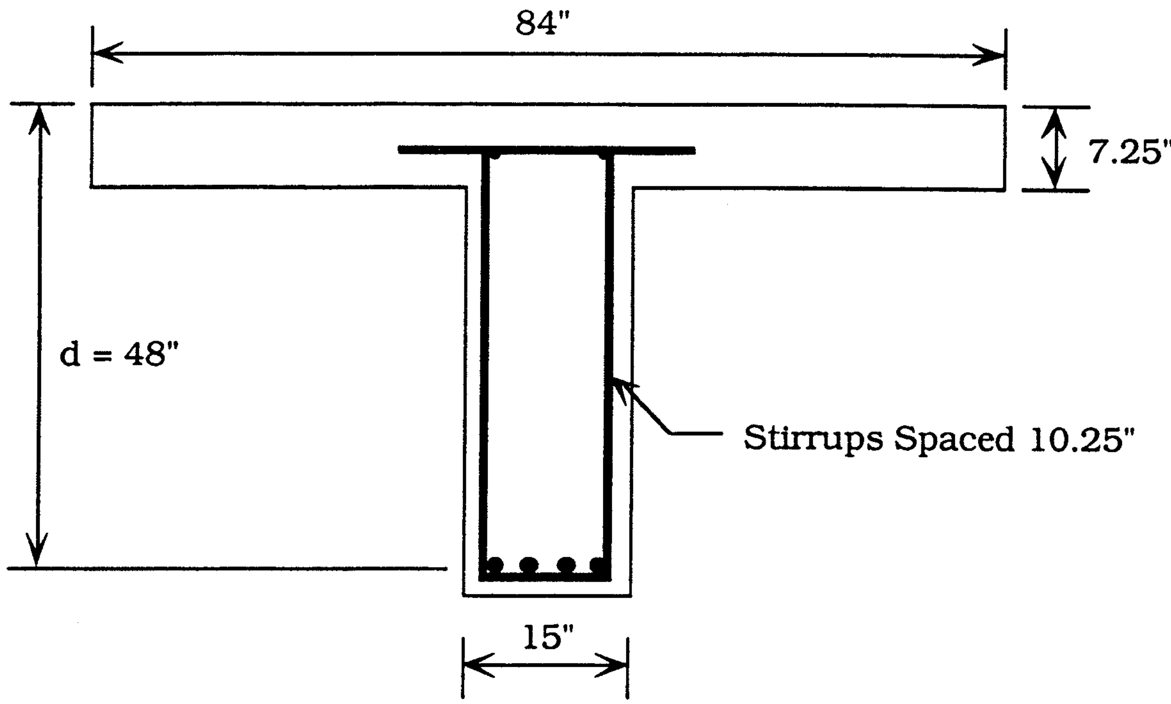

Layout of R/C Section C.

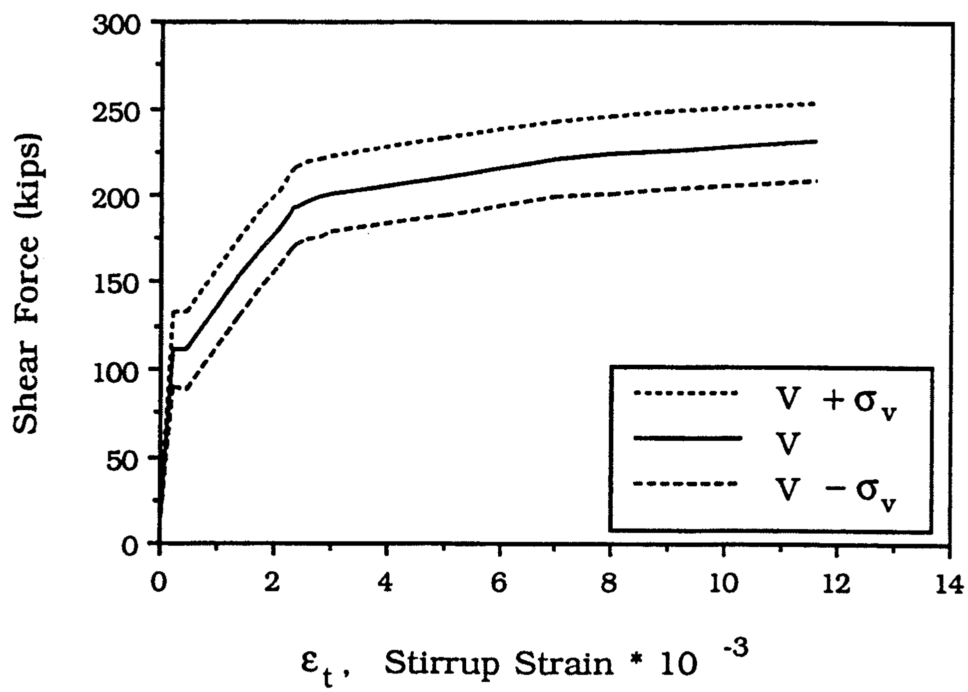

Fig. C-14 Shear Force - Shear Strain Curves for R/C Section C.

PRESTRESSED CONCRETE GIRDERS

Moment Capacity of Prestressed Concrete Girders

The parameters of resistance for prestressed concrete bridge girders are derived on the basis of the statistical data from Ellingwood, Galambos, MacGregor and Cornell (C-2) and Siriaksorn and Naaman (C-12). The simulations were performed using a computer program developed by Ting (C-8). The strains are assumed to be linearly distributed. Material properties are assumed to be uniform. The section is divided into a number of rectangular horizontal strips of a small depth. For given strains, stresses are calculated using material stress-strain curves. The bending moment is calculated as the resultant of the internal stress.

Uncracked and cracked sections are considered. The section is uncracked until the tension in concrete exceeds the tensile strength. In a cracked section all tension is resisted by steel. Ultimate stiffness corresponds to the prefailure part of the moment-curvature plot. The moment curvature relationship changes under a cyclic loading (trucks). If the total bending moment, M_Q, exceeds the cracking moment, M_{cr}, the section cracks and the tensile strength of concrete is reduced to zero. After the first cracking, the crack stays open any time M_Q exceeds decompression moment, M_d (if $M_Q < M_d$, then all concrete is compressed, if $M_Q > M_d$ then crack opens). For typical bridge girders, the ultimate moment is about twice the decompression moment, M_d. The section cracks for the first time under about 1.15 M_d.

The moment-curvature relationships are developed for typical AASHTO girders. The results are shown in Figs. C-15 to C-17. The solid line corresponds to the average, whereas the dash lines correspond to the average plus one and minus one standard deviation.

The results show that the bias factor for the ultimate moment is 1.04 and the coefficient of variation is about 0.045. The coefficient of variation is very small because all sections are under-reinforced and the ultimate moment is controlled by the prestressing tendons. For the analysis factor bias, $\lambda = 1.01$ and $V = 0.06$. Therefore, the bias factor for R, $\lambda_R = 1.05$ and $V_R = 0.075$.

Shear Capacity of Prestressed Concrete Girders

The shear capacity of prestressed concrete girders is calculated on the basis of the Modified Compression Field Theory (C-9; C-10). The parameters of resistance are simulated using the available test

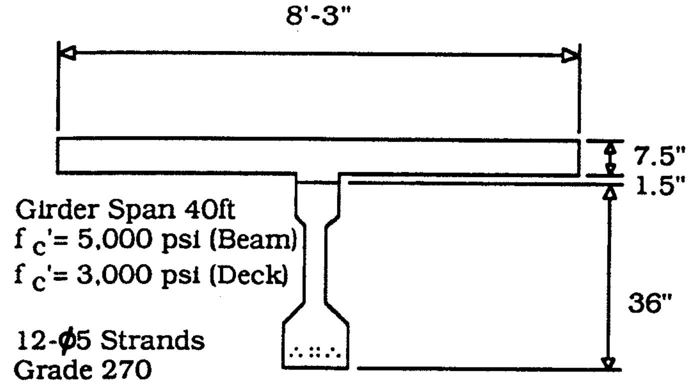

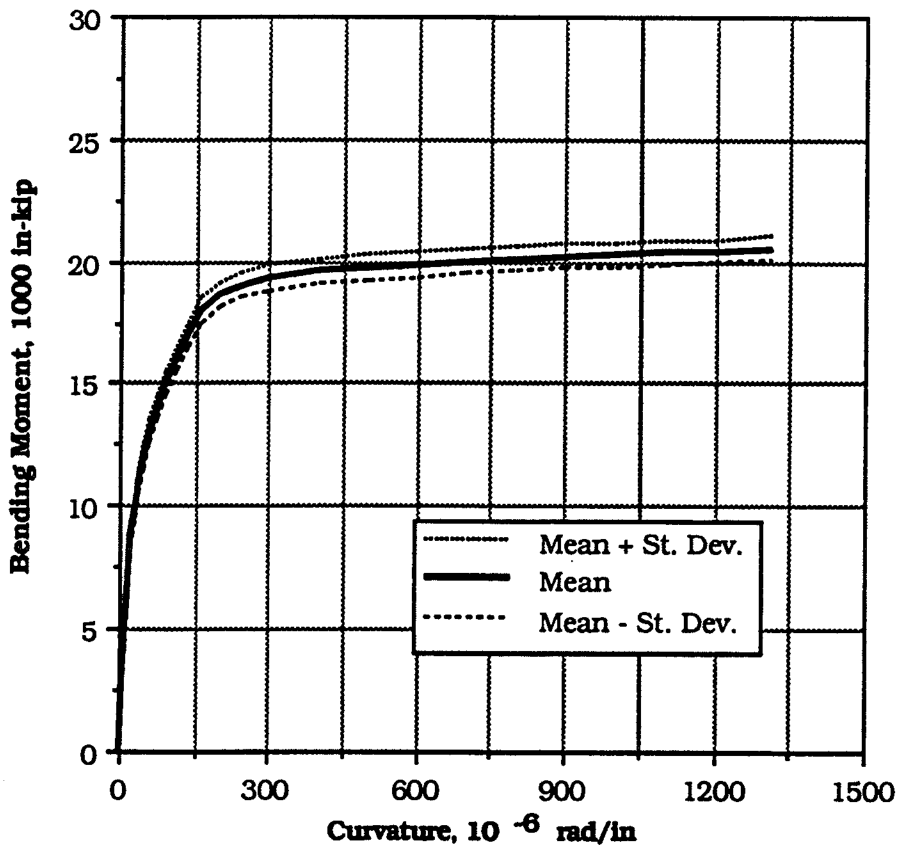

Fig. C-15 Moment-Curvature Curves for AASHTO II P/C Composite Girder.

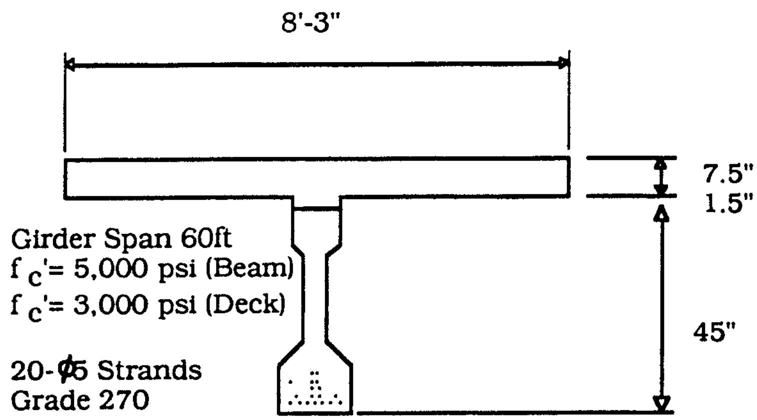

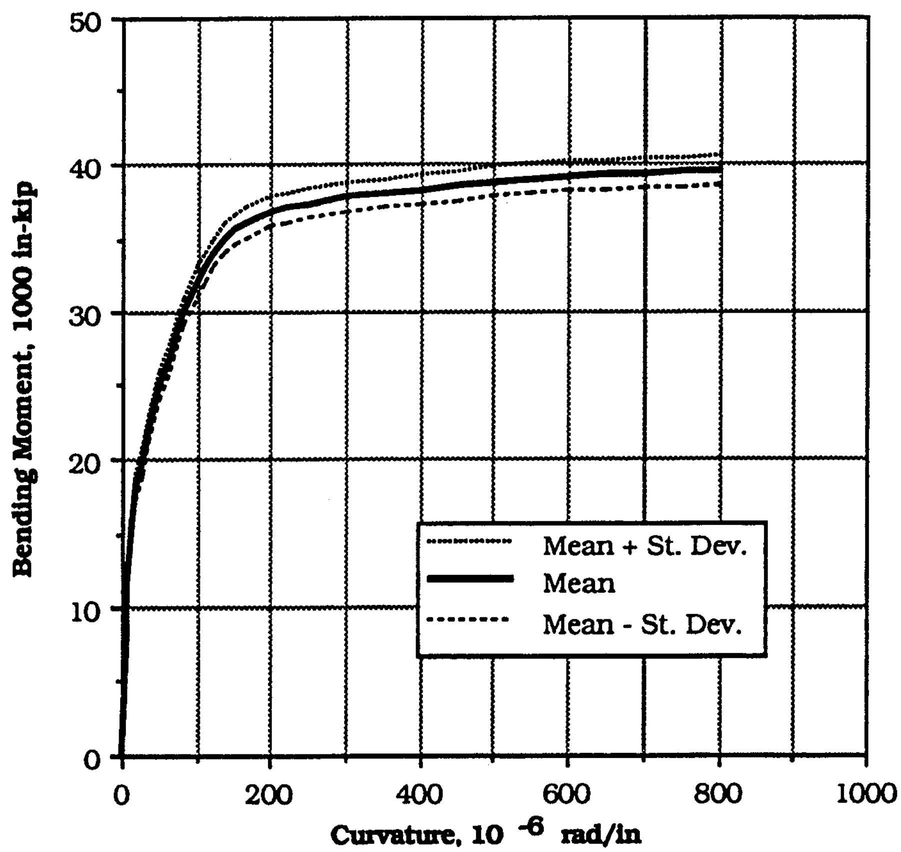

Fig. C-16 Moment-Curvature Curves for AASHTO III P/C Composite Girder.

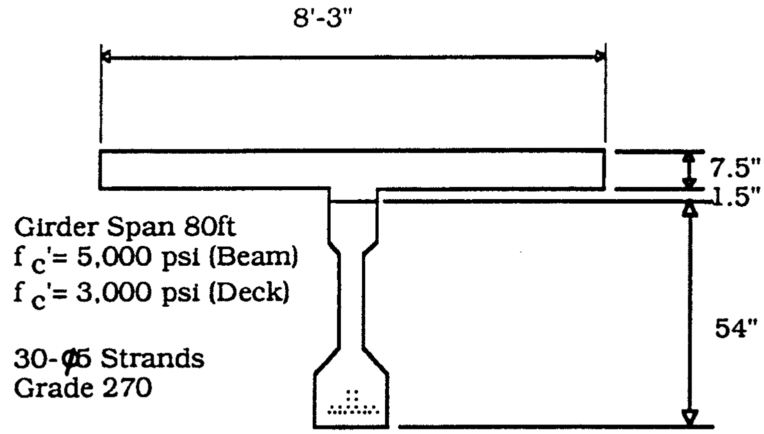

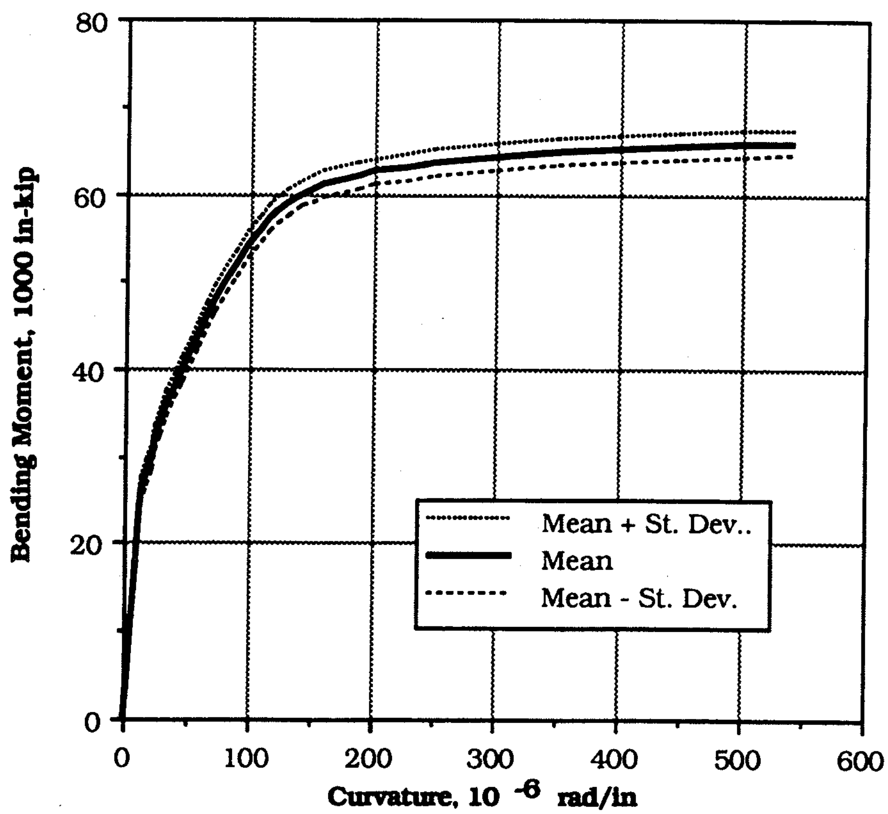

Fig. C-17 Moment-Curvature Curves for AASHTO IV P/C Composite Girder.

data and computer procedure developed by Yamani (C-11). The nominal (design) value of the shear capacity is calculated using the current AASHTO.

For typical AASHTO type girders, the resulting relationship between the shear force and shear strain is shown in Fig. C-18 to C-20. The curves correspond to the mean, mean plus one standard deviation and mean minus one standard deviation.

The parameters of FM are λ = 1.07 and V = 0.10. For P, λ = 1.075 and V = 0.10. Therefore, for the shear resistance, λ_R = 1.15 and V_R = 0.14.

Resistance of Components with High Strength Prestressing Bars

The resistance of these components is determined by the mechanical properties of the prestressing bars. The manufacturer tested 30 samples to determine the yield stress, F_y, and tensile strength (ultimate stress), F_u. Test results were obtained from the Dywidag Systems International.

The data is plotted on the normal probability paper in Fig. C-21. The calculated coefficients of variation are 0.03 for F_y and 0.01 for F_u. However, the lower tails of the CDF's show a higher variation, which is important in the reliability analysis. Therefore, the statistical parameters of R are assumed as for reinforced concrete T-beams.

SUMMARY OF RESISTANCE PARAMETERS

The parameters of resistance for steel girders, reinforced concrete T-beams and prestressed concrete girders are shown in Table 3.

References for Appendix C

C-1. Tabsh, S.W. "Reliability-Based Sensitivity Analysis of Girder Bridges," PhD Thesis, Department of Civil Engineering, University of Michigan, Ann Arbor, MI, (1990).

C-2. Ellingwood, B. Galambos, T.V., MacGregor, J.G. and Cornell C.A., "Development of a Probability Based Load Criterion for American National Standard A58", National Bureau of Standards, NBS Special Publication 577, Washington, D.C. (1980).

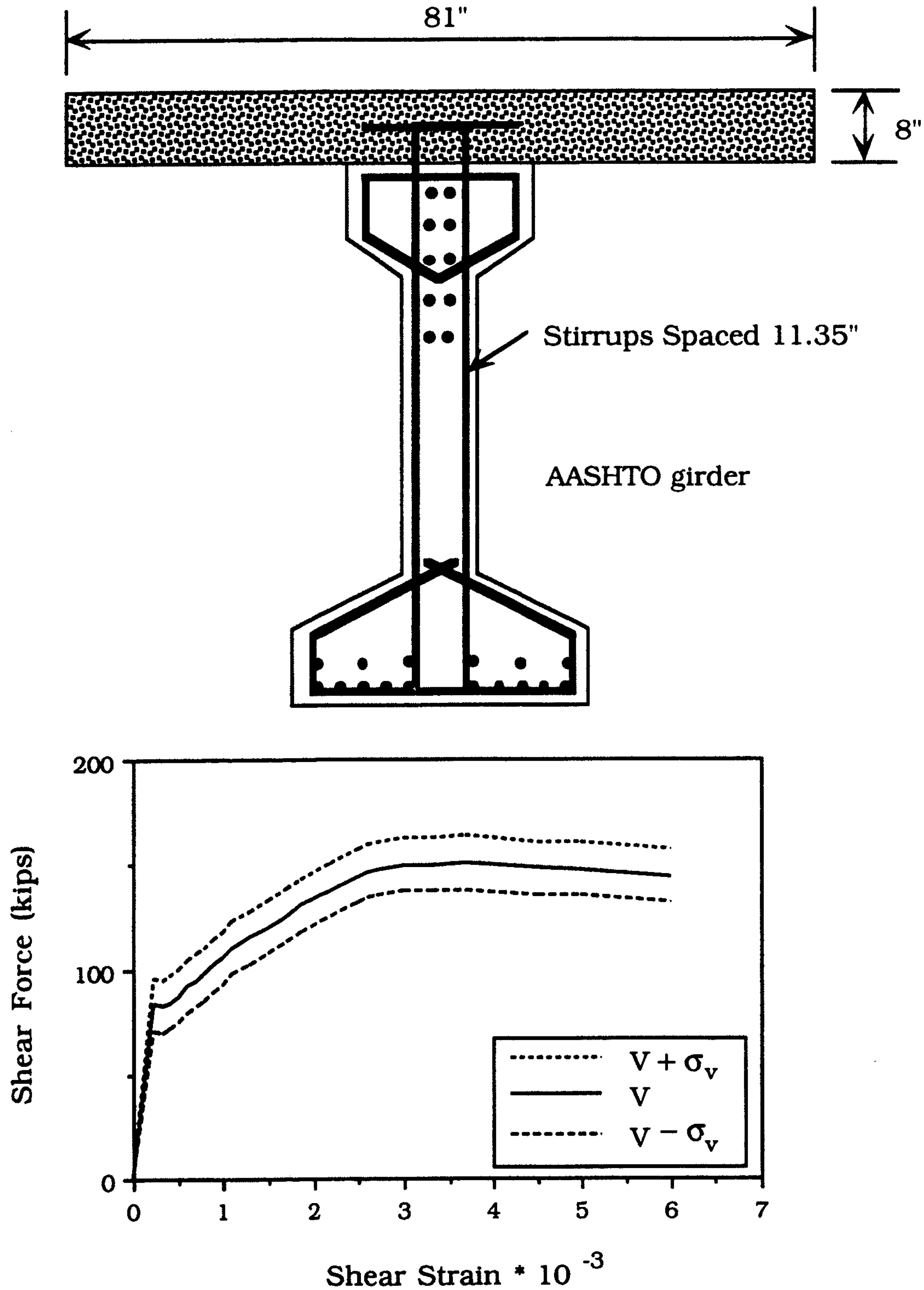

Fig. C-18 Shear Force - Shear Strain Curves for AASHTO II P/C Composite Girder.

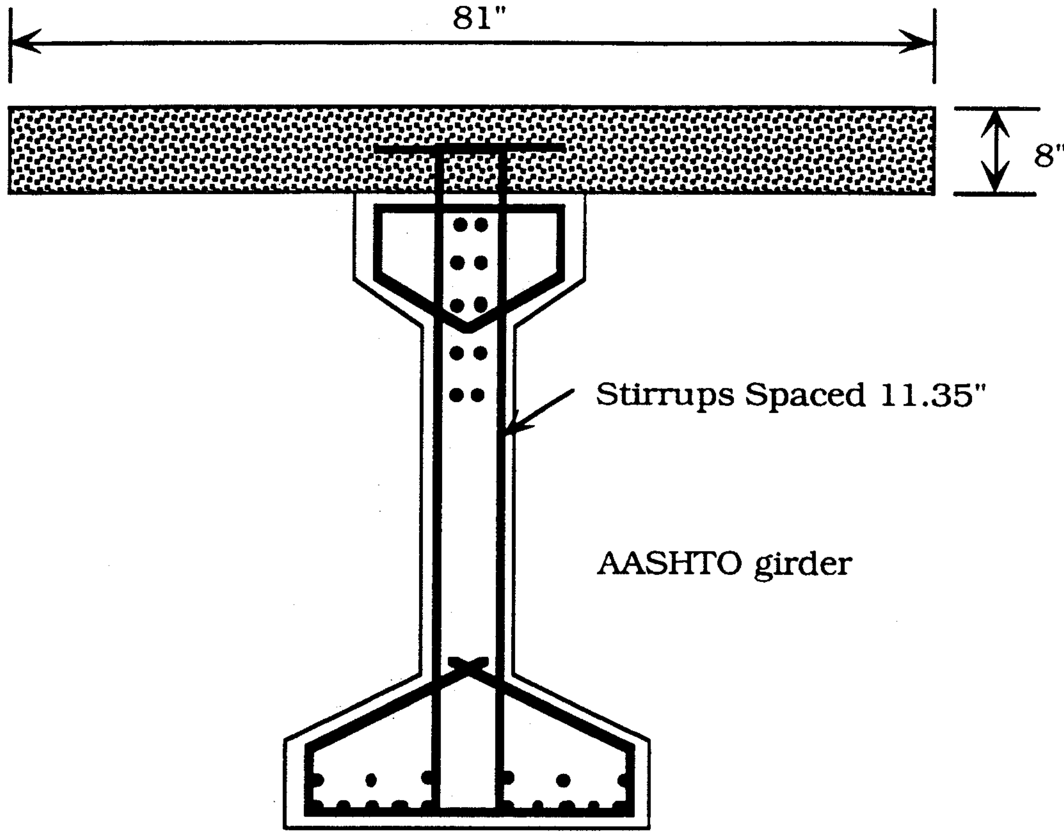

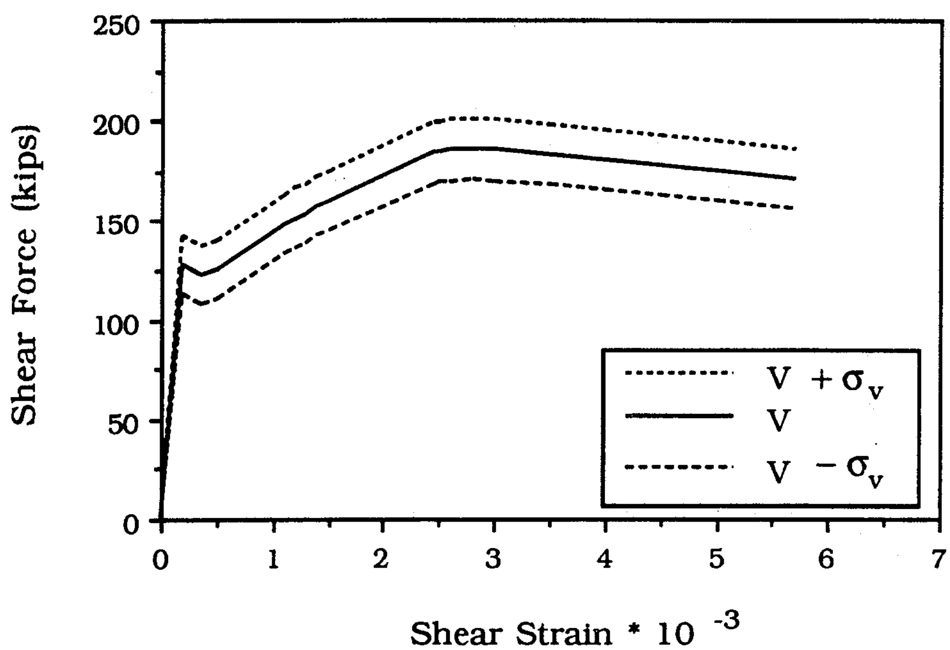

Fig. C-19 Shear Force - Shear Strain Curves for AASHTO III P/C Composite Girder.

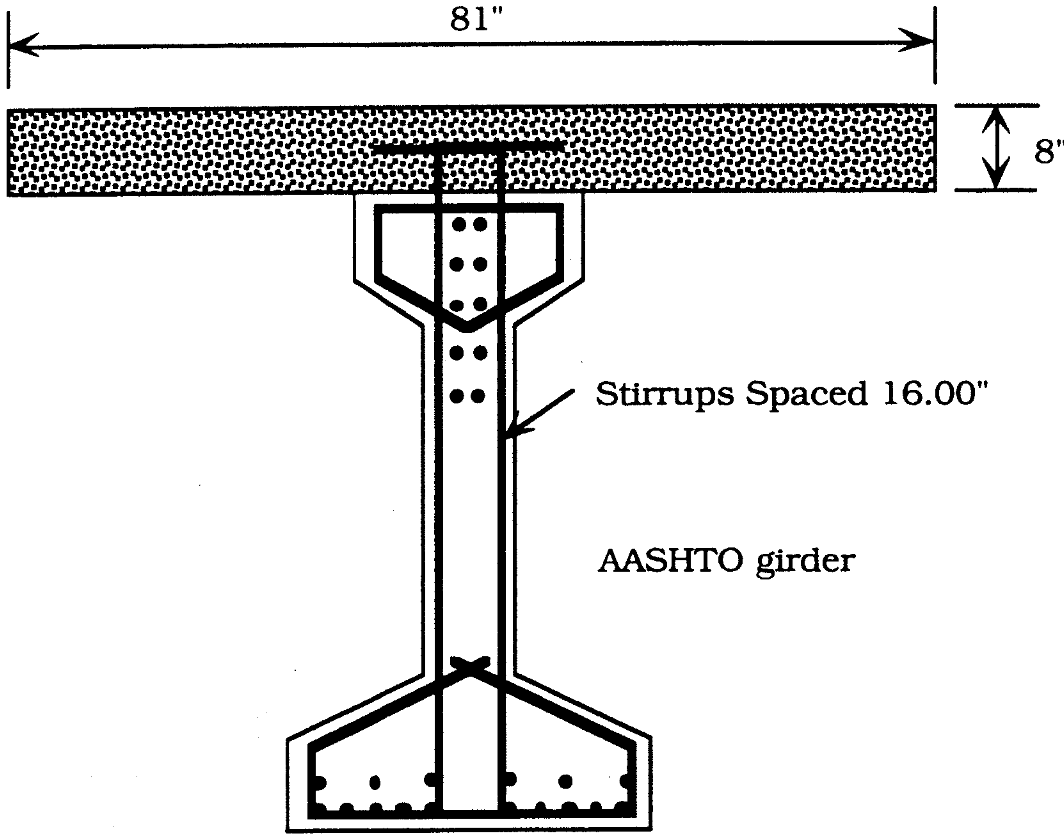

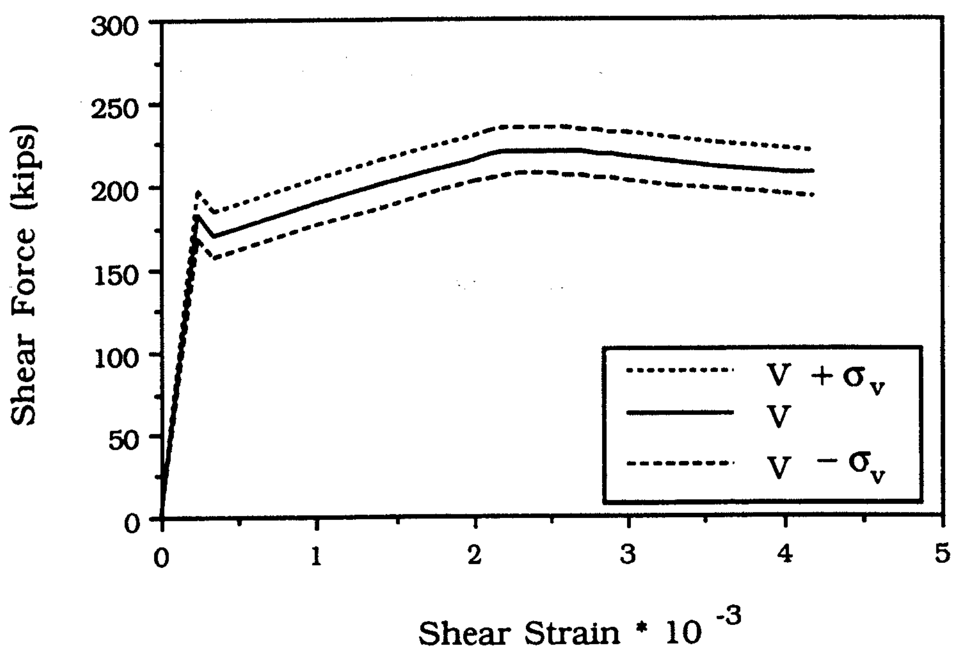

Fig. C-20 Shear Force - Shear Strain Curves for AASHTO IV P/C Composite Girder.

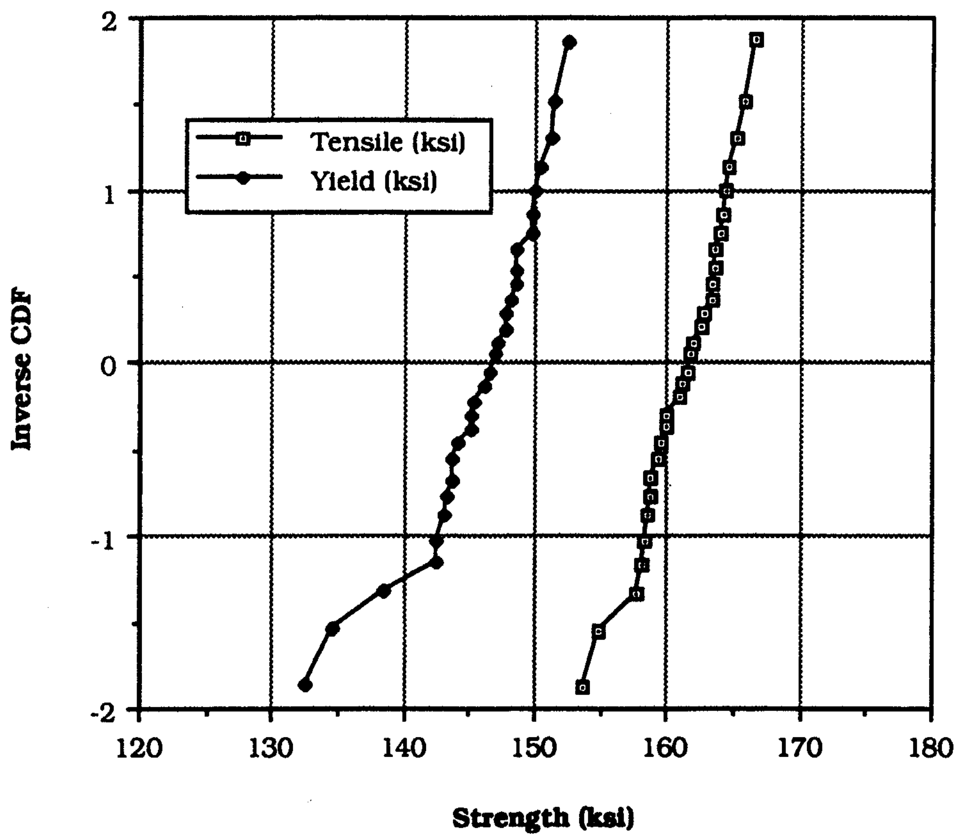

Fig. C-21. CDF's of F_y and F_u for the High-Strength Prestressing Bars.

C-3. Tantawi, H.M., "Ultimate Strength of Highway Girder Bridges", PhD Thesis, Department of Civil Engineering, University of Michigan, Ann Arbor, MI (1986).

C-4. Kennedy, D.J.L., "Study of Performance Factors for Section 10 Ontario Highway Bridge Design Code", Morrison, Hershfield, Burgess & Huggins, Ltd., Report No. 2805331, Toronto, Canada (1982).

C-5. Kurata, M. and Shodo, H., "The Plastic Design of Composite Girder Bridges, Comparison with Elastic Design", Doboka Gokkai-Shi, Japan (1967), translated by Arao, S., Civil Engineering Department, University of Ottawa, Canada.

C-6. Zhou, J-H. "System Reliability Models for Highway Bridge Analysis", PhD Thesis, Department of Civil Engineering, University of Michigan, Ann Arbor, MI (1987).

C-7. Zhou, J-H. and Nowak, A.S., "Integration Formulas for Functions of Random Variables," Journal of Structural Safety, 5, 1988, pp. 267-284.

C-8. Ting, S-C., "The Effects of Corrosion on the Reliability of Concrete Bridge Girders," PhD Thesis, Department of Civil Engineering, University of Michigan, Ann Arbor, MI (1989).

C-9. Vecchio, F. J., and Collins, M. P., "The response of Reinforced Concrete to In-Plane Shear and Normal Stresses", Research Final Report, University of Toronto, Department of Civil Engineering, Toronto, Canada (1982).

C-10. Vecchio, F. J. and Collins, M. P., "The Modified Compression Field Theory for Reinforced Concrete Elements Subjected to Shear", ACI Journal, Vol. 83, No. 2, (1986).

C-11. Yamani, A.S., "Reliability Evaluation of Shear Strength in Highway Girder Bridges," PhD Thesis, Department of Civil Engineering, University of Michigan, Ann Arbor, MI (1992).

C-12. Siriaksorn, A. and Naaman, A.E., "Reliability of Partially Prestressed Beams at Serviceability Limit States", Report No. 80-1, University of Illinois at Chicago Circle, Chicago, IL (1980).

APPENDIX D Reliability Analysis

The available reliability methods are presented in several publications (e.g. D-1; D-2). In this study the reliability analysis is performed using Rackwitz and Fiessler procedure, Monte Carlo simulations and special sampling techniques.

LIMIT STATES

Limit states are the boundaries between safety and failure. In bridge structures failure is defined as inability to carry traffic. Bridges can fail in many ways, or modes of failure, by cracking, corrosion, excessive deformations, exceeding carrying capacity for shear or bending moment, local or overall buckling, and so on. Some members fail in a brittle manner, some are more ductile. In the traditional approach, each mode of failure is considered separately.

There are two types of limit states. Ultimate limit states (ULS) are mostly related to the bending capacity, shear capacity and stability. Serviceability limit states (SLS) are related to gradual deterioration, user's comfort or maintenance costs. The serviceability limit states such as fatigue, cracking, deflection or vibration, often govern the bridge design. The main concern is accumulation of damage caused by repeated applications of load (trucks). Therefore, the model must include the load magnitude and frequency of occurrence, rather than just load magnitude as is the case in the ultimate limit states. For example, in prestressed concrete girders, a crack opening under heavy live load is not a problem in itself. However, a repeated crack opening may allow penetration of moisture and corrosion of the prestressing steel. The critical factors are both magnitude and frequency of load. Other serviceability limit states, vibrations or deflections, are related to bridge user's comfort rather than structural integrity.

A traditional notion of the safety limit is associated with the ultimate limit states. For example, a beam fails if the moment due to loads exceeds the moment carrying capacity. Let R represent the resistance (moment carrying capacity) and Q represent the load effect (total moment applied to the considered beam). Then the corresponding limit state function, g, can be written,

$$g = R - Q \qquad \text{(D-1)}$$

If $g > 0$, the structure is safe, otherwise it fails. The probability of failure, P_F, is equal to,

$$P_F = \text{Prob}\ (R - Q < 0) = \text{Prob}\ (g < 0) \qquad \text{(D-2)}$$

Let the probability density function (PDF) of R be f_R and PDF of Q be f_Q. Then let Z = R - Q. Z is also a random variable and it represents the safety margin, as shown in Fig. D-1.

In general, limit state function can be a function of many variables (load components, influence factors, resistance parameters, material properties, dimensions, analysis factors). A direct calculation of P_F may be very difficult, if not impossible. Therefore, it is convenient to measure structural safety in terms of a reliability index.

<u>RELIABILITY INDEX</u>

The reliability index, β, is defined as a function of P_F,

$$\beta = -\ \Phi^{-1}(P_F) \qquad \text{(D-3)}$$

where Φ^{-1} = inverse standard normal distribution function. Examples of β's and corresponding P_F's are shown in Table D-1.

There are various procedures available for calculation of β. These procedures vary with regard to accuracy, required input data and computing costs.

The simplest case involves a linear limit state function (Eq. D-1). If both R and Q are independent (in the statistical sense), normal random variables, then the reliability index is,

$$\beta = (m_R - m_Q)/(\sigma_R^2 + \sigma_Q^2)^{1/2} \qquad \text{(D-4)}$$

where m_R = mean of R, m_Q = mean of Q, σ_R = standard deviation of R and σ_Q = standard deviation of Q.

If both R and Q are lognormal random variables, then β can be approximated by

$$\beta = \ln\ (m_R/m_Q)/(V_R^2 + V_Q^2)^{1/2} \qquad \text{(D-5)}$$

where V_R = coefficient of variation of R and V_Q = coefficient of variation of Q. A different formula is needed for larger coefficients of variation.

Eq. D-4 and Eq. D-5 require the knowledge of only two parameters for each random variable, the mean and standard deviation (or coefficient of variation). Therefore the formulas belong to the

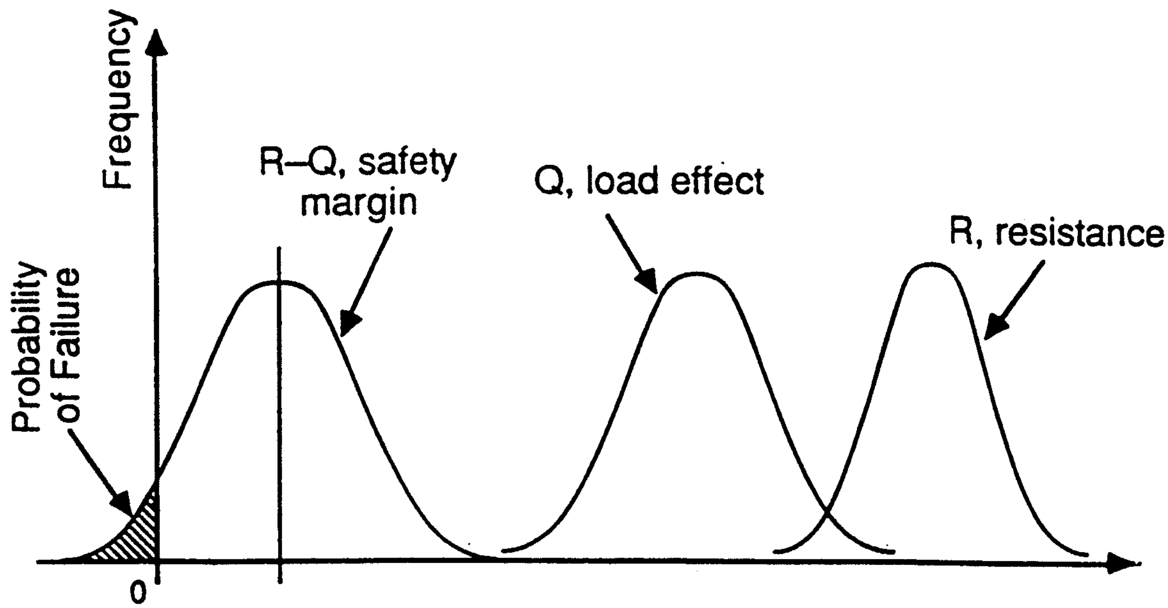

Fig. D-1. PDF's of Load, Resistance and Safety Reserve.

Table D-1. Probability of Failure vs. β.

reliability index β	reliability S $(= 1 - P_f)$	probability of failure P_f
0.0	0.500	$0.500\times10^{+0}$
0.5	0.691	$0.309\times10^{+0}$
1.0	0.841	$0.159\times10^{+0}$
1.5	0.933 2	0.668×10^{-1}
2.0	0.977 2	0.228×10^{-1}
2.5	0.993 79	0.621×10^{-2}
3.0	0.998 65	0.135×10^{-2}
3.5	0.999 767	0.233×10^{-3}
4.0	0.999 968 3	0.317×10^{-4}
4.5	0.999 996 60	0.340×10^{-5}
5.0	0.999 999 713	0.287×10^{-6}
5.5	0.999 999 981 0	0.190×10^{-7}
6.0	0.999 999 999 013	0.987×10^{-9}
6.5	0.999 999 999 959 8	0.402×10^{-10}
7.0	0.999 999 999 998 72	0.128×10^{-11}
7.5	0.999 999 999 999 968 1	0.319×10^{-13}
8.0	0.999 999 999 999 999 389	0.611×10^{-15}

second moment methods. If the parameters R an Q are not both normal or lognormal, then the formulas give only an approximate value of β. In such a case, the reliability index can be calculated using Rackwitz and Fiessler procedure, sampling techniques or by Monte Carlo simulations.

ITERATIVE NUMERICAL PROCEDURE

Rackwitz and Fiessler (D-3) developed an iterative procedure based on normal approximations to non-normal distributions at the so called design point. The design point is the point of maximum probability on the failure boundary (limit state function). For simplicity of the presentation, the method will be demonstrated for the case of two variables only; R, representing the structural resistance, and Q, representing the total load effect.

The mathematical representation of the failure boundary is the limit state function equal to zero, $g = R - Q = 0$. The design point, denoted by (R^*, Q^*), is located on the failure boundary, so $R^* = Q^*$.

Let F_R be the cumulative distribution function (CDF) and f_R the probability density function (PDF) for R. Similarly, F_Q and f_Q are the CDF and PDF for Q. Initial value of R^* (design point), is guessed first. Next, F_R is approximated by a normal distribution, F_R', such that

$$F_R'(R^*) = F_R(R^*) \tag{D-6}$$

and

$$f_R'(R^*) = f_R(R^*) \tag{D-7}$$

The standard deviation of R' is

$$\sigma_R' = \phi\{\Phi^{-1}[F_R(R^*)]\}/ f_R(R^*) \tag{D-8}$$

where ϕ = PDF of the standard normal random variable and Φ = CDF of the standard normal random variable.

The mean of R' is,

$$m_R' = R^* - \sigma_R' \Phi^{-1}[F_R(R^*)] \tag{D-9}$$

Similarly, F_Q is approximated by a normal distribution F_Q', such that

$$F_Q'(Q^*) = F_Q(Q^*) \tag{D-10}$$

$$f_Q'(Q^*) = f_Q(Q^*) \tag{D-11}$$

In this case $Q^* = R^*$. The standard deviation and mean of Q' are

$$\sigma_Q' = \phi\{\Phi^{-1}[F_Q(Q^*)]\}/ f_Q(Q^*) \tag{D-12}$$

and

$$m_Q' = Q^* - \sigma_Q' \, \Phi^{-1}[F_Q(Q^*)] \tag{D-13}$$

The reliability index is

$$\beta = (m_R' - m_Q')/ (\sigma_{R'}^2 + \sigma_{Q'}^2)^{1/2} \tag{D-14}$$

Next, a new design point can be calculated from the following equations

$$R^* = m_R' - \beta \, \sigma_R'^2 \;/\; (\sigma_R'^2 + \sigma_{Q'}^2)^{1/2} \tag{D-15}$$

$$Q^* = m_Q' - \beta \, \sigma_Q'^2 \;/\; (\sigma_R'^2 + \sigma_{Q'}^2)^{1/2} \tag{D-16}$$

Then, the second iteration begins; the approximating normal distributions are found for F_R and F_Q at the new design point. The reliability index is calculated using Eq. D-14, and the next design point is found from Eqs. D-15 and D-16. Calculations are continued until R^* and Q^* do not change in consecutive iterations. The procedure has been programmed and calculations can be carried out by the computer.

SIMULATION AND SAMPLING TECHNIQUES

Parameters of R and Q, or even the limit state function g, can be obtained by Monte Carlo simulations. Values of R, Q and g can be generated using special numerical procedures. If the means and standard deviations of R and Q are estimated then β can be calculated using Eq. D-4. If the mean, m_g, and standard deviation, σ_g, are derived directly for the limit state function g, then the reliability index is,

$$\beta = m_g/\sigma_g \tag{D-17}$$

Monte Carlo technique can be used to simulate full distribution functions of R and Q. Then β can be calculated using Rackwitz and Fiessler procedure. If the distribution function of g is generated, then the probability of failure corresponds to g = 0. For larger values of β, a considerable number of simulations is required to properly model the lower tail of the generated distribution. Otherwise, the results must be extrapolated. The accuracy of calculations depends mostly on the number of computer runs. However, in many practical cases the required computational effort is prohibitively expensive.

The means and coefficients of variation of R and Q can also be calculated using sampling techniques. Various numerical methods have been widely used. In the Latin Hypercube method, the selection of a value from the cumulative distribution function (CDF) of a variable is guaranteed non-repeated (D-4). This is done by stratifying the CDF, and assigning a value to each stratum. The value assigned within each stratum is randomly selected from within the range of the CDF stratum. In the simulation process, a stratum and its corresponding CDF value is only selected once. Hence the number of strata equals the number of simulations. If the number of strata is large, the CDF value for each stratum may be taken as the center point of the stratum.

Point estimate methods have been developed to limit the number of function evaluations in an analysis. Rosenblueth developed a 2n+1 point estimate (D-5) and a 2n point estimate (D-6). Gorman developed a 3 point estimate (D-7). These point estimate methods have successfully been used in civil engineering. Tantawi (D-8) used them in bridge reliability analysis. The use of the point estimate methods is convenient. However, errors may occur as the result of correlation between variables, high coefficients of variation, or nonlinear functions. Zhou (D-9) developed an efficient integration procedure, analogous to Gauss-Legendre integration, using weights and points to estimate integrals. The points and weights are predetermined in the independent standard normal variable space depending upon the number of points selected. The sample points in basic variable space are then obtained by various transformations.

RELIABILITY METHODS USED IN CALIBRATION

The statistical parameters of load and resistance are determined on the basis of the available data (truck surveys, material tests) by simulations. The techniques used in this study include Monte Carlo and the integration procedure developed by Zhou (D-9).

The reliability is measured in terms of the reliability index. It is assumed that the total load, Q, is a normal random variable with the parameters as described in APPENDIX B. The resistance is considered as a lognormal random variable. The parameters of R are listed in Table 3.

For given nominal (design) value of resistance, R_n, the procedure used to calculate the reliability index, β, is outlined below.

1. Given:

   resistance parameters: R_n, λ_R, V_R

   load parameters: m_Q, σ_Q

2. Calculate the mean resistance, $m_R = \lambda_R R_n$.

3. Assume the design point is $R^* = m_R (1 - k V_R)$, where k is unknown. Take k = 2 (initial guess), and calculate $R^* = m_R (1 - 2 V_R)$.

4. Value of the cumulative distribution function of R (lognormal), and the probability density function of R, for R* are,

$$F_R (R^*) = \Phi [(\ln R^* - \ln m_R)/ V_R] \qquad \text{(D-18)}$$

$$f_R (R^*) = \phi [(\ln R^* - \ln m_R)/ V_R] / (V_R R^*) \qquad \text{(D-19)}$$

Calculate the argument of function Φ and ϕ,

$$\alpha = (\ln R^* - \ln m_R)/ V_R \qquad \text{(D-20)}$$

5. Calculate the standard deviation and mean of the approximating normal distribution of R, at R*, using Eq. D-8 and D-9,

$$\sigma_{R'} = \phi \{\Phi^{-1}[\Phi(\alpha)]\} / [\phi (\alpha) / (V_R R^*)] = V_R R^* \qquad \text{(D-21)}$$

$$m_{R'} = R^* - \sigma_{R'} \Phi^{-1}[\Phi(a)] = R^* - \alpha \sigma_{R'} \qquad \text{(D-22)}$$

The load, Q, is normally distributed, therefore, the mean and standard deviation are m_Q and σ_Q.

6. Calculate the reliability index, β, using Eq. D-14,

$$\beta = (R^* - \alpha V_R R^* - m_Q) / [(V_R R^*)^2 + \sigma_Q^2]^{1/2} \qquad \text{(D-23)}$$

7. Calculate new design point using Eq. D-15,

$$R^* = m_{R'} - \beta (V_R R^*)^2 / [(V_R R^*)^2 + \sigma_Q^2]^{1/2} \qquad \text{(D-24)}$$

8. Check if the new design point is different than what was assumed in step 3. If the same, the calculation of β is completed, otherwise go to step 4 and continue. In practice, the reliability index can be obtained in one cycle of iterations.

The formula for reliability index can be expressed in terms of the given data (R_n, λ_R, V_R, m_Q, σ_Q) and parameter k. By replacing R* with $[R_n \lambda_R (1 - k V_R)]$, α with Eq. D-20, after some rearrangements, the formula can be presented as,

$$\beta = \frac{R_n \lambda_R (1 - kV_R)[1 - \ln(1 - kV_R)] - m_Q}{\sqrt{[R_n V_R \lambda_R (1 - kV_R)]^2 + \sigma_Q^2}} \tag{D-25}$$

References for Appendix D

D-1. Thoft-Christensen, P. and Baker, M.J., Structural Reliability Theory and Its Applications, Springer-Verlag, (1982), p. 267.

D-2. Melchers, R.E., "Structural Reliability Analysis and Prediction," Ellis Horwood Limited, Chichester, England, (1987).

D-3. Rackwitz, R. and Fiessler, B., "Structural Reliability under Combined Random Load Sequences", Computer and Structures, 9, (1978), pp. 489-494.

D-4. McKay, M.D., Beckman, R. and Conover, W.J., "A Comparison of Three Methods for Selecting Values of Input Variables in the Analysis of Output from a Computer Code", Technometrics, Vol. 21, No. 2, (1979), pp. 239-245.

D-5. Rosenbueth, E., "Point Estimates for Probability Moments", Proceedings of the Nature Academy of Sciences, Vol. 72, No. 10, (1975), pp. 3812-3814.

D-6. Rosenblueth, E., "Two Point Estimate in Probabilities", Applied Mathematical Modeling Journal, (1981) pp. 329-335.

D-7. Gorman, M.R., "Reliability of Structural Systems", Report No. 79-2, Civil Engineering Dept., Case Western Reserve University, Cleveland, (1979).

D-8. Tantawi, H.M., "Ultimate Strength of Highway Girder Bridges", PhD Thesis, Department of Civil Engineering, University of Michigan, Ann Arbor, MI, (1986).

D-9. Zhou, J-H. "System Reliability Models for Highway Bridge Analysis", PhD Thesis, Department of Civil Engineering, University of Michigan, Ann Arbor, MI, (1987).

APPENDIX E Reliability Indices for Current AASHTO

SELECTED BRIDGES

The code calibration is based on calculations performed for a selected set of structures. About 200 representative bridges were selected from various regions of the United States. The selection was based on structural type, material, and geographical location. Current and future trends were considered. The selected set also includes representative existing bridges. State DOT's were requested to provide the drawings and other relevant information. The information was obtained for 107 bridges.

The list of structures provided by State DOT's is given in Table E-1. Bridges are grouped by material (steel, reinforced concrete, prestressed concrete and wood), span (simple and continuous) and structural type (slab, beam, box, truss, arch). The requested items which were not provided are also listed in Table E-1.

For the selected bridges, moments and shears are calculated due to dead load components, live load and dynamic load. Nominal (design) values are calculated using current AASHTO. The mean maximum 75 year values of loads are obtained using the statistical parameters presented in this report. Resistance is calculated in terms of the moment carrying capacity and shear capacity. For each case, two values of the nominal (design (resistance) are considered, the actual resistance and the minimum required resistance. The actual resistance, R_{actual}, is the as-built load carrying capacity. It is calculated according to AASHTO. The minimum required resistance, R_{min}, is calculated as the minimum R which satisfies the AASHTO Specifications.

In general, the actual nominal resistance, R_{actual}, is larger than the minimum value required by AASHTO, R_{min}. The basic design requirement according to AASHTO is either expressed in terms of stresses (Allowable Stress Design),

$$D + L + I < R \qquad \text{(E-1)}$$

where D, L and I are stresses due to dead load, live load and impact, respectively, and R is allowable stress, or in terms of moments (or shears) (Load Factor Design),

$$1.3\,D + 2.17\,(L + I) < \phi R \qquad \text{(E-2)}$$

Table E-1. Selected Bridges.

Structural Type	Requested Span (ft)	Provided Span (ft)	State
Steel, Simple Span			
Rolled beams, non-composite	40' to 80'	48'	PA
		59'	MI
		83'	PA
Rolled beams, composite	50' to 80'	48'	PA
		49'	PA
		50'	PA
		51'	MI
		67'	PA
		76'	PA
		80'	PA
		86'	PA
Plate girder, non-composite	100' to 150'	78'	PA
		100'	PA
Plate girder, composite	100' to 180'	103'	MI
		109'	PA
		122'	MI
Box girder	100' to 180'	none	
Through truss	300' to 400'	300'	PA
		303'	PA
		311'	PA
		397'	PA
Deck truss	200' to 400'	200'	NY
		250'	NY
		300'	NY
		400'	NY
Pony truss	150'	100'	OK
		103'	PA
		300'	PA
Arch	300' to 500'	360'	NY
		436'	NY
		630'	NY
		730'	NY
Tied Arch	300' to 600'	535'	KY
Steel, Continuous Span			
Rolled beams	50'-65'-50' to 80'-100'-80	74'-60'	PA
		85'-80'-85'	MI
		76'-96'-80'-60'	PA

Table E-1. Selected Bridges - continued.

Structural Type	Requested Span (ft)	Provided Span (ft)	State
Steel, Continuous Span - continued			
Plate girder	100'-120'-100'	190'-180'	MI
		120'-150'-120'	MI
		200'-200'-200'	KY
		300-300-300-300	KY
		195-195-195-195	KY
		200-200-200-200-200-20(	KY
Box Grider	100'-120'-100' to 300-400-30	103-103-103	MD
		123-123-123	MD
		142-150-103	MD
		122-162-122	IL
		116-138-138-138-116	IL
		150-167-175-175-167-15(	IL
Through truss	400'	none	
Deck truss	400'	none	
Tied Arch	300'-500'	none	
Reinforced Concrete, Simple Span			
Slab	20' to 40'	30'	OK
T-beam	40' to 80'	40'	IL
		40'	OK
		43'	IL
		50', 50'	OK
		60'	IL
Arch-barrel	40'	none	
Arch-rib	60'	none	
Reinforced Concrete, Continuous Span			
Slab, two span	30'-30'	none	
	40'-40'	none	
Slab, three span	25'-25'-25'	none	
Solid Frame	40'	40'	CA
		48'	CA
T-beam, frame	55'	none	
T-beam, two span	50'-50'	62'-62'	CO
	0'-70'	71'-71'	CO

Table E-1. Selected Bridges - continued.

Structural Type	Requested Span (ft)	Provided Span (ft)	State
Reinforced Concrete, Continuous Span - continued			
T-beam, three span	40-50-40 to 50-70-50	38-50-38	TN
		40-51-40	TN
		0-51-40	TN
		46-56-39	TN
		47-65-47	TN
		53-73-53	TN
		50-71-42	TN
Arch		none	
Box, three span	60-80-60 to 75-90-75	69-119-96	MD
Prestressed Concrete, Simple Span			
Slab	30' to 40'	none	
Voided slab	30 to 50	none	
Double T	40 to 60	39	CO
Closed box CIP	125'	none	
AASHTO beam	50 to 100	76	MI
		76	CO
		102	TX
		102	PA
		105	PA
		103	MI
		110	CO
		118	TX
		120	CO
		130	TX
		138	CO
Bulb	60 to 120	none	
Box girder	80 to 120	74	PA
		74	PA
		82	CA
		95	CA
		102	CA
		104	CA
		116	CA
		118	CA
		120	CA
		125	CA
		125	CA

Table E-1. Selected Bridges - continued.

Structural Type	Requested Span (ft)	Provided Span	State
Prestressed Concrete, Continuous Span			
Slab	35-35 to 40-50-40	none	
Voided slab	50-70-50 to 105-105	none	
AASHTO beam	80 to 110	none	
Post-tensioned AASHTO beam	100-100	none	
Bulb		none	
Box		65-65	CA
		87-85	CA
		93-86	CA
		103-102	CA
		107-102	CA
		110-160	CA
		118-101	CA
		200-200	CA
		60-80-60	CA
		69-82-59	CA
		75-90-75	CA
		69-92-69	CA
		76-90-76	CA
		71-85-71	CA
		66-85-52	CA
Wood			
Sawn beam		18	MN
Glulam beam - nailed		49-50-49	MN
Glulam beam - dowelled		none	
Glulam beam - composite		none	
Truss		50, 100, 100, 4	MN
Arch		none	
Deck - nailed		32, 32, 32	MN
Deck - composite		none	
Deck - prestressed transversely		44	MN
Deck - prestressed longitudinally		none	

where D, L and I are moments (or shears) due to dead load, live load and impact, R is the moment (or shear) carrying capacity, and ϕ is the resistance factor. Values of the resistance factor are given in Table 4.

For given loads, D, L and I, the minimum required resistance, R_{min}, according to AASHTO, can be calculated from Eq. E-1 for Allowable Stress Design,

$$R_{min} = D + L + I \tag{E-3}$$

and from Eq. E-2, for the Load Factor Design,

$$R_{min} = [1.3\ D + 2.17\ (L + I)]/\phi \tag{E-4}$$

The statistical parameters (bias factor and coefficient of variation) of resistance are taken from Table 3.

Nominal (design) load components and resistance calculated for the selected bridges are listed in Table E-2. Columns are numbered and the explanation is provided below:

Column 1 - Bridge number, all structures are numbered for an easier reference.
Column 2 - State where the bridge is located.
Column 3 - Material, structural type, section type, SS = simple span, CS = continuous span.
Column 4 - Span length considered (ft).
Column 5 - Girder number; G1 = exterior girder, G2 = interior girder.
Column 6 - Girder spacing (ft).
Column 7 - Limit state considered, M = moment and S = shear.
Column 8 - Dead load due to the weight of factory made components.
Column 9 - Dead load due to the weight of cast in place components.
Column 10 - Dead load due to the weight of wearing surface (asphalt).
Column 11 - Dead load due to the weight of miscellaneous items.
Column 12 - Live load due to HS20 loading (AASHTO).
Column 13 - Impact according to AASHTO.
Column 14 - Minimum required resistance by AASHTO, R_{min}.
Column 15 - Actual resistance, R_{actual}.
Column 16 - Ratio of R_{actual}/R_{min}.

The ratio of R_{actual}/R_{min} is plotted vs. span in Fig. E-1 for moment in steel girders, Fig. E-2 for moment in prestressed concrete girders, and Fig. E-3 for shear in steel girders.

The analysis of the selected bridges provides information about actual values of load components. Girder spacing is between 4 and 10 ft for almost all considered cases. However, the selected bridges do

Table E-2. Load Components and Resistance for Selected Bridges.

No.	St.	Type	Span	Gr.	Space	F	D1	D2	D3	D4	LL	I	R min	R actual	Ratio
1	2	3	4	5	6	7	8	9	10	11	12	13	14	15	16
1	PA	S.S.	48.0	G1	6.5	S	3	16	2	26	20	6	118	276	2.3
	Steel					M	33	190	28	317	205	59	1310	2340	1.8
	beam			G2		S	3	16	5	0	39	11	138	276	2.0
						M	33	187	56	0	344	99	1320	2340	1.8
2	PA	S.S.	53.3	G1	6.8	S	3	19	3	24	23	7	128	358	2.8
	Steel					M	44	246	42	314	267	75	1580	2722	1.7
	beam			G2		S	3	17	6	1	41	11	147	358	2.4
						M	44	223	74	4	408	114	1582	2722	1.7
3	PA	S.S.	75.6	G1	7.0	S	6	27	5	29	27	7	160	497	3.1
	Steel					M	99	510	98	541	466	116	2884	4462	1.5
	beam			G2		S	6	27	8	1	44	11	173	497	2.9
						M	99	500	150	17	661	165	2788	4462	1.6
4	PA	S.S.	50.1	G1	6.0	S	3	15	2	21	20	6	109	261	2.4
	Steel					M	32	187	28	266	210	60	1256	2157	1.7
	beam			G2		S	3	14	5	0	36	10	128	261	2.0
						M	32	176	56	3	342	98	1303	2157	1.7
5	PA	S.S.	66.6	G1	8.5	S	6	28	9	22	37	10	186	724	3.9
	Steel					M	101	458	150	373	555	145	2925	5074	1.7
	beam			G2		S	6	28	13	0	50	13	198	724	3.7
						M	101	471	212	7	641	167	2782	5074	1.8
6	PA	S.S.	80.0	G1	8.0	S	11	34	11	15	42	10	207	889	4.3
	Steel					M	224	672	225	306	776	189	3951	10399	2.6
	beam			G2		S	11	34	14	2	49	12	213	889	4.2
						M	224	680	288	38	776	189	3695	10399	2.8
7	PA	S.S.	48.9	G1	1.8	S	2	9	1	20	0	0	41		
	Steel					M	25	105	12	238	0	0	494		
	beam			G2		S	3	10	4	0	25	7	92		
						M	33	125	51	0	207	59	849		
8	PA	S.S.	86.3	G1	7.0	S	12	28	5	40	23	6	170	540	3.2
	Steel					M	238	593	98	852	448	106	3518	5275	1.5
	beam			G2		S	12	28	9	1	45	11	184	540	2.9
						M	238	611	196	16	764	181	3428	5275	1.5

Table E-2. Load Components and Resistance - continued.

No.	St.	Type	Span	Gr.	Space	F	D1	D2	D3	D4	LL	I	R min	R actual	Ratio
1	2	3	4	5	6	7	8	9	10	11	12	13	14	15	16
9	PA	S.S.	109	G1	8.0	S	12	46	13	36	35	8	231	433	1.9
		Steel				M	291	1244	357	980	894	180	6062	8424	1.4
		plate		G2		S	12	46	20	1	51	11	235	433	1.8
						M	291	1258	533	14	1122	240	5680	8424	1.5
10	PA	S.S.	110	G1	37.8	S	25	151	43	26	613	131	1932		
		Steel				M	630	4218	1189	735	17857	3804	55807		
		plate		G2		S									
						M									
11	PA	S.S.	83	G1	4.8	S	13	25	0	0	24	6	112		
		Steel				M	258	509	0	9	462	111	2252		
		beam		G2		S	13	20	0	0	33	8	131		
						M	258	422	0	9	524	130	2316		
12	PA	S.S.	48	G1	5.5	S	3	11	0	18	16	5	85		
		Steel				M	37	128	0	215	161	47	946		
		beam		G2		S	4	13	0	6	33	10	122		
						M	44	158	0	69	296	86	1181		
13	PA	S.S.	78	G1	32.3	S	10	64	0	16	82	20	339		
		Steel				M	179	1242	0	262	1453	359	6118		
		plate		G2		S									
						M									
14	M	S.S.	51	G1	5.0	S	3	8	0	11	9	3	52	115	2.2
		Steel				M	37	97	0	138	96	27	620	1178	1.9
		beam		G2		S	3	11	0	0	31	9	106	222	2.1
						M	37	140	0	4	290	83	1045	2038	2.0
15	M	S.S.	47	G1	6.4	S	3	14	0	13	20	6	94	244	2.6
		Steel				M	36	161	0	150	198	57	1006	1851	1.8
		beam		G2		S	3	14	0	0	38	11	128	334	2.6
						M	36	166	0	0	329	95	1184	2286	1.9
16	M	S.S.	64	G1	6.4	S	5	18	0	17	21	6	111	211	1.9
		Steel				M	79	292	0	273	298	79	1654	2646	1.6
		beam		G2		S	5	19	0	0	40	11	140	274	2.0
						M	79	301	0	0	495	131	1854	3059	1.7

Table E-2. Load Components and Resistance - continued.

No.	St.	Type	Span	Gr.	Space	F	D1	D2	D3	D4	LL	I	R min	R actual	Ratio
1	2	3	4	5	6	7	8	9	10	11	12	13	14	15	16
17	M	S.S.	60	G1	6.4	S	4	17	0	16	21	6	107	289	2.7
		Steel				M	63	258	0	240	277	75	1492	2686	1.8
		beam		G2		S	4	18	0	0	39	11	137	384	2.8
						M	63	266	0	0	460	125	1696	3257	1.9
18	M	S.S.	59	G1	5.1	S	5	9	0	12	3	1	43		
		Steel				M	75	133	0	177	42	11	615		
		beam		G2		S	5	13	0	0	33	9	115		
						M	75	197	0	5	370	100	1379		
19	M	S.S.	122	G1	7.2	S	14	39	5	56	26	5	216		
		Steel				M	422	1195	143	1698	756	153	6468		
		plate		G2		S	14	44	8	1	49	10	213		
						M	422	1327	248	17	1275	259	5947		
20	M	S.S.	103	G1	5.5	S	12	26	0	30	16	4	132		
		Steel				M	304	675	0	775	395	86	3323		
		plate		G2		S	12	25	0	0	37	8	146		
						M	304	642	0	0	789	173	3316		
21	M	S.S.	45	G1	5.5	S	5	11	0	13	14	4	78		
		Steel				M	54	126	0	147	133	39	796		
		plate		G2		S	2	11	0	0	33	10	109		
						M	27	199	0	0	265	78	1038		
22	CO	S.S.	60	G1	7.2	S	32	0	3	7	30	8	163		
		P/S				M	481	0	49	106	403	109	1938	2413	1.2
		Double T		G2		S	32	0	4	0	61	16	252		
						M	481	0	59	0	807	218	2924		
23	CO	S.S.	39	G1	7.3	S	20	0	2	5	27	8	133		
		P/S				M	197	0	20	47	216	76	977	1270	1.3
		Double T		G2		S	20	0	3	0	55	17	217		
						M	193	0	24	0	423	129	1480	1805	1.2
24	CO	S.S.	76	G1	7.8	S	25	25	3	10	29	7	188		
		P/S				M	479	475	65	198	495	123	2920	3854	1.3
				G2		S	25	31	5	1	49	12	252		
						M	479	589	102	28	774	192	3653	4603	1.3

Table E-2. Load Components and Resistance - continued.

No.	St.	Type	Span	Gr.	Space	F	D1	D2	D3	D4	LL	I	R min	R actual	Ratio
1	2	3	4	5	6	7	8	9	10	11	12	13	14	15	16
25	CO	S.S.	98	G1	7.5	S	32	41	5	6	33	7	230		
		P/S				M	780	996	109	166	740	166	4632	6701	1.4
				G2		S	32	36	7	1	49	11	269		
						M	780	877	160	34	1009	227	5089	6701	1.3
26	CO	S.S.	120	G1	6.5	S	41	38	7	22	40	8	287		
		P/S				M	1218	1144	199	678	1133	231	7171	8725	1.2
				G2		S	41	36	7	1	44	9	264		
						M	1218	1095	212	48	1113	227	6253	8725	1.4
27	CO	S.S.	138	G1	6.3	S	55	46	6	43	30	6	318		
		P/S				M	1891	1578	196	1506	974	185	9235		
				G2		S	55	42	8	1	43	8	292		
						M	1891	1463	273	57	1274	242	8078		
28	CO	S.S.	110	G1	7.5	S	37	47	2	23	26	6	247		
		P/S				M	1019	1284	41	631	703	150	5718	8395	1.5
				G2		S	37	42	7	1	50	11	288		
						M	1019	1151	204	51	1162	248	6212	8395	1.4
29	TX	S.S.	102	G1	7.8	S	42	41	9	4	46	10	291		
		P/S				M	1069	1040	232	109	1107	244	6115	9294	1.5
		IV		G2		S	42	37	10	2	51	11	297	431	1.5
						M	1069	946	252	62	1099	242	5936		
30	TX	S.S.	118	G1	6.6	S	49	36	6	4	36	7	256		
		P/S				M	1431	1062	183	130	1104	227	6536	8758	1.3
		IV		G2		S	49	36	7	1	44	9	278		
						M	1431	1063	214	50	1104	227	6475	8289	1.3
31	TX	S.S.	130	G1	4.6	S	53	35	6	4	31	6	243		
		P/S				M	1737	1120	188	151	862	169	6392	9141	1.4
				G2		S	53	28	6	1	33	6	234	316	1.4
						M	1737	908	181	49	862	169	5975		
32	PA	S.S.		G1		S	59	129	9	9	24	5	391		
		P/S	102		10.2	M	1507	3285	222	193	582	128	8310	14968	1.8
		T-beam		G2		S	59	52	23	11	63	14	420		
						M	1507	1323	596	128	1441	317	8435	14968	1.8

Table E-2. Load Components and Resistance - continued.

No.	St.	Type	Span	Gr.	Space	F	D1	D2	D3	D4	LL	I	R min	R actual	Ratio
1	2	3	4	5	6	7	8	9	10	11	12	13	14	15	16
33	PA	S.S.	106	G1	6.8	S	47	35	6	34	23	5	258		
		P/S				M	1236	930	144	897	577	125	5692	8766	1.5
		T-beam		G2		S	47	38	11	4	46	10	293		
						M	1236	991	287	88	1013	220	6060	8241	1.4
34	MI	S.S.	103	G1	6.9	S	42	28	0	76	10	0	249		
		P/S				M	1090	731	0	1960	244	0	5445	8657	1.6
		T-beam		G2		S	42	40	0	0	46	10	269		
						M	1090	1034	0	0	995	218	5393	7820	1.5
35	MI	S.S.	76	G1	6.9	S	31	21	0	56	7	0	184		
		P/S				M	594	398	0	1064	133	0	2961	3908	1.3
		IV		G2		S	22	30	0	0	45	11	221		
						M	420	563	0	0	661	165	3071	3839	1.3
36	IL	S.S.	40	G1	6.5	S	0	19	0	7	19	6	103		
		P/S				M	0	191	0	67	156	47	860		
		T-beam		G2		S	0	22	0	0	36	11	153		
						M	0	220	0	0	244	73	1081		
37	IL	S.S.	43	G1	6.4	S	0	22	2	5	22	6	116		
		R.C.				M	0	234	26	61	193	57	1065		
		T-beam		G2		S	0	24	2	1	36	11	160		
						M	0	257	26	14	269	80	1271		
38	IL	S.S.	60	G1	6.5	S	0	40	4	13	26	7	170		
		R.C.				M	0	599	65	193	339	92	2275		
		T-beam		G2		S	0	41	7	0	39	11	200		
						M	0	620	105	0	437	118	2385		
39	OK	S.S.	50	G1	5.9	S	0	27	0	11	16	5	111		
		R.C.				M	0	341	0	148	171	49	1235		
		T-beam		G2		S	0	33	0	2	34	10	165		
						M	0	412	0	33	305	87	1589		
40	OK	S.S.	30	G1	6.7	S	0	17	0	0	28	8	117		
		R.C.				M	0	125	0	4	157	47	677		
		T-beam		G2		S	0	13	0	1	34	10	133		
						M	0	101	0	7	157	47	647		

Table E-2. Load Components and Resistance - continued.

No.	St.	Type	Span	Gr.	Space	F	D1	D2	D3	D4	LL	I	R min	R actual	Ratio
1	2	3	4	5	6	7	8	9	10	11	12	13	14	15	16
41	OK	S.S.	40	G1	6.7	S	0	24	0	0	31	9	139		
		R.C.				M	0	244	0	7	250	75	1145		
		T-beam		G2		S	0	20	0	1	37	11	154		
						M	0	201	0	13	250	75	1091		
42	OK	S.S.	50	G1	6.7	S	0	37	0	1	33	9	164		
		R.C.				M	0	460	0	13	345	99	1754		
		T-beam		G2		S	0	31	0	1	39	11	177		
						M	0	392	0	26	345	99	1675		
43	PA	S.S.	38	G1	9.3	S	12	15	3	12	31	9	166		
		P/S				M	111	146	31	112	235	70	1180		
		Box		G2		S	12	18	5	0	49	15	217		
						M	111	166	50	0	348	104	1405		
44	PA	S.S.	41	G1	9.3	S	13	17	4	13	32	10	175		
		P/S				M	129	170	36	131	265	80	1352		
		Box		G2		S	13	19	6	0	51	16	225		
						M	129	194	58	0	393	118	1603		
45	PA	S.S.	47	G1	9.3	S	15	19	4	15	33	10	188		
		P/S				M	172	227	48	174	329	95	1726		
		Box		G2		S	15	22	7	0	52	15	238		
						M	172	259	78	0	487	141	2024		
46	PA	S.S.	19	G1	9.75	S	4	8	2	7	22	7	103		
		P/S				M	20	39	7	31	82	25	357		
		Box		G2		S	4	9	3	0	39	12	154		
						M	20	44	13	0	135	40	480		
47	PA	S.S.	72	G1	9.5	S	27	33	6	25	36	9	255		
		P/S				M	485	595	112	441	589	150	3725		
		Box		G2		S	27	34	10	0	58	15	293		
						M	485	611	183	0	878	223	4054		
48	PA	S.S.	37	G1	9.3	S	10	15	3	12	33	10	172		
		P/S				M	90	138	32	109	243	73	1164		
		Box		G2		S	10	16	5	0	49	15	210		
						M	90	146	47	0	329	99	1296		

Table E-2. Load Components and Resistance - continued

No.	St.	Type	Span	Gr.	Space	F	D1	D2	D3	D4	LL	I	R min	R actual	Ratio
1	2	3	4	5	6	7	8	9	10	11	12	13	14	15	16
49	PA	S.S.	46	G1	9.3	S	14	19	4	15	36	11	198		
		P/S				M	160	221	50	174	350	102	1765		
		Box		G2		S	14	20	7	0	52	15	234		
						M	160	233	75	0	474	138	1935		
50	PA	S.S.	52	G1	10.2	S	18	24	5	19	34	10	211		
		P/S				M	229	304	58	244	381	108	2147		
		Box		G2		S	18	26	8	0	57	16	267		
						M	229	337	101	0	605	171	2552		
51	PA	S.S.	72	G1	7.3	S	30	26	8	26	25	6	216		
		P/S				M	533	456	146	467	402	102	3177		
		Box		G2		S	30	24	8	0	46	12	242		
						M	533	435	140	0	668	170	3258		
52	PA	S.S.	61	G1	9.1	S	21	24	8	20	37	10	230		
		P/S				M	317	370	118	297	494	133	2793		
		Box		G2		S	21	26	8	0	54	15	260		
						M	317	390	125	0	674	181	2935		
53	PA	S.S.	50	G1	9.5	S	17	21	7	18	32	9	200		
		P/S				M	206	261	83	220	365	104	2020		
		Box		G2		S	17	22	7	0	54	15	247		
						M	206	278	89	0	542	155	2259		
54	PA	S.S.	42	G1	9.4	S	11	16	4	13	32	9	172		
		P/S				M	120	168	38	138	275	82	1377		
		Box		G2		S	11	19	6	0	52	15	226		
						M	120	197	63	0	418	125	1671		
55	PA	S.S.	75	G1	4.0	S	25	8	3	11	17	4	129		
		P/S				M	475	157	63	213	292	73	1971		
		Box		G2		S	25	11	5	0	27	7	150		
						M	475	209	84	0	389	97	2054		
56	PA	S.S.	74	G1	4.0	S	28	0	2	32	14	4	140		
		P/S				M	513	0	28	592	237	60	2116		
		Box		G2		S	28	0	3	0	28	7	136		
						M	513	0	62	0	386	97	1795		

Table E-2. Load Components and Resistance - continued

No.	St.	Type	Span	Gr.	Space	F	D1	D2	D3	D4	LL	I	R min	Ract	Ratio
1	2	3	4	5	6	7	8	9	10	11	12	13	14	15	16
57	CA	S.S.	120	G1		S	0	1101	80	68	199	41	2523		
		P/S				M	0	16399	2377	2024	5605	1149	41696		
		Box													
58	CA	S.S.	104	G1		S	0	504	73	62	262	57	1792		
		P/S				M	0	13104	1893	1622	6383	1392	38476		
		Box													
59	CA	S.S.	82	G1		S	0	321	46	44	191	46	1234		
		P/S				M	0	6541	930	897	3576	865	20515		
		Box													
60	CA	S.S.	125	G1		S	0	565	74	71	201	40	1701		
		P/S				M	0	17648	2324	2227	5920	1184	44274		
		Box													
61	PA	C.S.	74-	G1	5.5	S	6	13	0	23	16	4			
		Steel	60			S	16	37	0	65	19	5			
		beam				S	4	9	0	15	16	4			
						M	83	190	0	329	226	57			
						M	-116	-256	0	-443	-142	-36			
						M	35	80	0	138	178	45			
				G2		S	6	16	0	8	34	9			
						S	16	46	0	23	40	10			
						S	4	11	0	6	33	8			
						M	83	235	0	119	414	104			
						M	-112	-316	0	-160	-260	-65			
						M	35	98	0	50	326	82			
62	MI	C.S.	190-	G1	7.9	S	31	44	0	61	23	4			
		Steel	180			S	94	137	0	188	25	4			
		plate				S	26	44	0	51	23	4			
						M	1120	1629	0	2241	884	141			
						M	-1707	-2483	0	-3414	-472	-74			
						M	786	1144	0	1573	797	131			
				G2		S	31	65	0	0	51	8			
						S	94	200	0	0	54	9			
						S	26	54	0	0	51	8			
						M	1120	2383	0	0	1681	267			
						M	-1707	-3632	0	0	-898	-147			
						M	786	1672	0	0	1515	248			

Table E-2. Load Components and Resistance - continued

No.	St.	Type	Span	Gr.	Space	F	D1	D2	D3	D4	LL	I	Rmin	Ract	Ratio
1	2	3	4	5	6	7	8	9	10	11	12	13	14	15	16
63	M	C.S.	120-	G1	7.8	S	11	33	0	63	11	0			
		Steel	150-			S	36	112	0	211	36	0			
		plate	120			M	241	737	0	1396	241	0			
						M	-447	-1370	0	-2596	-447	0			
						M	233	714	0	1353	233	0			
				G2		S	11	41	0	0	49	10			
						S	36	138	0	0	53	11			
						M	241	915	0	0	1007	206			
						M	-447	-1701	0	0	-603	123			
						M	233	886	0	0	1017	207			
64	M	C.s	30-	G1	7.5	S	1	6	0	4	20	6			
		steel	50-			S	5	30	0	20	27	8			
		I-bean	30			M	4	26	0	18	95	28			
						M	-18	-118	0	-79	-110	-33			
						M	13	86	0	57	143	43			
				G2		S	1	7	0	0	36	11			
						S	5	35	0	0	46	14			
						M	4	30	0	0	145	43			
						M	-18	-136	0	0	-168	-51			
						M	13	99	0	0	219	66			
65	M	C.S.	85-	G1	8.7	S	7	32	0	18	38	9			
		steel	80-			S	17	81	0	45	43	10			
		I-bean	85			M	117	550	0	307	598	142			
						M	-129	-608	0	-340	-369	-88			
						M	13	61	0	34	455	127			
				G2		S	7	34	0	0	51	12			
						S	17	86	0	0	57	14			
						M	117	586	0	0	693	165			
						M	-129	-648	0	0	-428	-102			
						M	13	65	0	0	527	126			
66	CA	C.S	1.7-	G1		S	0	217	34	18	182	46			
		P/S	4.5-			S	0	732	113	62	210	53			
		box	71			M	0	2890	447	243	2478	629			
						M	0	-5375	-832	-452	-1603	-407			
						M	0	2801	433	235	2516	639			

Table E-2. Load Components and Resistance - continued

No.	St.	Type	Span	Gr.	Space	F	D1	D2	D3	D4	LL	I	Rmin	R actual	Ratio
1	2	3	4	5	6	7	8	9	10	11	12	13	14	15	16
67	CA	C.S	66-	G1		S	0	196	30	17	179	47			
		P/S	85-			S	0	689	107	58	209	55			
		box	53			S	0	602	93	51	211	55			
						S	0	125	19	11	169	44			
						M	0	2369	367	199	2209	579			
						M	0	-4771	-738	-401	-1180	-309			
						M	0	2664	412	224	2218	581			
						M	0	-3774	-584	-317	-1633	-428			
						M	0	964	149	81	1580	414			
68	CA	C.S.	81-	G1	9.0	S		240			192				
		P/S	105-			S		435			213				
		box	81			M		3017			2535				
						M		-6044			-2387				
						M		4007			2642				
69	CA	C.S.	110-	G1	9.0	S		441			239				
		P/S	120-			S		719			263				
		box	100			S		659			263				
						M		7999			4150				
						M		-12245			-4005				
						M		6437			3659				
						M		10561			-3724				
						M		6182			3774				
70	CA	C.S.	160-	G1	8.8	S		636			209				
		P/S	195-			S		1086			272				
		box	112			S		996			270				
						M		16696			6057				
						M		-32669			-7516				
						M		18810			5956				
						M		-24176			-6712				
						M		3974			4141				
71	CA	S.S.	130	G1	8.0	S		2661			991				
		P/S				M		86161			30149				
		box													
72	CA	S.S.	139	G1	9.4	S		4114			1345				
		P/S				M		142231			42308				
		box													

Table E-2. Load Components and Resistance - continued

No.	St.	Type	Span	Gr.	Space	F	D1	D2	D3	D4	LL	I	R min	R actu	Ratio
1	2	3	4	5	6	7	8	9	10	11	12	13	14	15	16
73	CA	C.S.	200-	G1		S		899			228				
		P/S	200			S		1571			309				
		box				M		29028			7719				
						M		-55945			10444				
74	CA	C.S.	65-	G1	not	S		194			190				
		P/S	65		const.	S		324			210				
		box				M		2067			2138				
						M		-3762			-1622				
75	CA	C.S.	8.5-	G1	9.0	S		382			240				
		P/S	99			S		639			261				
		box				M		6213			4111				
						M		-11012			-3763				
76	CA	C.S.	3.5-	G1	10.7	S		396			218				
		P/S	102			S		656			237				
		box				S		387			218				
						M		6805			3821				
						M		-11474			-3569				
						M		6439			3767				
76	CA	C.S.	109-	G1	9.9	S		502			260				
		P/S	109			S		850			283				
		box				M		9168			4967				
						M		-16666			-4920				
77	CA	C.S.	.75-	G1	8.8	S		1082			493				
		P/S	123			S		1785			571				
		box				S		1046			493				
						M		22750			11761				
						M		-40093			-11490				
						M		20976			11566				
78	CA	C.S.	135-	G1	8.7	S		1030			422				
		P/S	132			S		1693			514				
		box				S		985			422				
						M		23350			9579				
						M		-37095			-10294				
						M		20999			9345				

Table E-2. Load Components and Resistance - continued

No.	St.	Type	Span	Gr.	Space	F	D1	D2	D3	D4	LL	I	R min	R actual	Ratio
1	2	3	4	5	6	7	8	9	10	11	12	13	14	15	16
79	CA	C.S.	146-	G1	9.9	S		713			267				
		P/S	144			S		1207			338				
		box				S		729			267				
						M		1678			6934				
						M		-32030			-8131				
						M		17713			7017				

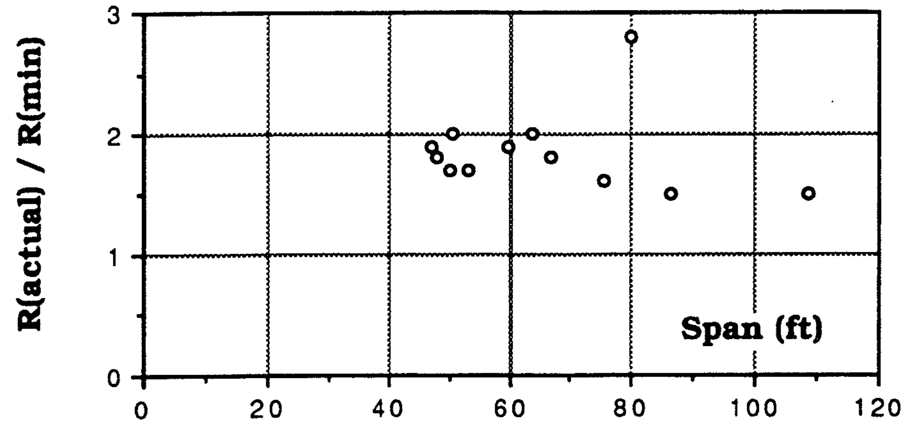

Fig. E-1. Ratio of R_{actual}/R_{min} for Moment in Steel Girder Bridges.

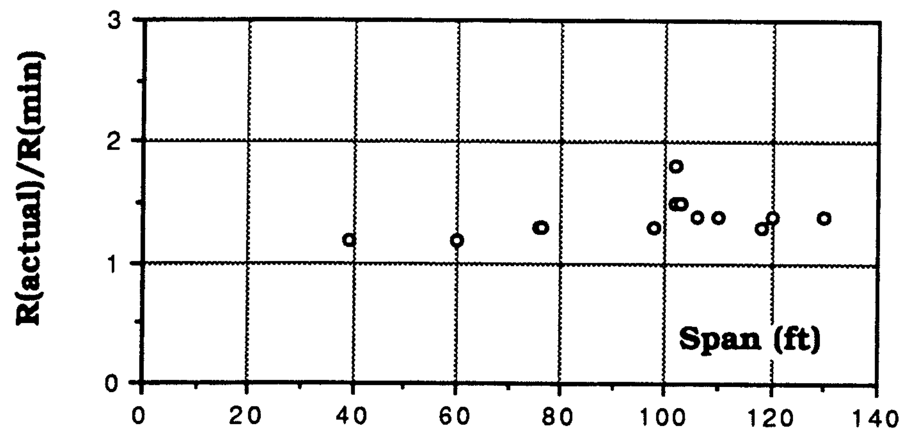

Fig. E-2. Ratio of R_{actual}/R_{min} for Moment in Prestressed Concrete Girder Bridges.

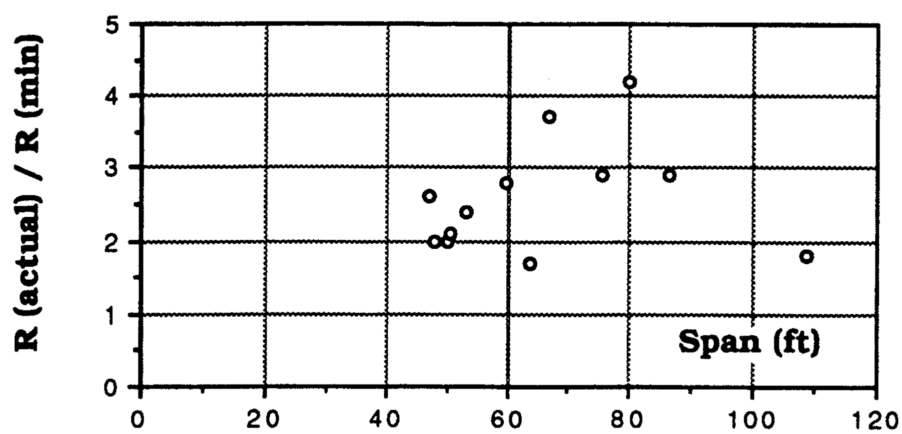

Fig. E-3. Ratio of R_{actual}/R_{min} for Shear in Steel Girder Bridges.

not cover a full range of spans and other parameters. Therefore, additional bridges are designed as a part of this study. The analysis is focused on girder bridges, including steel non-composite and composite beams, reinforced concrete T-beams and prestressed concrete AASHTO type girders, with spans from 30 to 200 ft. Five girder spacings are considered: 4, 6, 8, 10 and 12 ft. Typical cross sections are assumed. In all considered cases, the actual resistance, R_{actual}, is made equal exactly to R_{min}. This means that the sections are neither overdesigned nor underdesigned. Separate designs are carried out for moments and shears.

The calculated load components and resistance are summarized in tables. In the analysis, live loads are distributed using girder distribution factors (GDF) specified by AASHTO. For the moments, the calculated nominal (design) loads and resistance, R_{min}, are given in Tables E-3 through E-6 for non-composite steel, composite steel, reinforced concrete T-beams and prestressed AASHTO type girders, respectively. For shears, the results are presented in Tables E-7 to E-9.

For each considered case, the mean and standard deviation is calculated for the total load effect. The results are also shown in Tables E-3 to E-9, including span length, girder spacing, D_1, D_2, D_3, LL (static part of live load), I (dynamic part of live load), mQ (mean total load effect), sQ (standard deviation of total load effect) and R_{min}. The moments are given in k-ft and shears in kips.

CALCULATED RELIABILITY INDICES

The reliability indices are calculated for girder bridges and the limit states (moment and shear) described by the representative load components and resistance listed in Tables E-3 through E-9. The results are presented in Table E-10 to E-13, for simple span moments in non-composite steel, composite steel, reinforced concrete and prestressed concrete girders, respectively. For shears the results are given in Tables E-14 to E-16. For each considered case, given are: the span length, girder spacing, mean total load, m_Q, standard deviation of total load, σ, nominal (design) value of resistance, R_n, bias factor for resistance, λ, coefficient of variation of resistance, V, and the reliability index, β.

The reliability indices are also presented in Fig. 8 to 11 for moments in non-composite steel, composite steel, reinforced concrete and prestressed concrete. For shears the results are shown in Fig. 12 to 14.

Table E-3. Representative Load Components and Resistance for Non-Composite Steel Girder Bridges, Moments.

Span (ft)	Space (ft)	D1 (k-ft)	D2 (k-ft)	D3 (k-ft)	LL (k-ft)	I (%)	mQ (k-ft)	sQ (k-ft)	R(min) (k-ft)
30	4	8	61	12	103	30	321	43	395
30	6	8	84	18	154	30	428	57	578
30	8	9	104	24	205	30	526	70	756
30	10	10	130	30	256	30	629	83	945
30	12	11	160	36	308	30	733	95	1138
60	4	41	245	49	293	27	916	106	1243
60	6	54	335	73	440	27	1227	140	1813
60	8	77	414	97	587	27	1525	172	2381
60	10	95	521	122	733	27	1839	203	2979
60	12	113	639	146	880	27	2158	234	3592
90	4	263	552	109	489	23	1920	186	2509
90	6	284	754	164	733	23	2506	245	3524
90	8	304	931.5	219	978	23	3046	299	4505
90	10	324	1172	273	1222	23	3639	354	5569
90	12	354	1438	328	1467	23	4258	409	6679
120	4	540	981	194	685	20	3157	276	4019
120	6	630	1341	292	1027	20	4148	364	5625
120	8	684	1656	389	1369	20	5026	446	7126
120	10	720	2083	486	1712	20	5983	529	8748
120	12	810	2556	583	2054	20	7030	613	10501
200	4	3000	2725	540	1491	15	9096	617	11878
200	6	3500	3725	810	2236	15	11714	806	16045
200	8	4000	4600	1080	2982	15	14148	982	20050
200	10	4500	5788	1350	3727	15	16875	1171	24461
200	12	5000	7100	1620	4473	15	19705	1365	29035

Table E-4. Representative Load Components and Resistance for Composite Steel Girder Bridges, Moments.

Span (ft)	Space (ft)	D1 (k-ft)	D2 (k-ft)	D3 (k-ft)	LL (k-ft)	I (%)	mQ (k-ft)	sQ (k-ft)	R(min) (k-ft)
30	4	7	61	12	103	30	320	43	394
30	6	7	84	18	154	30	426	57	576
30	8	8	104	24	205	30	525	70	755
30	10	9	130	30	256	30	628	83	944
30	12	10	160	36	308	30	731	95	1136
60	4	39	245	49	293	27	914	106	1241
60	6	48	335	73	440	27	1221	140	1806
60	8	70	414	97	587	27	1518	172	2372
60	10	84	521	122	733	27	1828	203	2965
60	12	103	639	146	880	27	2148	234	3579
90	4	258	552	109	489	23	1915	186	2502
90	6	268	754	164	733	23	2490	244	3504
90	8	286	931.5	219	978	23	3028	299	4482
90	10	303	1172	273	1222	23	3617	354	5542
90	12	339	1438	328	1467	23	4242	409	6659
120	4	502	981	194	685	20	3118	276	3970
120	6	607	1341	292	1027	20	4124	364	5595
120	8	650	1656	389	1369	20	4991	446	7081
120	10	681	2083	486	1712	20	5943	529	8698
120	12	773	2556	583	2054	20	6992	613	10453
200	4	2780	2725	540	1491	15	8870	610	11592
200	6	3303	3725	810	2236	15	11511	800	15789
200	8	3790	4600	1080	2982	15	13932	976	19777
200	10	4190	5788	1350	3727	15	16556	1163	24058
200	12	4875	7100	1620	4473	15	19577	1362	28873

Table E-5. Representative Load Components and Resistance for Reinforced Concrete T-Beam Bridges, Moments.

Span (ft)	Space (ft)	D1 (k-ft)	D2 (k-ft)	D3 (k-ft)	LL (k-ft)	I (%)	mQ (k-ft)	sQ (k-ft)	R(min) (k-ft)
30	4	0	107	12	94	30	361	44	467
30	6	0	129	18	141	30	467	58	655
30	8	0	150	24	188	30	566	71	841
30	10	0	174	30	235	30	665	84	1032
30	12	0	236	36	282	30	801	97	1277
60	4	0	460	49	269	27	1100	114	1558
60	6	0	630	73	403	27	1481	151	2250
60	8	0	720	97	538	27	1767	183	2827
60	10	0	878	122	672	27	2116	216	3502
60	12	0	1035	146	807	27	2458	249	4176
90	4	0	1420	109	448	23	2561	230	3541
90	6	0	1720	164	672	23	3228	293	4719
90	8	0	1923	219	896	23	3774	347	5757
90	10	0	2278	273	1120	23	4466	409	7015
90	12	0	2683	328	1344	23	5200	472	8345
120	4	0	2790	194	628	20	4501	387	6133
120	6	0	3330	292	942	20	5587	482	7965
120	8	0	3870	389	1255	20	6646	575	9796
120	10	0	4590	486	1569	20	7874	679	11888
120	12	0	5400	583	1883	20	9182	788	14109

Table E-6. Representative Load Components and Resistance for Prestressed Concrete Girder Bridges, Moments.

Span (ft)	Space (ft)	D1 (k-ft)	D2 (k-ft)	D3 (k-ft)	LL (k-ft)	I (%)	mQ (k-ft)	sQ (k-ft)	R(min) (k-ft)
30	4	43	61	12	103	30	357	43	441
30	6	43	84	18	154	30	463	57	622
30	8	43	104	24	205	30	561	70	801
30	10	43	130	30	256	30	663	83	988
30	12	43	160	36	308	30	765	95	1179
60	4	262	245	49	293	27	1144	108	1531
60	6	262	335	73	440	27	1442	142	2084
60	8	262	414	97	587	27	1716	173	2622
60	10	262	521	122	733	27	2011	204	3197
60	12	262	639	146	880	27	2312	234	3786
90	4	832	552	109	489	23	2506	197	3249
90	6	832	754	164	733	23	3071	253	4237
90	8	832	932	219	978	23	3590	306	5192
90	10	832	1172	273	1222	23	4162	360	6229
90	12	832	1438	328	1467	23	4750	414	7300
120	4	1899	981	194	685	20	4557	314	5786
120	6	1899	1341	292	1027	20	5455	393	7275
120	8	1899	1656	389	1369	20	6277	469	8705
120	10	1899	2083	486	1712	20	7198	549	10281
120	12	1899	2556	583	2054	20	8152	629	11917
200	4	5650	2725	540	1491	15	11826	733	15323
200	6	5650	3725	810	2236	15	13928	885	18840
200	8	5650	4600	1080	2982	15	15848	1036	22195
200	10	5650	5788	1350	3727	15	18059	1204	25956
200	12	5650	7100	1620	4473	15	20375	1382	29880

Table E-7. Representative Load Components and Resistance for Steel Girder Bridges, Shears.

Span (ft)	Space (ft)	D1 (k)	D2 (k)	D3 (k)	LL (k)	I (%)	mQ (k)	sQ (k)	R(min) (k)
30	4	1	8	2	21	30	49	7	73
30	6	1	11	2	30	30	63	9	103
30	8	1	14	3	39	30	77	11	134
30	10	1	17	4	47	30	92	12	162
30	12	2	21	5	56	30	106	14	193
60	4	3	16	3	24	27	73	9	96
60	6	4	22	5	35	27	96	12	137
60	8	5	28	6	47	27	118	14	180
60	10	6	35	8	57	27	142	17	220
60	12	8	43	10	68	27	166	19	264
90	4	12	25	5	26	23	103	11	122
90	6	13	34	7	37	23	133	15	169
90	8	14	41	10	49	23	161	18	216
90	10	14	52	12	60	23	192	21	263
90	12	16	64	15	72	23	223	24	314
120	4	18	33	6	26	20	124	12	143
120	6	21	45	10	38	20	162	16	198
120	8	23	55	13	51	20	196	19	251
120	10	24	69	16	62	20	232	23	304
120	12	27	85	19	74	20	271	26	363
200	4	60	55	11	33	15	208	16	246
200	6	70	75	16	50	15	267	21	333
200	8	80	92	22	66	15	323	25	417
200	10	90	116	27	83	15	384	30	510
200	12	100	142	32	99	15	447	35	604

Table E-8. Representative Load Components and Resistance for Reinforced Concrete T-Beam Bridges, Shears.

Span (ft)	Space (ft)	D1 (k)	D2 (k)	D3 (k)	LL (k)	I (%)	mQ (k)	sQ (k)	R(min) (k)
30	4	0	14	2	20	30	54	7	78
30	6	0	17	2	28	30	69	9	107
30	8	0	20	3	37	30	83	11	139
30	10	0	23	4	45	30	97	13	165
30	12	0	31	5	53	30	116	14	201
60	4	0	31	3	23	27	85	10	110
60	6	0	42	5	33	27	113	12	156
60	8	0	48	6	44	27	135	15	197
60	10	0	59	8	53	27	160	18	240
60	12	0	69	10	64	27	186	20	285
90	4	0	63	5	24	23	131	13	155
90	6	0	76	7	35	23	165	16	206
90	8	0	85	10	46	23	194	19	253
90	10	0	101	12	56	23	229	23	305
90	12	0	119	15	67	23	265	26	362
120	4	0	93	6	25	20	169	15	197
120	6	0	111	10	36	20	210	19	254
120	8	0	129	13	47	20	250	23	314
120	10	0	153	16	58	20	295	27	378
120	12	0	180	19	69	20	343	31	448

Table E-9. Representative Load Components and Resistance for Prestressed Concrete Girder Bridges, Shears.

Span (ft)	Space (ft)	D1 (k)	D2 (k)	D3 (k)	LL (k)	I (%)	mQ (k)	sQ (k)	R(min) (k)
30	4	6	8	2	21	30	53	7	79
30	6	6	11	2	30	30	68	9	109
30	8	6	14	3	39	30	82	11	140
30	10	6	17	4	47	30	96	12	168
30	12	6	21	5	56	30	111	14	199
60	4	17	16	3	24	27	88	9	115
60	6	17	22	5	35	27	110	12	155
60	8	17	28	6	47	27	131	14	196
60	10	17	35	8	57	27	153	17	235
60	12	17	43	10	68	27	176	19	277
90	4	37	25	5	26	23	129	12	155
90	6	37	34	7	37	23	158	15	200
90	8	37	41	10	49	23	185	18	246
90	10	37	52	12	60	23	215	21	292
90	12	37	64	15	72	23	245	24	342
120	4	63	33	6	26	20	171	13	202
120	6	63	45	10	38	20	205	17	253
120	8	63	55	13	51	20	237	20	303
120	10	63	69	16	62	20	273	23	355
120	12	63	85	19	74	20	309	27	410
200	4	113	55	11	33	15	262	18	315
200	6	113	75	16	50	15	311	22	389
200	8	113	92	22	66	15	357	26	460
200	10	113	116	27	83	15	408	31	539
200	12	113	142	32	99	15	460	35	621

Table E-10. Reliability Indices for HS20 (AASHTO), Simple Span Moment in Non-Composite Steel Girders.

Span	Spacing	Load Effect (k-ft)		Resistance (k-ft)			β
(ft)	(ft)	mQ	σ	Rn	λ	V	
30	4	321	43	395	1.12	0.10	2.00
30	6	428	57	578	1.12	0.10	2.66
30	8	526	70	756	1.12	0.10	3.10
30	10	629	83	945	1.12	0.10	3.43
30	12	733	95	1138	1.12	0.10	3.69
60	4	916	106	1243	1.12	0.10	2.90
60	6	1227	140	1813	1.12	0.10	3.54
60	8	1525	172	2381	1.12	0.10	3.96
60	10	1839	203	2979	1.12	0.10	4.25
60	12	2158	234	3592	1.12	0.10	4.47
90	4	1920	186	2509	1.12	0.10	2.85
90	6	2506	245	3524	1.12	0.10	3.39
90	8	3046	299	4505	1.12	0.10	3.76
90	10	3639	354	5569	1.12	0.10	4.03
90	12	4258	409	6679	1.12	0.10	4.22
120	4	3157	276	4019	1.12	0.10	2.75
120	6	4148	364	5625	1.12	0.10	3.24
120	8	5026	446	7126	1.12	0.10	3.57
120	10	5983	529	8748	1.12	0.10	3.81
120	12	7030	613	10501	1.12	0.10	3.99
200	4	9096	617	11878	1.12	0.10	3.19
200	6	11714	806	16045	1.12	0.10	3.56
200	8	14148	982	20050	1.12	0.10	3.82
200	10	16875	1171	24461	1.12	0.10	4.00
200	12	19705	1365	29035	1.12	0.10	4.12

Table E-11. Reliability Indices for HS20 (AASHTO), Simple Span Moment in Composite Steel Girders.

Span	Spacing	Load Effect (k-ft)		Resistance (k-ft)			β
(ft)	(ft)	mQ	σ	Rn	λ	V	
30	4	320	43	394	1.12	0.10	2.00
30	6	426	57	576	1.12	0.10	2.66
30	8	525	70	755	1.12	0.10	3.10
30	10	628	83	944	1.12	0.10	3.43
30	12	731	95	1136	1.12	0.10	3.69
60	4	914	106	1241	1.12	0.10	2.90
60	6	1221	140	1806	1.12	0.10	3.54
60	8	1518	172	2372	1.12	0.10	3.96
60	10	1828	203	2965	1.12	0.10	4.25
60	12	2148	234	3579	1.12	0.10	4.47
90	4	1915	186	2502	1.12	0.10	2.84
90	6	2490	244	3504	1.12	0.10	3.39
90	8	3028	299	4482	1.12	0.10	3.76
90	10	3617	354	5542	1.12	0.10	4.03
90	12	4242	409	6659	1.12	0.10	4.23
120	4	3118	276	3970	1.12	0.10	2.74
120	6	4124	364	5595	1.12	0.10	3.24
120	8	4991	446	7081	1.12	0.10	3.57
120	10	5943	529	8698	1.12	0.10	3.81
120	12	6992	613	10453	1.12	0.10	3.99
200	4	8870	610	11592	1.12	0.10	3.18
200	6	11511	800	15789	1.12	0.10	3.56
200	8	13932	976	19777	1.12	0.10	3.83
200	10	16556	1163	24058	1.12	0.10	4.01
200	12	19577	1362	28873	1.12	0.10	4.13

Table E-12. Reliability Indices for HS20 (AASHTO), Simple Span Moment in Reinforced Concrete T-Beams.

Span	Spacing	Load Effect (k-ft)		Resistance (k-ft)			β
(ft)	(ft)	mQ	σ	Rn	λ	V	
30	4	361	44	467	1.14	0.13	2.24
30	6	467	58	655	1.14	0.13	2.73
30	8	566	71	841	1.14	0.13	3.07
30	10	665	84	1032	1.14	0.13	3.32
30	12	801	97	1277	1.14	0.13	3.53
60	4	1100	114	1558	1.14	0.13	2.97
60	6	1481	151	2250	1.14	0.13	3.42
60	8	1767	183	2827	1.14	0.13	3.71
60	10	2116	216	3502	1.14	0.13	3.92
60	12	2458	249	4176	1.14	0.13	4.08
90	4	2561	230	3541	1.14	0.13	2.94
90	6	3228	293	4719	1.14	0.13	3.28
90	8	3774	347	5757	1.14	0.13	3.53
90	10	4466	409	7015	1.14	0.13	3.71
90	12	5200	472	8345	1.14	0.13	3.84
120	4	4501	387	6133	1.14	0.13	2.88
120	6	5587	482	7965	1.14	0.13	3.16
120	8	6646	575	9796	1.14	0.13	3.37
120	10	7874	679	11888	1.14	0.13	3.52
120	12	9182	788	14109	1.14	0.13	3.63

Table E-13. Reliability Indices for HS20 (AASHTO), Simple Span Moment in Prestressed Concrete Girders.

Span	Spacing	Load Effect (k-ft)		Resistance (k-ft)			β
(ft)	(ft)	mQ	σ	Rn	λ	V	
30	4	357	43	441	1.05	0.08	1.90
30	6	463	57	622	1.05	0.08	2.58
30	8	561	70	801	1.05	0.08	3.05
30	10	663	83	988	1.05	0.08	3.41
30	12	765	95	1179	1.05	0.08	3.71
60	4	1144	108	1531	1.05	0.08	2.98
60	6	1442	142	2084	1.05	0.08	3.62
60	8	1716	173	2622	1.05	0.08	4.07
60	10	2011	204	3197	1.05	0.08	4.42
60	12	2312	234	3786	1.05	0.08	4.68
90	4	2506	197	3249	1.05	0.08	2.95
90	6	3071	253	4237	1.05	0.08	3.49
90	8	3590	306	5192	1.05	0.08	3.88
90	10	4162	360	6229	1.05	0.08	4.18
90	12	4750	414	7300	1.05	0.08	4.41
120	4	4557	314	5786	1.05	0.08	2.90
120	6	5455	393	7275	1.05	0.08	3.34
120	8	6277	469	8705	1.05	0.08	3.68
120	10	7198	549	10281	1.05	0.08	3.94
120	12	8152	629	11917	1.05	0.08	4.15
200	4	11826	733	15323	1.05	0.08	3.23
200	6	13928	885	18840	1.05	0.08	3.65
200	8	15848	1036	22195	1.05	0.08	3.96
200	10	18059	1204	25956	1.05	0.08	4.20
200	12	20375	1382	29880	1.05	0.08	4.37

Table E-14. Reliability Indices for HS20 (AASHTO), Shear in Steel Girders.

Span	Spacing	Load Effect (k)		Resistance (k)			β
(ft)	(ft)	mQ	σ	Rn	λ	V	
30	4	49	7	73	1.14	0.105	3.36
30	6	63	9	103	1.14	0.105	3.90
30	8	77	11	134	1.14	0.105	4.36
30	10	92	12	162	1.14	0.105	4.49
30	12	106	14	193	1.14	0.105	4.69
60	4	73	9	96	1.14	0.105	2.66
60	6	96	12	137	1.14	0.105	3.23
60	8	118	14	180	1.14	0.105	3.66
60	10	142	17	220	1.14	0.105	3.85
60	12	166	19	264	1.14	0.105	4.06
90	4	103	11	122	1.14	0.105	2.04
90	6	133	15	169	1.14	0.105	2.53
90	8	161	18	216	1.14	0.105	2.92
90	10	192	21	263	1.14	0.105	3.11
90	12	223	24	314	1.14	0.105	3.32
120	4	124	12	143	1.14	0.105	1.92
120	6	162	16	198	1.14	0.105	2.37
120	8	196	19	251	1.14	0.105	2.71
120	10	232	23	304	1.14	0.105	2.89
120	12	271	26	363	1.14	0.105	3.07
200	4	208	16	246	1.14	0.105	2.32
200	6	267	21	333	1.14	0.105	2.74
200	8	323	25	417	1.14	0.105	3.02
200	10	384	30	510	1.14	0.105	3.22
200	12	447	35	604	1.14	0.105	3.37

Table E-15. Reliability Indices for HS20 (AASHTO), Shear in Reinforced Concrete T-Beams.

Span	Spacing	Load Effect (k)		Resistance (k)			β
(ft)	(ft)	mQ	σ	Rn	λ	V	
30	4	54	7	78	1.20	0.155	2.89
30	6	69	9	107	1.20	0.155	3.25
30	8	83	11	139	1.20	0.155	3.60
30	10	97	13	165	1.20	0.155	3.70
30	12	116	14	201	1.20	0.155	3.82
60	4	85	10	110	1.20	0.155	2.34
60	6	113	12	156	1.20	0.155	2.72
60	8	135	15	197	1.20	0.155	3.03
60	10	160	18	240	1.20	0.155	3.16
60	12	186	20	285	1.20	0.155	3.31
90	4	131	13	155	1.20	0.155	1.91
90	6	165	16	206	1.20	0.155	2.22
90	8	194	19	253	1.20	0.155	2.47
90	10	229	23	305	1.20	0.155	2.60
90	12	265	26	362	1.20	0.155	2.73
120	4	169	15	197	1.20	0.155	1.85
120	6	210	19	254	1.20	0.155	2.09
120	8	250	23	314	1.20	0.155	2.30
120	10	295	27	378	1.20	0.155	2.42
120	12	343	31	448	1.20	0.155	2.53

Table E-16. Reliability Indices for HS20 (AASHTO), Shear in Prestressed Concrete Girders.

Span	Spacing	Load Effect (k)		Resistance (k)			β
(ft)	(ft)	mQ	σ	Rn	λ	V	
30	4	53	7	79	1.15	0.14	2.93
30	6	68	9	109	1.15	0.14	3.35
30	8	82	11	140	1.15	0.14	3.72
30	10	96	12	168	1.15	0.14	3.82
30	12	111	14	199	1.15	0.14	3.98
60	4	88	9	115	1.15	0.14	2.39
60	6	110	12	155	1.15	0.14	2.80
60	8	131	14	196	1.15	0.14	3.13
60	10	153	17	235	1.15	0.14	3.27
60	12	176	19	277	1.15	0.14	3.44
90	4	129	12	155	1.15	0.14	1.94
90	6	158	15	200	1.15	0.14	2.26
90	8	185	18	246	1.15	0.14	2.53
90	10	215	21	292	1.15	0.14	2.67
90	12	245	24	342	1.15	0.14	2.82
120	4	171	13	202	1.15	0.14	1.91
120	6	205	17	253	1.15	0.14	2.16
120	8	237	20	303	1.15	0.14	2.38
120	10	273	23	355	1.15	0.14	2.49
120	12	309	27	410	1.15	0.14	2.61
200	4	262	18	315	1.15	0.14	2.06
200	6	311	22	389	1.15	0.14	2.32
200	8	357	26	460	1.15	0.14	2.51
200	10	408	31	539	1.15	0.14	2.66
200	12	460	35	621	1.15	0.14	2.78

TARGET RELIABILITY INDEX

The calculated reliability indices served as a basis for the selection of the target reliability index, β_T.

The most important parameters which determine the reliability index are girder spacing and span length. In general, β's are higher for larger girder spacing. This is due to more conservative values of GDF (girder distribution factor) compared to shorter spacings, as shown in Fig. 3. It is assumed that the safety level determined for simple span moment and corresponding to girder spacing of 6 ft and span of 60 ft is acceptable. Therefore, for girder bridges, the target reliability index is taken as $\beta_T = 3.5$.

To achieve a uniform safety level for all materials, spans and girder spacings, the load and resistance factors are calculated in Appendix F of this report.

APPENDIX F Load and Resistance Factors

LOAD FACTORS

The objective in the selection of load and resistance factors is closeness to the target reliability index, β_T . For each load component, X_i, load factor, γ_i, can be considered as a function of the bias factor (mean to nominal ratio), λ_i, and the coefficient of variation, V_i,

$$\gamma_i = \lambda_i (1 + kV_i) \qquad \text{(F-1)}$$

where k is a constant.

The relationship between the nominal (design) load, mean load and factored load is shown in Fig. F-1. The shaded area in Fig. F-1 is equal to the probability of exceeding the factored load value. The parameters of bridge load components are summarized in Table F-1.

Various sets of load factors, corresponding to different values of k, are presented in Table F-2. The relationship is also shown in Fig. F-2.

Recommended values of load factors correspond to k = 2. For simplicity of the designer, one factor is specified for D_1 and D_2, $\gamma = 1.25$. For D_3, weight of asphalt, $\gamma = 1.50$. For live load and impact, the value of load factor corresponding to k = 2 is $\gamma = 1.60$. However, a more conservative value of $\gamma = 1.70$ is proposed for the LRFD code.

RELIABILITY-BASED RESISTANCE FACTORS

The relationship between the nominal (design) resistance, mean resistance and factored resistance is shown in Fig. F-3. The shaded area in Fig. F-3 is equal to the probability of exceeding the factored resistance value.

In the selection of resistance factors, the acceptance criterion is closeness to the target value of the reliability index, β_T. Various sets of resistance factors, ϕ, are considered. Resistance factors used in the code are rounded off to the nearest 0.05. For each value of ϕ, the minimum required resistance, R_{LRFD}, is determined from the following equation,

$$R_{LRFD} = [1.25\,D + 1.50\,D_A + 1.70\,(L + I)]/\phi \qquad \text{(F-3)}$$

where D is dead load except of D_A, which is the weight of asphalt surface. The load factors are equal to the recommended values.

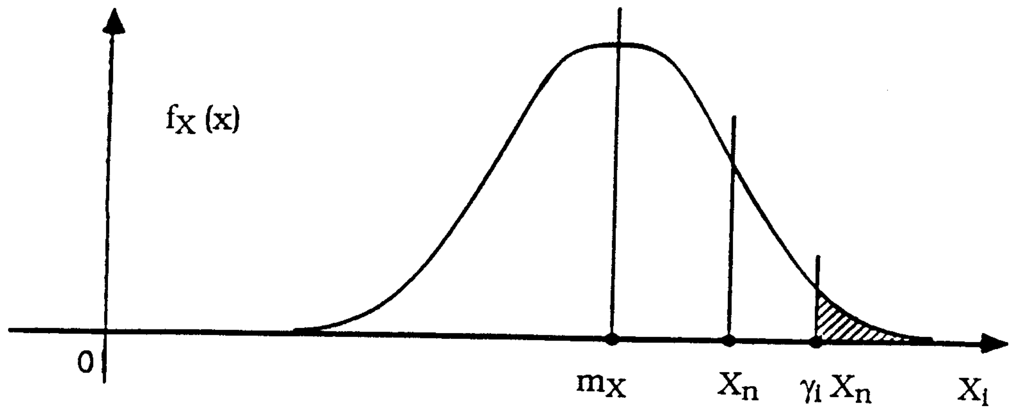

Fig. F-1. Probability Density Function, f_X (x), of Load Component, X_i; Mean Load, m_X, Nominal (design) Load, X_n, and Factored Load, $\gamma_i X_n$.

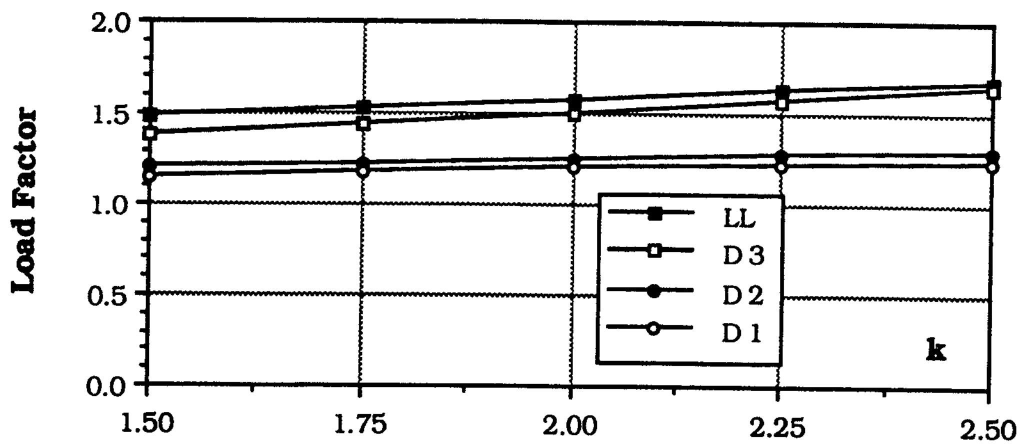

Fig. F-2. Load Factors vs. k.

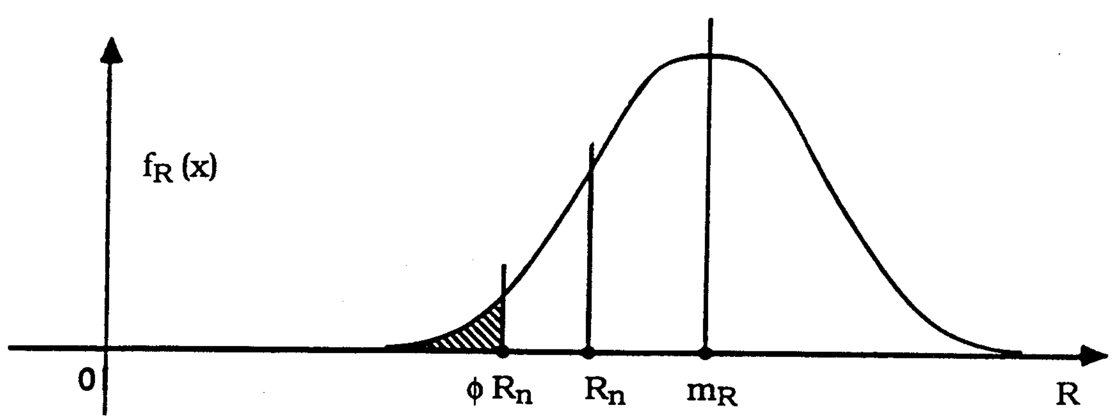

Fig. F-3. Probability Density Function, f_R (x), of Resistance, R; Mean Resistance, m_R, Nominal (design) Resistance, R_n, and Factored Resistance, ϕR_n.

Table F-1. Parameters of Bridge Load Components.

Load Component	Bias Factor	Coefficient of Variation
Dead load , D_1	1.03	0.08
Dead load, D_2	1.05	0.10
Dead load, D_3	1.00	0.25
Live load (with impact)	1.10-1.20	0.18

Table F-2. Considered Sets of Load Factors.

Load Component	k = 1.5	k = 2.0	k = 2.5
Dead load , D_1	1.15	1.20	1.24
Dead load, D_2	1.20	1.25	1.30
Dead load, D_3	1.375	1.50	1.65
Live load (with impact)	1.40-1.50	1.50-1.60	1.60-1.70

Table F-3. Considered Resistance Factors.

Material	Limit State	Resistance Factors, ϕ	
		Lower	Upper
Non-Composite Steel	Moment	0.95	1.00
	Shear	0.95	1.00
Composite Steel	Moment	0.95	1.00
	Shear	0.95	1.00
Reinforced Concrete	Moment	0.85	0.90
	Shear	0.90	0.95
Prestressed Concrete	Moment	0.95	1.00
	Shear	0.90	0.95

The calculations are performed using the load components listed in Tables E-3 to E-9 (see Appendix E). For a given resistance factor, material, span and girder spacing, a value of R_{LRFD} is calculated using Eq. F-3. Then, for each value of R_{LRFD} and corresponding loads, the reliability index is computed. For easier comparison with the current AASHTO, a resistance ratio, r, is defined as

$$r = R_{LRFD} / R_{HS20} \tag{F-4}$$

Resistance ratio is a measure of the actual change of the code requirements. Value of $r > 1$ corresponds to LRFD code being more conservative than current AASHTO, and $r < 1$ corresponds to LRFD being less conservative than the current AASHTO.

Values of r and β are calculated for live load factor, $\gamma = 1.70$. For comparison, the results are also shown for live load factor, $\gamma = 1.60$. The calculations are performed for the resistance factors, ϕ, listed in Table F-3.

The results of calculations are presented in tables and figures. For moments, resistance ratios and reliability indices are listed in Table F-4 for non-composite steel girders, Table F-5 for composite steel girders, Table F-6 for reinforced concrete T-beams and Table F-7 for prestressed concrete girders, and for shears in Tables F-8, F-9 and F-10, for steel, reinforced concrete and prestressed concrete, respectively. The tabulated data includes span length, girder spacing, mean total load, m_Q, standard deviation of total load, σ_Q, minimum resistance required by the current AASHTO, R_{HS20}, resistance ratios, r, and reliability indices, β.

The reliability indices are plotted vs. span in Fig. F-4 to F-10. The resistance ratios are shown in Fig. F-11 to F-17 for girder spacing 4, 6, 8, 10 and 12 ft. In practice, the reliability indices for bridges designed by the LRFD code do not depend on girder spacing.

OTHER RESISTANCE FACTORS

For some cases, there is no statistical data available, or the available data is incomplete, so that calculation of the reliability index is not possible. In such cases, resistance factors can be determined on the basis of the current specification. The current AASHTO is considered as acceptable, in particular for the spans in the range from 40 to 60 ft. Therefore, resistance factors are calculated so that the required nominal (design) resistance is the same for the LRFD Code and current AASHTO for spans in this range. For other spans, the required resistance can be different in LRFD Code and current AASHTO.

Table F-4. Reliability Indices and Resistance Ratios for LRFD Code, Simple Span Moments in Non-Composite Steel Girder Bridges.

Span	Space	Load		R(HS20)	$\phi = 0.95$		$\phi = 1.00$		$\phi = 0.95$		$\phi = 1.00$	
(ft)	(ft)	Effect		(k-ft)	$\gamma = 1.6$		$\gamma = 1.6$		$\gamma = 1.7$		$\gamma = 1.7$	
		mQ	σ		r	β	r	β	r	β	r	β
30	4	321	43	395	1.29	3.80	1.23	3.44	1.36	4.12	1.29	3.77
30	6	428	57	578	1.18	3.80	1.12	3.45	1.24	4.13	1.17	3.78
30	8	526	70	756	1.11	3.81	1.05	3.45	1.16	4.13	1.10	3.78
30	10	629	83	945	1.06	3.81	1.00	3.46	1.11	4.13	1.05	3.78
30	12	733	95	1138	1.02	3.82	0.97	3.46	1.07	4.14	1.01	3.78
60	4	916	106	1243	1.13	3.82	1.08	3.45	1.18	4.11	1.12	3.75
60	6	1227	140	1813	1.04	3.83	0.99	3.46	1.08	4.12	1.03	3.75
60	8	1525	172	2381	0.98	3.84	0.93	3.46	1.02	4.12	0.97	3.76
60	10	1839	203	2979	0.94	3.84	0.90	3.47	0.98	4.12	0.93	3.75
60	12	2158	234	3592	0.91	3.84	0.87	3.47	0.95	4.12	0.90	3.75
90	4	1920	186	2509	1.14	3.83	1.08	3.45	1.18	4.08	1.12	3.71
90	6	2506	245	3524	1.06	3.83	1.01	3.45	1.10	4.09	1.04	3.71
90	8	3046	299	4505	1.01	3.84	0.96	3.45	1.05	4.09	0.99	3.71
90	10	3639	354	5569	0.97	3.83	0.93	3.45	1.01	4.08	0.96	3.71
90	12	4258	409	6679	0.95	3.83	0.90	3.44	0.98	4.07	0.93	3.69
120	4	3157	276	4019	1.15	3.83	1.09	3.44	1.19	4.06	1.13	3.68
120	6	4148	364	5625	1.08	3.83	1.03	3.44	1.11	4.06	1.06	3.68
120	8	5026	446	7126	1.04	3.84	0.98	3.45	1.07	4.07	1.01	3.68
120	10	5983	529	8748	1.00	3.83	0.95	3.44	1.03	4.06	0.98	3.67
120	12	7030	613	10501	0.98	3.82	0.93	3.43	1.01	4.04	0.96	3.66
200	4	9096	617	11878	1.08	3.81	1.03	3.40	1.10	3.97	1.05	3.57
200	6	11714	806	16045	1.03	3.82	0.98	3.41	1.06	3.98	1.00	3.58
200	8	14148	982	20050	1.00	3.82	0.95	3.42	1.02	3.99	0.97	3.59
200	10	16875	1171	24461	0.98	3.81	0.93	3.41	1.00	3.98	0.95	3.58
200	12	19705	1365	29035	0.96	3.80	0.91	3.39	0.98	3.96	0.93	3.56

Table F-5. Reliability Indices and Resistance Ratios for LRFD Code, Simple Span Moments in Composite Steel Girder Bridges.

Span	Space	Load		R(HS20)	$\phi = 0.95$		$\phi = 1.00$		$\phi = 0.95$		$\phi = 1.00$	
(ft)	(ft)	Effect		(k-ft)	$\gamma = 1.6$		$\gamma = 1.6$		$\gamma = 1.7$		$\gamma = 1.7$	
		mQ	σ		r	β	r	β	r	β	r	β
30	4	320	43	394	1.29	3.79	1.23	3.44	1.36	4.12	1.29	3.77
30	6	426	57	576	1.18	3.80	1.12	3.45	1.24	4.13	1.17	3.78
30	8	525	70	755	1.11	3.81	1.05	3.45	1.16	4.13	1.10	3.78
30	10	628	83	944	1.06	3.81	1.00	3.45	1.11	4.13	1.05	3.78
30	12	731	95	1136	1.02	3.82	0.97	3.46	1.07	4.13	1.01	3.78
60	4	914	106	1241	1.14	3.82	1.08	3.45	1.18	4.11	1.12	3.75
60	6	1221	140	1806	1.04	3.82	0.99	3.46	1.08	4.12	1.03	3.75
60	8	1518	172	2372	0.98	3.83	0.93	3.46	1.02	4.12	0.97	3.76
60	10	1828	203	2965	0.94	3.84	0.90	3.47	0.98	4.12	0.93	3.75
60	12	2148	234	3579	0.91	3.84	0.87	3.46	0.95	4.12	0.90	3.75
90	4	1915	186	2502	1.14	3.83	1.08	3.45	1.18	4.08	1.12	3.71
90	6	2490	244	3504	1.06	3.83	1.01	3.45	1.10	4.09	1.04	3.71
90	8	3028	299	4482	1.01	3.83	0.96	3.45	1.05	4.09	0.99	3.71
90	10	3617	354	5542	0.97	3.83	0.92	3.45	1.01	4.08	0.96	3.71
90	12	4242	409	6659	0.95	3.83	0.90	3.44	0.98	4.07	0.93	3.69
120	4	3118	276	3970	1.15	3.83	1.09	3.44	1.19	4.06	1.13	3.68
120	6	4124	364	5595	1.08	3.83	1.03	3.44	1.11	4.06	1.06	3.68
120	8	4991	446	7081	1.04	3.84	0.98	3.45	1.07	4.07	1.01	3.68
120	10	5943	529	8698	1.00	3.83	0.95	3.44	1.03	4.06	0.98	3.67
120	12	6992	613	10453	0.98	3.82	0.93	3.43	1.01	4.04	0.96	3.66
200	4	8870	610	11592	1.08	3.81	1.03	3.41	1.11	3.98	1.05	3.58
200	6	11511	800	15789	1.03	3.82	0.98	3.41	1.06	3.99	1.00	3.59
200	8	13932	976	19777	1.00	3.83	0.95	3.42	1.02	4.00	0.97	3.60
200	10	16556	1163	24058	0.98	3.82	0.93	3.41	1.00	3.98	0.95	3.58
200	12	19577	1362	28873	0.96	3.80	0.91	3.39	0.98	3.96	0.93	3.56

Table F-6. Reliability Indices and Resistance Ratios for LRFD Code, Simple Span Moments in Reinforced Concrete T-Beam Bridges.

Span	Space	Load		R(HS20)	$\phi = 0.85$		$\phi = 0.90$		$\phi = 0.85$		$\phi = 0.90$	
(ft)	(ft)	Effect		(k-ft)	$\gamma = 1.6$		$\gamma = 1.6$		$\gamma = 1.7$		$\gamma = 1.7$	
		mQ	σ		r	β	r	β	r	β	r	β
30	4	361	44	467	1.34	4.00	1.27	3.68	1.40	4.24	1.33	3.93
30	6	467	58	655	1.24	4.01	1.18	3.69	1.30	4.26	1.23	3.94
30	8	566	71	841	1.18	4.02	1.11	3.69	1.23	4.26	1.16	3.95
30	10	665	84	1032	1.13	4.02	1.07	3.70	1.18	4.27	1.12	3.95
30	12	801	97	1277	1.09	4.01	1.03	3.69	1.14	4.25	1.07	3.94
60	4	1100	114	1558	1.18	3.95	1.11	3.62	1.22	4.15	1.15	3.83
60	6	1481	151	2250	1.09	3.95	1.03	3.62	1.13	4.15	1.07	3.82
60	8	1767	183	2827	1.04	3.96	0.99	3.63	1.08	4.17	1.02	3.84
60	10	2116	216	3502	1.01	3.96	0.95	3.63	1.04	4.16	0.99	3.84
60	12	2458	249	4176	0.98	3.96	0.92	3.63	1.01	4.16	0.96	3.83
90	4	2561	230	3541	1.15	3.82	1.09	3.47	1.18	3.97	1.12	3.64
90	6	3228	293	4719	1.10	3.84	1.04	3.50	1.13	4.01	1.07	3.67
90	8	3774	347	5757	1.06	3.87	1.00	3.53	1.09	4.04	1.03	3.71
90	10	4466	409	7015	1.03	3.87	0.97	3.53	1.06	4.04	1.00	3.71
90	12	5200	472	8345	1.00	3.87	0.95	3.53	1.03	4.03	0.98	3.70
120	4	4501	387	6133	1.15	3.73	1.08	3.38	1.17	3.86	1.11	3.52
120	6	5587	482	7965	1.10	3.77	1.04	3.42	1.13	3.91	1.07	3.57
120	8	6646	575	9796	1.07	3.79	1.01	3.44	1.10	3.93	1.04	3.59
120	10	7874	679	11888	1.05	3.79	0.99	3.44	1.07	3.93	1.01	3.59
120	12	9182	788	14109	1.03	3.78	0.97	3.44	1.05	3.92	0.99	3.58

Table F-7. Reliability Indices and Resistance Ratios for LRFD Code, Simple Span Moments in Prestressed Concrete Girder Bridges.

Span	Space	Load		R(HS20)	$\phi = 0.95$		$\phi = 1.00$		$\phi = 0.95$		$\phi = 1.00$	
(ft)	(ft)	Effect		(k-ft)	$\gamma = 1.6$		$\gamma = 1.6$		$\gamma = 1.7$		$\gamma = 1.7$	
		mQ	σ		r	β	r	β	r	β	r	β
30	4	357	43	441	1.26	3.86	1.20	3.43	1.32	4.24	1.26	3.80
30	6	463	57	622	1.17	3.86	1.11	3.43	1.22	4.23	1.16	3.80
30	8	561	70	801	1.10	3.85	1.05	3.42	1.15	4.23	1.09	3.80
30	10	663	83	988	1.05	3.85	1.00	3.42	1.10	4.23	1.05	3.80
30	12	765	95	1179	1.02	3.86	0.97	3.43	1.06	4.23	1.01	3.80
60	4	1144	108	1531	1.11	3.96	1.06	3.49	1.15	4.27	1.09	3.80
60	6	1442	142	2084	1.04	3.95	0.99	3.48	1.07	4.27	1.02	3.81
60	8	1716	173	2622	0.99	3.94	0.94	3.48	1.02	4.27	0.97	3.81
60	10	2011	204	3197	0.95	3.94	0.90	3.48	0.98	4.27	0.93	3.81
60	12	2312	234	3786	0.92	3.94	0.87	3.47	0.95	4.26	0.91	3.80
90	4	2506	197	3249	1.11	3.97	1.05	3.47	1.14	4.23	1.08	3.74
90	6	3071	253	4237	1.05	3.97	1.00	3.48	1.08	4.25	1.03	3.76
90	8	3590	306	5192	1.01	3.97	0.96	3.49	1.04	4.26	0.99	3.78
90	10	4162	360	6229	0.98	3.97	0.93	3.48	1.01	4.25	0.96	3.77
90	12	4750	414	7300	0.95	3.96	0.90	3.48	0.98	4.24	0.93	3.76
120	4	4557	314	5786	1.11	3.93	1.05	3.42	1.13	4.15	1.08	3.64
120	6	5455	393	7275	1.06	3.97	1.01	3.46	1.09	4.20	1.04	3.70
120	8	6277	469	8705	1.03	3.98	0.98	3.48	1.06	4.23	1.00	3.73
120	10	7198	549	10281	1.00	3.98	0.95	3.48	1.03	4.23	0.98	3.73
120	12	8152	629	11917	0.98	3.97	0.93	3.47	1.01	4.22	0.96	3.73
200	4	11826	733	15323	1.07	3.88	1.01	3.35	1.08	4.05	1.03	3.53
200	6	13928	885	18840	1.03	3.94	0.98	3.42	1.05	4.13	1.00	3.61
200	8	15848	1036	22195	1.00	3.98	0.95	3.46	1.02	4.17	0.97	3.66
200	10	18059	1204	25956	0.98	3.98	0.93	3.46	1.00	4.18	0.95	3.66
200	12	20375	1382	29880	0.96	3.97	0.91	3.45	0.98	4.17	0.93	3.66

Table F-8. Reliability Indices and Resistance Ratios for LRFD Code, Simple Span Shears in Steel Girder Bridges.

Span (ft)	Space (ft)	Load Effect mQ	σ	R(HS20) (k-ft)	$\phi = 0.95$ $\gamma = 1.6$ r	β	$\phi = 1.00$ $\gamma = 1.6$ r	β	$\phi = 0.95$ $\gamma = 1.7$ r	β	$\phi = 1.00$ $\gamma = 1.7$ r	β
30	4	49	7	73	1.09	3.96	1.04	3.62	1.15	4.28	1.09	3.94
30	6	63	9	103	1.01	3.96	0.96	3.62	1.06	4.28	1.01	3.95
30	8	77	11	134	0.94	3.97	0.89	3.63	0.99	4.29	0.94	3.95
30	10	92	12	162	0.92	3.97	0.88	3.63	0.97	4.29	0.92	3.95
30	12	106	14	193	0.90	3.97	0.85	3.63	0.94	4.29	0.89	3.95
60	4	73	9	96	1.22	4.05	1.16	3.70	1.28	4.35	1.22	4.01
60	6	96	12	137	1.13	4.05	1.07	3.71	1.18	4.35	1.12	4.01
60	8	118	14	180	1.06	4.06	1.01	3.71	1.11	4.35	1.05	4.01
60	10	142	17	220	1.03	4.06	0.98	3.71	1.08	4.35	1.02	4.01
60	12	166	19	264	1.00	4.06	0.95	3.71	1.04	4.35	0.99	4.00
90	4	103	11	122	1.29	3.89	1.23	3.53	1.35	4.16	1.28	3.81
90	6	133	15	169	1.21	3.89	1.15	3.54	1.26	4.17	1.20	3.81
90	8	161	18	216	1.15	3.90	1.09	3.54	1.20	4.17	1.14	3.82
90	10	192	21	263	1.12	3.90	1.06	3.54	1.16	4.17	1.10	3.81
90	12	223	24	314	1.09	3.90	1.03	3.54	1.13	4.16	1.07	3.81
120	4	124	12	143	1.34	4.08	1.27	3.72	1.39	4.33	1.32	3.98
120	6	162	16	198	1.26	4.08	1.20	3.72	1.31	4.33	1.25	3.98
120	8	196	19	251	1.21	4.09	1.15	3.73	1.25	4.34	1.19	3.98
120	10	232	23	304	1.18	4.08	1.12	3.72	1.22	4.33	1.16	3.98
120	12	271	26	363	1.15	4.07	1.09	3.71	1.19	4.32	1.13	3.96
200	4	208	16	246	1.27	4.17	1.21	3.80	1.31	4.37	1.25	4.00
200	6	267	21	333	1.21	4.17	1.15	3.80	1.25	4.37	1.18	4.01
200	8	323	25	417	1.17	4.18	1.11	3.81	1.20	4.38	1.14	4.02
200	10	384	30	510	1.14	4.17	1.08	3.80	1.17	4.37	1.11	4.01
200	12	447	35	604	1.11	4.16	1.06	3.78	1.14	4.35	1.09	3.99

Table F-9. Reliability Indices and Resistance Ratios for LRFD Code, Simple Span Shears in Reinforced Concrete T-Beam Bridges.

Span (ft)	Space (ft)	Load Effect		R(HS20) (k-ft)	$\phi = 0.90$ $\gamma = 1.6$		$\phi = 0.95$ $\gamma = 1.6$		$\phi = 0.90$ $\gamma = 1.7$		$\phi = 0.95$ $\gamma = 1.7$	
		mQ	σ		r	β	r	β	r	β	r	β
30	4	54	7	78	1.16	3.65	1.10	3.38	1.21	3.87	1.15	3.61
30	6	69	9	107	1.08	3.66	1.03	3.39	1.14	3.88	1.08	3.62
30	8	83	11	139	1.01	3.66	0.96	3.39	1.06	3.89	1.01	3.63
30	10	97	13	165	0.99	3.67	0.94	3.40	1.04	3.89	0.99	3.63
30	12	116	14	201	0.97	3.65	0.92	3.38	1.01	3.87	0.96	3.61
60	4	85	10	110	1.28	3.65	1.21	3.38	1.33	3.85	1.26	3.58
60	6	113	12	156	1.19	3.64	1.13	3.37	1.24	3.84	1.17	3.57
60	8	135	15	197	1.13	3.66	1.07	3.38	1.18	3.85	1.11	3.59
60	10	160	18	240	1.10	3.65	1.04	3.38	1.15	3.85	1.09	3.58
60	12	186	20	285	1.07	3.65	1.01	3.37	1.11	3.84	1.05	3.57
90	4	131	13	155	1.31	3.44	1.24	3.15	1.35	3.60	1.28	3.33
90	6	165	16	206	1.25	3.46	1.18	3.17	1.29	3.63	1.22	3.35
90	8	194	19	253	1.20	3.48	1.14	3.20	1.24	3.65	1.18	3.38
90	10	229	23	305	1.18	3.48	1.11	3.20	1.22	3.65	1.15	3.37
90	12	265	26	362	1.15	3.47	1.09	3.19	1.19	3.64	1.12	3.37
120	4	169	15	197	1.33	3.47	1.26	3.18	1.37	3.62	1.29	3.34
120	6	210	19	254	1.28	3.50	1.22	3.22	1.32	3.65	1.25	3.37
120	8	250	23	314	1.24	3.52	1.18	3.23	1.28	3.67	1.21	3.39
120	10	295	27	378	1.22	3.51	1.16	3.23	1.26	3.67	1.19	3.39
120	12	343	31	448	1.20	3.51	1.13	3.22	1.23	3.65	1.17	3.38

Table F-10. Reliability Indices and Resistance Ratios for LRFD Code, Simple Span Shears in Prestressed Concrete Girder Bridges.

Span	Space	Load		R(HS20)	$\phi = 0.90$		$\phi = 0.95$		$\phi = 0.90$		$\phi = 0.95$	
(ft)	(ft)	Effect		(k-ft)	$\gamma = 1.6$		$\gamma = 1.6$		$\gamma = 1.7$		$\gamma = 1.7$	
		mQ	σ		r	β	r	β	r	β	r	β
30	4	53	7	79	1.17	3.78	1.10	3.49	1.22	4.03	1.16	3.74
30	6	68	9	109	1.08	3.79	1.03	3.50	1.14	4.03	1.08	3.75
30	8	82	11	140	1.01	3.79	0.96	3.50	1.06	4.04	1.01	3.75
30	10	96	12	168	0.99	3.79	0.94	3.50	1.04	4.03	0.99	3.75
30	12	111	14	199	0.96	3.79	0.91	3.50	1.01	4.03	0.96	3.75
60	4	88	9	115	1.26	3.72	1.19	3.42	1.31	3.94	1.24	3.64
60	6	110	12	155	1.18	3.73	1.12	3.44	1.23	3.95	1.16	3.66
60	8	131	14	196	1.12	3.74	1.06	3.44	1.16	3.96	1.10	3.67
60	10	153	17	235	1.09	3.74	1.03	3.44	1.13	3.96	1.07	3.67
60	12	176	19	277	1.06	3.74	1.00	3.44	1.10	3.95	1.04	3.66
90	4	129	12	155	1.29	3.51	1.22	3.19	1.33	3.69	1.26	3.38
90	6	158	15	200	1.23	3.52	1.17	3.21	1.27	3.71	1.21	3.41
90	8	185	18	246	1.18	3.53	1.12	3.22	1.22	3.72	1.16	3.42
90	10	215	21	292	1.16	3.53	1.10	3.22	1.20	3.73	1.14	3.42
90	12	245	24	342	1.13	3.53	1.07	3.22	1.17	3.72	1.11	3.42
120	4	171	13	202	1.29	3.53	1.23	3.22	1.33	3.69	1.26	3.38
120	6	205	17	253	1.26	3.56	1.19	3.25	1.29	3.73	1.23	3.42
120	8	237	20	303	1.22	3.58	1.16	3.27	1.26	3.75	1.19	3.45
120	10	273	23	355	1.20	3.59	1.14	3.28	1.24	3.76	1.17	3.46
120	12	309	27	410	1.18	3.59	1.11	3.28	1.21	3.76	1.15	3.46
200	4	262	18	315	1.25	3.49	1.19	3.17	1.28	3.62	1.21	3.30
200	6	311	22	389	1.22	3.53	1.15	3.21	1.25	3.67	1.18	3.35
200	8	357	26	460	1.19	3.55	1.12	3.24	1.22	3.70	1.15	3.39
200	10	408	31	539	1.16	3.56	1.10	3.25	1.19	3.71	1.13	3.40
200	12	460	35	621	1.14	3.56	1.08	3.25	1.17	3.71	1.11	3.40

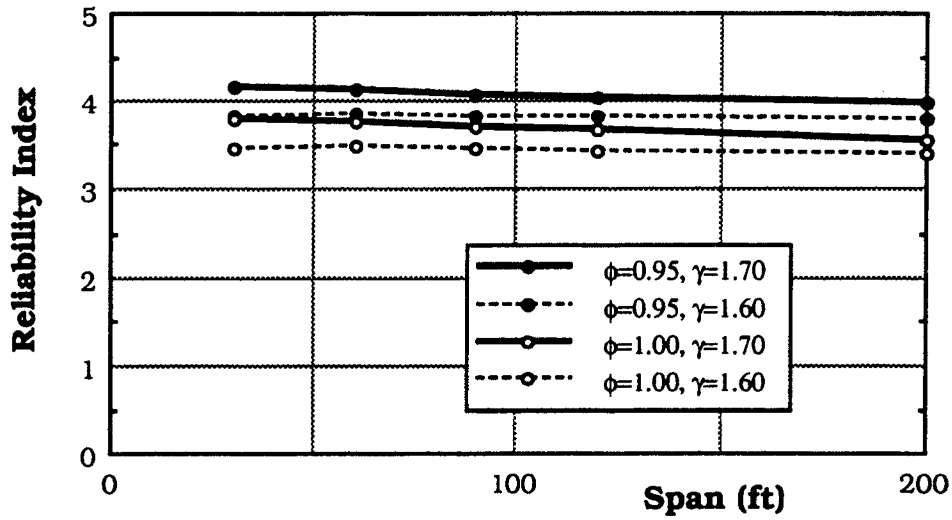

Fig. F-4. Reliability Indices for LRFD Code, Simple Span Moments in Non-Composite Steel Girders.

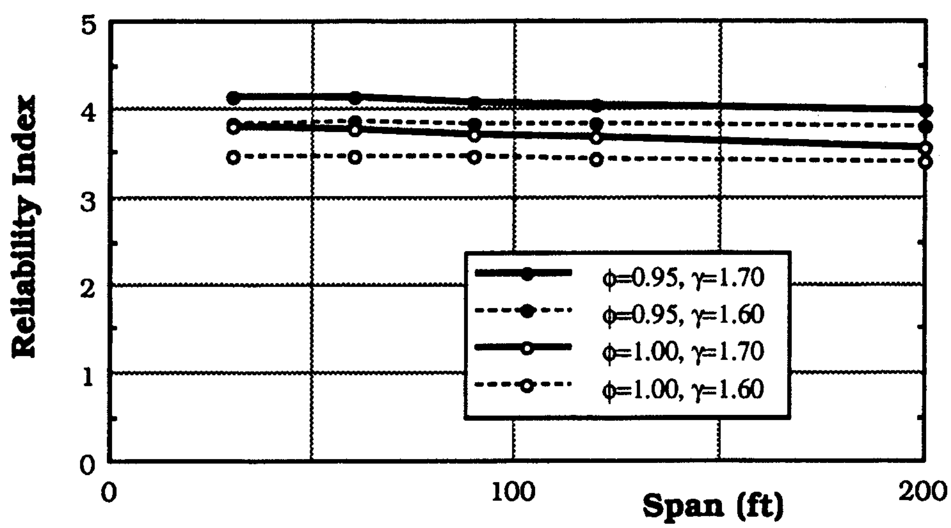

Fig. F-5. Reliability Indices for LRFD Code, Simple Span Moments in Composite Steel Girders.

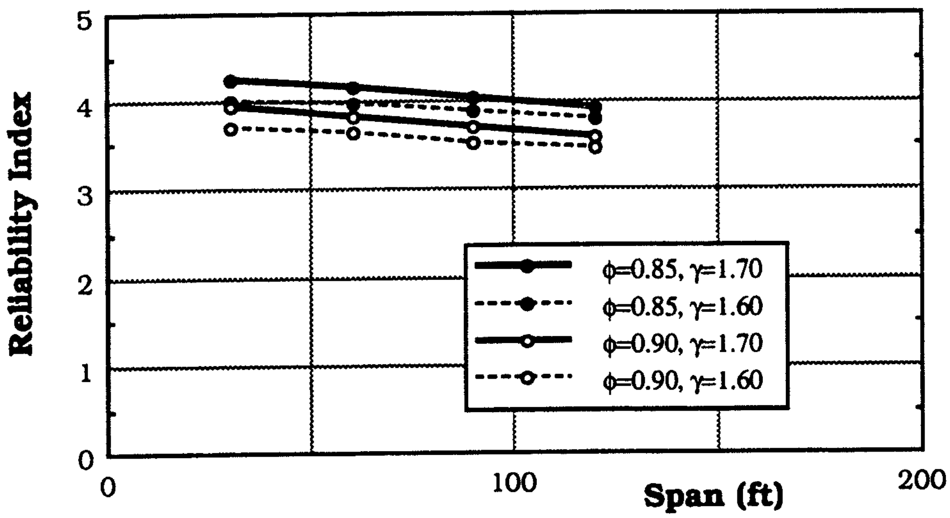

Fig. F-6. Reliability Indices for LRFD Code, Simple Span Moments in Reinforced Concrete T-Beams.

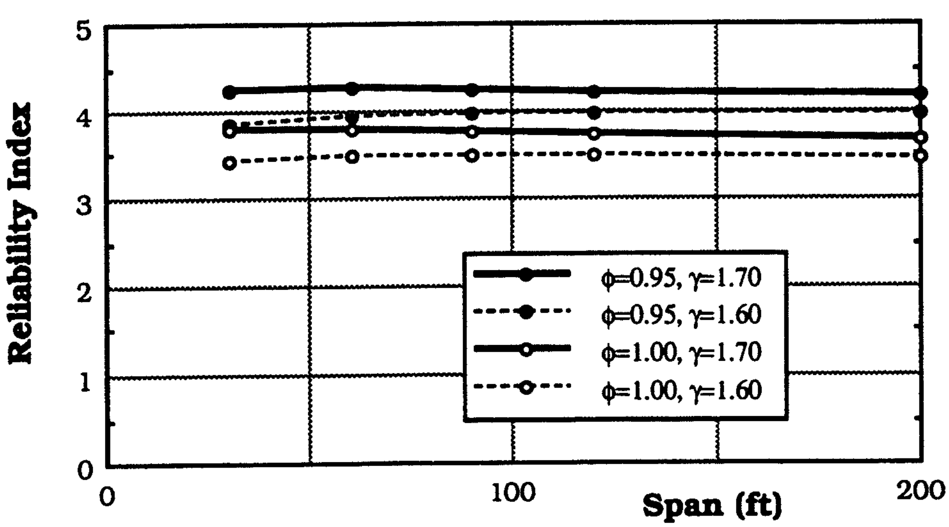

Fig. F-7. Reliability Indices for LRFD Code, Simple Span Moments in Prestressed Concrete Girders.

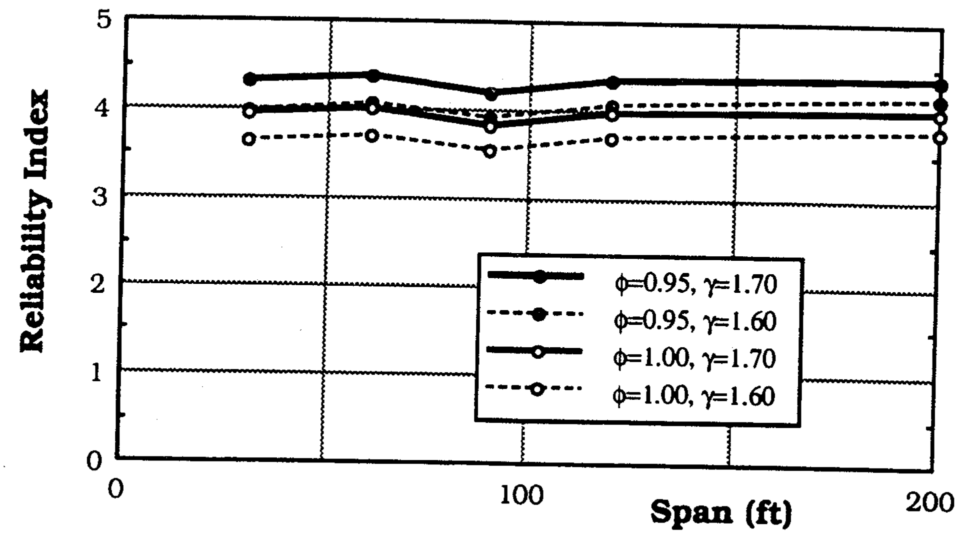

Fig. F-8. Reliability Indices for LRFD Code, Simple Span Shears in Steel Girders.

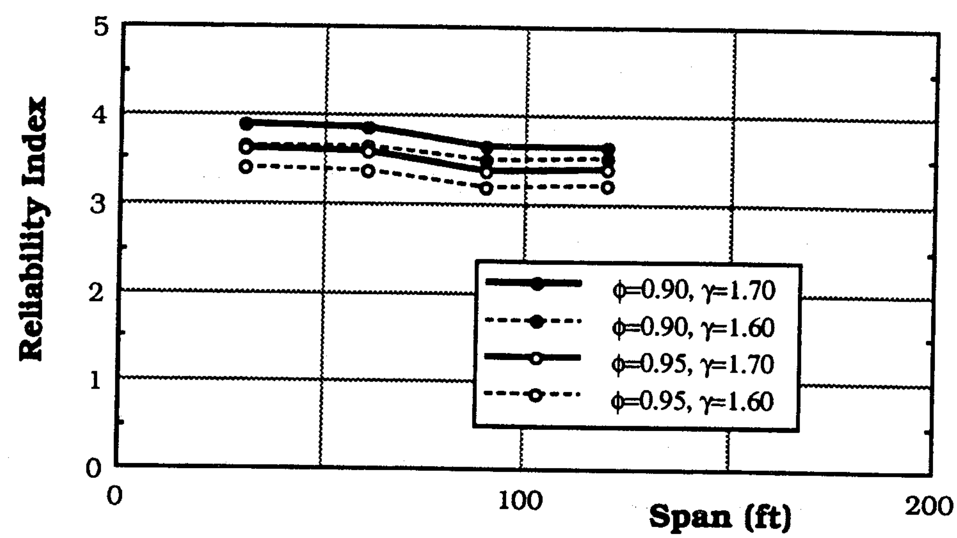

Fig. F-9. Reliability Indices for LRFD Code, Simple Span Shears in Reinforced Concrete T-Beams.

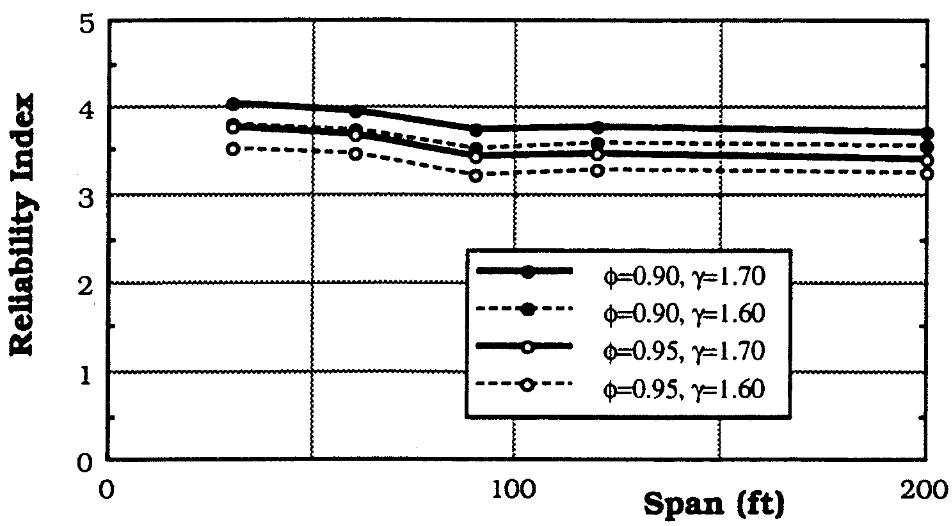

Fig. F-10. Reliability Indices for LRFD Code, Simple Span Shears in Prestressed Concrete Girders.

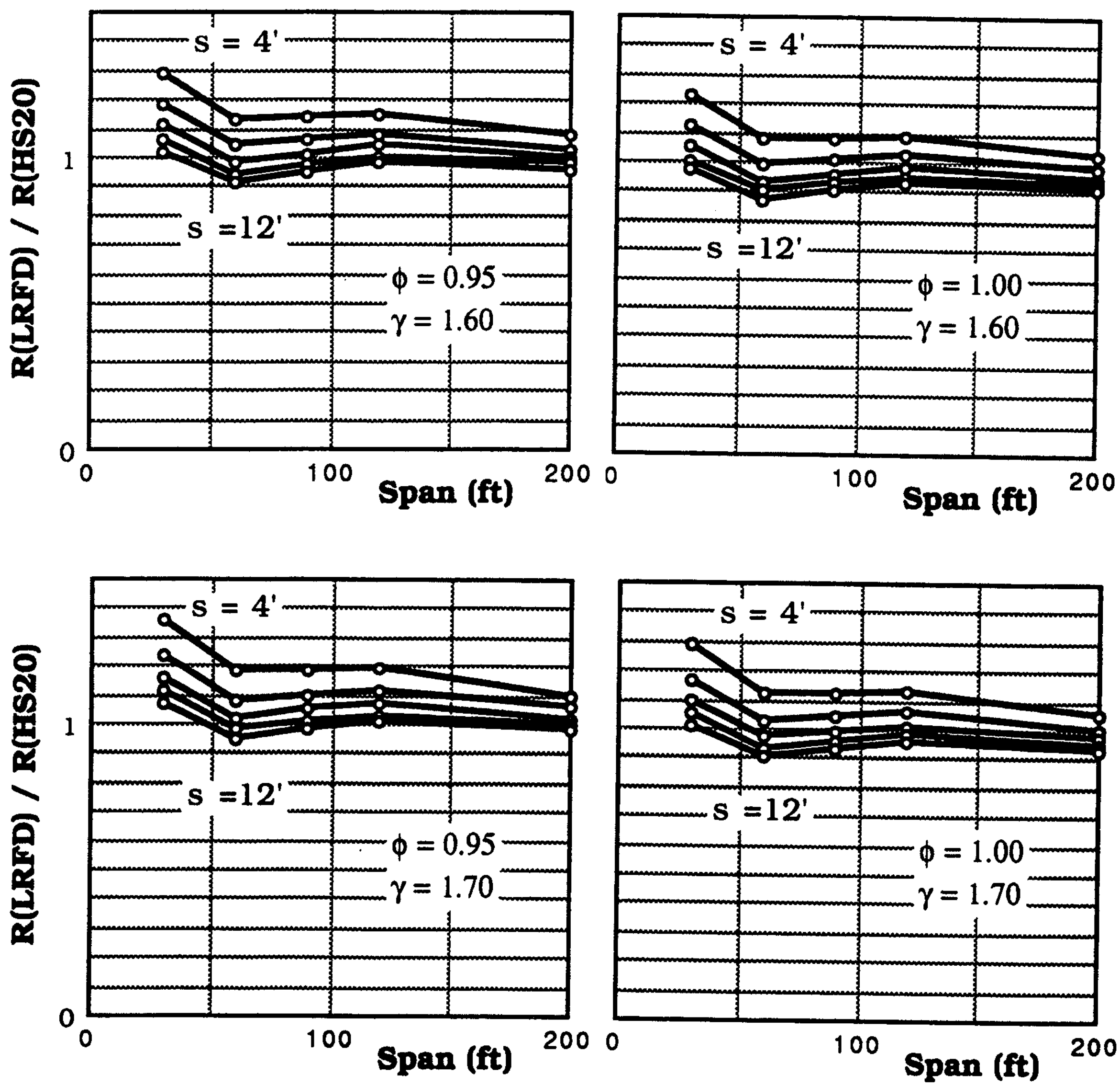

Fig. F-11. Resistance Ratios, $r = R_{LRFD} / R_{HS20}$, for Simple Span Moment, Non-Composite Steel Girder Bridges, for Girder Spacing s = 4, 6, 8, 10 and 12 ft.

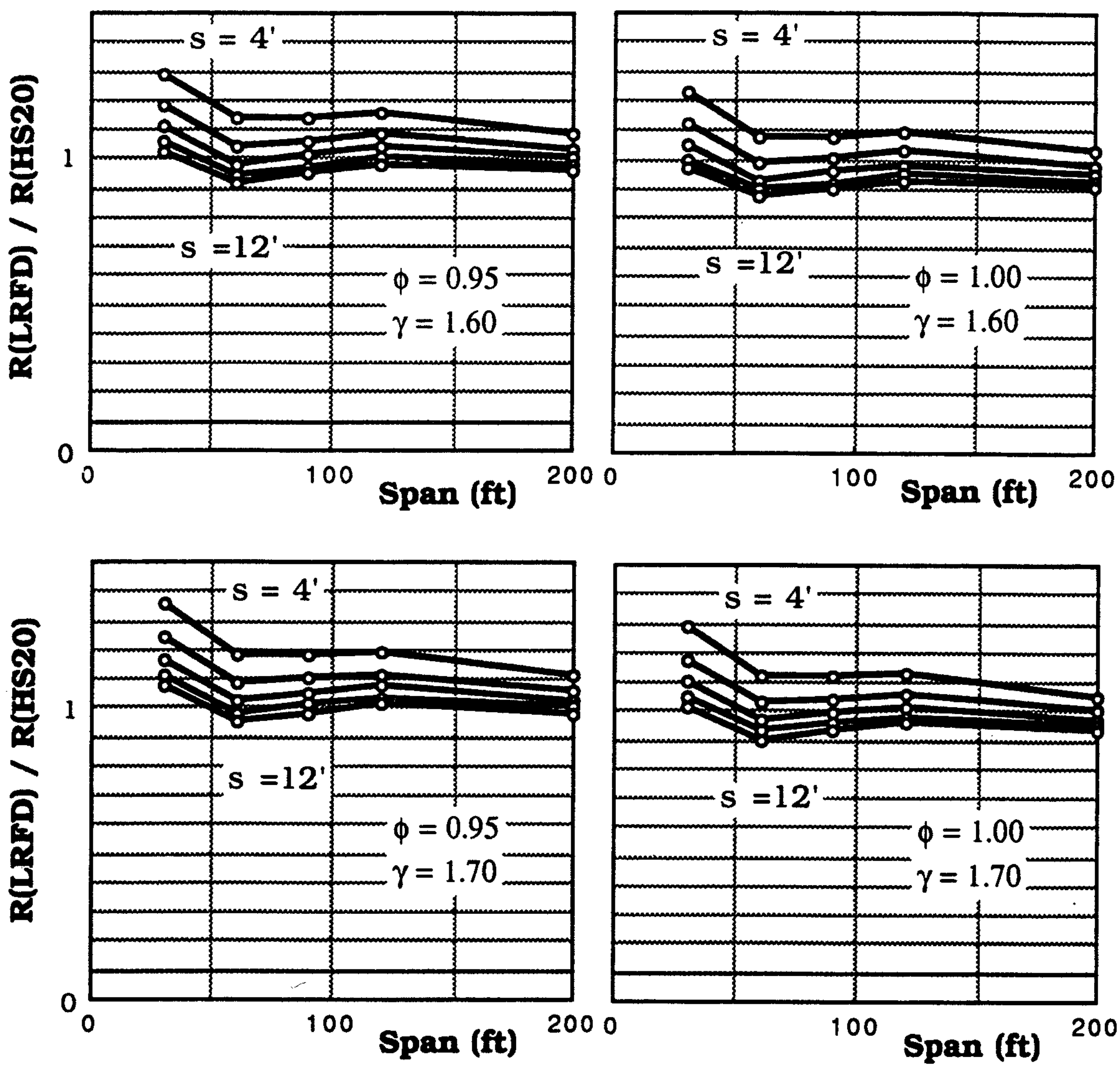

Fig. F-12. Resistance Ratios, $r = R_{LRFD} / R_{HS20}$, for Simple Span Moment, Composite Steel Girder Bridges, for Girder Spacing s = 4, 6, 8, 10 and 12 ft.

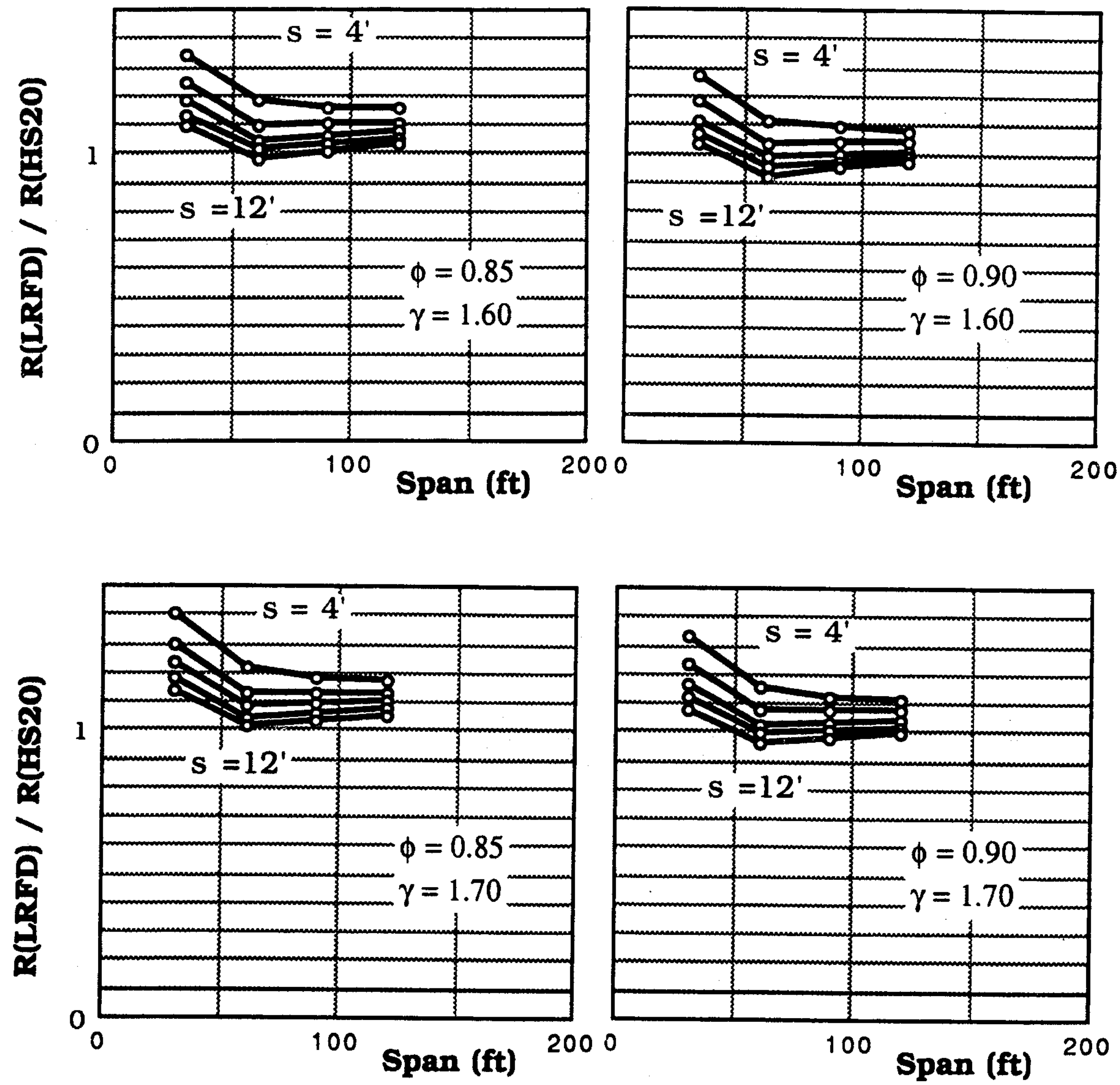

Fig. F-13. Resistance Ratios, r = R_{LRFD} / R_{HS20}, for Simple Span Moment, Reinforced Concrete T-Beam Bridges, for Girder Spacing s = 4, 6, 8, 10 and 12 ft.

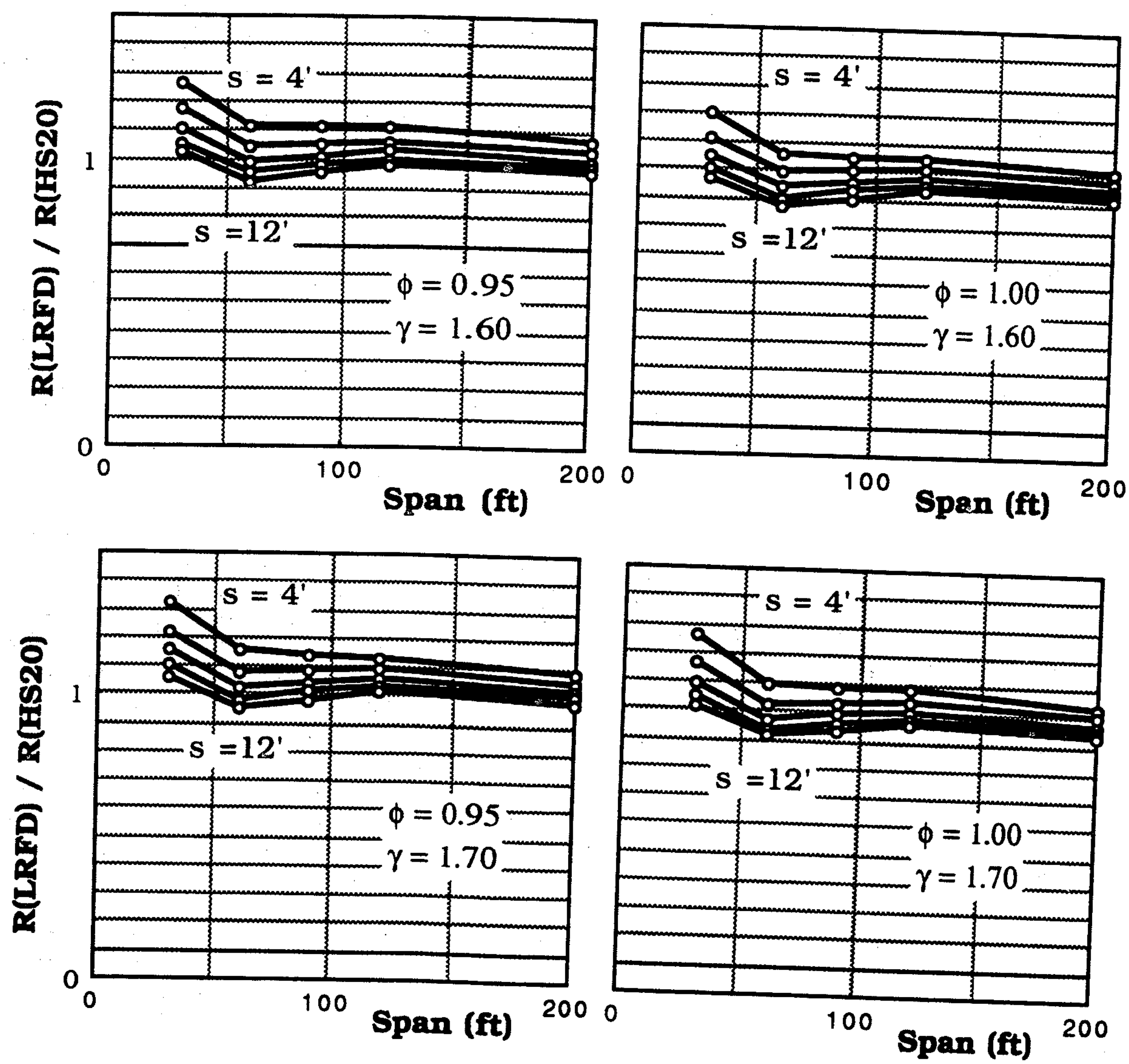

Fig. F-14. Resistance Ratios, r = R_{LRFD} / R_{HS20}, for Simple Span Moment, Prestressed Concrete Girder Bridges, for Girder Spacing s = 4, 6, 8, 10 and 12 ft.

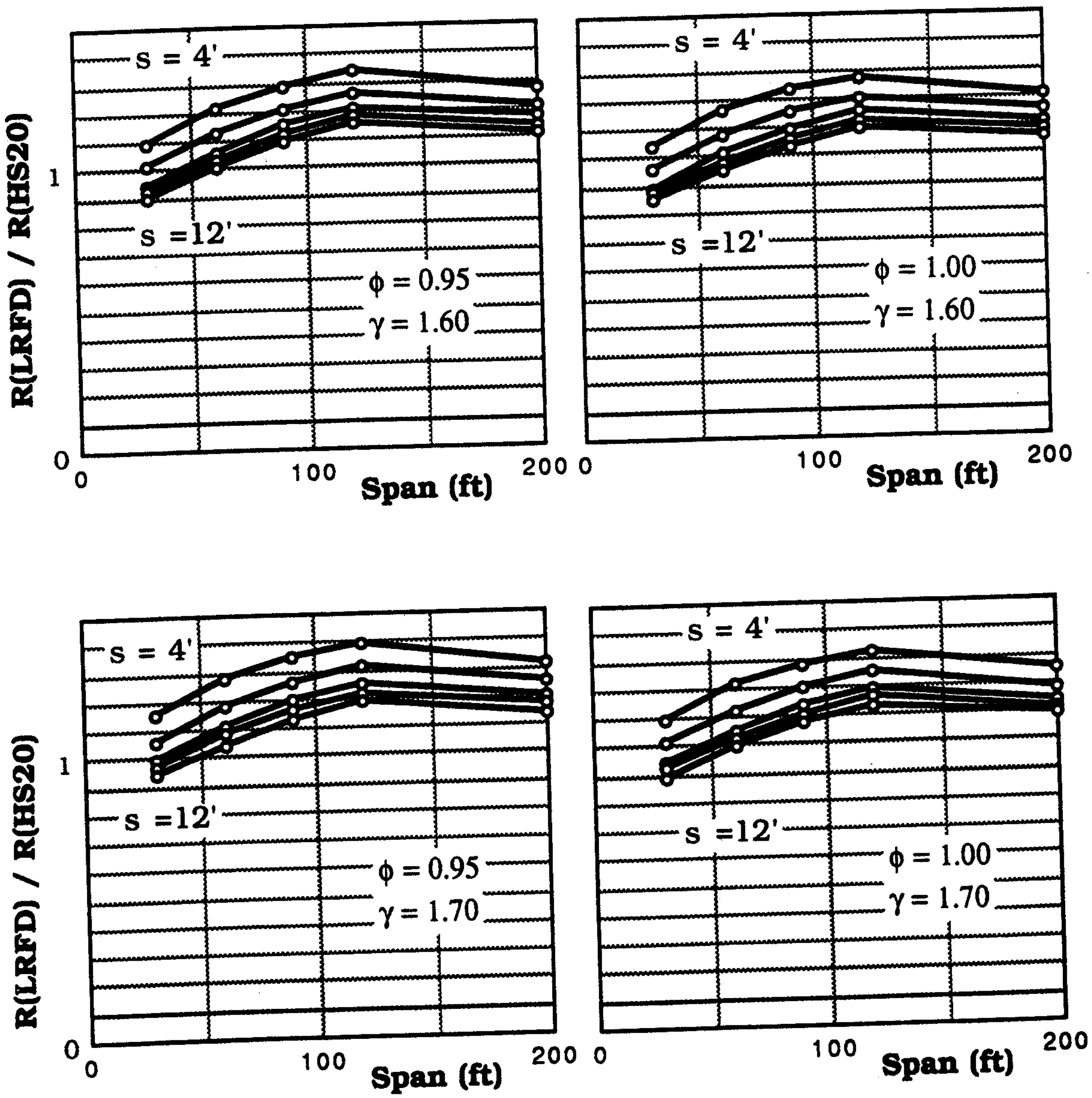

Fig. F-15. Resistance Ratios, $r = R_{LRFD} / R_{HS20}$, for Simple Span Shear, Steel Girder Bridges, for Girder Spacing s = 4, 6, 8, 10 and 12 ft.

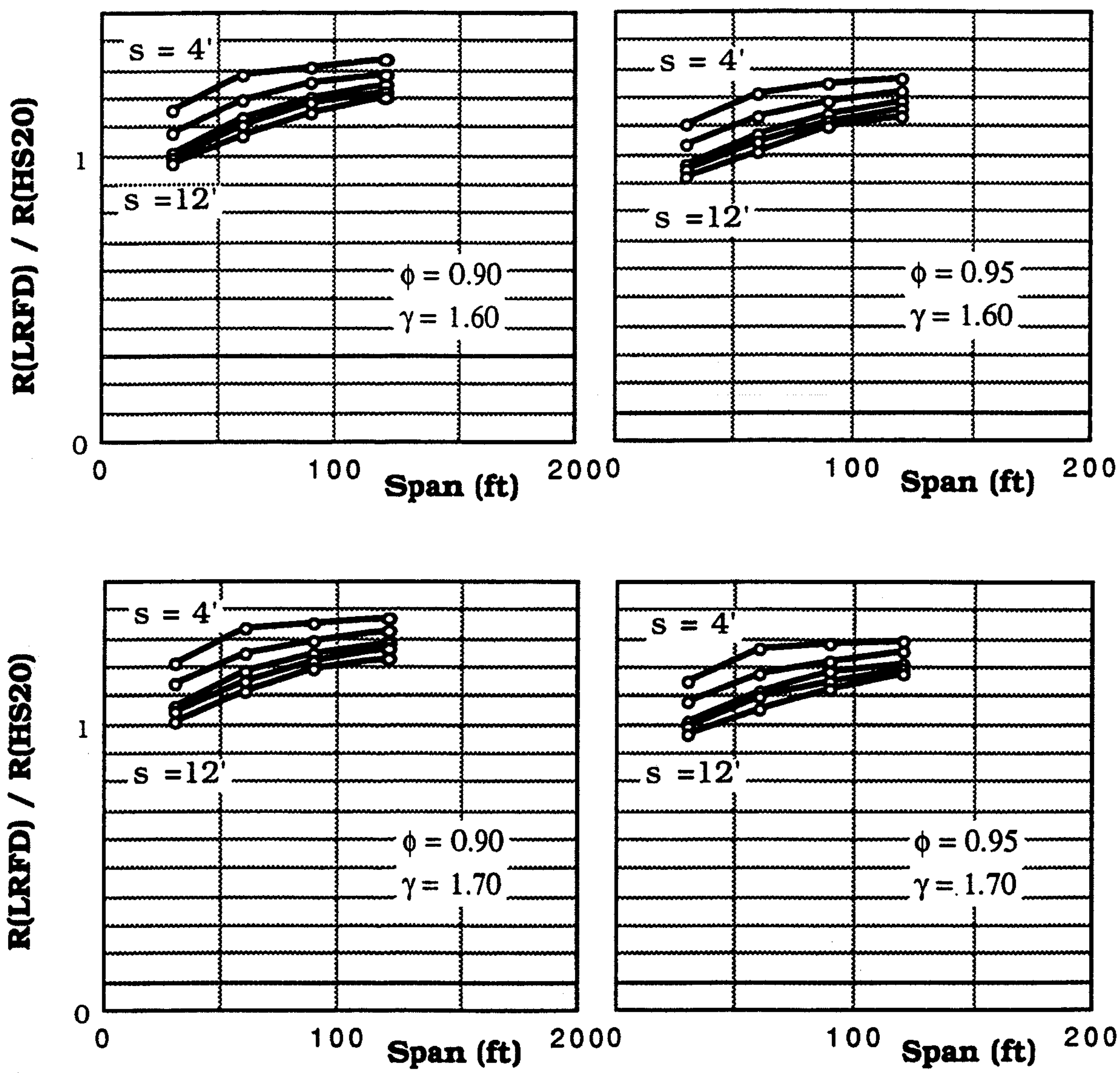

Fig. F-16. Resistance Ratios, $r = R_{LRFD} / R_{HS20}$, for Simple Span Shears, Reinforced Concrete T-Beam Bridges, for Girder Spacing s = 4, 6, 8, 10 and 12 ft.

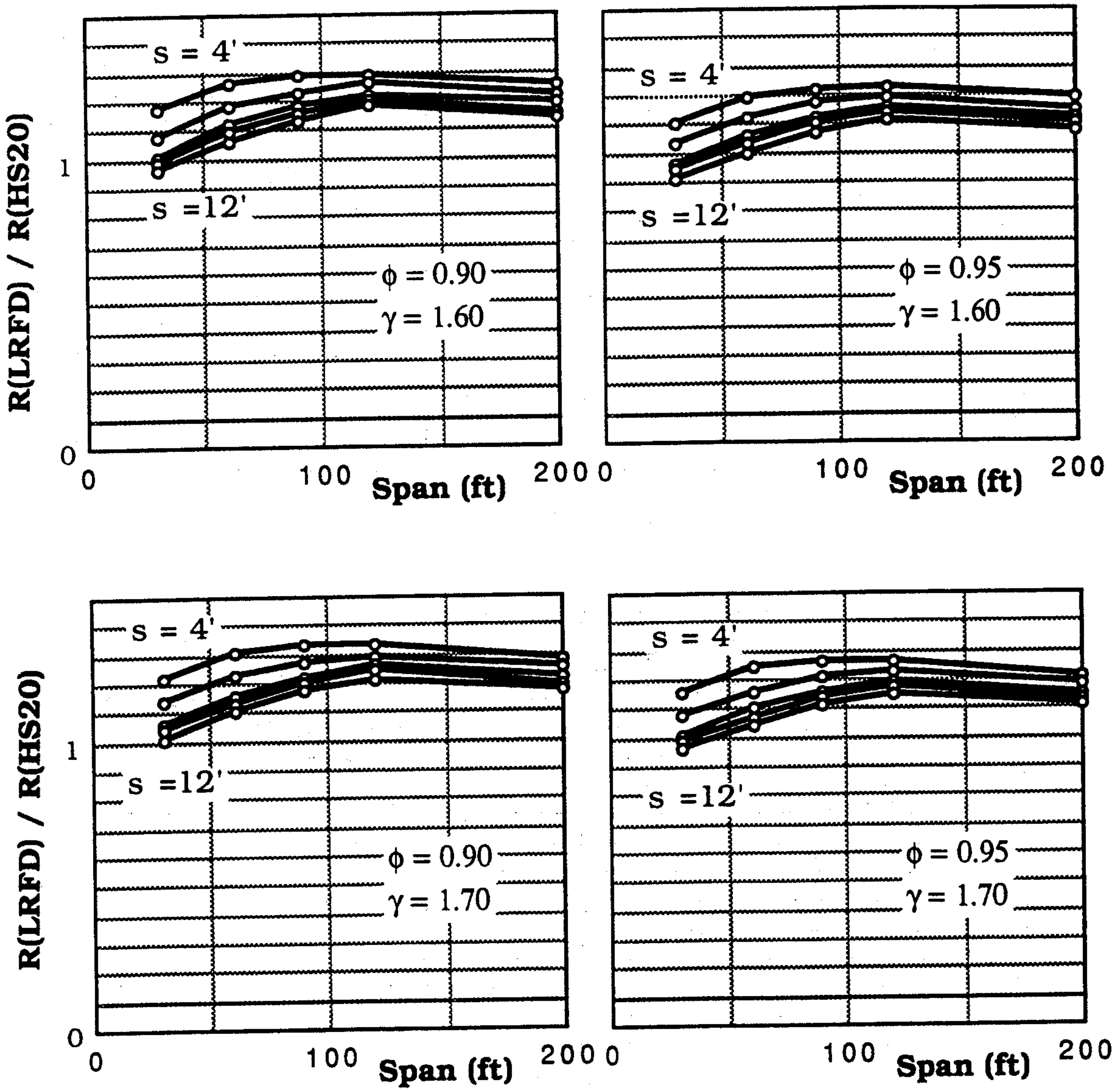

Fig. F-17. Resistance Ratios, $r = R_{LRFD} / R_{HS20}$, for Simple Span Shears, Prestressed Concrete Girder Bridges, for Girder Spacing s = 4, 6, 8, 10 and 12 ft.

The **Transportation Research Board** is a unit of the National Research Council, which serves the National Academy of Sciences and the National Academy of Engineering. The Board's mission is to promote innovation and progress in transportation by stimulating and conducting research, facilitating the dissemination of information, and encouraging the implementation of research results. The Board's varied activities annually draw on approximately 4,000 engineers, scientists, and other transportation researchers and practitioners from the public and private sectors and academia, all of whom contribute their expertise in the public interest. The program is supported by state transportation departments, federal agencies including the component administrations of the U.S. Department of Transportation, and other organizations and individuals interested in the development of transportation.

The National Academy of Sciences is a private, nonprofit, self-perpetuating society of distinguished scholars engaged in scientific and engineering research, dedicated to the furtherance of science and technology and to their use for the general welfare. Upon the authority of the charter granted to it by the Congress in 1863, the Academy has a mandate that requires it to advise the federal government on scientific and technical matters. Dr. Bruce M. Alberts is president of the National Academy of Sciences.

The National Academy of Engineering was established in 1964, under the charter of the National Academy of Sciences, as a parallel organization of outstanding engineers. It is autonomous in its administration and in the selection of its members, sharing with the National Academy of Sciences the responsibility for advising the federal government. The National Academy of Engineering also sponsors engineering programs aimed at meeting national needs, encourages education and research, and recognizes the superior achievements of engineers. Dr. William A. Wulf is president of the National Academy of Engineering.

The Institute of Medicine was established in 1970 by the National Academy of Sciences to secure the services of eminent members of appropriate professions in the examination of policy matters pertaining to the health of the public. The Institute acts under the responsibility given to the National Academy of Sciences by its congressional charter to be an adviser to the federal government and, upon its own initiative, to identify issues of medical care, research, and education. Dr. Kenneth I. Shine is president of the Institute of Medicine.

The National Research Council was organized by the National Academy of Sciences in 1916 to associate the broad community of science and technology with the Academy's purpose of furthering knowledge and advising the federal government. Functioning in accordance with general policies determined by the Academy, the Council has become the principal operating agency of both the National Academy of Sciences and the National Academy of Engineering in providing services to the government, the public, and the scientific and engineering communities. The Council is administered jointly by both the Academies and the Institute of Medicine. Dr. Bruce M. Alberts and Dr. William A. Wulf are chairman and vice chairman, respectively, of the National Research Council.

Abbreviations used without definitions in TRB publications:

AASHO	American Association of State Highway Officials
AASHTO	American Association of State Highway and Transportation Officials
ASCE	American Society of Civil Engineers
ASME	American Society of Mechanical Engineers
ASTM	American Society for Testing and Materials
FAA	Federal Aviation Administration
FHWA	Federal Highway Administration
FRA	Federal Railroad Administration
FTA	Federal Transit Administration
IEEE	Institute of Electrical and Electronics Engineers
ITE	Institute of Transportation Engineers
NCHRP	National Cooperative Highway Research Program
NCTRP	National Cooperative Transit Research and Development Program
NHTSA	National Highway Traffic Safety Administration
SAE	Society of Automotive Engineers
TCRP	Transit Cooperative Research Program
TRB	Transportation Research Board
U.S.DOT	United States Department of Transportation

TRANSPORTATION RESEARCH BOARD
National Research Council
2101 Constitution Avenue, N.W.
Washington, D.C. 20418